Novel Metrics and Regenerative Pathways for Securing Soil

By

Anilkumar Hunakunti

A thesis submitted to fulfil the requirements for the degree of

Doctor of Philosophy

2026

School of Life and Environmental Sciences

Faculty of Science

The University of Sydney

New South Wales, Australia

Statement of Originality

This is to certify that the content of this thesis is my own work. This thesis has not been submitted for any other degree or purpose.

I certify that the intellectual content of this thesis is the product of my own work, and that all assistance received in preparing this thesis and all sources have been acknowledged.

Anilkumar Hunakunti

Date: 02 March 2026

Acknowledgements

First of all, I would like to thank the PhD journey itself. It has taught me many things, especially how to understand the reality of nature in my own way. Of course, the journey has not been easy. It demanded deep focus and time, while I also had to balance my responsibilities as a parent and a family member. Sometimes, simply playing with my child made the PhD journey more joyful and helped me overcome moments of stress. I am deeply thankful to my family - my wife, my father, my mother, my sisters. Without their constant love and support, completing this PhD would not have been possible.

Thanks to the support of the Australian Research Council Laureate Fellowship and the Francis Henry Loxton Stipend scholarship, this research was made possible.

I would like to express my deepest gratitude to my supervisor, **Professor Alex McBratney**. This research introduces a novel concept in each chapter that began as simple ideas and questions during our discussions. Without him, those ideas would have remained just ideas, they became reality through his encouragement and intellectual generosity. I will always remember his support, guidance, expertise and patience.

I was also like to express my sincere gratitude to my co-supervisor, **Professor Budiman Minasny**, for his constant yet quiet support throughout my PhD journey. His constructive ideas, critical reviews of my papers, and valuable guidance have greatly improved the quality of my research. His expertise has been invaluable in shaping many aspects of this work.

Special thanks to **Dr. Balwant Singh**, my panel chair, and **Dr. Thomas Bishop Thomas** for their kind advice and support. My sincere thanks to **Dr. Anthony Whitbread** for his kindness and encouragement.

I would also like to thank **Dr. Julio Pachon** and **Dr. Andree Nekam,** not only as a colleague but as a friend. Finally, my sincere appreciation to the wonderful Soil Security Team-Thank you all for your support throughout my PhD journey.

Authorship attribution statement

Chapter 2 of this thesis is published as:

Anilkumar Hunakunti, Alex B McBratney, Budiman Minasny, Damien J Field (2025) Assessing Soil Erosion Vulnerability Using a Novel Capacity–Condition Framework (CCF): A Case Study from New South Wales, Australia. *International Soil and Water Conservation Research, 13(4), 771–794*.

I conceptualised along with my coauthors, performed the analysis, visualisation, and methodology, validation, writing-original draft, writing-review & editing.

Chapter 3 of this thesis is published as:

Anilkumar Hunakunti, Alex McBratney, Budiman Minasny (2025) Towards Soil security: Understanding Soil erosion footprint and their implications in NSW. *Soil security,* 19, 100184.

I conceptualised along with my coauthors, performed the analysis, visualisation, and methodology, validation, writing-original draft, writing-review & editing.

Chapter 4 of this thesis is published as:

Anilkumar Hunakunti, Alex McBratney, Budiman Minasny (2025) Introducing an exergy-based model for soil restoration: quantifying energy demands for SOC rebuilding, *Geoderma, 461, 117474*.

I conceptualised along with my coauthors, performed the analysis, visualisation, and methodology, validation, writing-original draft, writing-review & editing.

I designed the study with my co-authors and performed the analysis, validation, methodology, visualization and conceptualisation. I wrote the manuscript drafts.

Student name: Anilkumar Hunakunti

02 March 2026

As supervisor for the candidature upon which this thesis is based, I can confirm that the authorship attribution statements above are correct.

Alex McBratney, *Australian Research Council Laureate Fellow, Professor of Digital Agriculture & Soil Science, The University of Sydney*

02 March 2026

Statement on the Use of Generative Artificial Intelligence

During the preparation of this thesis, the author used ChatGPT (OpenAI, 2025) for the purpose of text enhancement, including sentence restructuring, paraphrasing for clarity, and grammar correction and improving the overall quality of the English expression. Following its use, the author reviewed and edited the content for possible errors, inaccuracies, and bias. The author takes full responsibility for the submitted thesis. All research design, analysis, interpretation, and conclusions presented in this thesis are entirely the author's own.

Abstract

Soil is a complex, dynamic, and self-organising system that provides essential services not just to humanity but to all life on Earth. Soil is under enormous pressure, especially on existing productive soils due to food security concerns; with the rise in population, more food must be grown on less soil, which leads to widespread degradation, often driven by human activity, both knowingly and unknowingly. Soil erosion is the major driver of soil degradation, causing other degradation processes such as nutrient loss, SOC loss, greenhouse gas emissions, loss of biodiversity, sedimentation and pollution.

Mitigating soil degradation requires systematic approaches to assessment and restoration. The concept of soil security has the potential to provide a structured framework that encompasses both soil degradation assessment and diverse restoration strategies. However, the concept is still evolving and requires metrics to assess soil conditions, as well as regenerative pathways to restore degraded soils. This thesis addresses this gap by introducing new metrics and regenerative pathways for soil security. The two metrics are the Soil Erosion Risk Capability (ERC) and the Soil Erosion Footprint, while the regenerative pathways include the exergy model for soil restoration and an opinion perspective that explores and proposes Quantum Soil Science as a novel regenerative pathway.

ERC quantifies the gap between a soil's inherent resistance to erosion and its erosion-altered state. To develop this metric, this thesis introduced a Capacity-Condition Framework (CCF), and quantified it using the concept of space-for-time substitution via genosoil, phenosoil and pedogenon concepts. The ERC was calculated across New South Wales (NSW), Australia, and the results suggest that the upper northwest and Coastal areas, where intensive dryland cropping and grazing on modified pastures occur, are at high risk of erosion and have lower capability to withstand future erosion.

This thesis introduced a generalised soil footprint framework to calculate different types of soil footprints. The flexible framework allows both complex and simple assessments of soil degradation, where individual soil footprints can be evaluated with respect to specific soil degradation processes or combined comprehensively to obtain an overall metric for soil security assessment. The main components of the framework used to calculate the soil footprint are threat to soil, Soil service ratio, and inherent mitigation capability. Two soil erosion footprints were calculated across NSW. Oats showed the highest erosion footprints, while wheat, barley, and legumes showed the lowest. AWC–related footprint was highest in coastal/dryland areas and lowest in irrigated systems.

Soil security depends not only on assessing soil degradation but also on the efficient restoration of degraded soils. This thesis introduces an exergy model for soil restoration, quantifying the energy needed to restore SOC in degraded soil to its reference state, based on the first-order differential equation. This model has potential as a regenerative

pathway tool, as it makes regenerative feasibility measurable, showing where and how much energy is needed for soil restoration. The results show that pedogenons with large SOC gaps and low recovery rates exhibited the highest exergy demands. Sensitivity analysis suggests that management goals focusing on reducing the SOC gap between genosoil and phenosoil and optimising the SOC recovery rate constant, K, are essential for energy-efficient restoration. This thesis conceptually explores whether there are opportunities to enhance the soil formation process itself in order to boost the soil's inherent ability to regenerate. It introduces a new way of thinking, called quantum thinking in soil management, to enhance soil process such as enzymatic decomposition and mineral weathering by recognising quantum processes like tunnelling and electron coherence, which could provide the hidden mechanisms that make soils resilient and regenerative thus proposing a new pathway for soil security.

Table of Contents

Statement of Originality i

Acknowledgements ii

Authorship Attribution Statement iii

Statement on the Use of Generative Artificial Intelligence iv

Abstract v

Chapter 1: Introduction 1

1.1 Overview 2

1.2 The Concept of Soil Security and Its Relevance to Reversing Soil Degradation 3

1.3 Soil Security and Soil Erosion Assessment 5

1.4 Soil Footprint Simple Indicator for Soil Security Assessment 7

1.5 Energy-Based Approaches in Soil Restoration 9

1.6 Quantum Pathways to Secure Soil 10

1.7 Aim & Objectives 12

1.8 References 14

Chapter 2: Assessing Soil Erosion Vulnerability Using a Novel Capacity–Condition Framework (CCF): A Case Study from New South Wales, Australia 22

2.1 Abstract 23

2.2 Introduction 24

2.3 Methods 27

2.3.1 Study Area 27

2.3.2 Overview of the Soil Erosion Risk Assessment Framework 30

2.3.3 Defining Capacity, Condition, and Erosion Risk 31

2.3.4 Indicators for Capacity and Condition 33

2.3.5 Two-Step Modelling Approach for Topsoil Thickness Mapping 37

2.3.6 Estimation of Capacity and Condition 39

2.4 Results 42

2.4.1 Remote Sensing Variables for Topsoil and Non-topsoil 42

2.4.2 Topsoil Thickness: Spatial Pattern and Genosoil-Phenosoil Comparison 45
2.4.3 Topsoil Thickness Model Performance 49
2.4.4 Clay Ratio Distribution and Relationship to Erosion Resistance in NSW 50
2.4.5 Capacity Utility maps.....50
2.4.6 Condition Utility maps 53
2.4.7 Quantifying Erosion Risk 55
2.5 Discussion 57
2.5.1 Challenges and Opportunities in Modelling Topsoil Thickness.....57
2.5.2 Soil Capacity for Erosion Resistance Using Genosoil Indicators.....60
2.5.3 Genosoil and Phenosoil Deviation and Its Effect on Soil Condition Utility.....61
2.5.4 Soil Erosion Risk.....63
2.5.5 Limitations and Future Perspectives 65
2.6 Conclusion 66
2.7 References 69
Chapter 3: Towards Soil Security: Understanding Soil Erosion Footprints and Their Implications in NSW 82
3.1 Abstract 83
3.2 Introduction 84
3.3 Materials and Methods 87
3.3.1 Study Area.....89
3.3.2 Soil Footprint 90
3.3.3 Soil Erosion Footprint 93
3.3.4 Erosion Rate and Erosion Risk Capability Estimation in ABARES Regions.....95
3.3.5 Estimation of Crop yield in ABARES Regions.....96
3.3.6 Estimation of Soil Service Ratio 96
3.3.7 Soil Erosion Footprint Analysis Based on Land Use Classification.....97
3.3.8 Impact on Crop Receipts Change in Soil Footprint.....98
3.4 Results and Discussion 100

3.4.1 Crop-Specific Soil Erosion Footprint Rankings Across NSW Regions 100

3.4.2 Crop Yield, Erosion Rate, and Risk Capabilities Across ABARES Regions 101

3.4.3 Relationship Between Soil Erosion Footprint and Crop Receipts in NSW 106

3.4.4 Impact of Soil Footprint on Crop Receipts Across Different Regions 109

3.4.5 Variation of AWC and Soil Service Ratio Mapping Across NSW 112

3.4.6 Soil Erosion Footprint Based on AWC as a Soil Service 112

3.4.7 Integrating Assessment of Soil Erosion Across Land Use Systems 115

3.5 Conclusion and Future Work 122

3.6 References 129

Chapter 4: Introducing an Exergy-Based Model for Soil Restoration - Quantifying Energy Demands for SOC Rebuilding 136

4.1 Abstract 137

4.2 Introduction 138

4.3 Methodology 140

4.3.1 Exergy-Based Soil Restoration: Conceptual Framework 140

4.3.2 Mathematical Framework 142

4.3.3 Exergy Calculation for Restoration 144

4.3.4 Thermodynamic Principles in SOC Restoration 145

4.3.5 Unit for Total Exergy 146

4.3.6 Pedogenon and Management-Specific Model Calculations 146

4.3.7 Calculating k: The Rate Constant for SOC Recovery 149

4.3.8 Calculating α: Energy Cost per unit increase in SOC 150

4.3.9 Variance Decomposition of Exergy Via Sobol Indices 153

4.4 Results 154

4.4.1 SOC Dynamics and Recovery Model 154

4.4.2 Understanding Exergy Demands and Recovery Efficiency 155

4.4.3 Pedogenon-Specific Exergy Cost Per Unit SOC Increase 159

4.4.4 Role of k, ΔSOC, and α in SOC Restoration 160

4.5 Discussion 162

4.5.1 Establishing an Exergy Framework for SOC Restoration 162

4.5.2 Towards Data-Driven Soil Restoration 164

4.5.3 Practical Implications for Soil Restoration 166

4.5.4 Future Directions 166

4.6 Conclusion 167

4.7 References 169

Chapter 5: Quantum Soil Science: A New Frontier for Soil Formation, Function, and Security 176

5.1 Abstract 177

5.2 Introduction 177

5.3 Quantum Contributions to Soil Formation and Function 180

5.4 Mineral Weathering and Electron Transfer 183

5.5 Enzymatic Reactions in Soil Organic Matter Decomposition 187

5.6 Quantum Tunnelling in Proton and Electron Transfers 188

5.7 Quantum Coherence in Enzyme Dynamics 190

5.8 Conceptual Framework: Linking Quantum Effects to Accelerated Soil Formation .191

5.8.1 External Drivers of Soil Processes 193

5.8.2 Quantum Processes in Soil Systems: Identification and Interpretive Value 193

5.8.3 Targeted Interventions and Accelerated Soil Formation 194

5.8.4 Reference Soils 195

5.9 Discussion 196

5.9.1 Limitations of Conventional Soil Indicators 196

5.9.2 Designing Interventions to Support Quantum Soil Processes 197

5.9.3 Integrating Quantum Thinking into Soil Management 199

5.9.4 Assessing Quantum Effects in Soil Systems 201

5.10 Conclusion 203

5.11 References 204

Chapter 6. Overall Discussion and Conclusions 214

6.1 Erosion Risk Capability as a Metric for Assessing Threats to Soil 215

6.2 Soil Footprint as a Metric of Soil Security 216

6.2.1 Soil Security Dimensions and Soil Footprint Framework..... 217

6.3 Exergy as a Regenerative Pathway for Restoring Soils..... 218

6.4 Quantum Soil Science as a Future Pathway for Accelerated Regeneration 219

6.5 A Holistic Vision for an Adaptive Soil Systems Framework..... 220

6.6 Future Directions..... 220

6.6 References 223

Chapter 1: Introduction

1.1 Overview

Soil is a complex system that provides essential services to humanity. However, since the Industrial Revolution, accelerated soil degradation, especially erosion, has threatened soil sustainability. Degradation of soil is often cumulative, latent, and challenging to reverse, necessitating proactive and systematic approaches to monitoring, mitigation, and restoration (Hussain et al., 2021; Blanco & Lal, 2023). The concept of soil security has the potential to provide a structured, comprehensive response to these challenges (McBratney et al., 2014). However, while it is gaining attention, the soil security concept is still evolving and requires metrics to assess soil conditions, as well as regenerative pathways to restore degraded soils. This thesis presents novel approaches to enhancing soil security through innovative metrics and regenerative frameworks. It introduces the Erosion Risk Capability (ERC), which integrates soil's intrinsic capacity to resist and mitigate erosion, providing a more practical measure of soil vulnerability, this framework is applied across NSW. The Soil Erosion Footprint is proposed as a framework to evaluate the interaction between erosion impacts and soil service capacities, applied to NSW.

This thesis also explores methods and develops an initial foundational framework for soil regeneration. Soil regeneration could be defined as the ability of soil to revive itself, recover from disturbances, and rebuild its functions, and deliver its essential services (Nwaogu et al., 2025). An exergy-based model is presented to quantify the energy required to restore soil organic carbon (SOC) in degraded soils. This framework is applied in the Lower Namoi Valley. The thermodynamic approach offers a way to regenerate soils efficiently by focusing restoration efforts where they are most needed, contributing to soil security. It also has several practical implications, such as guiding targeted soil restoration, supporting decision-making for land management practices, and enabling energy-aware soil policies. Taking inspiration from physics, this thesis proposes Quantum Soil Science as a novel regenerative pathway. It highlights how quantum processes like tunnelling and coherence may enhance soil formation and recovery, especially under degraded or energy-limited conditions. Integrating these mechanisms can support soil security by informing new metrics and targeted soil restoration strategies. Collectively, these novel metrics and regenerative pathways establish a

foundation for future interdisciplinary research and practical soil management strategies.

1.2 The concept of Soil Security and its relevance to reversing soil degradation

Over the past century, the assessment of soil has evolved based on changing societal priorities and scientific advancements (Karlen et al., 2019; Fan et al., 2025). Evidence from geomorphological and soil erosion studies indicates that soil degradation began with the onset of agriculture and intensified with land-use change, particularly under mechanised farming systems (Vanwalleghem et al., 2011; Vanwalleghem et al., 2017). Despite Soil's important role in food security, water security, climate regulation and biodiversity, it is often undervalued and overlooked in global sustainability agendas (Lal et al., 2021; Telo Da Gama, 2023) . Soil degradation is a critical issue alongside climate changes (Mandal & Roy, 2024). Many studies emphasise the severity of soil degradation, and numerous programs have been developed to address it (Hussain et al., 2021) (Albaladejo et al., 2021). Today, soil degradation is no longer seen as an isolated agricultural problem; it is increasingly recognised as a broader planetary issue (Kraamwinkel et al., 2021). It affects climate regulation, ecosystem stability, food security, and contributes to social and disaster-related risks (Kraamwinkel et al., 2021).

Currently, there are several frameworks that focus on soil. Earlier frameworks, such as the USDA's Land Capability Classification and the FAO's Land Evaluation System, primarily classified soils based on their ability to support agricultural uses without degradation (Klingebiel & Montgomery, 1961; FAO Soils Bulletin 32, 1976). As scientific understanding of soils deepened, especially in relation to their ecological roles and societal dependencies, concepts such as soil health, soil quality, soil condition, soil change, soil resilience, soil security and soil ecosystem services came into use (McBratney et al., 2014; Meersmans et al., 2024; Panagos et al., 2025). While these concepts are valuable, they are often narrowly defined and lack the integration of broader social-ecological dimensions within a single framework (Evangelista et al., 2023).

Soil degradation is a continuous process that rarely ends and quantifying how much soil has degraded remains a challenge (Gunawardena, 2022). This is why having a reference

state is essential for assessing soil degradation (Evangelista et al., 2023). Soil health, soil quality, and soil condition frameworks often place less emphasis on defining an explicit reference state (Evangelista et al., 2023). Without it, it is difficult to determine how much soil has changed (Jang et al., 2022) or to evaluate the effectiveness of restoration efforts.

The concept of soil security provides a comprehensive framework to address this gap by assessing soil in multiple dimensions - capacity, condition, capital, connectivity and codification, all of which are essential for sustainable soil management (McBratney et al., 2014). Among these, capacity and condition are influential dimensions for assessing soil degradation. Capacity refers to the soil's inherent ability to resist degradation, while condition refers to the current state of soil due to degradation and management deviations from the reference state, indicating whether the soil is in good or poor condition (Evangelista et al., 2023). Both dimensions contributed to a structured, reference-based framework for systematically assessing soil degradation and guiding appropriate management responses. Within this thesis, capacity is treated as the soil's intrinsic potential under its reference state, while condition reflects its current state under management and disturbance. Soil degradation primarily reduces condition relative to capacity. Only under severe and potentially irreversible changes such as substantial topsoil loss or structural collapse might the inherent capacity itself shift, representing a system-level transition or tipping point.

In practical terms, degradation is expressed as the widening gap between inherent capacity and current condition. For example, a soil with high clay content and a deep topsoil may initially resit erosion; however, repeated disturbance and vegetation removal can progressively weaken its structure and infiltration, increasing erosion susceptibility. In contrast, appropriate management can maintain or enhance soil conditions relative to capacity, emphasising the role of cumulative disturbance alongside soil type.

1.3 Soil security and soil erosion assessment

Securing soil and assessing soil degradation are crucial processes. It quantifies how well soils support food production, water filtration, climate regulation, and biodiversity, while also guiding sustainable management and broader policy decisions (Kopittke et al., 2025). Historically, soil degradation assessment evolved from land capability classification and visual surveys (Oluwatosin et al., 2006; Kapalanga, 2008). These approaches classified land based on its suitability for agriculture, using a ranking system where a higher rank indicated a greater risk of degradation. Land use was recommended based on capability to prevent inappropriate use and avoid degradation (Adams & Engert, 2023). With the recent advancement in assessing dynamic soil conditions, more advanced approaches have emerged, shifting from static evaluations to frameworks such as Soil Health and Soil Quality assessments (Oluwatosin et al., 2006; Lal, 2015; Tesfahunegn, 2014;Mandal et al., 2021).

The Soil Management Assessment Framework (SMAF), for example, quantifies soil quality or health by integrating biological, chemical, and physical indicators into a composite index (Andrews et al., 2004; Hu et al., 2025).

Globally, most soil erosion by water assessments have focused on the rate of soil erosion - meaning the amount of soil lost from a particular location (Borrelli et al., 2021). The most widely used model for this is the RUSLE model, which provides valuable information; however, it does not account for redeposited soil (Bui et al., 2011), which is important for soil condition. Across the literature, it is well emphasised that soil erosion negatively affects soil health and quality (Lal, 1993; Turner et al., 2018).

Many studies within soil health/quality framework (SMAF) assess soil erosion by computing a Soil Quality Index (SQI) using various chemical and physical indicators combined into a single score (Nosrati & Collins, 2019; Vaca et al., 2023). While this approach provides useful information on overall soil degradation, it is difficult to attribute changes in SQI specifically to soil erosion, because SQI integrates multiple degradation processes. For example, (Fang et al., 2024) found that soil erosion explained only a small portion of the variability in SQI, with an adjusted R^2 value of 0.28 (SQI-TDS) and 0.33 (SQI-

MDS). This suggests that the SQI may not fully capture the effects of erosion and that other degradation processes could also play a role (Sione et al., 2017).

The soil security assessment framework aims to evaluate soil based on three roles: soil functions, soil services, and threats to soil. Each role is further assessed across the five dimensions of soil security: capacity, condition, capital, connectivity, and codification. Threats to soil represent various forms of soil degradation and are often evaluated in terms of soil vulnerability (Evangelista et al., 2023). While the proposed framework has the potential to be applied to soil functions and services (Francos et al., 2025;Evangelista et al., 2025), it is still evolving and has not yet been fully implemented to address specific threats. It could be argued that cropping soil receiving external input and generating consistent economic returns represents a stable system. However, from a soil security perspective, short-term productivity does not necessarily indicate long-term stability. It may temporarily mask declining soil condition, increasing dependence on management while reducing resilience to future disturbances. Distinguishing between apparent productivity and underlying soil security is therefore essential. The framework identifies several key threats, many of which directly impact soil functions and services (Evangelista et al., 2023). Among them, accelerated soil erosion by water is particularly significant due to its rapid impact - it removes nutrient-rich topsoil, reducing soil fertility and crop yield, and leading to substantial economic losses and wider socio-economic consequences (Favis-Mortlock, 2020; Hossini et al., 2022; Borrelli et al., 2022). As soil erosion is a global issue, there are increasing international efforts, including the UN-led Global Soil Erosion Assessment (GSERmap), which aims to support erosion monitoring, mitigating, and policy development (Borrelli et al., 2021).

Soil erosion is induced by both natural and anthropogenic processes, which are widespread across both space and time (Poesen, 2018). These processes impact both the capacity and condition of soil over temporal and spatial scales. However, current methods face challenges in understanding both natural and anthropogenic erosion processes, as well as in assessing capacity and condition simultaneously across these dimensions (Nosrati, 2013; Mandal et al., 2021). To evaluate changes in soil functions and service caused by anthropogenic pressures, studies have distinguished between two types of soil: Genosoil and Phenosoil (Francos et al., 2024). These terms were initially

developed to assess how long-term land management affects soil condition and capability (Droogers & Bouma, 1997; Rossiter & Bouma, 2018) . Genosoil refers to the natural, less disturbed state of the soil, primarily influenced by natural processes, whereas Phenosoil represents current soil conditions affected by both natural and anthropogenic pressure (Román Dobarco et al., 2023). While this concept has been applied to the assessment of soil functions and services (Francos et al., 2024; Evangelista et al., 2025), its use in evaluating threats to soil - particularly soil erosion - within the soil security assessment framework remains limited and requires further exploration. Existing studies often examine soil condition or erosion rates independently, but lack a unified measure that captures the gap between inherent capacity and the current degraded state. This gap can be referred to as *erosion risk capability*, which serves as a metric to quantify how vulnerable the soil is to future erosion. The rationale and further details are provided in Chapter 3.

1.4 Soil footprint simple indicator for Soil Security Assessment

Soil degradation is driven by diverse factors and poses a significant threat to soil sustainability, undermining the capacity of soils to regenerate over time (Ludwig et al., 2018). Soil sustainability refers to the maintenance of soil functional integrity, while resilience is its ability to recover structure and function after disturbance (Ludwig et al., 2018). When resilience persists over time, enabling soils to rebuild structure and organic matter after disturbance (De Andrade Bonetti et al., 2017), it results in sustainable soil formation, where formation keeps pace with or exceeds degradation. Sustainable soil formation can be understood as the dynamic balance between soil forming (pedogenic) processes including biological, chemical, and physical processes and processes of degradation and loss (Bayata, 2024; Dror et al., 2022). It represents the foundation of soil resilience - enabling continuous regeneration and the sustained provision of functions and services essential for the planetary system. However, this balance is increasingly disrupted by accelerated erosion, anthropogenic pressures, and extreme climate events (Ludwig et al., 2018; García-Ruiz et al., 2013). When soil formation becomes unsustainable due to these threats, it can create a persistent imbalance between degradation processes and regeneration capacity, disrupting soil functions, services and mitigation capability (Lal, 2015; Abubakar et al., 2024) . The importance of sustainable

soil formation has received limited attention in soil assessment frameworks related to soil health, quality, and soil security, and indicators that reflect this regenerative balance are lacking (Rinot et al., 2019; Evangelista et al., 2023; Fan et al., 2025).

The Soil security concept, aimed at securing soil, involves the assessment of multiple dimensions and requires translating complex scientific assessments into simpler, more communicable terms (García-Gamero et al., 2024). Similar to the water security framework – which, despite its complexity, introduced the simple indicator of the water footprint (measuring how much water is consumed or polluted across products, processes, and regions) (Srinivasan et al., 2017; Varis et al., 2017; Ercin & Hoekstra, 2014) and the carbon footprint (used to assess the pressure of human activities) (Pandey et al., 2011). A comparable approach is needed for soil (García-Gamero et al., 2024): a quantifiable and communicable indicator that connects soil degradation to soil service. Such an indicator can help determine whether there is a balance between threats and the soil's capacity to provide essential functions and services. This balance is critical for supporting sustainable soil formation and identifying where targeted interventions are most needed.

The soil footprint concept, recently introduced by García-Gamero et al., 2024, proposes a simple indicator for soil security that relates to its dimensions. They define soil footprints as the ratio of soil loss to crop productivity, representing how much soil service is compromised by a specific threat to soil (i.e., soil erosion). However, while this formulation marks an important step forward; it falls short of fully meeting the need outlined above. Specifically, it omits other soil degradation processes and soil services, such as salinization, contamination, carbon storage, water filtration, and nutrient cycling and soil's inherent ability to buffer or recover from degradation. There is a need for a soil footprint framework that expands the concept in both definition and application. Moreover, a general calculation framework that can flexibly apply the concept across regions and contexts is still lacking.

1.5 Energy-Based Approaches in Soil Restoration

Globally, soil degradation is already underway due to various factors such as unsustainable management, extreme events, climate change, overgrazing, and the decline of soil functions and services (Farooqi et al., 2024; Rhodes, 2014). While preventing further degradation is important, restoration is essential to recover lost functions and resilience, and to correct the imbalance between degradation and soil services and functions (Jiba et al., 2024; Raupp et al., 2024). This enhances soil's contribution to global sustainability goals (Lal et al., 2021). Furthermore, regenerative methods provide an actionable pathway to reverse degradation and rebuild essential soil functions, making them fundamental to achieving soil security (Das et al., 2025; Kumar et al., 2025).

Several studies have mentioned and practice implementing the restoration of soil, through restoration of soil health and quality (Macheroum et al., 2025; Raupp et al., 2024). The most widely applied methods for restoring degraded soil, such as composting, reduced tillage, cover cropping and agroecological design, play a vital role in rebuilding degraded soils. More often, an integrated approach combining several of these methods is most effective (Cerecetto et al., 2021; Khangura et al., 2023). However, the specific methods chosen for soil restoration depend on the type and severity of degradation, the local climate, soil type, and the desired land use (e.g., agriculture, ecological restoration) (Bhalerao & Jain, 2025; Zhao et al., 2005). And studies note that restoring Soil Organic Carbon is often chosen as the main indicator for restoration since SOC influences most of all other soil properties (Eze et al., 2023). The restoration is energy-intensive; to increase SOC in degraded soil, we need external inputs such as management, biomass incorporation, organic amendments, and fertilisers (Larney & Angers, 2012).

Most studies mainly focus on SOC mapping and losses across different land uses and climates. However, there is limited emphasis on the energy requirements for restoring SOC (Angelopoulou et al., 2019; Minasny et al., 2024; Wendt & Hauser, 2013). It is important to understand how much energy investment is needed to prioritise high-leverage areas where restoration yields the greatest return. This supports better national and local planning, especially where funds and labour are limited (Mu et al., 2022; Liu et al., 2025).

The thermodynamic concept may provide an alternative perspective for studying the restoration of degraded soil to its natural state. In the literature, most studies have advanced the use of thermodynamic concepts to study SOC, mainly in understanding microbial efficiency, decomposition rates, SOC quality, carbon turnover modelling, and SOC temperature response across various soil types and climates (Barros, 2021; Kästner et al., 2024; Bhanja et al., 2019). However, there are limited studies that apply these concepts for restoration modelling, translating thermodynamic insights into actionable frameworks for quantifying the energy required to restore degraded SOC to its natural state.

Within the broader thermodynamic context, Gibbs free energy, enthalpy, and entropy are more frequently adopted in SOC studies for analysing energy transformations (Kästner, et al., 2024; Barros, 2021). However, these concepts are often confined to specific conditions, such as reaction spontaneity or total system energy, and are limited in their application across different systems (Stoner, 2000). In soil restoration, restoring SOC in degraded soil often requires external energy input (such as organic amendments, fertilisers, cover crops) (Khan et al., 2024) . One concept, exergy, refers to the maximum useful work that a system can perform relative to a defined reference state. Exergy more adaptable and system-wide accounting of usable energy and has been widely adopted in fields such as ecology, industrial systems, and ecosystem health metrics (Silow & Mokry, 2010; Bilgen & Sarıkaya, 2015). However, its application remains limited in the field of SOC restoration.

Utilising the exergy concept to model energy demand for restoration may provide a new pathway to secure soil, as soil security depends on the capacity to rebuild degraded soils. It may help support resource-efficient planning by identifying where restoration should be prioritised, where energy costs are lowest, or returns are highest.

1.6. Quantum Pathways to Secure Soil

Soil degradation affects the soil's capacity and condition to provide essential services and functions (Evangelista et al., 2023). It also disrupts the natural process of soil formation, indirectly constraining soil regeneration (Baumhardt et al., 2015). These consequences lead to risks to soil security, which is especially concerning because soil

formation is governed by processes that occur at the molecular scale (Du & Bi, 2025; Kögel-Knabner & Rumpel, 2018). Soil formation fundamentally depends on molecular interactions such as mineral weathering, organic matter decomposition, and microbial activity (Kleber et al., 2021; Newcomb et al., 2017). Any acceleration of its degradation affects these molecular processes.

Soil-forming processes are often modelled using classical principles of physics and chemistry to explain and predict soil processes. For instance, mineral weathering models use the Arrhenius principle, where the mineral dissolution rate is a function of temperature (Brantley, 2008). In the context of soil organic matter decomposition, the Michaelis-Menten equation is used to describe the relationship between reaction velocity and substrate concentration under steady-state conditions (Wang & Allison, 2019). This provides insight into how enzymes facilitate the breakdown of organic matter in soils. Microbial respiration is commonly represented through first-order kinetics (Zhou et al., 2021). However, these classical models often don't represent the real complexity of soils. Studies noted that these models do not explain the unexpectedly rapid or efficient behaviour observed in natural soils, particularly under cold, low-energy, or microscopic conditions (Pot et al., 2021; Vereecken et al., 2016; Yan et al., 2023). Even under carbon limitation and freezing temperatures, microbial communities in alpine and cold ecosystems can maintain enzyme activity, demonstrating a biochemical resilience not readily explained by classical models (Shan et al., 2024).

This suggests the need to explore new concepts and theories to better understand soil processes and improve modelling approaches. One such theory, quantum mechanics, has not been widely explored in soil science. Quantum theory suggests that subatomic particles can tunnel through activation energy barriers rather than fully overcoming them (Schreiner, 2020). This could help explain how soils maintain enzyme activity at low temperatures, where classical models predict minimal or no activity. Quantum principles such as proton tunnelling, electron coherence, and vibrational quantisation have been widely studied in enzymology, molecular biology, and materials science for their ability to enhance reaction efficiency, especially under low-energy constraints (Devault, 1980; Truhlar et al., 2002; Kim et al., 2021). This aspect is discussed in detail in Chapter 5.

These subatomic phenomena are not widely studied in soil science. It is worth investigating whether quantum processes play a role in soil processes. If such processes can be identified, they could inform the design of soil management strategies that focus on the micro-environment to stimulate soil processes and enhance soil formation. This could be one way to look at generative pathways for securing soil.

1.7. Aim & Objectives

The understanding from the previous sections shows that the soil security concept provides a promising assessment framework for evaluating soil degradation, especially soil erosion accelerated by both natural and anthropogenic pressures. However, the operationalisation of soil security is still ongoing, particularly in relation to the development of novel metrics that can quantify threats to soil. In addition, while soil restoration is recognised as essential for securing soils, current approaches provide limited insight into the energetic feasibility and prioritisation of restoration interventions.

The aim of the thesis is to support the operationalisation of soil security by introducing novel metrics and regenerative pathways through the development of new assessment frameworks, an exergy-based restoration model, and the exploration of advanced concepts such as quantum mechanics in looking for new regenerative pathways for soil security. Therefore, this research attempts to present practical tools and conceptual advancements that support soil security under rising anthropogenic pressures.

The specific objective of the thesis is to:

1) Introducing Erosion Risk Capability as a new metric/indicator for Soil erosion Vulnerability by developing a new Capacity-condition Framework (CCF) for calculating Erosion Risk capability across NSW.
2) Introducing a generalised soil footprint metric/indicator for soil security, which accommodates various degradation processes, integrates multiple services, and includes soil mitigation capability. The metric is applied to calculate soil footprint across NSW for one degradation process (soil erosion) and services (available water capacity (AWC) and crop yield).

3) To develop an exergy-based model to quantify the energy demand for SOC restoration in degraded soils to their natural state, providing examples of exergy calculation for different soil types and management.
4) Exploring quantum mechanical principles in soil, such as tunnelling and coherent, and their roles in soil processes such as mineral weathering and enzymatic decomposition. Proposing a conceptual quantum thinking in soil management to design the soil management strategies.

The proposed research fits within the broader context of global policy and sustainability goals. The proposed metrics and frameworks align with and support global sustainability efforts, particularly the Sustainable Development Goals (SDGs). They contribute to SDG 15 (Life on Land) and its target on Land Degradation Neutrality (LDN) by providing quantitative tools to monitor soil degradation, restoration feasibility, and ecosystem service loss.

The ERCI provides spatial assessment of soil erosion vulnerability, while the soil footprint framework offers flexible and comprehensive monitoring of soil degradation, including threats such as salinity, compaction, and acidification. The exergy-based restoration model supports strategic planning for restoration by optimising energy inputs for regenerative impact. These tools not only address scientific gaps but also offer actionable insights for policymakers, land managers, and stakeholders.

1.8. References

Abubakar, G. A., Gabasawa, A. I., Sale, L. A., & Obemah, D. N. (2024). Advantages and Disadvantages of Soil Regeneration. In S. A. Aransiola, B. R. Babaniyi, A. B. Aransiola, & N. R. Maddela (Eds.), Prospects for Soil Regeneration and Its Impact on Environmental Protection (pp. 297–305). Springer Nature Switzerland. https://doi.org/10.1007/978-3-031-53270-2_13

Adams, V. M., & Engert, J. E. (2023). Australian agricultural resources: A national scale land capability map. Data in Brief, 46, 108852. https://doi.org/10.1016/j.dib.2022.108852

Albaladejo, J., Díaz-Pereira, E., & De Vente, J. (2021). Eco-Holistic Soil Conservation to support Land Degradation Neutrality and the Sustainable Development Goals. CATENA, 196, 104823. https://doi.org/10.1016/j.catena.2020.104823

Andrews, S. S., Karlen, D. L., & Cambardella, C. A. (2004). The Soil Management Assessment Framework: A Quantitative Soil Quality Evaluation Method. Soil Science Society of America Journal, 68(6), 1945–1962. https://doi.org/10.2136/sssaj2004.1945

Angelopoulou, T., Tziolas, N., Balafoutis, A., Zalidis, G., & Bochtis, D. (2019). Remote Sensing Techniques for Soil Organic Carbon Estimation: A Review. Remote Sensing, 11(6), 676. https://doi.org/10.3390/rs11060676

Barros, N. (2021). Thermodynamics of Soil Microbial Metabolism: Applications and Functions. Applied Sciences, 11(11), 4962. https://doi.org/10.3390/app11114962

Baumhardt, R., Stewart, B., & Sainju, U. (2015). North American Soil Degradation: Processes, Practices, and Mitigating Strategies. Sustainability, 7(3), 2936–2960. https://doi.org/10.3390/su7032936

Bayata, A. (2024). Soil Degradation: Contributing Factors and Extensive Impacts on Agricultural Practices and Ecological Systems- Systematic Review. Journal of Agriculture and Environmental Sciences, 13.

Bhalerao, A., & Jain, A. (2025). Soil Restoration: Methods and Challenges. In J. A. Parray (Ed.), Soil and Land Use Change (pp. 45–53). Springer Nature Switzerland. https://doi.org/10.1007/978-3-031-93075-1_5

Bhanja, S. N., Wang, J., Shrestha, N. K., & Zhang, X. (2019). Microbial kinetics and thermodynamic (MKT) processes for soil organic matter decomposition and dynamic oxidation-reduction potential: Model descriptions and applications to soil N2O emissions. Environmental Pollution, 247, 812–823. https://doi.org/10.1016/j.envpol.2019.01.062

Blanco, H., & Lal, R. (2023). Restoration and Management of Degraded Soils. In H. Blanco & R. Lal, Soil Conservation and Management (pp. 331–361). Springer Nature Switzerland. https://doi.org/10.1007/978-3-031-30341-8_14

Bilgen, S., & Sarıkaya, İ. (2015). Exergy for environment, ecology and sustainable development. Renewable and Sustainable Energy Reviews, 51, 1115–1131. https://doi.org/10.1016/j.rser.2015.07.015

Borrelli, P., Alewell, C., Alvarez, P., Anache, J. A. A., Baartman, J., Ballabio, C., Bezak, N., Biddoccu, M., Cerdà, A., Chalise, D., Chen, S., Chen, W., De Girolamo, A. M.,

Gessesse, G. D., Deumlich, D., Diodato, N., Efthimiou, N., Erpul, G., Fiener, P., … Panagos, P. (2021). Soil erosion modelling: A global review and statistical analysis. Science of The Total Environment, 780, 146494. https://doi.org/10.1016/j.scitotenv.2021.146494

Borrelli, P., Ballabio, C., Yang, J. E., Robinson, D. A., & Panagos, P. (2022). GloSEM: High-resolution global estimates of present and future soil displacement in croplands by water erosion. Scientific Data, 9(1), 406. https://doi.org/10.1038/s41597-022-01489-x

Brantley, S. L. (2008). Kinetics of Mineral Dissolution. In S. L. Brantley, J. D. Kubicki, & A. F. White (Eds.), Kinetics of Water-Rock Interaction (pp. 151–210). Springer New York. https://doi.org/10.1007/978-0-387-73563-4_5

Bui, E. N., Hancock, G. J., & Wilkinson, S. N. (2011). 'Tolerable' hillslope soil erosion rates in Australia: Linking science and policy. Agriculture, Ecosystems & Environment, 144(1), 136–149. https://doi.org/10.1016/j.agee.2011.07.022

Cao, H., Liu, J., Ma, S., Wu, X., Fu, Y., & Gao, Y. (2024). Selection of Suitable Organic Amendments to Balance Agricultural Economic Benefits and Carbon Sequestration. Plants, 13(17), 2428. https://doi.org/10.3390/plants13172428

Cerecetto, V., Smalla, K., Nesme, J., Garaycochea, S., Fresia, P., Sørensen, S. J., Babin, D., & Leoni, C. (2021). Reduced tillage, cover crops and organic amendments affect soil microbiota and improve soil health in Uruguayan vegetable farming systems. FEMS Microbiology Ecology, 97(3), fiab023. https://doi.org/10.1093/femsec/fiab023

Das, S., Dutta, S., Roy Choudhury, M., Garai, S., Mukherjee, S., Sengupta, S., Jana, S., Dey, S., Dhar, A., Dutta, S., & Awasthi, A. (2025). Regenerating rural soil and ecosystems: A 15-year systematic review of emerging methods and technologies. Science of The Total Environment, 990, 179926. https://doi.org/10.1016/j.scitotenv.2025.179926

De Andrade Bonetti, J., Anghinoni, I., De Moraes, M. T., & Fink, J. R. (2017). Resilience of soils with different texture, mineralogy and organic matter under long-term conservation systems. Soil and Tillage Research, 174, 104–112. https://doi.org/10.1016/j.still.2017.06.008

Droogers, P., & Bouma, J. (1997). Soil Survey Input in Exploratory Modeling of Sustainable Soil Management Practices. Soil Science Society of America Journal, 61(6), 1704–1710. https://doi.org/10.2136/sssaj1997.03615995006100060023x

Dror, I., Yaron, B., & Berkowitz, B. (2022). The Human Impact on All Soil-Forming Factors during the Anthropocene. ACS Environmental Au, 2(1), 11–19. https://doi.org/10.1021/acsenvironau.1c00010

Du, H., & Bi, J. (2025). The formation mechanisms, stability, and dynamic effects of soil aggregates under specific environments (0). Resources Economics Research Board. https://doi.org/10.50908/grb.4.0_445

Ercin, A. E., & Hoekstra, A. Y. (2014). Water footprint scenarios for 2050: A global analysis. Environment International, 64, 71–82. https://doi.org/10.1016/j.envint.2013.11.019

Evangelista, S. J., Field, D. J., McBratney, A. B., Minasny, B., Ng, W., Padarian, J., Román Dobarco, M., & Wadoux, A. M. J.-C. (2023). A proposal for the assessment of soil security: Soil functions, soil services and threats to soil. Soil Security, 10, 100086. https://doi.org/10.1016/j.soisec.2023.100086

Evangelista, S. J., McBratney, Alex., & Minasny, B. (2025). Approaches to assessing soil nutrient cycling condition: A case study in the Hunter valley Wine district. Soil Security, 20, 100198. https://doi.org/10.1016/j.soisec.2025.100198

Eze, S., Magilton, M., Magnone, D., Varga, S., Gould, I., Mercer, T. G., & Goddard, M. R. (2023). Meta-analysis of global soil data identifies robust indicators for short-term changes in soil organic carbon stock following land use change. Science of The Total Environment, 860, 160484. https://doi.org/10.1016/j.scitotenv.2022.160484

Fan, Y., Zhang, C., Hu, W., Khan, K. S., Zhao, Y., & Huang, B. (2025). Development of soil quality assessment framework: A comprehensive review of indicators, functions, and approaches. Ecological Indicators, 172, 113272. https://doi.org/10.1016/j.ecolind.2025.113272

Fang, H., Zhai, Y., & Li, C. (2024). Evaluating the impact of soil erosion on soil quality in an agricultural land, northeastern China. Scientific Reports, 14(1), 15629. https://doi.org/10.1038/s41598-024-65646-5

Farooqi, Z. U. R., Sohail, M., Alserae, H., Qadir, A. A., Hussain, T., Ilic, P., Riaz, S., & Zafar, Z. (2024). Management of Soil Degradation: A Comprehensive Approach for Combating Soil Degradation, Food Insecurity, and Climate Change. In A. Banerjee, M. K. Jhariya, A. Raj, & T. Mechergui (Eds.), Ecosystem Management (1st ed., pp. 55–78). Wiley. https://doi.org/10.1002/9781394231249.ch3

Favis-Mortlock, D. (2020). Erosion by Water: Accelerated. In B. D. Fath, S. E. Jørgensen, & M. Cole (Eds.), Managing Soils and Terrestrial Systems (2nd ed., pp. 25–33). CRC Press. https://doi.org/10.1201/9780429346255-5

Francos, N., McBratney, A. B., Field, D. J., Minasny, B., Pachon, J. C., Padarian, J., Hunakunti, A., Ng, W., Evangelista, S. J., & O'Donoghue, T. (2024). Valuing and integrating soil roles in assessing the capital dimension of soil security: An Australian case study. Soil Security, 16, 100141. https://doi.org/10.1016/j.soisec.2024.100141

Francos, N., Ng, W., Evangelista, S., Styc, Q., Sharififar, A., Pachon, J., & McBratney, A. (2025). Assessing Soil Condition and Capacity Using the Global Pedogenon Map Within the Americas' Horse Latitudes. CATENA, 259, 109372. https://doi.org/10.1016/j.catena.2025.109372

García-Gamero, V., Vanwalleghem, T., & Peñuela, A. (2024). Soil footprint: A simple indicator to communicate and quantify soil security. Soil Security, 16, 100156. https://doi.org/10.1016/j.soisec.2024.100156

García-Ruiz, J. M., Nadal-Romero, E., Lana-Renault, N., & Beguería, S. (2013). Erosion in Mediterranean landscapes: Changes and future challenges. Geomorphology, 198, 20–36. https://doi.org/10.1016/j.geomorph.2013.05.023

Gunawardena, U. A. D. P. (2022). Soil Degradation: Causes, Consequences, and Analytical Tools. In P. Panwar, G. Shukla, J. A. Bhat, & S. Chakravarty (Eds.), Land Degradation Neutrality: Achieving SDG 15 by Forest Management (pp. 155–170). Springer Nature Singapore. https://doi.org/10.1007/978-981-19-5478-8_9

Hossini, H., Karimi, H., Mustafa, Y. T., & Al-Quraishi, A. M. F. (2022). Role of Effective Factors on Soil Erosion and Land Degradation: A Review. In A. M. F. Al-Quraishi, Y. T. Mustafa, & A. M. Negm (Eds.), Environmental Degradation in Asia (pp. 221–235). Springer International Publishing. https://doi.org/10.1007/978-3-031-12112-8_11

Hu, X., Machmuller, M. B., Blecker, S. W., Buchanan, C. M., Aksland, I. B., Firth, A. G., & Ippolito, J. A. (2025). Comparing the Soil Management Assessment Framework to the Haney Soil Health Test Across Managed Agroecosystems. Agronomy, 15(3), 643. https://doi.org/10.3390/agronomy15030643

Hussain, M. I., Abideen, Z., & Qureshi, A. S. (2021). Soil Degradation, Resilience, Restoration and Sustainable Use. In E. Lichtfouse (Ed.), Sustainable Agriculture Reviews 52 (Vol. 52, pp. 335–365). Springer International Publishing. https://doi.org/10.1007/978-3-030-73245-5_10

Jang, H. J., Román Dobarco, M., Minasny, B., McBratney, A., & Jones, E. (2022). Developing and testing of pedogenons in the lower Namoi valley, NSW, Australia. Geoderma, 428, 116182. https://doi.org/10.1016/j.geoderma.2022.116182

Jiba, W., Manyevere, A., & Mashamaite, C. V. (2024). The Impact of Ecological Restoration on Soil Quality in Humid Region Forest Habitats: A Systematic Review. Forests, 15(11), 1941. https://doi.org/10.3390/f15111941

Kapalanga, T. S. (2008). A Review of Land Degradation Assessment Methods.

Karlen, D. L., Veum, K. S., Sudduth, K. A., Obrycki, J. F., & Nunes, M. R. (2019). Soil health assessment: Past accomplishments, current activities, and future opportunities. Soil and Tillage Research, 195, 104365. https://doi.org/10.1016/j.still.2019.104365

Kästner, M., Maskow, T., Miltner, A., Lorenz, M., & Thiele-Bruhn, S. (2024). Assessing energy fluxes and carbon use in soil as controlled by microbial activity—A thermodynamic perspective A perspective paper. Soil Biology and Biochemistry, 193, 109403. https://doi.org/10.1016/j.soilbio.2024.109403

Kästner, M., Maskow, T., Miltner, A., Lorenz, M., Thiele-Bruhn, S., Bölscher, T., Blagodatsky, S., Streck, T., Pagel, H., & Blagodatskaya, E. (2024). Gibbs energy or enthalpy—What is relevant for microbial C-turnover in soils? Global Change Biology, 30(2), e17183. https://doi.org/10.1111/gcb.17183

Khan, M. T., Aleinikovienė, J., & Butkevičienė, L.-M. (2024). Innovative Organic Fertilizers and Cover Crops: Perspectives for Sustainable Agriculture in the Era of Climate Change and Organic Agriculture. Agronomy, 14(12), 2871. https://doi.org/10.3390/agronomy14122871

Khangura, R., Ferris, D., Wagg, C., & Bowyer, J. (2023). Regenerative Agriculture—A Literature Review on the Practices and Mechanisms Used to Improve Soil Health. Sustainability, 15(3), 2338. https://doi.org/10.3390/su15032338

Kleber, M., Bourg, I. C., Coward, E. K., Hansel, C. M., Myneni, S. C. B., & Nunan, N. (2021). Dynamic interactions at the mineral–organic matter interface. Nature Reviews Earth & Environment, 2(6), 402–421. https://doi.org/10.1038/s43017-021-00162-y

Kögel-Knabner, I., & Rumpel, C. (2018). Advances in Molecular Approaches for Understanding Soil Organic Matter Composition, Origin, and Turnover: A Historical Overview. In Advances in Agronomy (Vol. 149, pp. 1–48). Elsevier. https://doi.org/10.1016/bs.agron.2018.01.003

Kopittke, P. M., Harper, S. M., Asio, L. G., Asio, V. B., Batalon, J. T., Batuigas, A. M. T., Gonzaga, A. B., Gonzaga, N. R., De Guzman, M. T. L., Lumanao, D. M., McKenna, B. A., Soyon, G. B., Vergara, J. R. M., & Sanchez, P. B. (2025). Soil degradation: An

integrated model of the causes and drivers. International Soil and Water Conservation Research, 13(4), 744–755. https://doi.org/10.1016/j.iswcr.2025.07.010

Kraamwinkel, C. T., Beaulieu, A., Dias, T., & Howison, R. A. (2021). Planetary limits to soil degradation. Communications Earth & Environment, 2(1), 249. https://doi.org/10.1038/s43247-021-00323-3

Kumar, A., Antoniella, G., Blasi, E., & Chiti, T. (2025). Recent advances in regenerative sustainable agricultural strategies for managing soil carbon and mitigating climate change consequences. CATENA, 258, 109208. https://doi.org/10.1016/j.catena.2025.109208

Lal, R. (1993). Tillage effects on soil degradation, soil resilience, soil quality, and sustainability. Soil and Tillage Research, 27(1–4), 1–8. https://doi.org/10.1016/0167-1987(93)90059-X

Lal, R. (2015). Restoring Soil Quality to Mitigate Soil Degradation. Sustainability, 7(5), 5875–5895. https://doi.org/10.3390/su7055875

Lal, R., Bouma, J., Brevik, E., Dawson, L., Field, D. J., Glaser, B., Hatano, R., Hartemink, A. E., Kosaki, T., Lascelles, B., Monger, C., Muggler, C., Ndzana, G. M., Norra, S., Pan, X., Paradelo, R., Reyes-Sánchez, L. B., Sandén, T., Singh, B. R., … Zhang, J. (2021). Soils and sustainable development goals of the United Nations: An International Union of Soil Sciences perspective. Geoderma Regional, 25, e00398. https://doi.org/10.1016/j.geodrs.2021.e00398

Larney, F. J., & Angers, D. A. (2012). The role of organic amendments in soil reclamation: A review. Canadian Journal of Soil Science, 92(1), 19–38. https://doi.org/10.4141/cjss2010-064

Liu, Y., Zhang, C., Xie, M., & Xie, J. (2025). Optimal ecological restoration strategy development based on value-cost trade-offs. Global Ecology and Conservation, 58, e03500. https://doi.org/10.1016/j.gecco.2025.e03500

Ludwig, M., Wilmes, P., & Schrader, S. (2018). Measuring soil sustainability via soil resilience. Science of The Total Environment, 626, 1484–1493. https://doi.org/10.1016/j.scitotenv.2017.10.043

Macheroum, A., Sayada, N., & Chenchouni, H. (2025). Restoration of soil quality and improvement of physicochemical properties through grazing exclusion in arid and semi-arid rangelands. CATENA, 249, 108646. https://doi.org/10.1016/j.catena.2024.108646

Mandal, D., Chandrakala, M., Alam, N. M., Roy, T., & Mandal, U. (2021). Assessment of soil quality and productivity in different phases of soil erosion with the focus on land degradation neutrality in tropical humid region of India. CATENA, 204, 105440. https://doi.org/10.1016/j.catena.2021.105440

Mandal, D., & Roy, T. (2024). Climate Change Impact on Soil Erosion and Land Degradation. In H. Pathak, D. Chatterjee, S. Saha, & B. Das (Eds.), Climate Change Impacts on Soil-Plant-Atmosphere Continuum (Vol. 78, pp. 139–161). Springer Nature Singapore. https://doi.org/10.1007/978-981-99-7935-6_5

McBratney, A., Field, D. J., & Koch, A. (2014). The dimensions of soil security. Geoderma, 213, 203–213. https://doi.org/10.1016/j.geoderma.2013.08.013

Meersmans, J., Colinet, G., & Negassa, W. (2024). Editorial: Soil health, functions, and ecosystem services: insights into soil parameters and methods of integration. Frontiers in Environmental Science, 12, 1358548. https://doi.org/10.3389/fenvs.2024.1358548

Minasny, B., Bandai, T., Ghezzehei, T. A., Huang, Y.-C., Ma, Y., McBratney, A. B., Ng, W., Norouzi, S., Padarian, J., Rudiyanto, Sharififar, A., Styc, Q., & Widyastuti, M. (2024). Soil Science-Informed Machine Learning. Geoderma, 452, 117094. https://doi.org/10.1016/j.geoderma.2024.117094

Mu, Y., Guo, Y., Li, X., Li, P., Bai, J., Linke, S., & Cui, B. (2022). Cost-effective integrated conservation and restoration priorities by trading off multiple ecosystem services. Journal of Environmental Management, 320, 115915. https://doi.org/10.1016/j.jenvman.2022.115915

Newcomb, C. J., Qafoku, N. P., Grate, J. W., Bailey, V. L., & De Yoreo, J. J. (2017). Developing a molecular picture of soil organic matter–mineral interactions by quantifying organo–mineral binding. Nature Communications, 8(1), 396. https://doi.org/10.1038/s41467-017-00407-9

Nosrati, K. (2013). Assessing soil quality indicator under different land use and soil erosion using multivariate statistical techniques. Environmental Monitoring and Assessment, 185(4), 2895–2907. https://doi.org/10.1007/s10661-012-2758-y

Nosrati, K., & Collins, A. L. (2019). A soil quality index for evaluation of degradation under land use and soil erosion categories in a small mountainous catchment, Iran. Journal of Mountain Science, 16(11), 2577–2590. https://doi.org/10.1007/s11629-019-5567-8

Oluwatosin, G. A., Adeyolanu, O. D., Ogunkunle, A. O., & Idowu, O. J. (2006). [DE LA CLASIFICACIÓN DEL POTENCIAL A LA CALIDAD DEL SUELO: UNA EVALUACIÓN].

Panagos, P., Orgiazzi, A., Lugato, E., Vandenesch, G., Thannberger, L., Neff, J. C., Reijneveld, A., Mathijs, E., Chapot, P., Guerrini, S., Štyriaková, D., Kremers, J., Martin, P., Van Der Tol, R., Burgeon, V., Kalimeri, E., & Van Eynde, E. (2025). Healthy soils as a booster to EU competitiveness. Land Use Policy, 158, 107755. https://doi.org/10.1016/j.landusepol.2025.107755

Pandey, D., Agrawal, M., & Pandey, J. S. (2011). Carbon footprint: Current methods of estimation. Environmental Monitoring and Assessment, 178(1–4), 135–160. https://doi.org/10.1007/s10661-010-1678-y

Poesen, J. (2018). Soil erosion in the Anthropocene: Research needs. Earth Surface Processes and Landforms, 43(1), 64–84. https://doi.org/10.1002/esp.4250

Pot, V., Gerke, K. M., Ebrahimi, A., Garnier, P., & Baveye, P. C. (2021). Editorial: Microscale Modelling of Soil Processes: Recent Advances, Challenges, and the Path Ahead. Frontiers in Environmental Science, 9, 818038. https://doi.org/10.3389/fenvs.2021.818038

Raupp, P., Carrillo, Y., & Nielsen, U. N. (2024). Soil Health to Enhance Ecological Restoration and Conservation. Journal of Sustainable Agriculture and Environment, 3(4), e70022. https://doi.org/10.1002/sae2.70022

Rhodes, C. J. (2014). Soil Erosion, Climate Change and Global Food Security: Challenges and Strategies. Science Progress, 97(2), 97–153. https://doi.org/10.3184/003685014X13994567941465

Rinot, O., Levy, G. J., Steinberger, Y., Svoray, T., & Eshel, G. (2019). Soil health assessment: A critical review of current methodologies and a proposed new approach. Science of The Total Environment, 648, 1484–1491. https://doi.org/10.1016/j.scitotenv.2018.08.259

Román Dobarco, M., Padarian Campusano, J., McBratney, A. B., Malone, B., & Minasny, B. (2023). Genosoil and phenosoil mapping in continental Australia is essential for soil security. Soil Security, 13, 100108. https://doi.org/10.1016/j.soisec.2023.100108

Rossiter, D. G., & Bouma, J. (2018). A new look at soil phenoforms – Definition, identification, mapping. Geoderma, 314, 113–121. https://doi.org/10.1016/j.geoderma.2017.11.002

Schreiner, P. R. (2020). Quantum Mechanical Tunneling Is Essential to Understanding Chemical Reactivity. Trends in Chemistry, 2(11), 980–989. https://doi.org/10.1016/j.trechm.2020.08.006

Shan, C., Wang, M., Yang, Y., Shen, F., Ji, L., & Yang, L. (2024). Microbial carbon and nitrogen limitation in Larix gmelinii forests along an altitudinal gradient: Evidence from ecoenzymatic stoichiometry and vector analysis. Applied Soil Ecology, 195, 105257. https://doi.org/10.1016/j.apsoil.2023.105257

Silow, E. A., & Mokry, A. V. (2010). Exergy as a Tool for Ecosystem Health Assessment. Entropy, 12(4), 902–925. https://doi.org/10.3390/e12040902

Sione, S. M. J., Wilson, M. G., Lado, M., & González, A. P. (2017). Evaluation of soil degradation produced by rice crop systems in a Vertisol, using a soil quality index. CATENA, 150, 79–86. https://doi.org/10.1016/j.catena.2016.11.011

Srinivasan, V., Konar, M., & Sivapalan, M. (2017). A dynamic framework for water security. Water Security, 1, 12–20. https://doi.org/10.1016/j.wasec.2017.03.001

Stoner, C. D. (2000). Inquiries into the Nature of Free Energy and Entropy in Respect to Biochemical Thermodynamics. Entropy, 2(3), 106–141. https://doi.org/10.3390/e2030106

Telo Da Gama, J. (2023). The Role of Soils in Sustainability, Climate Change, and Ecosystem Services: Challenges and Opportunities. Ecologies, 4(3), 552–567. https://doi.org/10.3390/ecologies4030036

Tesfahunegn, G. B. (2014). Soil Quality Assessment Strategies for Evaluating Soil Degradation in Northern Ethiopia. Applied and Environmental Soil Science, 2014, 1–14. https://doi.org/10.1155/2014/646502

Turner, B. L., Fuhrer, J., Wuellner, M., Menendez, H. M., Dunn, B. H., & Gates, R. (2018). Scientific case studies in land-use driven soil erosion in the central United States: Why soil potential and risk concepts should be included in the principles of soil health. International Soil and Water Conservation Research, 6(1), 63–78. https://doi.org/10.1016/j.iswcr.2017.12.004

Vaca, R., Del Águila, P., Yañez-Ocampo, G., Lugo, J. A., & De La Portilla-López, N. (2023). Soil Quality Assessment in Response to Water Erosion and Mining Activity. Agriculture, 13(7), 1380. https://doi.org/10.3390/agriculture13071380

Varis, O., Keskinen, M., & Kummu, M. (2017). Four dimensions of water security with a case of the indirect role of water in global food security. Water Security, 1, 36–45. https://doi.org/10.1016/j.wasec.2017.06.002

Vanwalleghem, T., Amate, J. I., De Molina, M. G., Fernández, D. S., & Gómez, J. A. (2011). Quantifying the effect of historical soil management on soil erosion rates in Mediterranean olive orchards. Agriculture, Ecosystems & Environment, 142(3–4), 341–351. https://doi.org/10.1016/j.agee.2011.06.003

Vanwalleghem, T., Gómez, J. A., Infante Amate, J., González De Molina, M., Vanderlinden, K., Guzmán, G., Laguna, A., & Giráldez, J. V. (2017). Impact of historical land use and soil management change on soil erosion and agricultural sustainability during the Anthropocene. Anthropocene, 17, 13–29. https://doi.org/10.1016/j.ancene.2017.01.002

Vereecken, H., Schnepf, A., Hopmans, J. W., Javaux, M., Or, D., Roose, T., Vanderborght, J., Young, M. H., Amelung, W., Aitkenhead, M., Allison, S. D., Assouline, S., Baveye, P., Berli, M., Brüggemann, N., Finke, P., Flury, M., Gaiser, T., Govers, G., … Young, I. M. (2016). Modeling Soil Processes: Review, Key Challenges, and New Perspectives. Vadose Zone Journal, 15(5), 1–57. https://doi.org/10.2136/vzj2015.09.0131

Wang, B., & Allison, S. D. (2019). Emergent properties of organic matter decomposition by soil enzymes. Soil Biology and Biochemistry, 136, 107522. https://doi.org/10.1016/j.soilbio.2019.107522

waogu, C., Minasny, B., Field, D. J., & Cherubin, M. R. (2025). Conceptualizing core aspects of circular economy in soil: A critical review and analysis. Critical Reviews in Environmental Science and Technology, 55(11), 805–835. https://doi.org/10.1080/10643389.2025.2454689

Wendt, J. W., & Hauser, S. (2013). An equivalent soil mass procedure for monitoring soil organic carbon in multiple soil layers. European Journal of Soil Science, 64(1), 58–65. https://doi.org/10.1111/ejss.12002

Yan, Z., Wang, Z., Fu, Z., Zhang, Y., Peng, X., & Zheng, J. (2023). Microscale heterogeneity controls macroscopic soil heterotrophic respiration by regulating resource availability and environmental stress. Biogeochemistry, 164(2), 431–449. https://doi.org/10.1007/s10533-023-01044-9

Zhao, W. Z., Xiao, H. L., Liu, Z. M., & Li, J. (2005). Soil degradation and restoration as affected by land use change in the semiarid Bashang area, northern China. CATENA, 59(2), 173–186. https://doi.org/10.1016/j.catena.2004.06.004

Zhou, J., Chen, S., Yan, L., Wang, J., Jiang, M., Liang, J., Zhang, X., & Xia, J. (2021). A Comparison of Linear Conventional and Nonlinear Microbial Models for Simulating Pulse Dynamics of Soil Heterotrophic Respiration in a Semi-Arid Grassland. Journal of Geophysical Research: Biogeosciences, 126(5), e2020JG006120. https://doi.org/10.1029/2020JG006120

Chapter 2: Assessing Soil Erosion Vulnerability Using a Novel Capacity–Condition Framework (CCF): A Case Study from New South Wales, Australia

This chapter is published at:

Anilkumar Hunakunti, Alex B McBratney, Budiman Minasny, Damien J Field (2025) Assessing Soil Erosion Vulnerability Using a Novel Capacity–Condition Framework (CCF): A Case Study from New South Wales, Australia. International Soil and Water Conservation Research, 13(4), 771–794

2.1 Abstract

Soil erosion by water poses a critical threat to long-term soil sustainability. However, challenges remain in capturing how both natural and human-induced erosion processes interact over space and time to influence soil degradation. Current assessment methods often overlook how erosion simultaneously weakens the soil's inherent resistance (capacity) and degrades its current state (condition)-key drivers of long-term vulnerability and two core dimensions of soil security. To address this, we present a Capacity-Condition (CCF) framework, which quantifies erosion vulnerability using the erosion risk capability metric, which captures the gap between a soil's inherent resistance to erosion (capacity) and its erosion-altered state (condition). The framework employs the pedogeonon concept, identifying unique landscape units where the same soil-forming factors operate over time. Within each pedogeonon, two soil states are compared: genosoil (conditions influenced by natural erosion) and phenosoil (present state shaped by both natural and human-accelerated erosion). Capacity is assessed using genosoil indicators (clay ratio and topsoil thickness), and condition is evaluated using the phenosoil/genosoil ratio for the same indicators. Utility functions standardize these indicators on a 0-1 scale, enabling their aggregation into composite scores. When applied to New South Wales (NSW), Australia, the framework identified regions most vulnerable to erosion. Coastal areas and the upper northwest, characterized by intensive dry cropping and grazing on modified pastures, exhibited the highest risk values, indicating a lower capability to withstand future erosion. Conversely, regions with mixed land use-including grazing on native vegetation, intensive horticulture, and irrigated cropping-showed moderate risk, demonstrating the framework's utility for targeted, spatially explicit soil conservation and land management planning. The lowest erosion risk was observed in floodplain and low-disturbance regions, particularly the lower Riverina Murray and parts of far western NSW.

2.2. Introduction

Earth is a dynamic system shaped over geological timescales by processes such as tectonics, weathering, erosion, and volcanism. Soil erosion, a fundamental natural process (Harmon and Doe, 2001; Osman, 2014; Poesen, 2018), plays a key role in landscape evolution and ecological development (Hancock et al., 2019). However, human activities and extreme weather events driven by climate change are significantly accelerating this natural process (García-Ruiz et al., 2013). This widespread phenomenon, primarily driven by water and wind erosion, disrupts entire ecosystems and may even contribute to climate change by impacting the Earth's overall balance (entropy) (Bridges and Oldeman, 1999; Lal, 2001; Pimentel and Kounang, 1998; Webb et al., 2017). The consequences of accelerated erosion extend far beyond the landscape, posing a major threat to interconnected security issues such as soil security, food security, water security, energy security and human security (Lal, 2009; Amundson et al., 2015; Pozza and Field, 2020; Evangelista et al., 2023).

A common approach for assessing soil erosion globally is estimating the rate of soil loss per unit land area (Borrelli et al., 2021). While this provides valuable information, if often overlooks erosion's direct impact on the soil itself. Models like RUSLE estimate total erosion on slopes but don't account for redeposited soil, which means they don't capture the net loss of soil (Bui et al., 2011).

Erosion reduces soil's ability to perform essential functions and provide vital services, making it even more vulnerable to further degradation (Verheijen et al., 2009). Numerous studies and the European Commission recognise soil erosion as a major threat to soil (Verheijen et al., 2009; Evangelista et al., 2023a; European Commission, 2006). Soil erosion is widely recognised as a primary process that negatively affects soil quality, health (Lal, 1993; Turner et al., 2018; Are et al., 2018) and security.

Established methods for assessing soil erosion within these frameworks often involve developing a quantitative soil quality index (SQI) by combining various chemical and physical indicators, both qualitative and quantitative (Karlen and Stott, 2015; Vaca et al., 2023; Herrick et al., 2018; Are et al., 2018; Nosrati and Collins, 2019). Other approaches, such as Ecosystem Function Analysis (EFA), focus on evaluating soil functional

performance (e.g. stability, infiltration, and nutrient cycling) through integrative field-based indicators. However, while these methods provide valuable insights, they can also be resource intensive and may not always capture the full extent of cumulative effects over time, particularly given the challenges in standardization, methodological accessibility, spatial scale issues, and the dynamic nature of soil conditions (Bastida et al., 2008; Gholamhosseinian et al., 2022).

SQIs, though useful for overall soil health/quality assessments, assess erosion indirectly through changes in various soil properties (Nosrati and Collins, 2019; Chen et al., 2023). While this approach is informative, encompassing a wide range of properties into a single score can obscure the specific dynamics of erosion and its distinct impacts on soil condition. Using multiple properties in SQIs can lead to uncertainty about the cause behind the SQI score. For example, a lower SOC value might indicate erosion (Rajan et al., 2010), but it could also be due to an increased decomposition rate or poor land management practices (Lal, 2007; Parihar et al., 2019). Similarly, acidic soil pH may result from processes unrelated to erosion, such as atmospheric deposition (e.g. acid rain) (Matsumoto et al., 2018) or reflect inherent soil characteristics. Reduced nutrient availability could point to erosion (Bashagaluke et al., 2018), but fertilizer use (Smith et al., 2007), or excessive crop uptake could also be contributing factors (Tan et al., 2005). The SQI score combines these changes into a single value, which reflects the combined effects of various factors on the measured soil properties (Mandal et al., 2021) . While it suggests soil degradation, it is difficult to pinpoint erosion as the sole culprit (Fang et al., 2024). Other processes likely contribute to the changes in the measured soil properties (Tesfahunegn, 2014;Sione et al., 2017).

These observations highlight the need for a more direct and separate assessment framework for soil erosion (Fang et al., 2024). Existing challenges in soil erosion assessment include understanding the interactions between natural and anthropogenic erosion process, scaling erosion assessment across space and time (Poesen 2018). As a result, erosion may not only affect the soil's current condition but also reduce its capacity for future resistance to erosion (Evangelista et al., 2023). Currently, approaches to simultaneously assess soil erosion often have limitations in explicitly linking how erosion processes reduce the soil's inherent resistance (capacity) and degrade its present

condition (Nosrati, 2013; Nosrati & Collins, 2019; Mandal et al., 2021; Fang et al., 2024). Recognizing this linkage is important for assessing long-term vulnerability. Addressing these challenges, in this study, we present a framework that addresses both spatial and temporal erosion dynamics by integrating the genosoil–phenosoil concept within a pedogeonon-based assessment approach. This framework leveraging the concept of soil security (McBratney et al., 2014), which involves assessing multiple dimensions of soil function to ensure its long-term sustainability (McBratney et al., 2014; Evangelista et al., 2023). By simultaneously quantifying the soil's inherent resistance (capacity) and its erosion-altered state (condition), this approach provides a more complete measure of erosion vulnerability. By utilising the pedogeonon concept (Román Dobarco et al., 2021), this approach enables standardised assessments over large areas.

A pedogeonon is a distinct space within a landscape defined by consistent soil-forming factors. Within this space, we compare genosoil (representing the natural, less disturbed state of the soil, primarily influenced by natural erosion processes) with phenosoil (reflecting the current soil conditions affected by both natural and accelerated erosion processes driven by human activities) (Huang et al., 2018; Evangelista et al., 2024; Francos et al., 2024). Both genosoil and phenosoil exist within a relative timeframe, but genosoil reflects a past and ongoing less disturbed state. This approach, based on space-for-time substitution (Jang et al., 2022; Lovell et al., 2023), provides:

Consistent Spatial Framework: Ensures that erosion dynamics are assessed within a well-defined area, eliminating variability from comparing different locations (Jang et al., 2023).

Temporal Consistency: By comparing genosoil (indicators) and phenosoil (indicators), the method captures temporal changes in soil due to human impact, providing a clear picture of how soil properties have evolved (Wadoux et al., 2024; Styc et al., 2025).

In our framework, we evaluate two dimensions of soil security capacity and condition to capture both the soil's inherent resistance to erosion and its current, erosion-altered state (Evangelista et al., 2023; Evangelista et al., 2024). "Capacity" refers to the soil's intrinsic ability to resist erosive forces, while "condition" reflects its present state following erosion (Evangelista et al., 2023). Both dimensions are quantified using two key

indicators clay ratio and topsoil thickness with capacity evaluated relative to the genosoil (reference state) and condition assessed using the phenosoil/genosoil ratio (Wadoux et al., 2024; Tang et al., 2024).

Specifically, clay ratio reflects inherent capacity: higher clay content strengthens soil structure and aggregate stability (Jesús Melej et al., 2024), thereby increasing resistance to erosion, while lower clay content indicates reduced capacity and increased vulnerability (Bouyoucos, 1935). Topsoil thickness reflects current condition; thinner topsoil signifies a more degraded state due to past erosion impacting fertility, water retention, and structural integrity (Kaihura et al., 1997) though its remaining thickness still contributes to current capacity. Moreover, changes in clay ratio also reflect condition, with lower ratios signalling erosion-induced degradation (Wischmeier and Mannering, 1969; Toy et al., 2002; Parwada and Van Tol, 2019). Thus, clay ratio and topsoil thickness together capture both capacity and condition. Each indicator is transformed via a utility function to yield normalized scores, from which we calculate average capacity and condition (Andrews et al., 2002 Wadoux et al., 2024; Ng et al., 2024) . By quantifying the gap between these two dimensions, we derive the erosion risk capability metric a direct measure of soil erosion vulnerability. In our framework, a larger gap between inherent capacity and current condition indicates higher erosion risk, and vice versa. The main objective of this study is to develop and test this new framework for assessing soil water erosion risk across a large area, such as New South Wales (NSW).

2.3 Methods

2.3.1. Study area

Spanning 808,444 square kilometres in southeastern Australia, New South Wales (NSW) encompasses extensive agricultural lands that support livestock and the cultivation of crops such as wheat, barley, cotton, and canola, along with a thriving horticultural sector. The region is characterised by diverse ecosystems, including forests, woodlands to heathlands and grasslands, find protection in national parks and reserves (Fig.1).

From the western rangelands with temperatures surpassing 40℃ to ‘alpine’ peaks dipping below 0℃, NSW diverse geography significantly influences its climate and vegetation.

Coastal and central regions experience moderate warmth, with temperatures from 20-30℃ in summers and 8-20°C in winters. Rainfall varies from below 250 mm in the arid far west to 600-1200 mm on the rainy mountain slopes, supporting diverse ecosystems and agricultural activities. Severe erosion was observed in parts of the study area, particularly where prolonged grazing pressure and intense rainfall have led to exposed subsoil, gully formation, and vertical soil loss . Fig. 2 presents a series of representative photographs from the Upper Hunter Valley, located in the eastern part of NSW, where erosion is notably intensified by grazing impacts and concentrated runoff in sloped pasture landscapes.

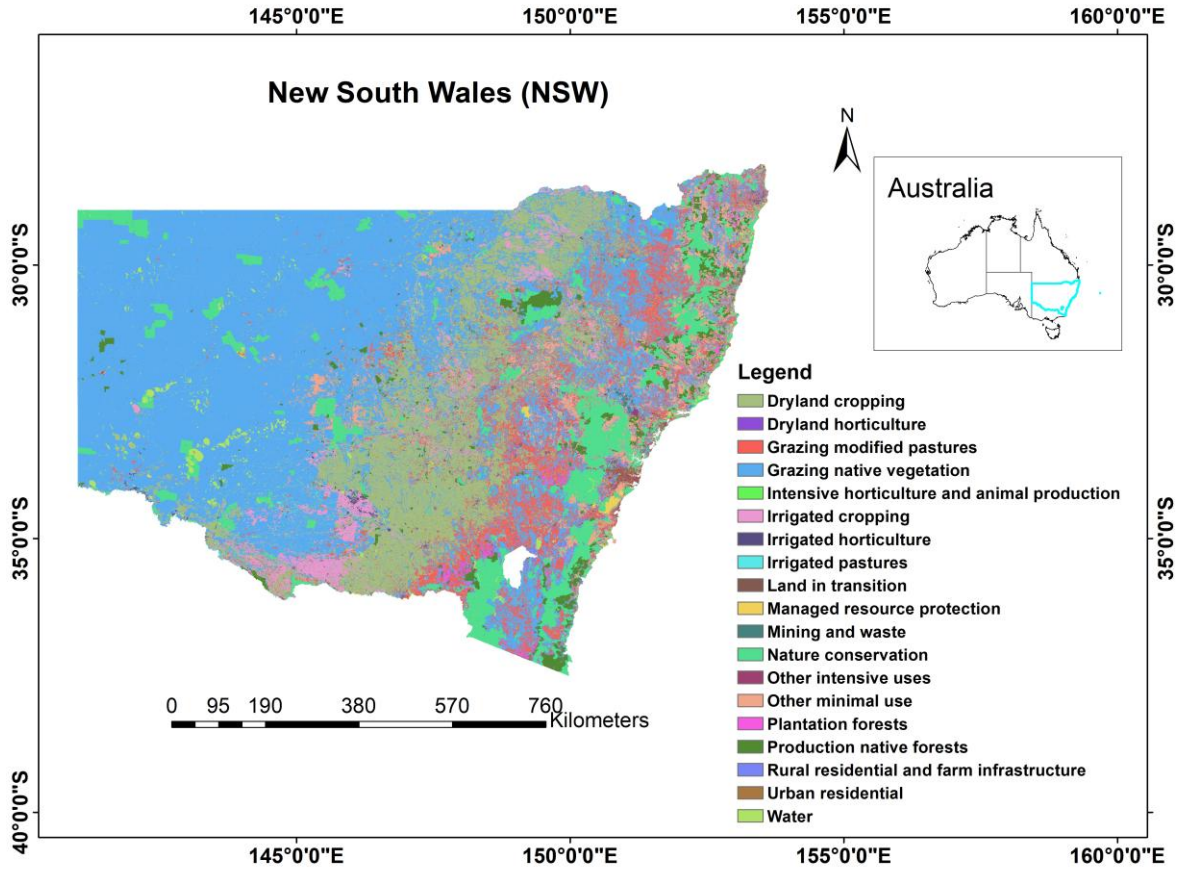

Fig. 1 Land Use Map of New South Wales (NSW), Sourced from the Department of Agriculture, Fisheries and Forestry.

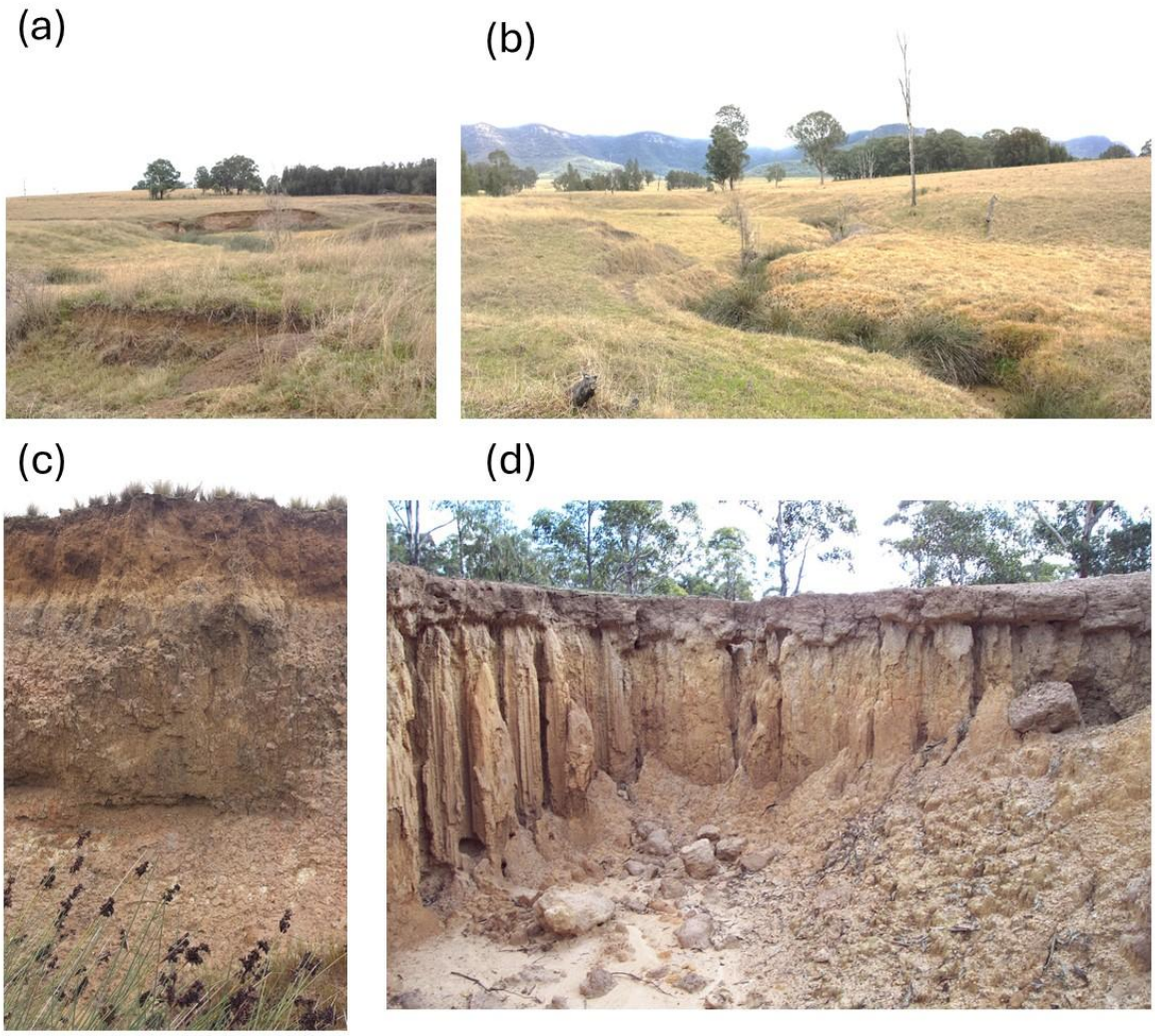

Fig. 2 Representative soil erosion features in the Upper Hunter Valley, NSW, under varying grazing intensities. (a) Active gully in heavily grazed pasture. (b) Early-stage gully in moderately grazed land. (c) Profile showing reduced topsoil thickness. (d) Severe gully with exposed subsoil and vertical piping.

2.3.2 Overview of the Soil Erosion Risk Assessment framework

The proposed general framework for assessing soil erosion is illustrated in Fig. 3. The first step involves selecting indicators for capacity and condition, based on expert opinion or knowledge, to establish a minimum data set for the study area. Once the indicators are chosen, they are transformed into unitless utility values to account for different measurement units. This transformation method is commonly used in soil security, health, and quality assessments (Andrews et al., 2002; Volchko et al., 2014; Evangelista et al., 2023; Evangelista et al., 2024; Wadoux et al., 2024).

The utility curves differ based on indicator role: upper asymptotic sigmoid curves are applied for condition- related indicators (clay ratio and topsoil thickness) and capacity-related topsoil thickness, reflecting a “more is better” relationship. Conversely, a lower asymptotic curve was used for capacity-related clay ratio, indicating a “less is better” relationship. These utility functions are developed separately for capacity and condition indicators. Capacity corresponds to the genosoil, while condition is based on the comparison between phenosoil and genosoil.

The development of these utility functions includes calculating the mean values of genosoil and phenosoil indicators within each corresponding pedogeon (unique spatial unit), using the pedogeon map from the study by Román Dobarco et al., 2021. The function outputs a value from 0 (least capacity/condition) to 1 (highest capacity/condition), providing a relative measure of deviation from the optimum state (genosoil). These values are represented graphically in utility graphs.

After developing the utility functions, capacity and condition values are aggregated to estimate the final capacity and condition for the study area. The average capacity is calculated as the mean of the capacity for clay ratio and topsoil thickness for genosoil. Similarly, the average condition is calculated as the mean of the condition for clay ratio and topsoil thickness for phenosoil/genosoil. Finally, capacity and condition are mapped using these utility functions, resulting in utility maps. By comparing the utility map for capacity with the utility map for condition, we can assess the soil erosion risk.

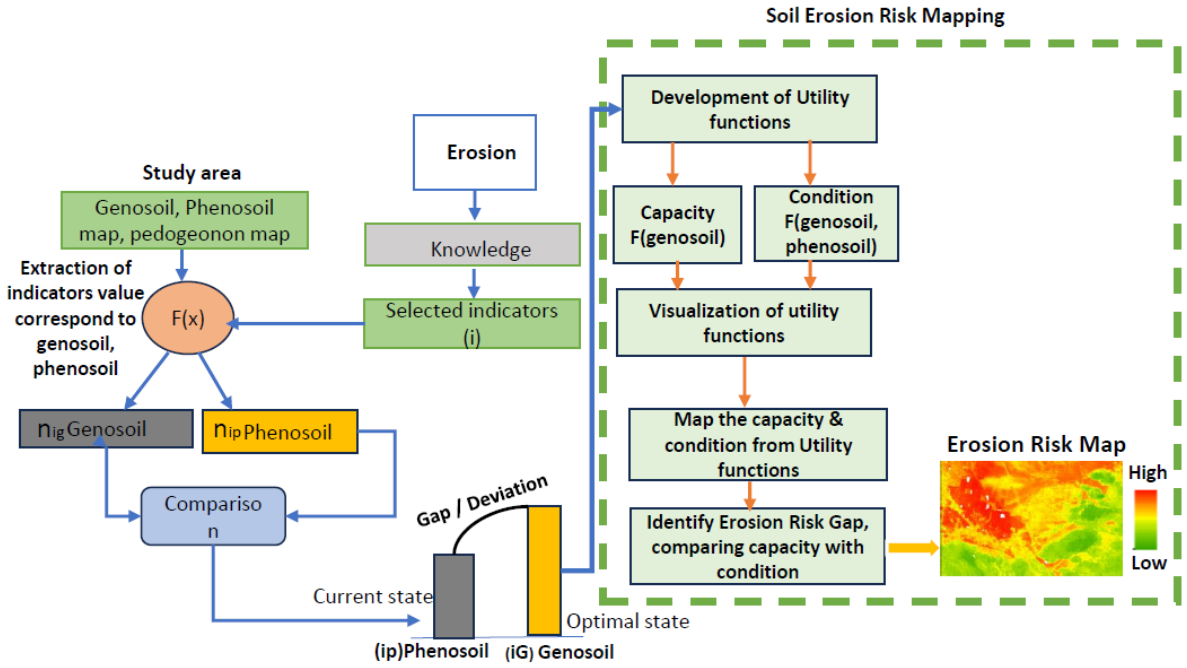

Fig. 3 The Capacity–Condition Framework (CCF) for assessing soil erosion vulnerability.

2.3.3. Defining Capacity, Condition, and Erosion Risk

Erosion, the detachment and transport of soil particles by wind and water, is influenced by the force required to dislodge these particles (Toy et al., 2002; Foster et al., 2015; Blanco and Lal, 2023). Cohesive soils rich in clay particles demonstrate stronger resistance to erosion compared to non-cohesive, sandy soils due to the higher force needed for particle detachment (Foster et al., 2015). Topsoil thickness also plays a critical role. Studies by Mielke and Schepers, 1986; Guo et al., 2021 demonstrate a positive correlation between topsoil thickness and plant growth, highlighting the importance of vegetation in binding soil particles. Conversely, Kaihura et al., 1997 found that decreasing topsoil thickness negatively impacts water holding capacity and essential soil properties, ultimately reducing plant growth and increasing erosion vulnerability.

The concept of assessing erosion involves two critical factors: a soil's inherent capacity to resist erosion and its current condition. Inherent capacity is determined using genosoil indicators, representing the natural resilience of the soil to erosion. The capacity can vary

over time and space due to both natural process and human activities (Bouyoucos, 1935; Couper, 2003; Wang et al., 2024). For instance, sandy soils with low clay content are more vulnerable to erosion under similar conditions compare to higher clay content (Wischmeier and Mannering, 1969; Toy et al., 2002; Parwada and Van Tol, 2019).

Erosion is a gradual process that occurs over time and space, as cumulative erosive forces modify soil condition (Turkelboom et al., 2008; Dotterweich et al., 2012). The current condition is assessed by examining the ratio of phenosoil to genosoil for the same indicators, reflecting the cumulative impact of both natural and human-induced erosion. This approach leads to the concept of erosion risk capability, defined as the difference between a soil's inherent capacity and its current condition (Fig.4). A larger gap between these two factors indicates a higher risk of erosion, as the soil's current state may no longer align with its natural capacity (Table 1).

To quantify erosion risk capability, the utility values $U^{(risk)}$ are calculated as follows:

$$U^{(risk)} = C - Con \quad (1)$$

where C is the inherent capacity and Con soil's current state. Higher $U^{(risk)}$ values indicate a larger gap and thus a greater erosion risk, while negative $U^{(risk)}$ values, where conditions exceed capacity, signify lower erosion risk. This calculation assumes both indicators are standardized on a 0–1 utility scale and that a linear gap reflects risk magnitude. Risk Classification Criteria: The erosion risk levels (high, moderate, low) were classified based on natural breaks in the utility difference distribution and expert knowledge (see Table 1).

Table 1. Classification of Erosion Risk Based on Capacity–Condition Utility Gaps

Erosion Risk Category	Capability Gap description	Inherent Capacity	Current Condition	Utility Gap $U^{(risk)}$
High	Low	High	Low	>0.515
Moderate	High	Good	Low	0.172-0.517
Low	High	Poor	Moderate	-0.763-0.172
Very Low/Negative	Low	Poor	High	< -0.763

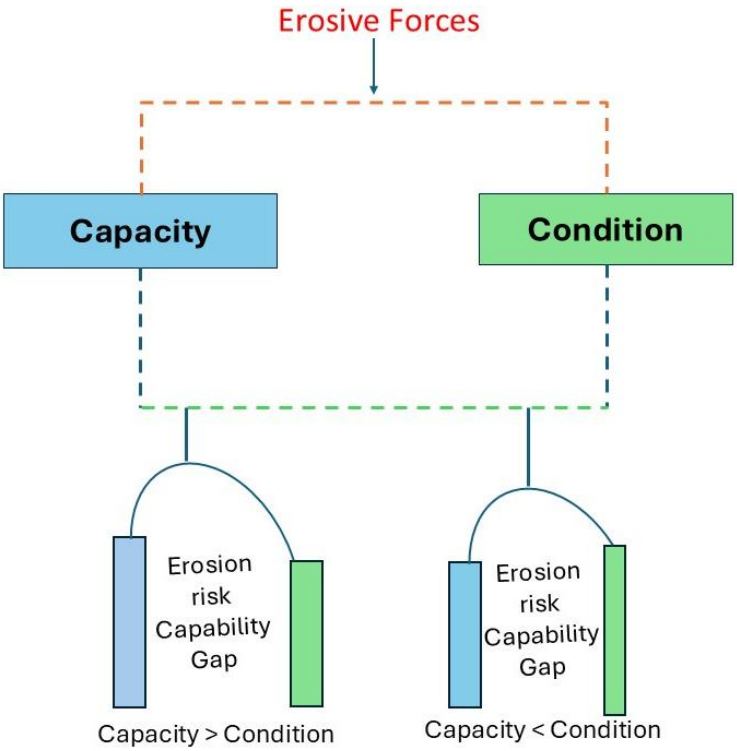

Fig. 4 Conceptual Framework for Assessing Soil Erosion Risk Based on Condition and Capacity of soil. The framework evaluates soil erosion risk by comparing soil condition and capacity against erosive forces. A larger gap between condition and capacity bars indicates a higher erosion risk, while a smaller gap suggest a lower risk.

2.3.4. Indicators for capacity and condition

Following the framework described in Section 2.3.2, clay ratio and topsoil thickness were selected as indicators for both soil capacity (genosoil) and condition (phenosoil relative to genosoil). These indicators satisfy the framework requirements and can be applied consistently across large spatial extents.

Clay ratio, widely used in erosion studies (Bouyoucos, 1935; Sarkar and Mishra, 2018; Kusre et al., 2018; Olaniya et al., 2020; Pinheiro Junior et al., 2022; Raj et al., 2023), is a simple and stable over time, with lower ratios indicating higher resistance to erosion. Topsoil thickness, a crucial parameter in erosion assessment, varies with erosion and

indicates soil condition (Zhang et al., 2021; Zhang et al., 2024). Thicker topsoil indicates better conditions, while erosion reduces topsoil thickness (Zhang et al., 2021). The selected indicators are described in detail in the following subsections.

2.3.4.1. Clay ratio Indicator

The clay ratio (CR) was calculated as the proportion of non-clay particles (sand and silt) relative to the clay content using the formula (Bouyoucos, 1935).

$$CR = \frac{Sand\% + Silt\%}{Clay\%} \quad (2)$$

To perform these calculations, we utilized the Soil and Landscape Gird of Australia (SLGA) data, provided by TERN (Malone and Searle, 2022). The SLGA offers comprehensive soil and landscape attribute information across Australia with a spatial resolution of 90m. we extracted sand, silt and clay percentages over New South Wales (NSW) using Google Earth Engine Image collection "CSIRO/SLGA".

2.3.4.2. Topsoil Thickness (TST) indicator

We utilized A1 horizon data from the publicly accessible Terrestrial Ecosystem Research Network (TERN) Soil Data Federator, developed by CSIRO and Industry & Environment Department NSW (https://espade.environment.nsw.gov.au). The database provides upper and lower depth measurements for various locations. To ensure data integrity, we pre-processed the datasets to address any missing values and outliers. Both datasets from TERN and eSPADE were standardised to the same unit (metres).

We then combined the two databases, carefully checking for, and removing any, intersecting data points to avoid duplication. This computation resulted in a total of 6619 observations; the spatial distribution of sample locations is shown in Fig.5.

For locations where topsoil was absent, we utilized the rock outcrop data. These locations were obtained from Geoscience Australia via their portal (https://portal.ga.gov.au/). Field site specimen measured data filtered based on type, focusing specifically on rock outcrop specimens within areas of relief >200m. The total number of topsoil absence locations across the NSW amounted to 1092, as illustrated in Fig.5.

For topsoil thickness modelling, we employed a two-step approach using different sets of covariates, following the SCORPAN framework (McBratney et al., 2003). The probability of topsoil presence was modelled using 24 covariates (supplementary, Table 1), and topsoil thickness prediction utilized 38 covariates (supplementary, Table 2).

For the topsoil probability model, 6 out of the 24 covariates were computed from remote-sensing data, derived from multi-sensor and multi-temporal images, covering soil indices, temporal stability, and spectral reflectance characteristics. We processed Landsat-8 and Sentinel-1 images spanning four years (2019-2022) using the Google Earth Engine (GEE) cloud computing platform. Landsat-8 provides high-resolution optical imagery, while Sentinel-1 offers radar data with VV and VH polarizations. Using four years of data captures topsoil presence and absence more accurately, minimizes noise, and accounts for seasonal variations in spectral signatures, thereby improving soil property identification.

Sentinel-1 Ground Range Detected (GRD) data, including VV and VH polarization images, were processed within GEE and expressed in backscatter coefficient decibel units (Mullissa et al., 2021). Landsat surface reflectance (SR) data, with less than 2% cloud cover, were pre-processed to mask clouds and shadows using quality bands before computing indices (Yan et al., 2022). For VV and VH, the temporal mean for both polarizations were calculated using GEE's collection-level method. Other optical indices were calculated in GEE involved by defining user functions based on specific band combinations (Table 2) and generating temporal statistics (mean, maximum, and standard deviation) over four years. To ensure consistency in resolution before modelling, remote sensing covariates computed in GEE were resampled to match the SLGA covariates at a 90m resolution.

Table 2. Derived Remote Sensing Variables for Topsoil probability modeling

Satellite	Variables	Abbreviation	Calculation	Description

Landsat-8	Temporal stability of Soil brighness – coefficient of variation (CV)	SBI-CV	$\mathrm{CV}_{\mathrm{BI}} = \frac{\sigma_{\mathrm{BI}}}{\mu_{\mathrm{BI}}} * 100\%$ standard deviation (σ_{BI}), BI mean (μ_{BI}) $\mathrm{SBI} = \frac{\sqrt{\mathrm{Red}^2 + \mathrm{Green}^2}}{2}$ (Escadafal, 1989)	Quantifies temporal fluctuation in exposed soil
Landsat-8	SWIR Reflectance temporal standard deviation	Std SWIR	StdDev(imageCollection)	Represents variations in SWIR reflectance over time
Landsat-8	Maximum NDVI	Max NDVI	$\mathrm{NDVI} = \frac{\mathrm{NIR} - \mathrm{Red}}{\mathrm{NIR} + \mathrm{Red}}$ (Ke et al., 2015)	Highest NDVI value, indicating peak vegetation Vigor
Landsat-8	Mean NDVI	Mean NDVI	ImageCollection.mean()	Average NDVI value; reflectance overall vegetation health
Sentinel-1	Temporal Mean VV Backscatter coefficient	Mean VV	ImageCollection.mean()	VV backscatter intensity; relates to vegetation cover/surface roughness and soil moisture (Hoskera et al., 2020)
Sentinel-1	Temporal mean VH Backscatter coefficient	Mean VH	ImageCollection.mean()	VH backscatter intensity; sensitive to soil moisture & vegetation structure (Baghdadi et al., 2018)

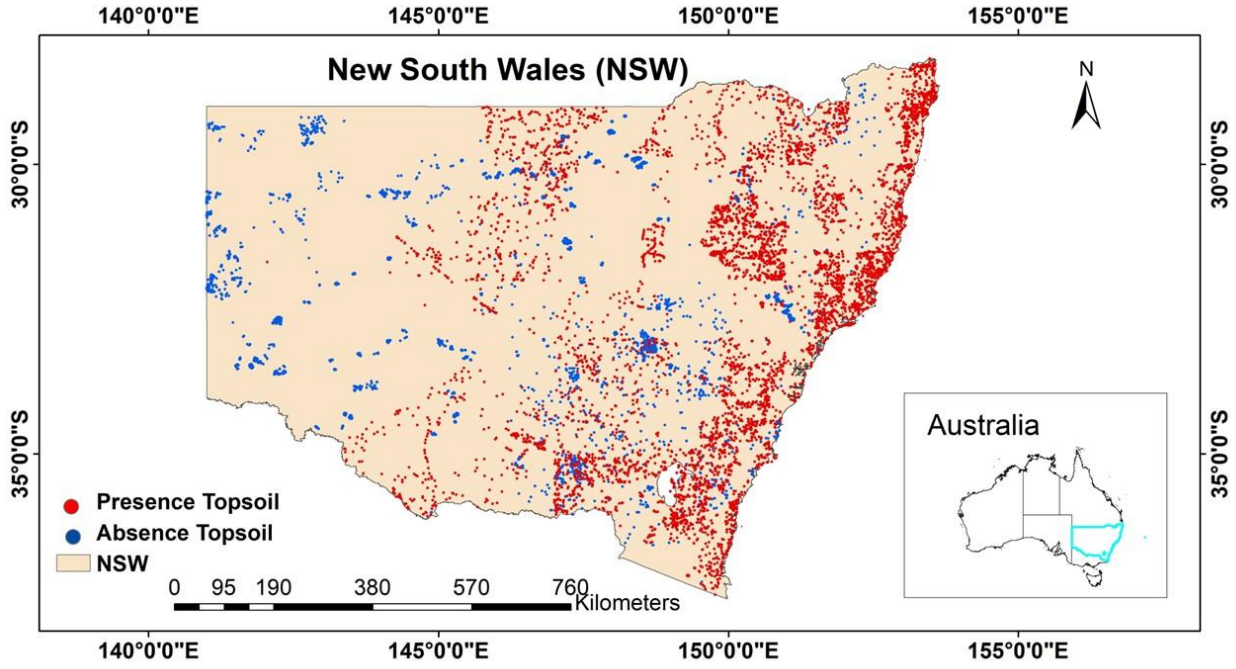

Fig.5 Topsoil Thickness Measurements and Non-Topsoil Locations Across NSW

2.3.5. Two-step modelling approach for topsoil thickness mapping

Our two-part modelling approach (Fig.6) first characterizes topsoil presence (or absence). We utilise a training dataset encompassing both topsoil and rock outcrop's locations, along with covariates detailed in supplementary, s1, To address potential class imbalances, a stratified random sampling technique is employed, dividing the data into a 70:30 training-validation split with equal representation of topsoil and non-topsoil locations. This approach ensures robust model development by mitigating bias (Raschka, 2020). A probability threshold (95th percentile) was used to classify areas with a high likelihood of topsoil presence for further thickness prediction.

In the second step of predicting topsoil thickness, we utilise a set of covariates (supplementary, s2) along with observed topsoil thickness data. This data split into 70% training and 30% validation sets. Throughout the modelling process (both presence and thickness), we utilize the Random Forest (RF) algorithm, a well-established choice for mapping and soil thickness estimation (Hounkpatin et al., 2018; Yamashita et al., 2024). To ensure optimal performance and prevent overfitting, we employ a grid search with 10-fold cross-validation on the training data for hyperparameter tuning (Ye et al., 2021).

Finally, the prediction thickness map was masked using the 95% probability map from the first step to exclude areas with low topsoil presence.

To quantify the uncertainty associated with our topsoil thickness predictions, we employ the bootstrap method. This technique involves generating 100 new datasets by sampling with replacement from the original training data. Each of these bootstrapped datasets is used to train a separate RF model. The standard deviation of the predictions from all 100 models provides a measure of prediction variability.

Model performance evaluation is conducted multiple metrics on the unseen test set, including mean error (ME), root mean square error (RMSE), squared Pearson's correlation coefficient (r2), determination coefficient (R^2) or modelling efficiency coefficient (MEC) (Wadoux, 2023; Wadoux et al., 2023). The probability model's evaluation includes metrics such as accuracy, precision, recall, F1 score (Lagomarsino et al., 2017; Yamashita et al., 2024).

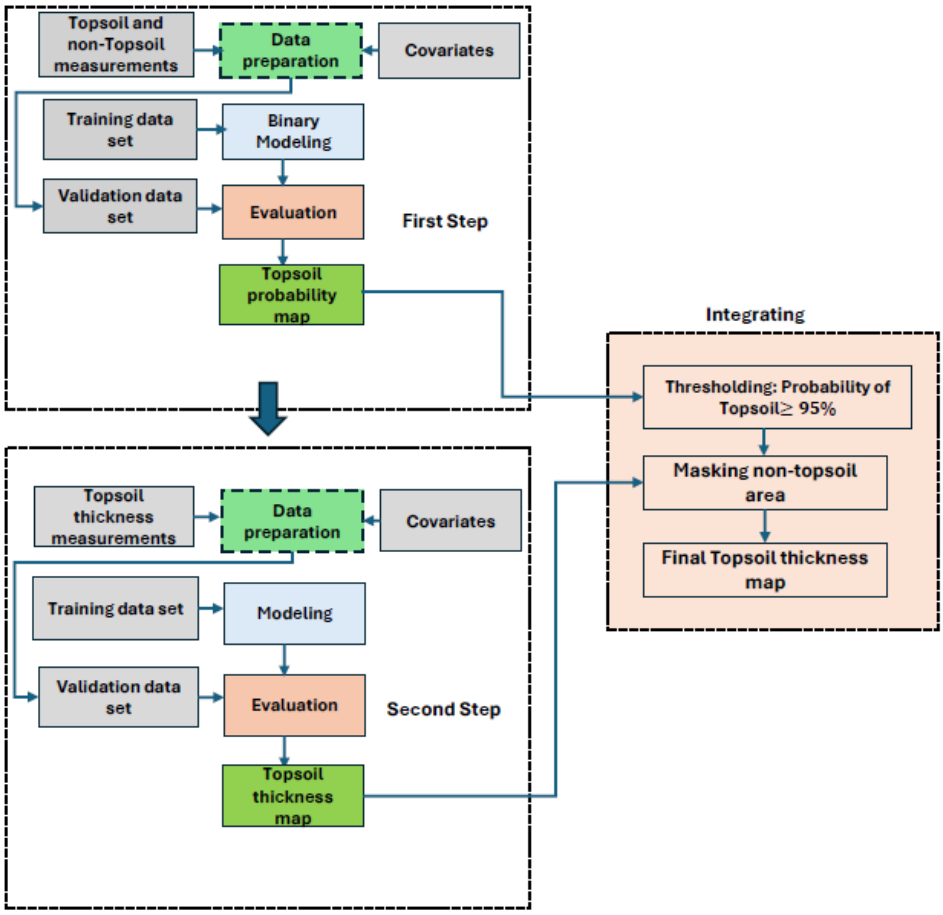

Fig. 6 General Workflow for Mapping Topsoil Thickness

2.3.6. Estimation of capacity and condition

To estimate capacity and condition, we first used the genosoil and phenosoil maps of topsoil thickness and clay ratio produced in Section 2.3.6.1. We then calculated the mean values of these indicators within each pedogeon unit, based on the pedogeon map developed by Román Dobarco et al. 2021. The mean genosoil values were used to represent capacity, while the ratio of phenosoil to genosoil means was used to represent condition (Wadoux et al., 2024; Tang et al., 2024). These values were then transformed into unitless scores (ranging from 0 to 1) through indicator-specific utility functions. Finally, the utility scores for each indicator of capacity and condition were averaged to derive the overall capacity and condition values for the study area (Fig. 3). Further details are discussed in the following sections.

2.3.6.1 Genosoil and phenosoil indicators

Genosoil refers to the natural state of soil formed under minimal human influence, reflecting long-term soil-forming processes and predominantly natural erosion (McBratney et al., 2019). For example, Jang et al., 2022 described in lower Namoi valley in NSW, Pedogenon I, where genosoil by woodland vegetation on Pilliga Sandstone, while the corresponding phenosoil is under non-irrigated cropping, indicating anthropogenic alteration influence on soil (Yang et al., 2020; Jang et al., 2023).

In contrast, phenosoil represents the current state of the same soil following anthropogenic modifications such as agriculture, land clearing, and land management (McBratney et al., 2019), where both natural and human-induced erosion processes dominate. For instance, Jang et al., 2022 described in lower Namoi valley in NSW, Pedogenon E, genosoil where sclerophyll forests dry on sandy plains, while the phenosoil corresponds to areas now used for irrigated cropping, highlighting land-use-driven changes in erosion-relevant soil properties (Nearing et al., 2017).

Genosoil and phenosoil locations across New South Wales (NSW) were previously identified and mapped by Román Dobarco et al., 2023. To map genosoil and phenosoil indicators (clay ratio and topsoil thickness), we applied a Random Forest (RF) modeling approach across NSW, method used described in section 2.5, using the same covariates but with distinct vegetation inputs to differentiate between genosoil and phenosoil conditions: Genosoil mapping used pre-European settlement vegetation (1788) as a proxy for natural soil conditions prior to major anthropogenic disturbance (source : https://pid.geoscience.gov.au/ dataset/ga/42356) (Tang et al., 2024). Phenosoil mapping used current vegetation data to reflect present-day land use and human-induced changes (Tang et al., 2024). The training datasets were derived from the genosoil and phenosoil locations mapped in Román Dobarco et al., 2023, ensuring representative data for both natural and modified soil states. In total, four maps were generated: genosoil and phenosoil for both topsoil thickness and clay ratio. These maps served as inputs to estimate erosion-related capacity and condition in the next steps.

2.3.6.2. Estimation of capacity

The soil's capacity to resist erosion across the study area was quantified using utility functions applied to the genosoil indicators:

$$C = U_C(I_{Geno}) \quad (3)$$

In this context, U_C is the utility function that transforms genosoil indicator value I_{Geno} into a unitless score ranging from 0 to 1. The utility function U_C , developed by integrating theoretical knowledge, established an inverse relationship between clay ratio and susceptibility to erosion (Bouyoucos, 1935) . Recognizing that smaller clay ratios indicate greater resistance to erosion, this relationship is modelled using an S-shaped curve. This curve reflects soil behaviour, where erosion resistance increases with clay content. The specific utility functions are described as:

$$(U_{CR}) = 1 + \frac{1}{1+e^{a(geno\ CR-b)}} \quad (4)$$

$$(U_{TST}) = 1 + \frac{1}{1+e^{-c(geno\ TST-d)}} \quad (5)$$

Where U_{CR} and U_{TST} are utility scores for genosoil indicator - clay ratio and topsoil thickness. Geno CR and Geno TST refer to the genosoil values for clay ratio and topsoil thickness, respectively, derived from spatial predictions using RF models trained with genosoil data (see section 2.3.6.). The parameters a, b, and d were calibrated by fitting sigmoid utility functions to observed indicator distributions across pedogenons. The utility graphs Fig. 12 a, b.

The overall capacity was then calculated as:

$$C = \frac{U_{CR} + U_{TST}}{2} \quad (6)$$

2.3.6.3 Estimation of condition

To estimate the current condition of the soil affected by erosion, we use a similar S-Shaped curve approach through the utility function:

$$Con = U_{Con}\left(\frac{I_{pheno}}{I_{Geno}}\right) \quad (7)$$

Here, U_{Con} is the utility function that transforms the ratio of the phenosoil indicator value I_{pheno} (clay ratio and Topsoil thickness) to the genosoil indicator value I_{Geno} (clay ratio and Topsoil thickness) into a unitless score ranging from 0 to 1, representing the soil's condition. The utility function is defined as:

$$(U^*_{CR}) = 1 + \frac{1}{1+e^{-a(\frac{phnoCR}{geno\ CR}-b)}} \quad (8)$$

$$(U^*_{TST}) = 1 + \frac{1}{1+e^{-c(\frac{pheTST}{genoTST}-d)}} \quad (9)$$

Where U^*_{CR} and U^*_{TST} are utility scores for the ratios of phenosoil to genosoil clay ratio and topsoil thickness, respectively. The parameters a, b, c and d are carefully optimized to achieve the best fit with the observed data patterns. The utility graphs Fig.12 c, d.

The overall condition was calculated as:

$$Con = \frac{U^*_{CR} + U^*_{TST}}{2} \quad (10)$$

2.4. Results

2.4.1. Remote sensing variables for Topsoil and Non-topsoil

The Kernel density curves, and box plots were utilized to visually analyze the distribution disparities between topsoil presence and absence locations across five variables: VV backscatter coefficient, VH backscatter coefficient, Maximum NDVI, Std SWIR, and CV-SBI. These visualizations revealed distinct patterns in the distribution of these variables between topsoil presence and absence locations, with all variables displaying statistically significant differences between the two categories.

VV and VH backscatter coefficients: Both backscatter coefficient displayed a wider spread in rock outcrop locations (indicating higher variability) compared to the narrower spread observed in topsoil areas (suggesting more uniform responses) (Fig.7 a, b.). Specifically, peak probability for VV backscatter occurred at -11 dB (probability: 0.22) in rock outcrops and -14 dB (probability:0.28) in topsoil locations. A similar pattern was observed for VH backscatter, with a peak probability of 12 dB (Probability: 0.23) in rock outcrops and -13 dB (probability:0.28) in topsoil locations. These trends were further corroborated by the boxplots, which consistently showed higher backscatter response in rock outcrops regions. This contrast was evident in the box plots, showing higher backscatter responses for rock outcrop regions.

Std SWIR: Kernel density plots showed topsoil areas exhibited a narrower spread, indicating more consistent SWIR reflectance behavior, while rock outcrops displayed a wider spread, suggesting greater variability in SWIR reflectance value The peak reflectance probability for Std SWIR in topsoil locations occurred at 900 (probability:0.24), while for rock outcrop locations, it occurred at 800 (probability:0.22) (Fig.7 c). This variability was also evident in the boxplots, which showed a higher overall SWIR response in rock outcrop regions compared to topsoil locations.

Max NDVI: Topsoil curves exhibited a peak at a specific Max-NDVI value with a narrow spread, suggesting consistent vegetation cover. In contrast, rock outcrop curve displayed a peak at a higher max-NDVI value with a wider spread, indicating a different and more variable vegetation response (Fig.7 d). This suggests that vegetation cover may be sparser and variable on rock outcrops compared to topsoil areas.

CV-SBI: The topsoil curve exhibited a narrower spread, signifying consistent soil brightness over time. Conversely, the rock outcrop curve displayed a wider spread and potentially higher values, indicating greater variability and potentially higher soil brightness in rock outcrops locations (Fig.7 e). Specifically, the peak probability for CV-BI in topsoil locations occurred at 57% (Probability:0.32), while for rock outcrop locations, it occurred at 76% (probability:0.33). These findings underscore the utility of these variables in distinguishing between topsoil and rock outcrop areas. These findings align with the boxplots, which depicted higher variability and responses for rock outcrop areas.

a)

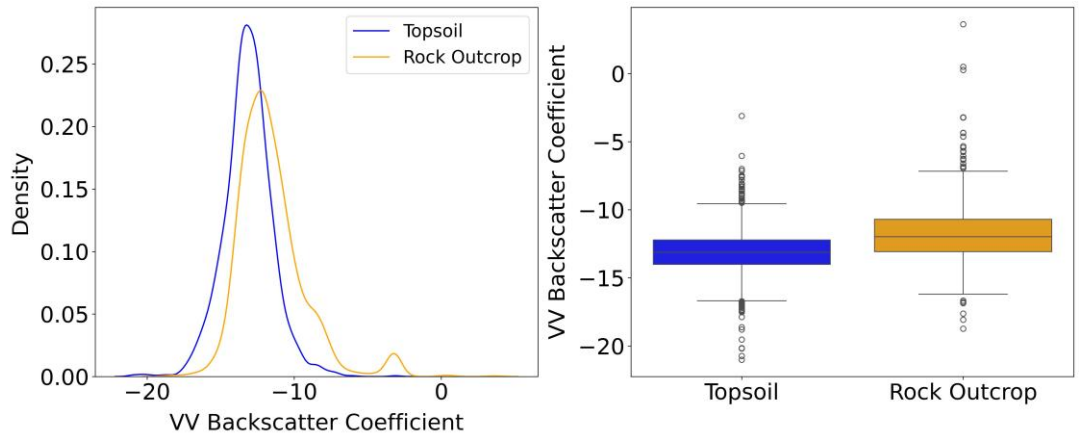

b)

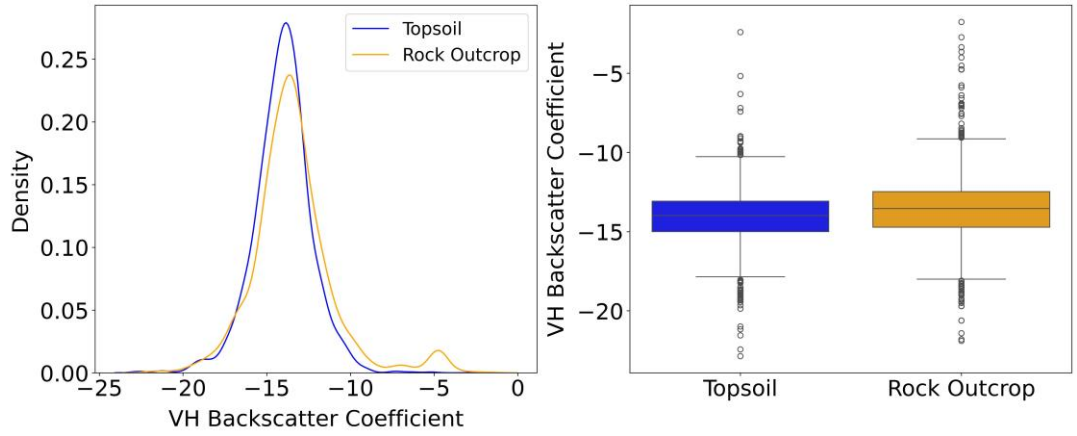
Topsoil
Rock Outcrop
Density
VH Backscatter Coefficient
VH Backscatter Coefficient
Topsoil
Rock Outcrop

c)

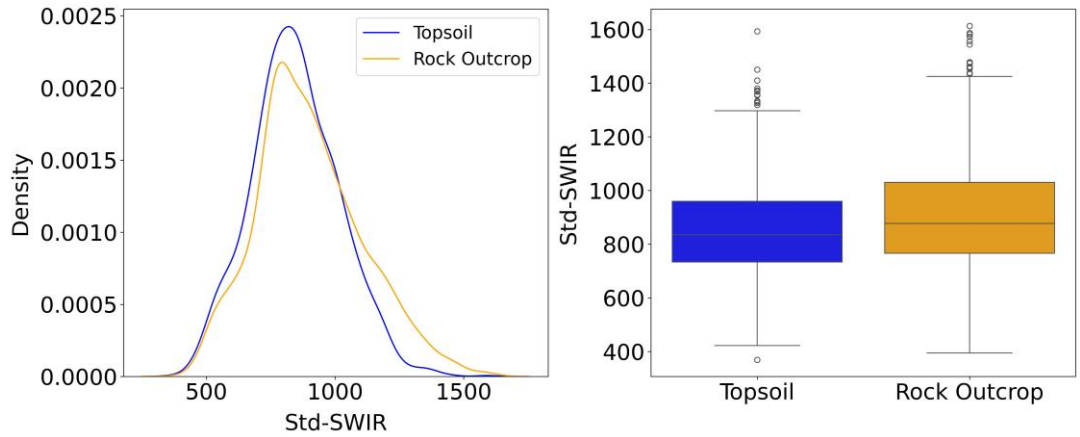
Topsoil
Rock Outcrop
Density
Std-SWIR
Std-SWIR
Topsoil
Rock Outcrop

d)

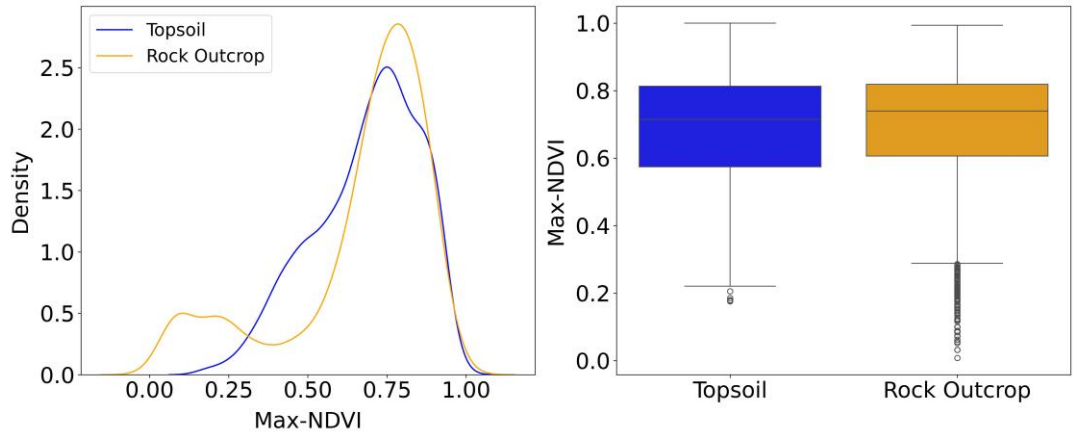
Topsoil
Rock Outcrop
Density
Max-NDVI
Max-NDVI
Topsoil
Rock Outcrop

e)

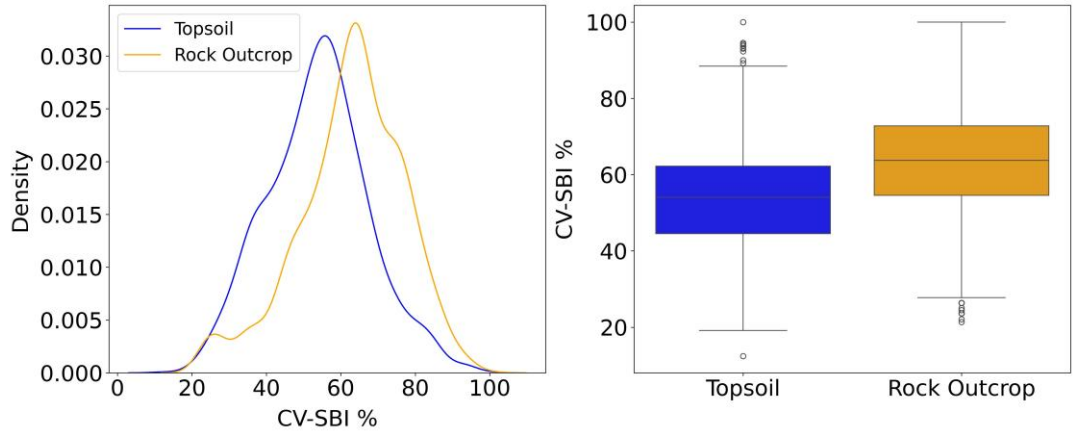

Fig. 7 Spectral Variation Between Topsoil and Rock outcrop. Panels show (a) VH backscatter , (b) VH backscatter, (c) Standard Deviation of SWIR, (d) Max-NDVI, and (e) Coefficient Variation of SBI Index

2.4.2. Topsoil Thickness: Spatial pattern and genosoil-phenosoil comparison

Fig.8a shows a typical topsoil thickness of 0.10 meters in the study area, with frequency decreasing as the values deviate from this point. The average thickness is 0.158 m (15.8cm) with a moderate variation of 0.088 m (8.8cm) around this mean, mirrored the median of 0.15 m (15 cm). Quartile analysis shows 25% of measurements fall below 0.1 m (10cm) while another 25% exceed 0.2 m (20cm). Finally, a 95% confidence interval suggests the true average thickness is likely between 0.156 and 0.160 m.

Topsoil thickness varied across land uses (Fig.8 b). Irrigated horticulture had the highest mean (0.20 m), while dry cropland and managed resource protection had the lowest (0.14 m). other land uses (dry horticulture, grazing native vegetation, intensive horticulture, nature conservation, plantation forest, and production native forest) displayed intermediate depths (Mean: 0.14-0.17m, SD: 0.06-0.10m). See S3 for detailed statistics,supplementary.

The comparison of top-soil thickness between Phenosoils and Genosoils indicated significant differences, with Genosoils consistently showing larger mean and median values (Fig.8 c). Statistical analysis, including a t- test (t-statistic =-4.326, p-value < 0.001), confirmed this disparity. Phenosoils had a mean thickness of 0.1488 m

(SD=0.082, var = 0.0067), while Genosoils exhibited a higher mean of 0.1606 m (SD =0.0884, Var =0.0078).

(a)

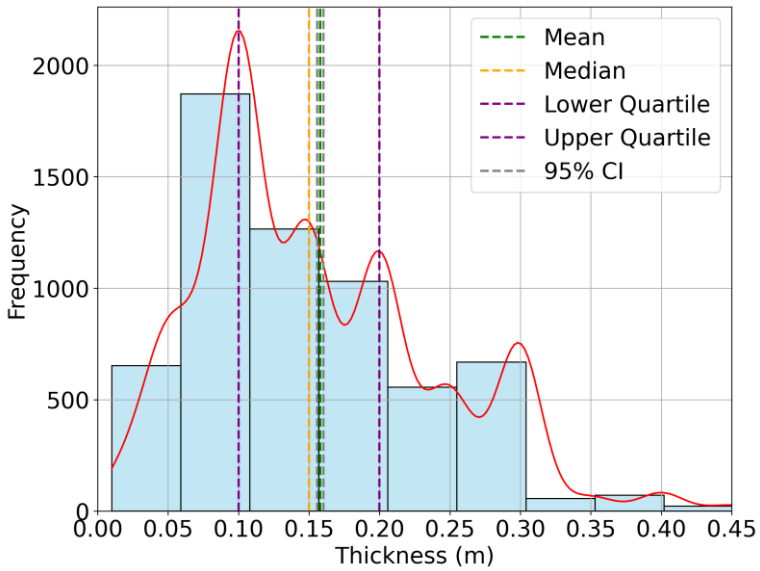

(b)

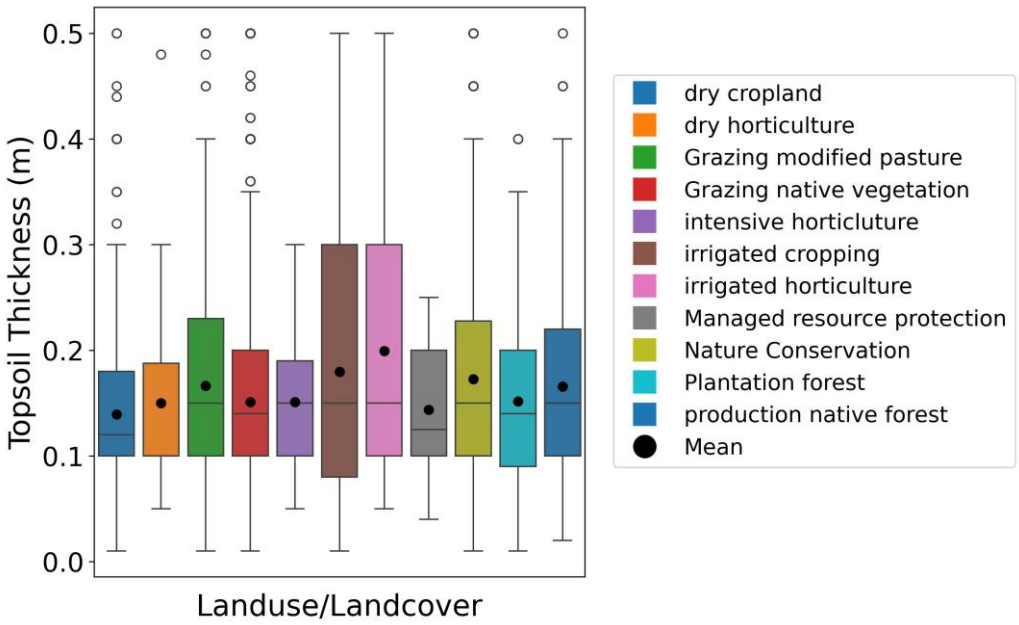

(c)

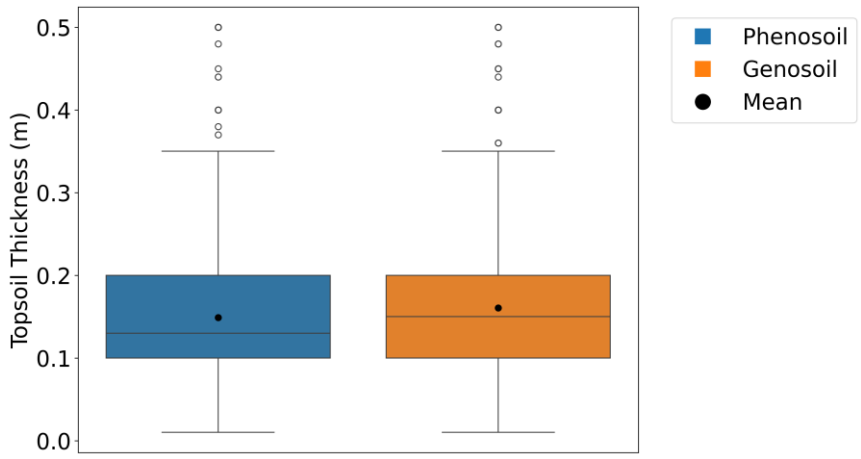

Fig. 8 Spatial Distribution of Topsoil Thickness Measurements. (a) Histogram of measured topsoil thickness, (b) box plot for the topsoil thickness across different land use class, (c) comparison of topsoil thickness between Genosoil and Phenosoil

(a)

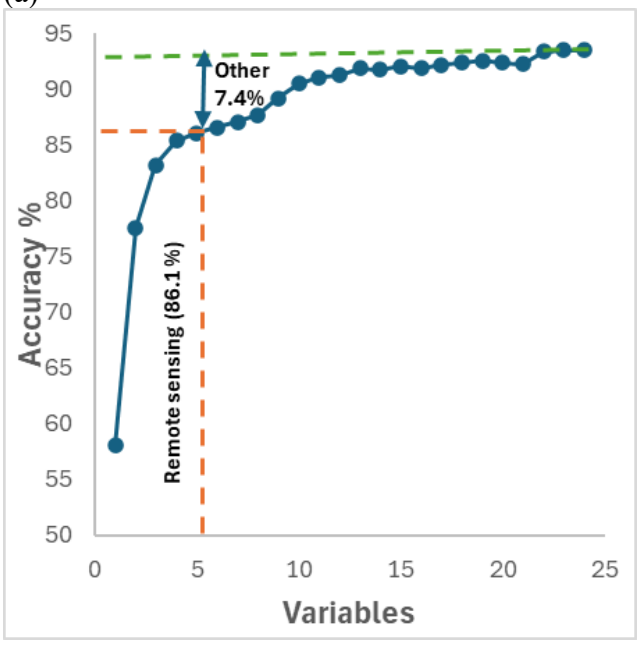

(b)

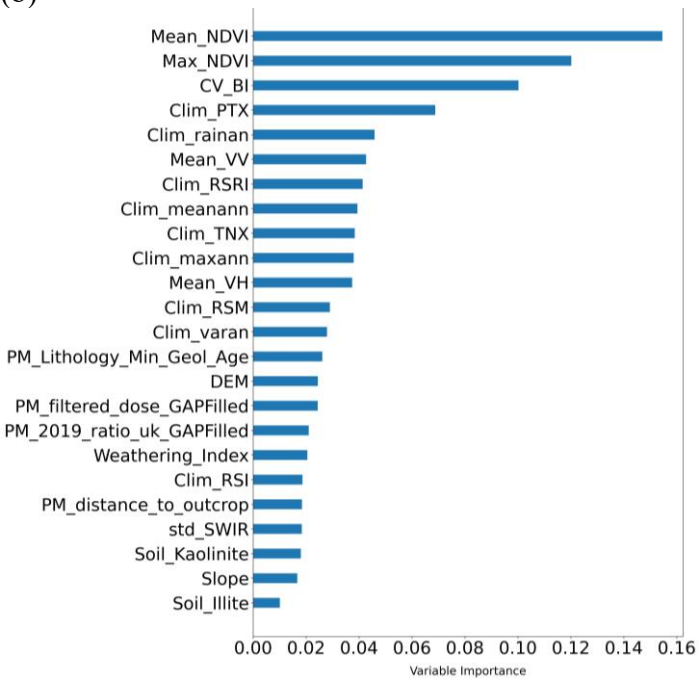

(c)

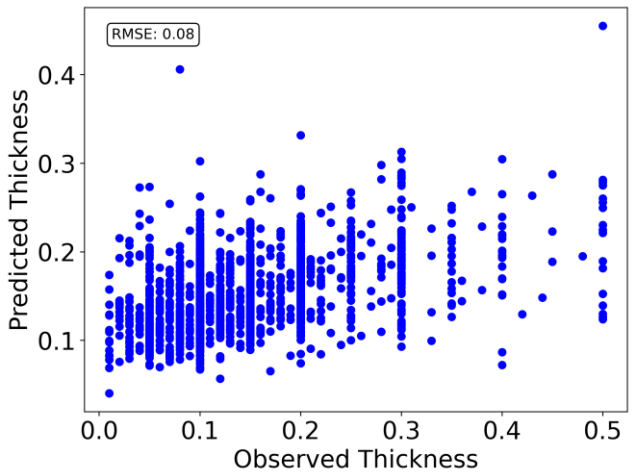

(d)

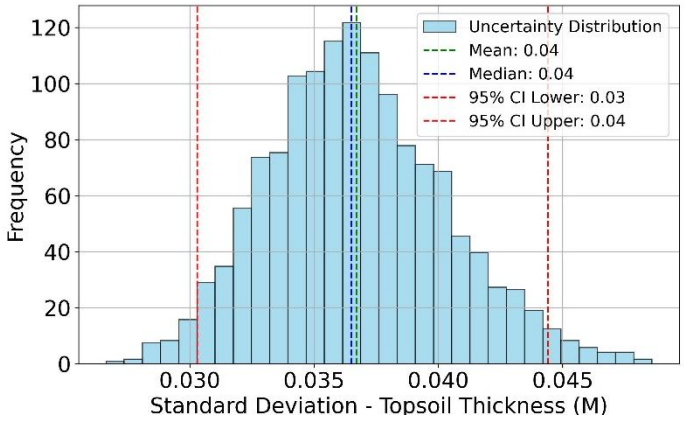

(e)

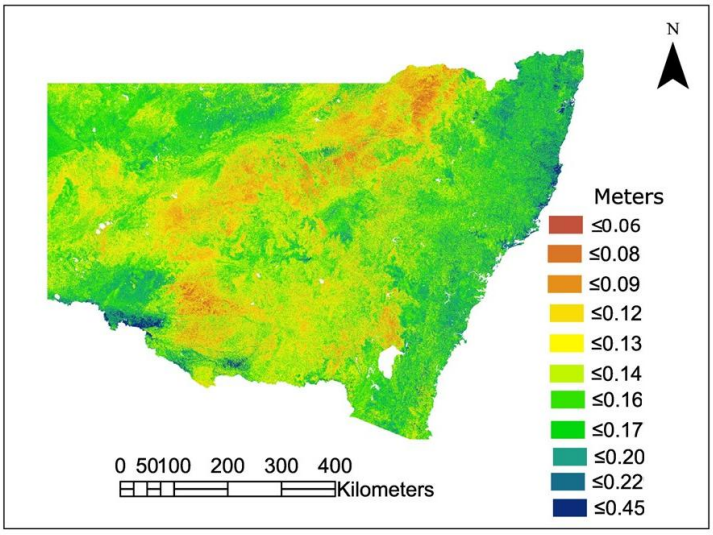

Fig. 9 (a) Contribution of variables to Model Accuracy. (b) Variable Importance in the Model (c) Validation Between Predicted Topsoil Thickness and Observed Topsoil Thickness. (d) Uncertainty Analysis with a 95% Confidence Interval for Topsoil Thickness Predictions. (e) Map of Predicted Topsoil Thickness

2.4.3. Topsoil thickness model performance

The results obtained demonstrate the robust performance of the RF model in predicting the presence/absence of topsoil. With an accuracy of 93.54%, the model exhibits high precision (91.08%) and recall (96.27%), indicating its capability to accurately classify both positive and negative instances. The F1-score of 93.60% further confirms the model's balanced performance in terms of precision and recall. Additionally, the specificity value of 90.90% showcases the model's ability to effectively identify true negative cases. The Matthews Correlation Coefficient (MCC) of 0.87 highlights strong agreement between the predictions and the actual labels.

To dissect the accuracy of our model, we employed a stepwise approach, gradually incorporating variables. The results, as illustrated in Fig.9 a, demonstrate that remote sensing variables were the key drivers of accuracy, contributing 86.1%. While other variables played a role, their combined contribution was 7.4%. The variable importance in the model also showed that remote sensing variables particularly MeanNDVI, MaxNDVI, and CV-BI, contributed more to the model than the rest of the variables (Fig.9 b) .

The topsoil thickness predicted RF model exhibited moderate performance on the test set, with a root mean squared error (RMSE) of 0.08 m. The model achieved an R^2 value of 0.217 (Fig.9 c). Furthermore, an uncertainty analysis provided stable results, with a 95% confidence interval for topsoil thickness predictions ranging from 0.03 to 0.04 m (Fig.9 d).

There is a notable variation of topsoil thickness over NSW, with thicker topsoil near the coast from the northeast coast to southeast coast and in the river basins. The topsoil is thinner in some parts of the west and south NSW. Deeper topsoil is seen in the areas of riverine sediment deposition. In context of land use, the higher thickness of soil can be seen in the Irrigated Cropping and Irrigated horticulture (Fig.9 e, Fig.8 b, Fig.1). Thinner topsoil can be seen in the dry cropping.

2.4.4. Clay ratio distribution and Relationship to Erosion Resistance in NSW

The range of clay ratio values varies from less than 2.65 to more than 24.93 across NSW. Very small values of clay ratio (less than 2.65) indicate areas with potentially inherently soil have higher resistance to erosion, while higher values (approximately 24.93) suggest areas with potentially lower resistance to erosion (Fig.10). Clay ratios less than 2.65 region have larger clay contents varying from 38.82% to 64%, moderate clay ratio values 4.18 to 7.81 have clay contents 28.94 % to 20.9 %, while high clay ratio varies greater than 7.81 have clay content less than 20.9%.

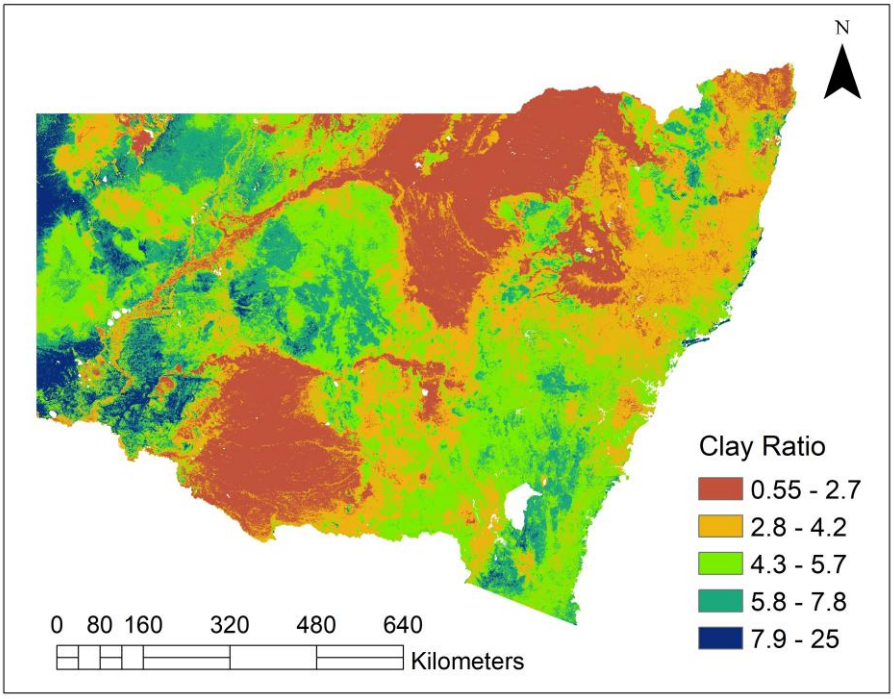

Fig.10 Map of clay ratio

2.4.5. Capacity Utility maps

The clay ratio- capacity utility map illustrates varying erosion resistance across NSW (Fig.11 g), with higher utility values indicating greater erosion resistance due to high clay content (median ~ 46%), moderate sand content (median ~ 42%), and lower silt content (median ~ 11.32%) (Fig.11 m). High-capacity regions, shown in darker shades, are found in areas such as the Northwest, Central West, Riverina, and Murray, where the soil composition is conducive to resisting erosion. Conversely, lower capacity regions,

characterized by high sand content (median ~ 79%), lower clay content (median ~ 12.5%), and low silt content (median ~ 6.9%), are predominantly observed in the central, western, and southeast regions (Fig.11 n).

The topsoil thickness capacity utility map (Fig.11 h) highlights differences in erosion resistance based on topsoil depth. High-capacity areas, represented in darker shades (utility values up to 1), are mainly located in coastal and highland regions, where thicker topsoil provides better erosion resistance. Conversely, low-capacity areas, indicated by lighter shades (utility values as low as 0.23), are prevalent in the central and western parts of NSW, where thinner topsoil results in lower inherent capacity.

The average-capacity utility map, integrating both clay ratio- capacity utility map and topsoil thickness -capacity utility map, reveals comprehensive erosion resistance across NSW (Fig.11 i). High-capacity regions, shown in darker shades (utility values ranging 0.781 to 1), are typically found in coastal and highland areas where both high clay content and thick topsoil combine to provide strong resistance to erosion. Low-capacity areas, indicated by lighter shades (utility values ranging 0 to 0.325), are prevalent in central and western NSW, where either or both indicators are less favourable.

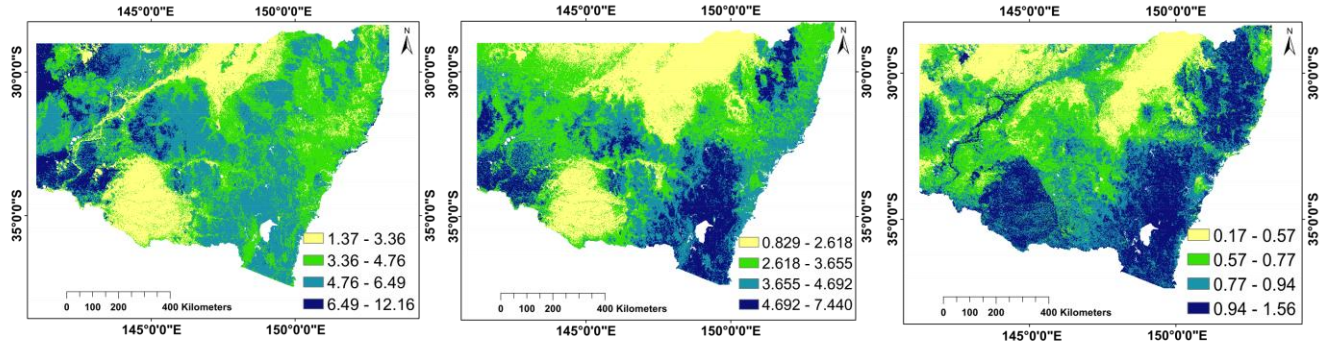

(a) Geno:Clay ratio (b) Pheno:Clay ratio (c) Pheno/Geno:Clay ratio

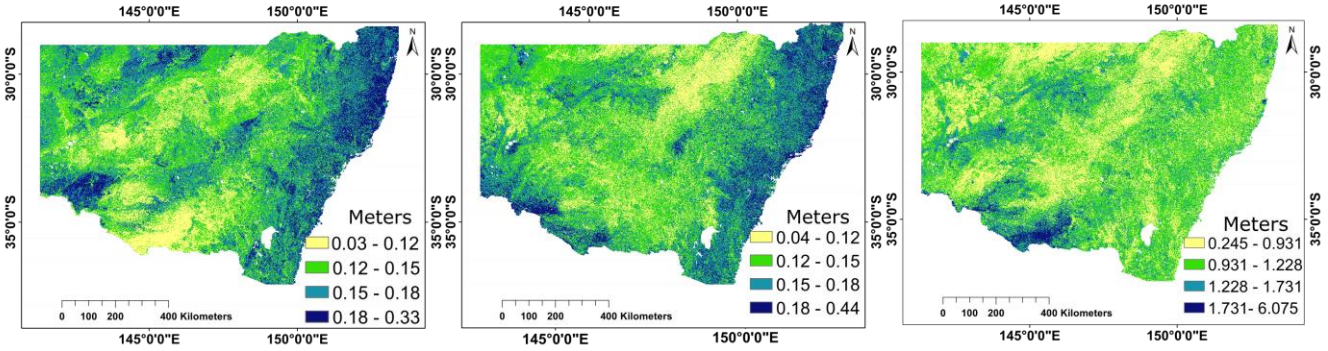

(d) Geno:Topsoil Thickness (e) Pheno:Topsoil Thickness (f) Pheno/Geno:Topsoil Thickness

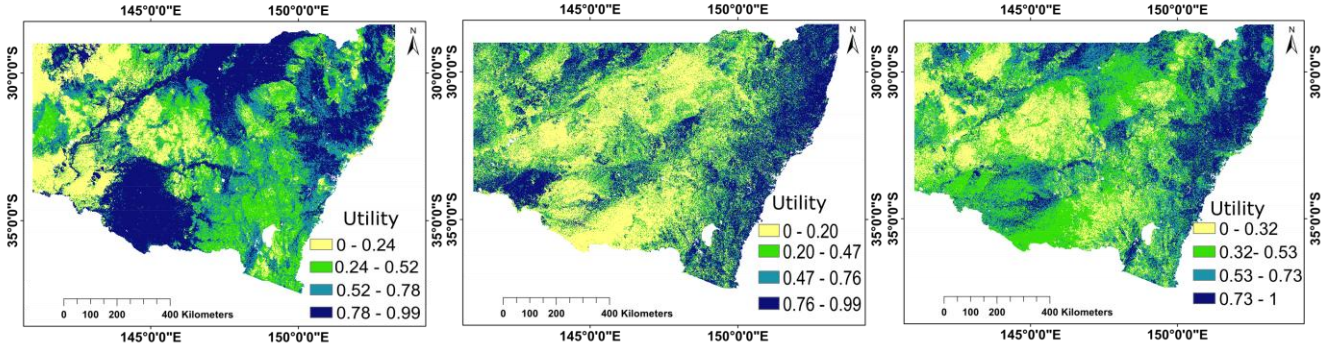

(g) Capacity:Clay ratio (h) Capacity:Topsoil Thickness (i) Avg:Capcity

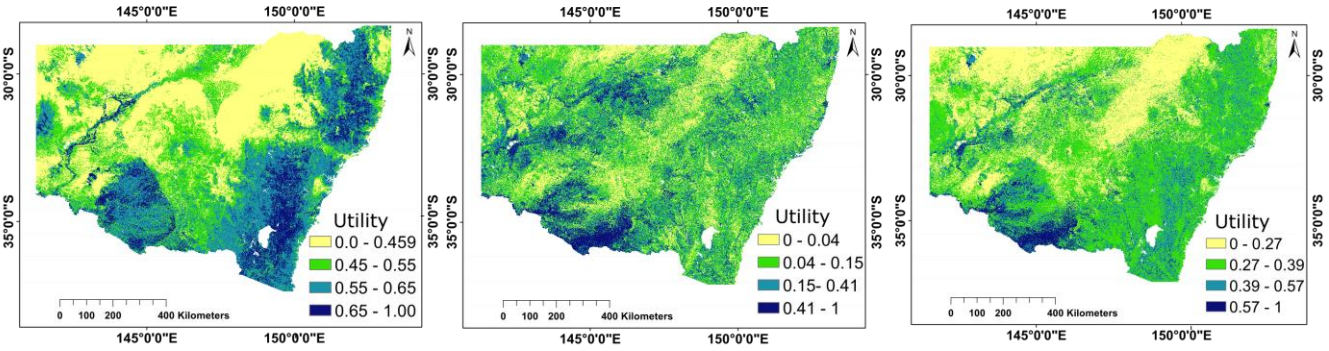

(j) Condition:Clay ratio (k) Condition:Topsoil Thickness (l) Avg:Condition

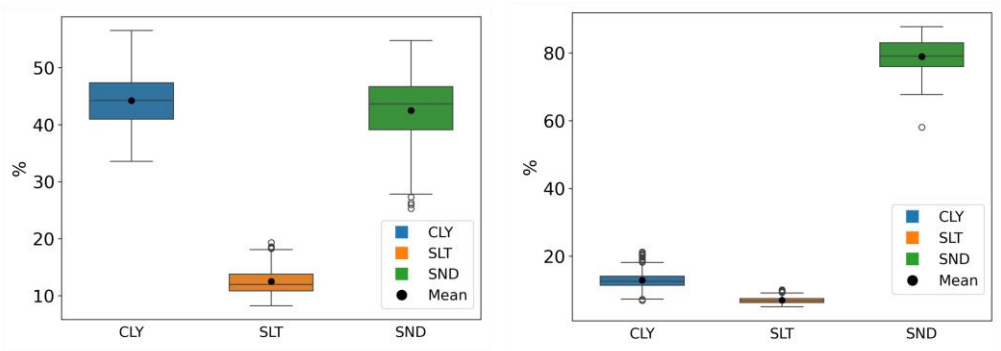

(m) Higher Utility locations (n) Lower Utility locations

Fig. 11 The first row shows maps of the clay ratio indicator for genosoil, phenosoil, and their deviation. The Second row displays maps of topsoil thickness for genosoil, phenosoil, and their deviation. The third row presents capacity utility maps for clay ratio, topsoil thickness, and the average capacity map. The fourth row illustrates condition utility maps for clay ratio, topsoil thickness, and average condition map. The fifth row depicts the textural composition of the capacity utility map for the clay ratio indicator at lower and higher locations.

2.4.6. Condition Utility maps

The condition utility map for clay ratio reveals the spatial variation between phenosoil and genosoil. Areas with high utility values indicate a low deviation in clay ratio between phenosoil and genosoil, while areas with low utility values show a high deviation in clay ratio (Fig.11 j). High condition areas (utility values: 0.655 to 1) are found in the coastal areas and some parts of the Riverina. Moderate condition areas (utility values: 0.459 to 0.655), indicating partial alteration, are scattered across various parts of NSW, including central regions and the Riverina. Low condition areas (utility values: 0. to 0.459) are prevalent in the North west and Far west regions.

The condition utility map for topsoil thickness highlights regions with varying degrees of soil preservation (Fig.11 k). High utility values (0.411 to 1), found in some coastal regions, highlands, parts of the Riverina, and the far west, indicate areas with well-preserved topsoil thickness due to continuous deposition processes. Regions such as Barham, Deniliquin, and Bourke benefit from natural deposition, leading to high resistance to further erosion. Moderate utility values (0.157 to 0.411) in central regions and scattered parts of NSW. Conversely, low utility values (0 to 0.157) are prevalent in dry cropping areas, particularly in some parts of the central west and far west regions.

The average condition utility map reveals regions with varying soil conditions across NSW (Fig.11 l). High condition areas (utility values: 0.572 to 1) are observed in the some parts coastal regions, some parts of the far west and Riverina .Moderate to low condition areas (utility values: 0 to 0.572) are spread across NSW, typically showing low condition in clay ratio and moderate condition in topsoil thickness.

(a) Capacity- Clay ratio

(b) Capacity- Topsoil Thickness

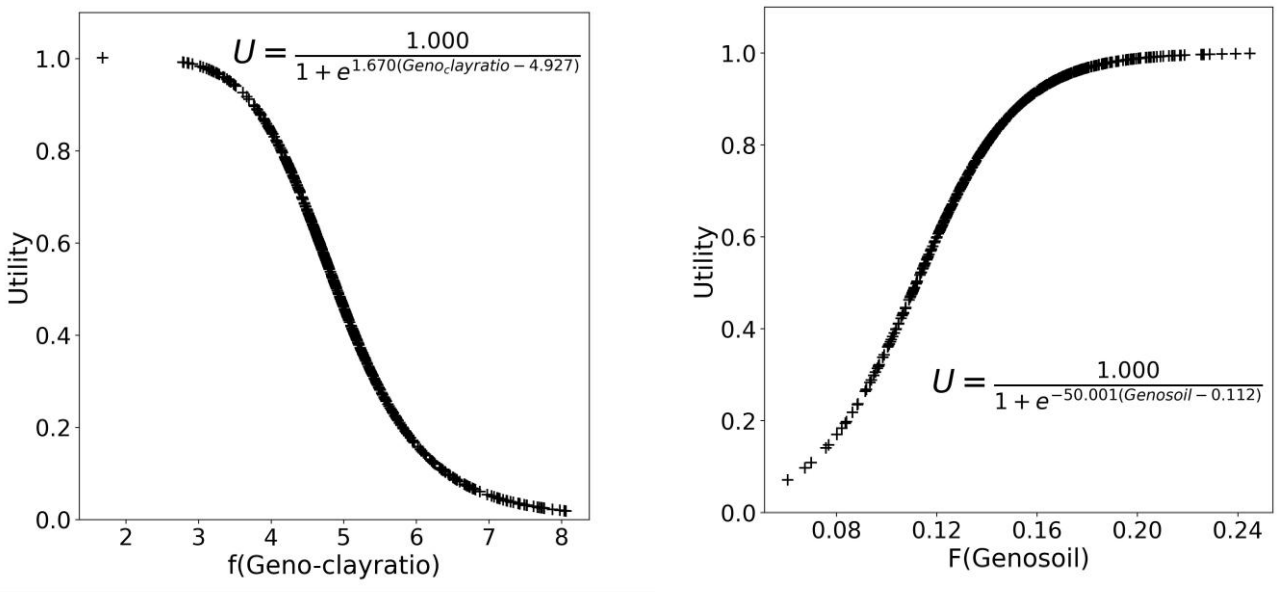

(c) Condition- Clay ratio

(d) Condition- Topsoil Thickness

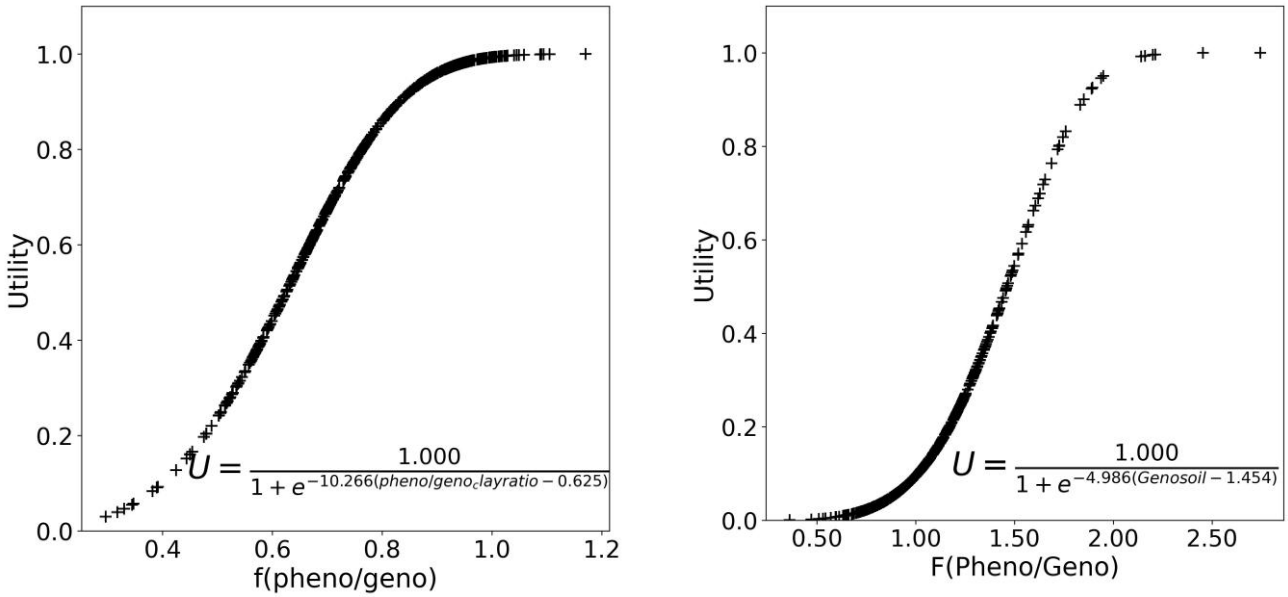

Fig. 12 First row shows capacity utility graphs for clay ratio and Topsoil thickness. The Second row presents condition utility graphs for clay ratio and Topsoil thickness.

2.4.7. Quantifying Erosion Risk

The erosion risk map (Fig. 13) illustrates spatial variation across NSW based on the difference between average capacity and condition utility values, as described in Section 2.3. The classified map reveals three primary risk categories: high, moderate, and low erosion risk.

High-risk areas (Dark Blue to Blue): These regions show the largest utility gaps (values > 0.517), indicating highly degraded conditions relative to the soil's inherent capacity. They are mostly located in the northwest dryland cropping zones, where phenosoil conditions have deviated substantially from natural genosoil capacity.

Moderate-risk areas (Cyan to Green): These zones fall within a moderate gap range (0.172 < $U^{(risk)}$≤ 0.517), often found in mixed land-use areas or regions undergoing transitional management

Low-risk areas (Light Green to Yellow): Representing small or negative utility gaps (-0.763 < $U^{(risk)}$≤ 0.172), these areas indicate well-preserved or slightly improved conditions, typically observed in floodplain zones or areas with low disturbance.

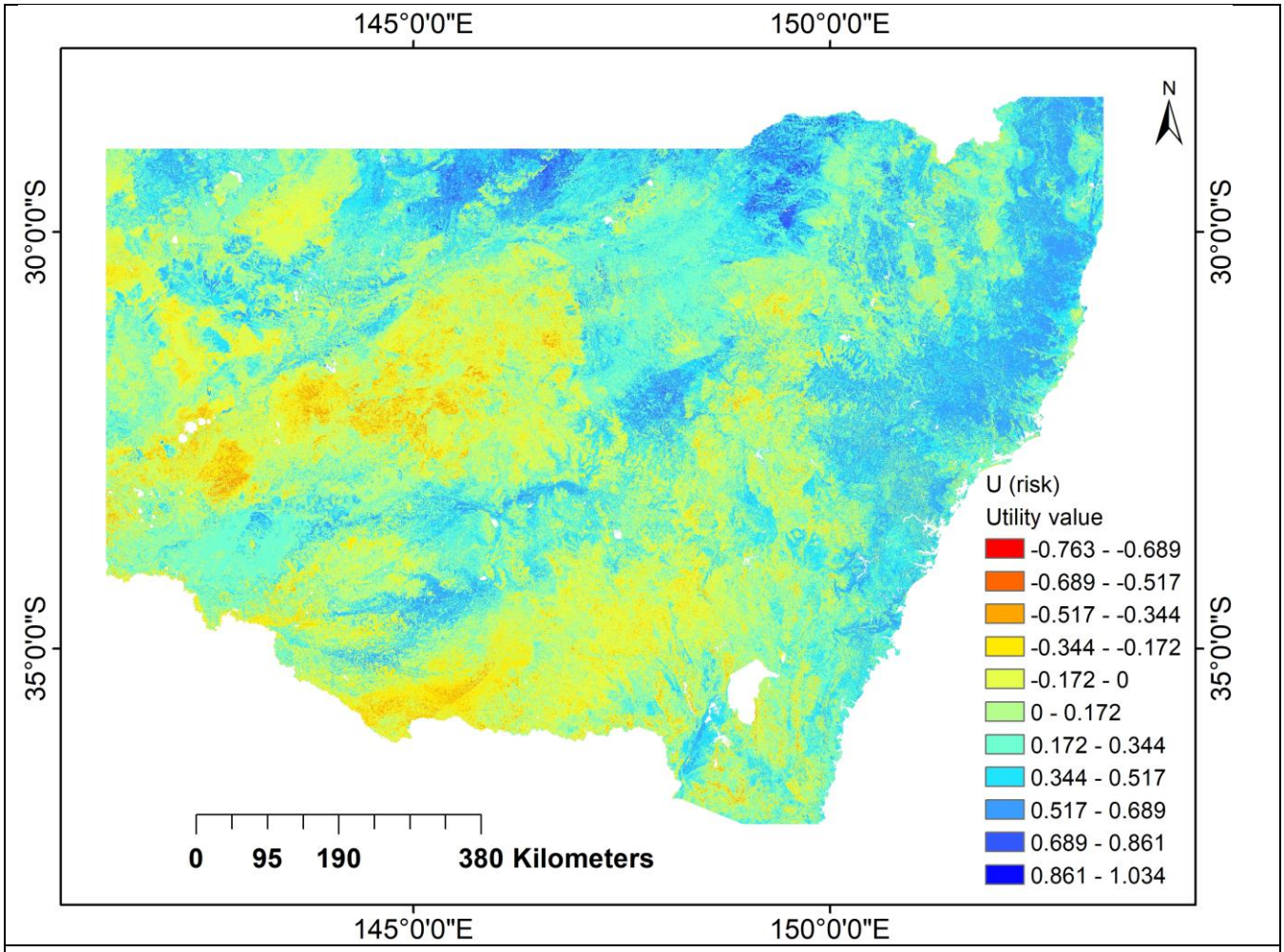

Fig. 13 Soil Erosion Risk Map of NSW

2.5. Discussion

2.5.1. Challenges and Opportunities in Modelling Topsoil Thickness

The prediction of topsoil thickness in this study achieved a modest R^2 =0.21, but low RMSE = 0.08 m, and low uncertainty. The model performed well for average thickness but struggled with specific ranges. This discrepancy is likely due to the challenges of correlating topsoil thickness with variables that have significant spatial and temporal variability (Fig.14a). Topsoil thickness changes over time due to factors like erosion and land-use practices (Zhang et al., 2024), complicating its correlation with variables measured at specific times.

Fig.14b illustrates that static variable such as geographic location and altitude contributed more significantly to the model than dynamic variables. This dominance underscores the difficulty of aligning dynamic variables with the spatial-temporal patterns of topsoil thickness. The lower R^2 of other models tested suggests that the model choice might be less critical than the selection of variables that capture the Spatio-temporal dynamics of topsoil thickness (Fig.14c).

Our top-soil thickness map aligns with land cover pattern (Fig.8 b). Dryland cropping areas (lower thickness) likely experience reduced organic matter and erosion due to erratic rainfall and a lack of consistent moisture, leading to sparse vegetation (Freebairn et al., 2015; Osman, 2018; (https://www.soe.epa.nsw.gov.au/all-themes/land/soil-condition-2018; Lal, 2004; Blanco-Canqui and Lal, 2010). Consequently, soil organic matter content decreases, and the soil formation rate slows, leading to significant topsoil loss over time (Hartemink et al., 2020).

Conversely, thicker topsoil was observed in coastal regions, especially near valley bottoms, due to frequent flood events (Eyre and Twigg, 1997; Speer and Leslie, 2000; Rolfe et al., 2020). These floods deposit eroded soil from upstream, contributing to thicker topsoil layer (Gregorich et al., 1998). Additionally, higher rainfall in these regions (exceeding 600 mm) facilitates active mineral redistribution (Yang et al., 2023a; Carroll-MacDonald et al., 2023), further influencing topsoil development. Dark blue areas on the map, representing the highest topsoil thickness, align with ground observation thickness and are often located in floodplain areas near rivers, where regular sediment deposition

during floods occurs. For instance, the Murray River and its adjacent floodplain shows thicker topsoil due to frequent flooding (Boulton and Lloyd, 1992; Mac Nally et al., 2011).

(a)

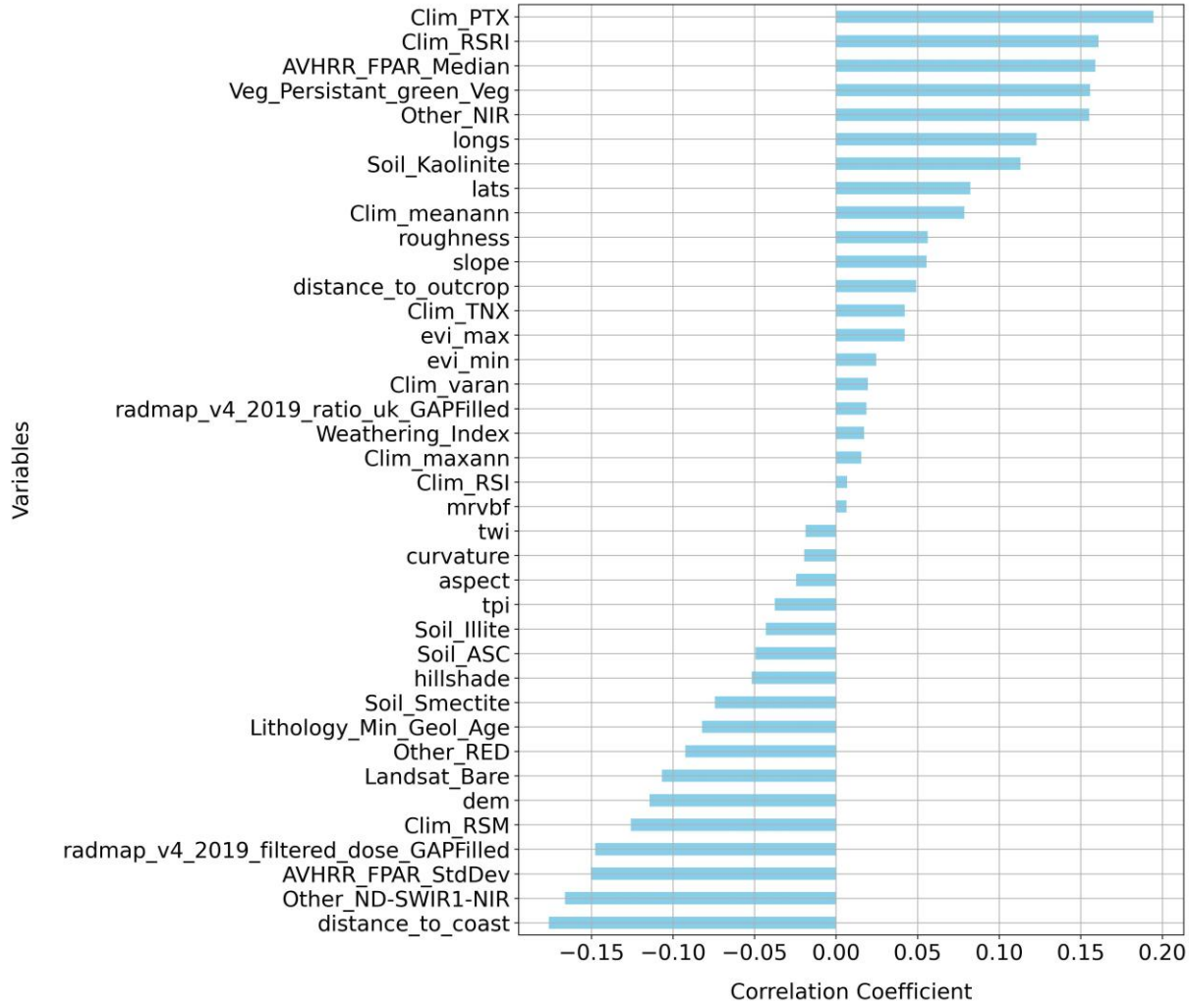

(b)

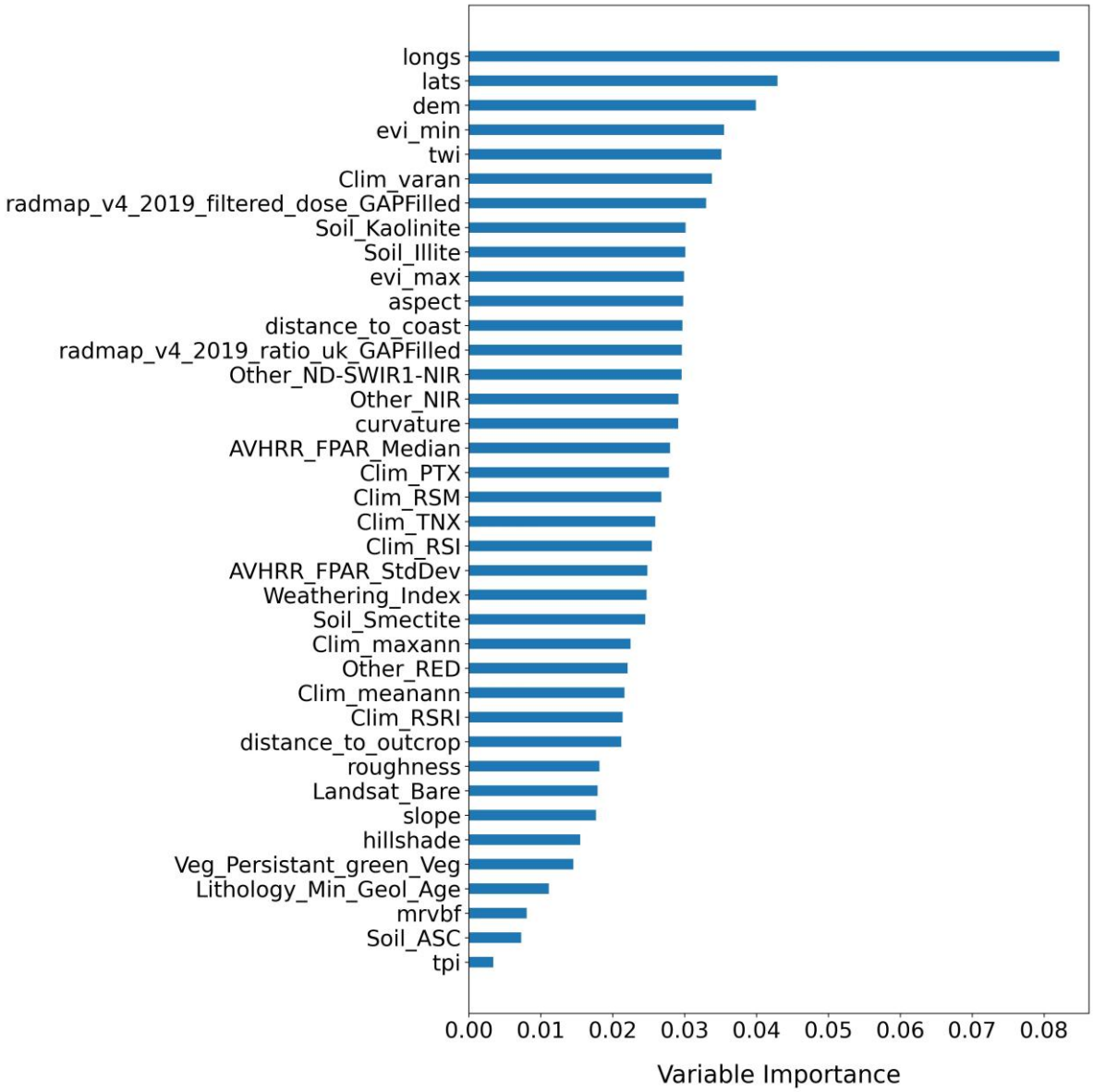
longs
lats
dem
evi_min
twi
Clim_varan
radmap_v4_2019_filtered_dose_GAPFilled
Soil_Kaolinite
Soil_Illite
evi_max
aspect
distance_to_coast
radmap_v4_2019_ratio_uk_GAPFilled
Other_ND-SWIR1-NIR
Other_NIR
curvature
AVHRR_FPAR_Median
Clim_PTX
Clim_RSM
Clim_TNX
Clim_RSI
AVHRR_FPAR_StdDev
Weathering_Index
Soil_Smectite
Clim_maxann
Other_RED
Clim_meanann
Clim_RSRI
distance_to_outcrop
roughness
Landsat_Bare
slope
hillshade
Veg_Persistant_green_Veg
Lithology_Min_Geol_Age
mrvbf
Soil_ASC
tpi
0.00
0.01
0.02
0.03
0.04
0.05
0.06
0.07
0.08
Variable Importance

(c)

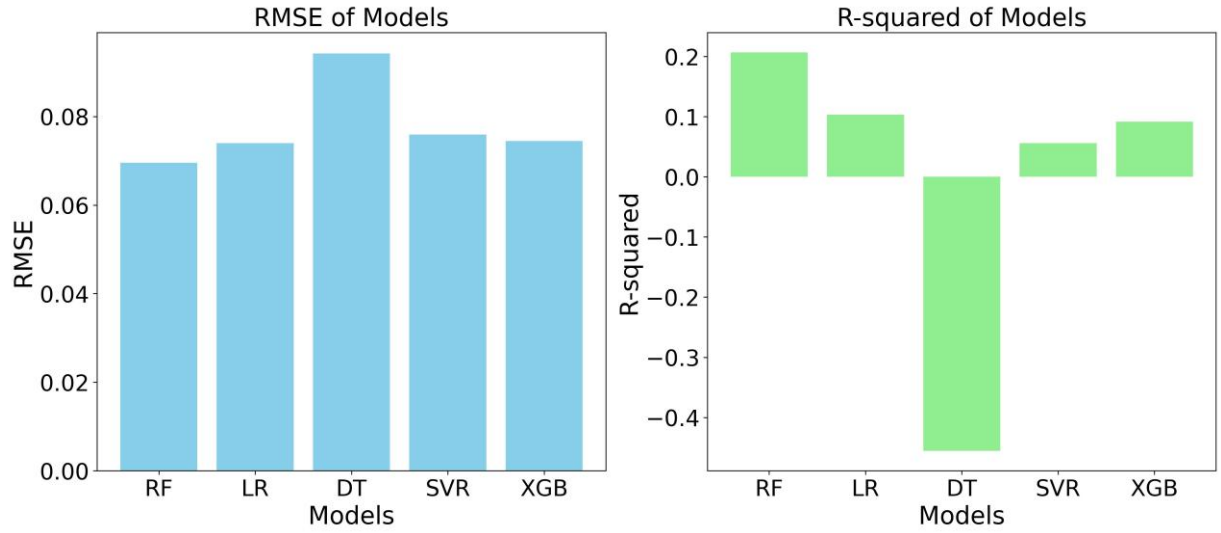

Fig. 14 (a) Pearson correlation coefficients of variables used in the model with topsoil thickness measurements, (b) variable importance in modeling topsoil thickness, (c) Comparison of different machine learning models (RF: Random Forest, LR: Linear Regression, DT: Decision Tree, SVR: Support Vector Regression, XGB: XGBoost) for predicting topsoil thickness.

2.5.2. Soil Capacity for Erosion Resistance Using Genosoil Indicators

Clay particles offer superior binding capacity compared to sand and slit, leading to greater aggregate stability and resistance to erosion (Bouyoucos, 1935; Lundekvam and Skoien, 1998; Parwada and Van Tol, 2019; Agassi, 2023). Unlike commonly used indicators such as the RUSLE soil erodibility K-factor, which is influenced by land use and external factors, and is therefore less reliable for assessing inherent soil properties over a longer timeframe (Ferreira et al., 2015; Wang and Zhang, 2021; Baskan, 2022),and soil surface shear strength, which is also affected by moisture and land use (Havaee et al., 2015; Wei et al., 2019; Wang et al., 2023) , Clay content provides a stable foundation for assessing erosion resistance, since higher clay levels are linked to stronger aggregate stability and higher critical shear stress thresholds, resulting in more resilient soils over time (Grissinger, 1966; Jesús Melej et al., 2024; Kulesza et al., 2024).

The clay ratio-capacity utility map revealed that regions with large clay content exhibited grater erosion resistance. High-capacity regions, such as the Northwest, Central West, Riverina, and Murray, benefit from this soil composition, as evidenced by their high utility values. These areas have a median clay content of approximately 46%, which significantly contributed to their resilience against erosion (Grissinger, 1966; Moragoda et al., 2022; Ayoubi et al., 2022).

The topsoil thickness-capacity utility map highlighted the crucial role of topsoil depth in erosion resistance. Higher topsoil thickness corresponds to better soil erosion resistance (Mielke and Schepers, 1986; Guo et al., 2021), as seen in the coastal regions and floodplains across NSW, where topsoil deposition is high. These regions exhibit high utility values ranging from 0.83 to 0.99. In contrast, low-capacity areas with thinner topsoil, such as the importance of topsoil thickness in mitigating erosion.

The average capacity utility map is more reliable than single-factor maps. High-capacity areas (0.781 to 0.99 utility) have favourable clay and topsoil levels, while low-capacity areas (0.0019 to 0.234) have less favorable clay or topsoil, or both. This underscores the importance of incorporating multiple soil properties such as texture and topsoil thickness into capacity estimation, as these jointly influence erosion resistance, hydrological response, and long-term soil productivity (Fu et al., 2011; Zhang et al., 2021).

2.5.3. Genosoil and Phenosoil Deviation and Its Effect on Soil Condition Utility

Our analysis of the NSW clay ratio condition map reveals significant spatial variability in the phenosoil-to-genosoil clay ratio, with an average of 0.50 ± 0.13 indicating moderate variability across the state. Regions exhibiting high utility values generally demonstrate minimal deviation, suggesting low anthropogenic disturbance and well-preserved soil profiles (Jang et al., 2022; Ng et al., 2024), eg: coastal and Riverina-Murray areas. Conversely, lower utility value regions, predominantly in northwest and associated with intensive cropping, display pronounced deviations in clay ratio. This spatial pattern is consistent with findings from southeastern Australia, where soil characteristics and erosion have been shown to be shaped by both natural topographic controls and long-

term land use such as grazing and pasture management (Senanayake et al., 2024, Senanayake et al., 2024).

Condition utility map due to topsoil thickness is driven by the difference (0.18 ± 0.19) between genosoil and phenosoil. Genosoil represents, undisturbed soil conditions (McBratney et al., 2019; Evangelista et al., 2024) and tends to have higher topsoil thickness compared to phenosoils across NSW (Fig.8 c). This difference likely reflects the cumulative effects of erosion over time, influenced by both natural and anthropogenic processes leading to long-term landscape change (Poesen, 2018). Genosoils primarily experiencing primarily natural erosion processes, while phenosoils show additional impacts from human activities such as agriculture and land management, which can accelerate topsoil loss (Schumm and Harvey, 2015; Vanwalleghem et al., 2017; Evangelista et al., 2024). This accelerated loss, particularly evident in agricultural regions practicing dry cropping, farming practices like vegetation clearance and tillage significantly drive soil erosion (Quinton & Fiener, 2024). Small soil condition utility values are predominantly found in these agricultural regions. In these areas, a high deviation between phenosoil and genosoil is observed (Fig.15). This suggests a greater human influence on soil development, as evidenced by the substantial difference between the reference (genosoil) and the current state (phenosoil) (Jang et al., 2023). Intensive cultivation practices are likely to contribute to this phenomenon by accelerating erosion processes (Loughran et al., 2004).

Conversely, areas with large soil condition values tend to exhibit minimal deviation between genosoil and phenosoils (Fig.15), potentially due to factors that minimized historical land-use change and associated soil disturbances, as evidenced by studies on erosion (Fanning, 1999) and land-use impacts on soil properties(Parker and Chartres, 1983; Banks, 2019). This minimal disruption might have preserved a thicker topsoil and a more favorable soil profile development (Parker and Chartres, 1983; Rob Banks, 2019).

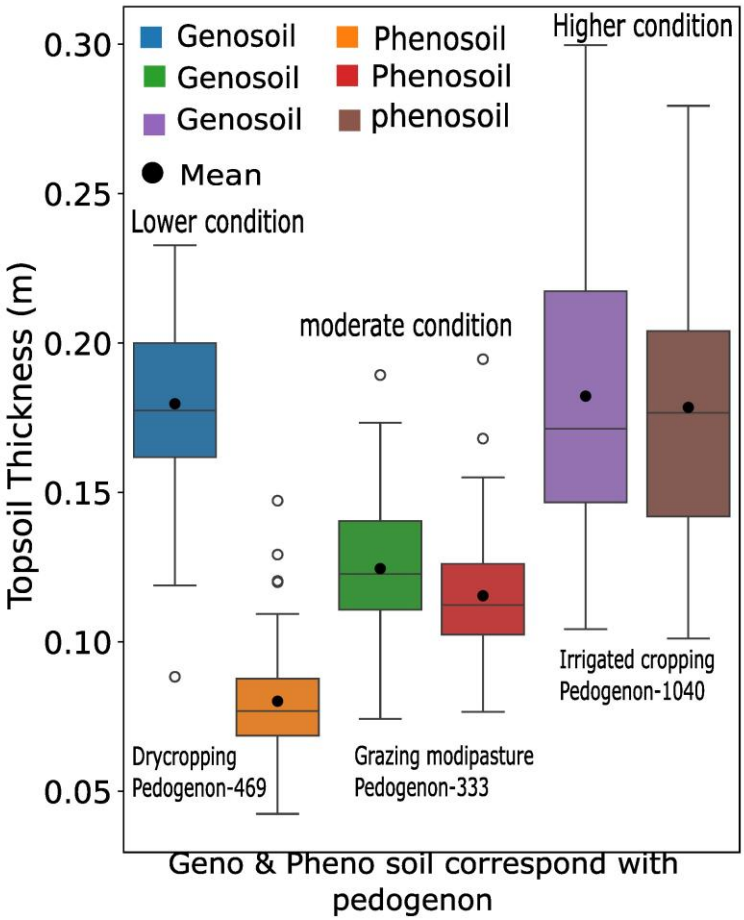

Fig.15 Deviation between genosoil and phenosoil for topsoil thickness in the pedogenon

2.5.4. Soil Erosion Risk

Our analysis of soil erosion risk in NSW leverages the concept of soil resilience, defined as the difference between a soil's inherent capacity and its current condition utility (Lal, 1997; Blanco-Canqui & Lal, 2010). The erosion risk map (Fig.13) visualizes this difference, revealing complex spatial patterns across the state. By examining the gap between inherent capacity and current soil condition (Wadoux et al., 2024), we gain valuable insights into a soil's ability to resist further erosion.

Our analysis and erosion risk mapping reveal interesting and complex patterns of high to low erosion risk throughout NSW. The cereal belt of NSW observed varying risks, with high erosion risk particularly in the upper northwest region dominated by dryland cropping, modified pastures, and grazing native vegetation. This region exhibits a significant gap between capacity and condition, leading to high erosion risk. Intensive agricultural

practices frequently disturb the soil, reducing its soil condition (Whitbread et al., 1998; Dalal & Chan, 2001; Koch et al., 2015). Despite exhibiting lower water erosion rates (< 100 kg/ha/yr) (Yang et al., 2023), these areas remain at high risk due to thinner topsoil layers and higher clay content (Fig.8 b). These conditions, while supporting intensive cropping, also increase the soil's vulnerability to degradation (Farquharson et al., 2003). Moderate to low risk is observed in regions with grazing native vegetation, dry cropping, modified pasture and irrigated cropping. The lower Riverina Murray region shows more spatial patterns where condition exceeds capacity, with negative utility values prevalent. This could be due to floodplain topsoil deposition and improved management practices (Wallbrink et al. 1996; Rayburg et al., 2023;Nordblom et al., 2023; Schrader et al., 2024).

In the far western region of NSW, our analysis shows a range from high to low erosion risk. Most of the land use in this area involves grazing native vegetation. The low erosion risk areas with negative utility values coincide with regions of high wind erosion rates (McTainsh, G.H. *et al*. 2011; Yang et al., 2023), which match low water erosion rates. Erosion rates generally range from 100 to 500 kg/ha/yr (Yang et al., 2023). This balance may help maintain soil conditions closer to their inherent capacity despite erosion pressures, due to reduced human disturbance and improved management practices in the Far West region (Leys et al., 2023).

In the coastal regions, a similar pattern is observed with low to high erosion risk, predominately high in sloped and hilly areas. The high erosion risk in these regions is due to high erosion rates (> 2000 to > 5000 kg/ha/yr) (Yang et al., 2023). The gap between capacity and condition is significant due to high rainfall and hilly topography (Yang & Yu, 2015), resulting in low current soil conditions. Lower to moderate risk is observed at the bottom of hilly areas near rivers, where the gap between capacity and condition is small, and in some cases, condition even exceeds capacity due to topsoil deposition. These areas may also experience reduced rainfall erosivity compared to upper slopes, as rainfall erosivity tends to decrease with increasing elevation (Yang & Yu, 2015; Zhu et al., 2025), further contributing to their relatively stable erosion condition.

2.5.5 Limitations and future perspectives

This framework utilises clay ratio and topsoil thickness parameters particularly relevant to water erosion to assess the soil's ability to withstand erosive forces rather than categorizing specific erosion types, making it versatile for various scenarios. While wind erosion also affects topsoil thickness (Tuo et al., 2018; Gholami et al., 2024), the current framework does not evaluate this aspect; therefore, future research should integrate wind-related variables such as surface roughness and wind speed to enhance its applicability. Additionally, although the framework assumes an inverse relationship between clay ratio and erosion vulnerability, further investigation is needed to determine if this holds across all landscapes or if region-specific adjustments to the utility functions are required.

Topsoil thickness inherently captures topographic influences (Gessler et al., 2000), as steeper slopes typically have thinner topsoil due to increased runoff and displacement , while flatter areas accumulate deeper soil layers (Benedict, 1970; Zhang et al., 2024). In this framework, genosoil represents natural erosion processes, while phenosoil reflects both natural and human-induced erosion, allowing for the assessment of anthropogenic influences on soil degradation. While erosion is affected by climate and land management (Guo et al., 2019), the emphasis on intrinsic soil properties ensures a consistent and scalable baseline for risk assessment.

This study helps prioritize soil conservation in vulnerable areas (e.g., dryland zones), recommending rehabilitation, erosion controls, and sustainable farming (Zhao et al., 2013 ;Ricci et al., 2020; Martínez-Mena et al., 2020), plus cover crops/reduced tillage for high-risk areas (Lal, 2015; Nunes et al., 2018). Their long-term effectiveness requires accounting for climate impacts on future erosion patterns(Borrelli et al., 2020).

Climate change is expected to intensify rainfall variability, increase extreme weather events, and shift vegetation cover factors that affect erosion processes (Z. Li & Fang, 2016; Borrelli et al., 2020; Eekhout & De Vente, 2022). Some regions may face more erosion due to intense rainfall (N. Li et al., 2024), while others may see reduced water erosion (Chen et al., 2024). In this study, future climate projection scenarios were not considered. The framework proposed here is based on inherent soil properties that

reflect long-term erosion processes. However, it is important to examine how these indicators respond to dynamic, climate-induced changes.

Future studies should explore how this framework can be extended by linking soil properties to climate change variables for example, by assessing how capacity and condition may shift with projected changes in rainfall erosivity or land use. This could support adaptive strategies such as climate-informed land-use planning and dynamic soil health or condition monitoring. Such advancements could help guide targeted erosion mitigation and support proactive, resilient soil management under future climate uncertainty.

2.6 Conclusion

This study introduces a novel, CCF framework for assessing erosion risk. By balancing a soil's inherent resistance with its current state, the framework effectively identifies areas vulnerable to future erosion, even under low current erosion rates. This scalable approach offers valuable insights for land managers across vast regions.

Key strengths of the framework include:

- Scalability: It requires minimal data (clay ratio and topsoil thickness) for large-scale assessments.
- Soil security Focus: It captures areas under pressure from erosion, even with low current rates, by considering both inherent capacity and current conditions.

The framework effectively distinguishes high erosion risk areas (low capability to withstand future erosion) from low erosion risk areas (higher capability to withstand future erosion). The soil condition maps for New South Wales (NSW) revealed significant spatial variation due to the cumulative effects of erosion. Areas with intensive agricultural practices, particularly cropping areas especially dry cropping areas, exhibited higher risk of soil erosion, highlighting the substantial human influence on soil capacity and condition.

By prioritising areas most susceptible to future erosion based on both inherent capacity and current condition, the framework empowers land managers to develop effective strategies for sustainable land use and soil conditions across large regions. This facilitates more effective erosion management, crucial for mitigating erosion risk and sustaining soil in NSW and beyond.

Supplementary

S1. Covariates for top-soil probability mapping

Serial	Covariants	Description	SCORPAN Compor	Category	pixel s
1	Mean_NDVI	Mean value of the Normalized Difference Vegetation Index, indicating average vegetation health.	Organisms (O)	Remote Sensing	90m
2	Max_NDVI	Maximum value of the Normalized Difference Vegetation Index, indicating peak vegetation health.	Organisms (O)	Remote Sensing	90m
3	CV_BI	Coefficient of variation of the Bare Soil Index, reflecting temporal stability of bare soil.	Soil (S)	Remote Sensing	90m
4	Mean_VV	Mean value of VV polarization backscatter from Sentinel-1, indicating surface roughness/moisture.	Organisms (O)	Remote Sensing	90m
5	Mean_VH	Mean value of VH polarization backscatter from Sentinel-1, indicating surface roughness/moisture.	Organisms (O)	Remote Sensing	90m
6	std_SWIR	Standard deviation of short-wave infrared reflectance, indicating variability in soil/vegetation characteristics.	Soil (S)	Remote Sensing	90m
7	Clim_PTX	Maximum monthly precipitation (mm)	Climate (C)	Other	90m
8	Clim_rainan	Average Rainfall - Annual	Climate (C)	Other	90m
9	Clim_RSRI	Short-wave solar radiation - min difference between successive months (SRAD data)	Climate (C)	Other	90m
10	Clim_meannn	Average daily mean temperature - Annual	Climate (C)	Other	90m
11	Clim_TNX	Minimum temperature - monthly maximum (°C)	Climate (C)	Other	90m
12	Clim_maxxnn	Average daily max temperature - Annual	Climate (C)	Other	90m
13	Clim_RSM	Short-wave solar radiation - annual mean (SRAD data)	Climate (C)	Other	90m
14	Clim_varann	Rainfall Variability - Annual	Climate (C)	Other	90m
15	PM_Lithology_MIn_Geol_Age	Surface Geology of Australia 1:1 million scale dataset 2012 edition - Minimum Geologic Age	Parent material (P)	Other	90m
16	DEM	Digital Elevation Model, representing terrain elevation.	Relief (R)	Other	90m
17	PM_filtered_dose_GAPfilled	Radiometric grid of Australia (Radmap) v4 2019 - Filtered dose	Parent material (P)	Other	90m
18	PM_2019_ratio_uk_GAPfilled	Radiometric grid of Australia (Radmap) v4 2019 - Uranium Potassium ratio	Parent material (P)	Other	90m
19	Weathering_Index	Weathering Index	Parent material (P)	Other	90m
20	Clim_RSI	Short-wave solar radiation - monthly minimum (SRAD data)	Climate (C)	Other	90m
21	PM_distance_to_outcrop	Distance from the nearest rock outcrop	Parent material (P)	Other	90m
22	Soil_Kaolinite	Maps clay minerals – kaolinite in Australian soils - 0 - 20cmKaolinite content in the soil, representing the mineral composition of the soil.	Soil (S)	Other	90m
23	Slope	Slope of the terrain, influencing runoff and erosion processes.	Relief (R)	Other	90m
24	Soil_Illite	Maps clay minerals – illite in Australian soils - 0 - 20cm	Soil (S)	Other	90m

S2. Covariates for Topsoil thickness mapping

Serial	Covariants	Description	SCORPAN Component	Category	pixel size
1	longs	Longitude coordinates of the study area.	Space (S)	Other	90m
2	lats	Latitude coordinates of the study area.	Space (S)	Other	90m
3	dem	Elevation Model (DEM)	Relief (R)	Other	90m
4	evi_min	Dataset Minimum of the timeseries 2000 - 2008	Organisms (O)	Remote Sensing	90m
5	Clim_varan	Rainfall Variability - Annual	Climate (C)	Other	90m
6	radmap_v4_2019_filtered_dose_GAPfi	Radiometric grid of Australia (Radmap) v4 2019 - Filtered dose	Parent material (P)	Other	90m
7	Soil_illite	Maps clay minerals – illite in Australian soils - 0 - 20cm	Soil (S)	Other	90m
8	Soil_kaolinite	Maps clay minerals – kaolinite in Australian soils - 0 - 20cm	Soil (S)	Other	90m
9	aspect	Aspect derived from 3" SRTM DEM-S	Relief (R)	Other	90m
10	evi_max	Dataset Maximum of the timeseries 2000 - 2008	Organisms (O)	Remote Sensing	90m
11	distance_to_coast	Eucludian distance from the coastline	Space (S)	Other	90m
12	Other_ND-SWIR1-NIR	Barest Earth Landsat Imagery - ND-SWIR1-NIR	Organisms (O)	Remote Sensing	90m
13	radmap_v4_2019_ratio_uk_GAPfilled	Australia (Radmap) v4 2019 - Uranium Potassium ratio	Parent material (P)	Other	90m
14	Other_NIR	Barest Earth Landsat Imagery - NIR	Organisms (O)	Remote Sensing	90m
15	curvature	Plan Curvature derived from 1" SRTM DEM-S	Relief (R)	Other	90m
16	Clim_PTX	Maximum monthly precipitation (mm)	Climate (C)	Other	90m
17	AVHRR_FPAR_median	Land and Water algorithm Australia coverage - Median Value in Timeseries	Organisms (O)	Remote Sensing	90m
18	Clim_RSM	Short-wave solar radiation - annual mean (SRAD data)	Climate (C)	Other	90m
19	Clim_TNX	Minimum temperature - monthly maximum (°C)	Climate (C)	Other	90m
20	Clim_RSI	Short-wave solar radiation - monthly minimum (SRAD data)	Climate (C)	Other	90m
21	Weathering_Index	Weathering Index	Parent material (P)	Other	90m
22	AVHRR_FPAR_stddev	Land and Water algorithm Australia coverage - Standard Deviation of Value in Timeseries	Organisms (O)	Remote Sensing	90m
23	Soil_Smectite	Maps clay minerals – smectite in Australian soils - 0 - 20cm	Soil (S)	Other	90m
24	Clim_maxann	Average daily max temperature - Annual	Climate (C)	Other	90m
25	Clim_meannn	Average daily mean temperature - Annual	Climate (C)	Other	90m
26	Other_Red	Barest Earth Landsat Imagery - RED	Organisms (O)	Remote Sensing	90m
27	Clim_RSRI	Short-wave solar radiation - min difference between successive months(SRAD data)	Climate (C)	Other	90m
28	distance_to_outcrop	Distance from the nearest rock outcrop	Parent material (P)	Other	90m
29	roughness	Landscape Roughness	Relief (R)	Other	90m
30	Landsat_Bare	Barest Earth Landsat Imagery	Organisms (O)	Remote Sensing	90m
31	Slope	Slope derived from 1" SRTM DEM-S	Relief (R)	Other	90m
32	hillshade	Hillshade derived from 3 second SRTM Derived Digital Elevation Model (DEM) Version 1.0.	Relief (R)	Other	90m
33	Veg_Persistent_green_Veg	Landsat 2000-2010 Persistent Green-Vegetation Fraction	Organisms (O)	Remote Sensing	90m
34	Lithology_Min_Geol_Age	Surface Geology of Australia 1:1 million scale dataset 2012 edition - Minimum Geologic Age	Parent material (P)	Other	90m
35	mrvbf	Multi-resolution Valley Bottom Flatness	Relief (R)	Other	90m
36	Soil_ASC	Australian Soil Classification data, categorizing soil types.	Soil (S)	Other	90m
37	tpi	Topographic Position Index derived from 1" SRTM DEM-S	Relief (R)	Other	90m
38	twi	Topographic Wetness Index derived from 1" SRTM DEM-H	Relief (R)	Other	90m

S3. Summarizing statistics of topsoil thickness for each land use.

Land Use Category	Mean	Standard Deviation	Variance	Q1	Q2 (Median)	Q3	Min	Max
Dry Cropland	0.14	0.07	0.01	0.10	0.12	0.18	0.01	0.50
Dry Horticulture	0.15	0.10	0.01	0.10	0.10	0.19	0.05	0.48
Grazing Modified Pasture	0.17	0.09	0.01	0.10	0.15	0.23	0.01	0.50
Grazing Native Vegetation	0.15	0.09	0.01	0.10	0.14	0.20	0.01	0.50
Intensive Horticulture	0.15	0.08	0.01	0.10	0.15	0.19	0.05	0.30
Irrigated Cropping	0.18	0.12	0.01	0.08	0.15	0.30	0.01	0.50
Irrigated Horticulture	0.20	0.13	0.02	0.10	0.15	0.30	0.05	0.50
TST-Irrigated Pastures	0.19	0.15	0.02	0.10	0.10	0.20	0.10	0.50
Managed Resource Protection	0.14	0.06	0.00	0.10	0.12	0.20	0.04	0.25
Nature Conservation	0.17	0.10	0.01	0.10	0.15	0.23	0.01	0.50
Plantation Forest	0.15	0.09	0.01	0.09	0.14	0.20	0.01	0.40
Production Native Forest	0.17	0.09	0.01	0.10	0.15	0.22	0.02	0.50

2.7. References

Agassi, M. (2023). Soil Erosion, Conservation, and Rehabilitation (1st ed.). CRC Press. https://doi.org/10.1201/9781003418177

Amundson, R., Berhe, A. A., Hopmans, J. W., Olson, C., Sztein, A. E., & Sparks, D. L. (2015). Soil and human security in the 21st century. Science, 348(6235), 1261071. https://doi.org/10.1126/science.1261071

Andrews, S. S., Karlen, D. L., & Mitchell, J. P. (2002). A comparison of soil quality indexing methods for vegetable production systems in Northern California. Agriculture, Ecosystems & Environment, 90(1), 25–45. https://doi.org/10.1016/S0167-8809(01)00174-8

Are, K. S., Oshunsanya, S. O., & Oluwatosin, G. A. (2018). Changes in soil physical health indicators of an eroded land as influenced by integrated use of narrow grass strips and mulch. Soil and Tillage Research, 184, 269–280. https://doi.org/10.1016/j.still.2018.08.009

Ayoubi, S., Milikian, A., Mosaddeghi, M. R., Zeraatpisheh, M., & Zhao, S. (2022). Impacts of Clay Content and Type on Shear Strength and Splash Erosion of Clay–Sand Mixtures. Minerals, 12(11), 1339. https://doi.org/10.3390/min12111339

Baghdadi, N., Hajj, M. E., Choker, M., Zribi, M., Bazzi, H., Vaudour, E., Gilliot, J.-M., & Ebengo, D. M. (2018). Potential of Sentinel-1 Images for Estimating the Soil Roughness over Bare Agricultural Soils.

Banks, Robert Gordon (2019). Rapid soil development in response to land use change: case studies from the north New South Wales slopes and plains. England Tablelands. PhD thesis, School of Agriculture and Food Sciences, The University of Queensland. http://doi.org/10.14264/914u3q

Bashagaluke, J. B., Logah, V., Opoku, A., Sarkodie-Addo, J., & Quansah, C. (2018). Soil nutrient loss through erosion: Impact of different cropping systems and soil amendments in Ghana. PLOS ONE, 13(12), e0208250. https://doi.org/10.1371/journal.pone.0208250

Baskan, O. (2022). Analysis of spatial and temporal changes of RUSLE-K soil erodibility factor in semi-arid areas in two different periods by conditional simulation. Archives of Agronomy and Soil Science, 68(12), 1698–1710. https://doi.org/10.1080/03650340.2021.1922673

Bastida, F., Zsolnay, A., Hernández, T., & García, C. (2008). Past, present and future of soil quality indices:A biological perspective. Geoderma, 147(3–4), 159–171. https://doi.org/10.1016/j.geoderma.2008.08.007.

Blanco, H., & Lal, R. (2023). Wind Erosion. In H. Blanco & R. Lal, Soil Conservation and Management (pp. 73–88). Springer Nature Switzerland. https://doi.org/10.1007/978-3-031-30341-8_4

Blanco-Canqui, H., & Lal, R. (2010). Soil Resilience and Conservation. In H. Blanco-Canqui & R. Lal, Principles of Soil Conservation and Management (pp. 425–447). Springer Netherlands. https://doi.org/10.1007/978-1-4020-8709-7_16

Benedict, J. B. (1970). Downslope Soil Movement in a Colorado Alpine Region: Rates, Processes, and Climatic Significance. Arctic and Alpine Research, 2(3), 165–226. https://doi.org/10.1080/00040851.1970.12003576

Blanco-Canqui, H., & Lal, R. (2010). Principles of Soil Conservation and Management. Springer Netherlands. https://doi.org/10.1007/978-1-4020-8709-7

Borrelli, P., Alewell, C., Alvarez, P., Anache, J. A. A., Baartman, J., Ballabio, C., Bezak, N., Biddoccu, M., Cerdà, A., Chalise, D., Chen, S., Chen, W., De Girolamo, A. M., Gessesse, G. D., Deumlich, D., Diodato, N., Efthimiou, N., Erpul, G., Fiener, P., … Panagos, P. (2021). Soil erosion modelling: A global review and statistical analysis. Science of The Total Environment, 780, 146494. https://doi.org/10.1016/j.scitotenv.2021.146494

Borrelli, P., Robinson, D. A., Panagos, P., Lugato, E., Yang, J. E., Alewell, C., Wuepper, D., Montanarella, L., & Ballabio, C. (2020). Land use and climate change impacts on global soil erosion by water (2015-2070). Proceedings of the National Academy of Sciences, 117(36), 21994–22001. https://doi.org/10.1073/pnas.2001403117

Boulton, A. J., & Lloyd, L. N. (1992). Flooding frequency and invertebrate emergence from dry floodplain sediments of the river murray, Australia. Regulated Rivers: Research & Management, 7(2), 137–151. https://doi.org/10.1002/rrr.3450070203

Bouyoucos, G. J. (1935). The Clay Ratio as a Criterion of Susceptibility of Soils to Erosion 1. Agronomy Journal, 27(9), 738–741. https://doi.org/10.2134/agronj1935.00021962002700090007x

Bridges, E. M., & Oldeman, L. R. (1999). Global Assessment of Human-Induced Soil Degradation. Arid Soil Research and Rehabilitation, 13(4), 319–325. https://doi.org/10.1080/089030699263212

Bui, E. N., Hancock, G. J., & Wilkinson, S. N. (2011). 'Tolerable' hillslope soil erosion rates in Australia: Linking science and policy. Agriculture, Ecosystems & Environment, 144(1), 136–149. https://doi.org/10.1016/j.agee.2011.07.022

Carroll-MacDonald, T.-A., Rayburg, S., & Neave, M. (2023). Spatial Variability of Topsoil Properties on a Semi-Arid Floodplain. Soil Systems, 7(2), 42. https://doi.org/10.3390/soilsystems7020042

Chen, X., Zhang, X., Wei, Y., Zhang, S., Cai, C., Guo, Z., & Wang, J. (2023). Assessment of soil quality in a heavily fragmented micro-landscape induced by gully erosion. Geoderma, 431, 116369. https://doi.org/10.1016/j.geoderma.2023.116369

Chen, Y., Wei, T., Li, J., Xin, Y., & Ding, M. (2024). Future changes in global rainfall erosivity: Insights from the precipitation changes. Journal of Hydrology, 638, 131435. https://doi.org/10.1016/j.jhydrol.2024.131435

Couper, P. (2003). Effects of silt–clay content on the susceptibility of river banks to subaerial erosion. Geomorphology, 56(1–2), 95–108. https://doi.org/10.1016/S0169-555X(03)00048-5

Dalal, R. C., & Chan, K. Y. (2001). Soil organic matter in rainfed cropping systems of the Australian cereal belt. Soil Research, 39(3), 435. https://doi.org/10.1071/SR99042

Dotterweich, M., Rodzik, J., Zgłobicki, W., Schmitt, A., Schmidtchen, G., & Bork, H.-R. (2012). High resolution gully erosion and sedimentation processes, and land use changes since the Bronze Age and future trajectories in the Kazimierz Dolny area

(Nałęczów Plateau, SE-Poland). CATENA, 95, 50–62. https://doi.org/10.1016/j.catena.2012.03.001

Eekhout, J. P. C., & De Vente, J. (2022). Global impact of climate change on soil erosion and potential for adaptation through soil conservation. Earth-Science Reviews, 226, 103921. https://doi.org/10.1016/j.earscirev.2022.103921

Escadafal, R. (1989). Remote sensing of arid soil surface color with Landsat thematic mapper. Advances in Space Research, 9(1), 159–163. https://doi.org/10.1016/0273-1177(89)90481-X

Evangelista, S. J., Field, D. J., McBratney, A. B., Minasny, B., Ng, W., Padarian, J., Román Dobarco, M., & Wadoux, A. M. J.-C. (2023). A proposal for the assessment of soil security: Soil functions, soil services and threats to soil. Soil Security, 10, 100086. https://doi.org/10.1016/j.soisec.2023.100086

Evangelista, S. J., Field, D. J., McBratney, A. B., Minasny, B., Ng, W., Padarian, J., Román Dobarco, M., & Wadoux, A. M. J.-C. (2024). Soil security—Strategizing a sustainable future for soil. In Advances in Agronomy (Vol. 183, pp. 1–70). Elsevier. https://doi.org/10.1016/bs.agron.2023.10.001

European Commission (2006). Communication from the Commission to the Council, the EuropeanParliament, the European Economic and Social Committee and the Committee of the Regions: Thematic Strategy for Soil Protection. COM(2006) 231 final, Brussels.

Eyre, B., & Twigg, C. (1997). Nutrient Behaviour During Post-flood Recovery of the Richmond River Estuary, Northern NSW, Australia. Estuarine, Coastal and Shelf Science, 44(3), 311–326. https://doi.org/10.1006/ecss.1996.0124

Fang, H., Zhai, Y., & Li, C. (2024). Evaluating the impact of soil erosion on soil quality in an agricultural land, northeastern China. Scientific Reports, 14(1), 15629. https://doi.org/10.1038/s41598-024-65646-5.

Fanning, P. C. (1999). Recent landscape history in arid western New South Wales, Australia: A model for regional change. Geomorphology, 29(3–4), 191–209. https://doi.org/10.1016/S0169-555X(99)00014-8

Farquharson, R. J., Schwenke, G. D., & Mullen, J. D. (2003). Should we manage soil organic carbon in Vertosols in the northern grains region of Australia? Australian Journal of Experimental Agriculture, 43(3), 261. https://doi.org/10.1071/EA00163

Ferreira, V., Panagopoulos, T., Andrade, R., Guerrero, C., & Loures, L. (2015). Spatial variability of soil properties and soil erodibility in the Alqueva dam watershed, Portugal. https://doi.org/10.5194/sed-7-301-2015

Fu, Z., Li, Z., Cai, C., Shi, Z., Xu, Q., & Wang, X. (2011). Soil thickness effect on hydrological and erosion characteristics under sloping lands: A hydropedological perspective. Geoderma, 167–168, 41–53. https://doi.org/10.1016/j.geoderma.2011.08.013

Foster, G. R., Young, R. A., Römkens, M. J. M., & Onstad, C. A. (2015). Processes of Soil Erosion by Water. In R. F. Follett & B. A. Stewart (Eds.), ASA, CSSA, and SSSA Books (pp. 137–162). American Society of Agronomy, Crop Science Society of

America, Soil Science Society of America. https://doi.org/10.2134/1985.soilerosionandcrop.c9

Francos, N., McBratney, A. B., Field, D. J., Minasny, B., Pachon, J. C., Padarian, J., … O'Donoghue, T.(2024). Valuing and integrating soil roles in assessing the capital dimension of soil security: An Australian case study. Soil Security, 16, 100141. https://doi.org/10.1016/j.soisec.2024.100141.

Freebairn, D. M., Cornish, P. S., Anderson, W. K., Walker, S. R., Brett Robinson, J., & Beswick, A. R. (2015). Management Systems in Climate Regions of the World-Australia. In G. A. Peterson, P. W. Unger, & W. A. Payne (Eds.), Agronomy Monographs (pp. 837–878). American Society of Agronomy, Crop Science Society of America, Soil Science Society of America. https://doi.org/10.2134/agronmonogr23.2ed.c20

García-Ruiz, J. M., Nadal-Romero, E., Lana-Renault, N., & Beguería, S. (2013). Erosion in Mediterranean landscapes: Changes and future challenges. Geomorphology, 198, 20–36. https://doi.org/10.1016/j.geomorph.2013.05.023

Gregorich, E. G., Greer, K. J., Anderson, D. W., & Liang, B. C. (1998). Carbon distribution and losses: Erosion and deposition effects. Soil and Tillage Research, 47(3–4), 291–302. https://doi.org/10.1016/S0167-1987(98)00117-2

Grissinger, E. H. (1966). Resistance of selected clay systems to erosion by water. Water Resources Research, 2(1), 131–138. https://doi.org/10.1029/WR002i001p00131

Gessler, P. E., Chadwick, O. A., Chamran, F., Althouse, L., & Holmes, K. (2000). Modeling Soil–Landscape and Ecosystem Properties Using Terrain Attributes. Soil Science Society of America Journal, 64(6), 2046–2056. https://doi.org/10.2136/sssaj2000.6462046x

Gholamhosseinian, A., Bashtian, M. H., & Sepehr, A. (2022). Soil Quality: Concepts, Importance, Indicators, and Measurement. In Rakshit, A., Ghosh, S., Vasenev, V., Pathak, H., & Rajput, V. D. (Eds.), Soils in Urban Ecosystem (pp. 161–187). Singapore: Springer. https://doi.org/10.1007/978-981-16-8914-7-8.

Gholami, H., Mohammadifar, A., Song, Y., Li, Y., Rahmani, P., Kaskaoutis, D. G., Panagos, P., & Borrelli, P. (2024). An assessment of global land susceptibility to wind erosion based on deep-active learning modelling and interpretation techniques. Scientific Reports, 14(1), 18951. https://doi.org/10.1038/s41598-024-70125-y

Guo, L., Yang, Y., Zhao, Y., Li, Y., Sui, Y., Tang, C., Jin, J., & Liu, X. (2021). Reducing topsoil depth decreases the yield and nutrient uptake of maize and soybean grown in a glacial till. Land Degradation & Development, 32(9), 2849–2860. https://doi.org/10.1002/ldr.3868

Guo, Y., Peng, C., Zhu, Q., Wang, M., Wang, H., Peng, S., & He, H. (2019). Modelling the impacts of climate and land use changes on soil water erosion: Model applications, limitations and future challenges. Journal of Environmental Management, 250, 109403. https://doi.org/10.1016/j.jenvman.2019.109403

Hancock, G. R., Wells, T., Dever, C., & Braggins, M. (2019). Hillslope and point based soil erosion – an evaluation of a Landscape Evolution Model. Earth Surface Processes and Landforms, 44(5), 1163–1177. https://doi.org/10.1002/esp.4566

Harmon, R. S., & Doe, W. W. (Eds.). (2001). Landscape erosion and evolution modeling. Kluwer Academic/Plenum Publishers.

Hartemink, A. E., Zhang, Y., Bockheim, J. G., Curi, N., Silva, S. H. G., Grauer-Gray, J., Lowe, D. J., & Krasilnikov, P. (2020). Soil horizon variation: A review. In Advances in Agronomy (Vol. 160, pp. 125–185). Elsevier. https://doi.org/10.1016/bs.agron.2019.10.003

Havaee, S., Mosaddeghi, M. R., & Ayoubi, S. (2015). In situ surface shear strength as affected by soil characteristics and land use in calcareous soils of central Iran. Geoderma, 237–238, 137–148. https://doi.org/10.1016/j.geoderma.2014.08.016

Herrick, J. E., Weltz, M. A., Reeder, J. D., Schuman, C. E., & Simanton, J. R. (2018). Rangeland Soil Erosion and Soil Quality: Role of Soil Resistance, Resilience, and Disturbance Regime. In R. Lal (Ed.), Soil Quality and Soil Erosion (1st ed., pp. 209–233). CRC Press. https://doi.org/10.1201/9780203739266-13

Hoskera, A. K., Nico, G., Ahmed, M. I., & Whitbread, A. (2020). Accuracies of Soil Moisture Estimations Using a Semi-Empirical Model over Bare Soil Agricultural Croplands from Sentinel-1 SAR Data.

Hounkpatin, K. O. L., Schmidt, K., Stumpf, F., Forkuor, G., Behrens, T., Scholten, T., Amelung, W., & Welp, G. (2018). Predicting reference soil groups using legacy data: A data pruning and Random Forest approach for tropical environment (Dano catchment, Burkina Faso). Scientific Reports, 8(1), 9959. https://doi.org/10.1038/s41598-018-28244-w

Huang, J., McBratney, A. B., Malone, B. P., & Field, D. J. (2018). Mapping the transition from pre-European settlement to contemporary soil conditions in the Lower Hunter Valley, Australia. Geoderma, 329,27–42. https://doi.org/10.1016/j.geoderma.2018.05.016.

Jesús Melej, M., Acevedo, S. E., Contreras, C. P., Giraldo, C. V., Maurer, T., Calderón, F. J., & Bonilla, C. A. (2024). Changes in macroaggregate stability as a result of wetting/drying cycles of soils with different organic matter and clay contents. Geoderma, 448, 116965. https://doi.org/10.1016/j.geoderma.2024.116965

Jang, H. J., Dobarco, M. R., Minasny, B., Campusano, J. P., & McBratney, A. (2023). Assessing human impacts on soil organic carbon change in the Lower Namoi Valley, Australia. Anthropocene, 43, 100393. https://doi.org/10.1016/j.ancene.2023.100393

Jang, H. J., Román Dobarco, M., Minasny, B., McBratney, A., & Jones, E. (2022). Developing and testing of pedogenons in the lower Namoi valley, NSW, Australia. Geoderma, 428, 116182. https://doi.org/10.1016/j.geoderma.2022.116182

Kaihura, F. B., Kullaya, I., Kilasara, M., Lal, R., Singh, B. R., & Aune, J. B. (1997). Topsoil Thichkness Effects on Soil Properties and Maize (Zea mays) Yield in Three Ecoregions of Tanzania. Journal of Sustainable Agriculture, 9(1), 11–30. https://doi.org/10.1300/J064v09n01_04

Karlen, D. L., & Stott, D. E. (2015). A Framework for Evaluating Physical and Chemical Indicators of Soil Quality. In J. W. Doran, D. C. Coleman, D. F. Bezdicek, & B. A. Stewart (Eds.), SSSA Special Publications (pp. 53–72). Soil Science Society of America and American Society of Agronomy. https://doi.org/10.2136/sssaspecpub35.c4

Ke, Y., Im, J., Lee, J., Gong, H., & Ryu, Y. (2015). Characteristics of Landsat 8 OLI-derived NDVI by comparison with multiple satellite sensors and in-situ observations. Remote Sensing of Environment.

Kusre, B. C., Ghosh, P., & Nath, K. (2018). Prioritization of soil conservation measures using erodibility indices as criteria in Sikkim (India). Journal of Earth System Science, 127(6), 81. https://doi.org/10.1007/s12040-018-0981-9

Kulesza, S. E., Mathis, M. A., Alarcon, V. J., & Sassenrath, G. F. (2024). Critical shear stress variability in claypan soils with depth. Journal of Soil and Water Conservation, 79(2), 66–77. https://doi.org/10.2489/jswc.2024.00099

Koch, A., Chappell, A., Eyres, M., & Scott, E. (2015). Monitor Soil Degradation or Triage for Soil Security? An Australian Challenge. Sustainability, 7(5), 4870–4892. https://doi.org/10.3390/su7054870

Lagomarsino, D., Tofani, V., Segoni, S., Catani, F., & Casagli, N. (2017). A Tool for Classification and Regression Using Random Forest Methodology: Applications to Landslide Susceptibility Mapping and Soil Thickness Modeling. Environmental Modeling & Assessment, 22(3), 201–214. https://doi.org/10.1007/s10666-016-9538-y

Lal, R. (1997). Degradation and resilience of soils. Philosophical Transactions of the Royal Society of London. Series B: Biological Sciences, 352(1356), 997–1010. https://doi.org/10.1098/rstb.1997.0078

Lal, R. (1993). Tillage effects on soil degradation, soil resilience, soil quality, and sustainability. Soil and Tillage Research, 27(1–4), 1–8. https://doi.org/10.1016/0167-1987(93)90059-X

Lal, R. (2001). Soil degradation by erosion. Land Degradation & Development, 12(6), 519–539. https://doi.org/10.1002/ldr.472

Lal, R. (2004). Soil Carbon Sequestration Impacts on Global Climate Change and Food Security. Science, 304(5677), 1623–1627. https://doi.org/10.1126/science.1097396

Lal, R. (2007). Carbon Management in Agricultural Soils. Mitigation and Adaptation Strategies for Global Change, 12(2), 303–322. https://doi.org/10.1007/s11027-006-9036-7

Lal, R. (2009). Soils and world food security. Soil and Tillage Research, 102(1), 1–4. https://doi.org/10.1016/j.still.2008.08.001

Lal, R. (2015). Restoring Soil Quality to Mitigate Soil Degradation. Sustainability, 7(5), 5875–5895. https://doi.org/10.3390/su7055875.

Leys, J. F., Shields, T., Murphy, S. R., & Koen, T. (2023). Changes in land management practices have reduced wind erosion in the cropping areas of far south-western NSW, Australia. The Rangeland Journal, 44(6), 309–319. https://doi.org/10.1071/RJ22028

Loughran, R. J., Elliott, G. L., McFarlane, D. J., & Campbell, B. L. (2004). A Survey of Soil Erosion in Australia using Caesium-137. Australian Geographical Studies, 42(2), 221–233. https://doi.org/10.1111/j.1467-8470.2004.00261.x

Lovell, R. S. L., Collins, S., Martin, S. H., Pigot, A. L., & Phillimore, A. B. (2023). Space-for-timesubstitutions in climate change ecology and evolution. Biological Reviews, 98(6), 2243–2270. https://doi.org/10.1111/brv.13004.

Lundekvam, H., & Skoien, S. (1998). Soil erosion in Norway. An overview of measurements from soil loss plots. Soil Use and Management, 14(2), 84–89. https://doi.org/10.1111/j.1475-2743.1998.tb00620.x

Li, N., Zhao, H., Luo, Z., Wang, T., Yang, J., Li, L., & Que, S. (2024). Soil erosion prediction in multiple scenarios based on climate change and land use regulation policies in context of sustainable agriculture. CATENA, 247, 108525. https://doi.org/10.1016/j.catena.2024.108525

Li, Z., & Fang, H. (2016). Impacts of climate change on water erosion: A review. Earth-Science Reviews, 163, 94–117. https://doi.org/10.1016/j.earscirev.2016.10.004

Mac Nally, R., Cunningham, S. C., Baker, P. J., Horner, G. J., & Thomson, J. R. (2011). Dynamics of Murray-Darling floodplain forests under multiple stressors: The past, present, and future of an Australian icon. Water Resources Research, 47(12), 2011WR010383. https://doi.org/10.1029/2011WR010383

Matsumoto, S., Ogata, S., Shimada, H., Sasaoka, T., Hamanaka, A., & Kusuma, G. (2018). Effects of pH-Induced Changes in Soil Physical Characteristics on the Development of Soil Water Erosion. Geosciences, 8(4), 134. https://doi.org/10.3390/geosciences8040134

Martínez-Mena, M., Carrillo-López, E., Boix-Fayos, C., Almagro, M., García Franco, N., Díaz-Pereira, E., Montoya, I., & De Vente, J. (2020). Long-term effectiveness of sustainable land management practices to control runoff, soil erosion, and nutrient loss and the role of rainfall intensity in Mediterranean rainfed agroecosystems. CATENA, 187, 104352. https://doi.org/10.1016/j.catena.2019.104352

McBratney, A. B., Mendonça Santos, M. L., & Minasny, B. (2003). On digital soil mapping. Geoderma, 117(1–2), 3–52. https://doi.org/10.1016/S0016-7061(03)00223-4

McBratney, A., Field, D. J., & Koch, A. (2014). The dimensions of soil security. Geoderma, 213, 203–213. https://doi.org/10.1016/j.geoderma.2013.08.013

McBratney, Alex. B., Field, D., Morgan, C. L. S., & Huang, J. (2019). On Soil Capability, Capacity, and Condition. Sustainability, 11(12), 3350. https://doi.org/10.3390/su11123350

McTainsh, G.H., Leys, J.F., O'Loingsigh, T. & Strong, C.L., 2011. Wind erosion and land management in Australia during 1940–1949 and 2000–2009. Report prepared for the Australian Government Department of Sustainability, Environment, Water, Population and Communities, on behalf of the State of the Environment 2011 Committee, Canberra: DSEWPaC.

Mielke, L. N., & Schepers, J. S. (1986). Plant response to topsoil thickness on an eroded loess soil. Journal of Soil and Water Conservation, 41(1), 59.

Mullissa, A., Vollrath, A., Odongo-Braun, C., Slagter, B., Balling, J., Gou, Y., Gorelick, N., & Reiche, J. (2021). Sentinel-1 SAR Backscatter Analysis Ready Data Preparation in Google Earth Engine.

Moragoda, N., Kumar, M., & Cohen, S. (2022). Representing the role of soil moisture on erosion resistance in sediment models: Challenges and opportunities. Earth-Science Reviews, 229, 104032. https://doi.org/10.1016/j.earscirev.2022.104032

Malone, Brendan; & Searle, Ross (2022): Soil and Landscape Grid National Soil Attribute Maps - Clay (3" resolution) - Release 2. v5. CSIRO. Data Collection. https://doi.org/10.25919/hc4s-3130

Mandal, D., Chandrakala, M., Alam, N. M., Roy, T., & Mandal, U. (2021). Assessment of soil quality andproductivity in different phases of soil erosion with the focus on land degradation neutrality in tropical humidregion of India. CATENA, 204, 105440. https://doi.org/10.1016/j.catena.2021.105440.

Nearing, M. A., Xie, Y., Liu, B., & Ye, Y. (2017). Natural and anthropogenic rates of soil erosion. International Soil and Water Conservation Research, 5(2), 77–84. https://doi.org/10.1016/j.iswcr.2017.04.001

Nosrati, K. (2013). Assessing soil quality indicator under different land use and soil erosion using multivariate statistical techniques. Environmental Monitoring and Assessment, 185(4), 2895–2907. https://doi.org/10.1007/s10661-012-2758-y

Nosrati, K., & Collins, A. L. (2019). A soil quality index for evaluation of degradation under land use and soil erosion categories in a small mountainous catchment, Iran. Journal of Mountain Science, 16(11), 2577–2590. https://doi.org/10.1007/s11629-019-5567-8

Nordblom, T., Gurusinghe, S., Erbacher, A., & Weston, L. A. (2023). Opportunities and Challenges for Cover Cropping in Sustainable Agriculture Systems in Southern Australia. Agriculture, 13(3), 688. https://doi.org/10.3390/agriculture13030688

Nunes, M. R., Van Es, Schindelbeck, R., Ristow, A. J., & Ryan, M. (2018). No-till and cropping systemdiversification improve soil health and crop yield. Geoderma, 328, 30–43. https://doi.org/10.1016/j.geoderma.2018.04.031.

Ng, W., Evangelista, S. J., Padarian, J., Pachon, J., O'Donoghue, T., Xue, P., Francos, N., & McBratney, A. B. (2024). Estimating surrogates, utility graphs and indicator sets for soil capacity and security assessments using legacy data. Soil Research, 62(2). https://doi.org/10.1071/SR23138

Okujeni, A., Kowalski, K., Lewińska, K. E., Schneidereit, S., & Hostert, P. (2024). Multidecadal grassland fractional cover time series retrieval for Germany from the Landsat and Sentinel-2 archives. Remote Sensing of Environment, 302, 113980. https://doi.org/10.1016/j.rse.2023.113980

Olaniya, M., Bora, P. K., Das, S., & Chanu, P. H. (2020). Soil erodibility indices under different land uses in Ri-Bhoi district of Meghalaya (India). Scientific Reports, 10(1), 14986. https://doi.org/10.1038/s41598-020-72070-y

Osman, K. T. (2014). Soil Degradation, Conservation and Remediation. Springer Netherlands. https://doi.org/10.1007/978-94-007-7590-9

Osman, K. T. (2018). Dryland Soils. In K. T. Osman (Ed.), Management of Soil Problems (pp. 15–36). Springer International Publishing. https://doi.org/10.1007/978-3-319-75527-4_2

Parihar, C. M., Singh, A. K., Jat, S. L., Ghosh, A., Dey, A., Nayak, H. S., Parihar, M. D., Mahala, D. M., Yadav, R. K., Rai, V., Satayanaryana, T., & Jat, M. L. (2019). Dependence of temperature sensitivity of soil organic carbon decomposition on nutrient management options under conservation agriculture in a sub-tropical Inceptisol. Soil and Tillage Research, 190, 50–60. https://doi.org/10.1016/j.still.2019.02.016

Parker, C. J., & Chartres, C. J. (1983). The effects of recent land use changes on red podzolic soils near Sydney, N.S.W., Australia. CATENA, 10(1–2), 61–76. https://doi.org/10.1016/S0341-8162(83)80005-8

Parwada, C., & Van Tol, J. (2019). Effects of litter quality on macroaggregates reformation and soil stability in different soil horizons. Environment, Development and Sustainability, 21(3), 1321–1339. https://doi.org/10.1007/s10668-018-0089-z

Pimentel, D., & Kounang, N. (1998). Ecology of Soil Erosion in Ecosystems. Ecosystems, 1(5), 416–426. https://doi.org/10.1007/s100219900035

Pinheiro Junior, C. R., Salvador, C. A., Tavares, T. R., Abreu, M. C., Fagundes, H. S., Almeida, W. S., Silva Neto, E. C., Anjos, L. H. C., & Pereira, M. G. (2022). Lithic soils in the semi-arid region of Brazil: Edaphic characterization and susceptibility to erosion. Journal of Arid Land, 14(1), 56–69. https://doi.org/10.1007/s40333-022-0002-3

Poesen, J. (2018). Soil erosion in the Anthropocene: Research needs. Earth Surface Processes and Landforms, 43(1), 64–84. https://doi.org/10.1002/esp.4250

Pozza, L. E., & Field, D. J. (2020). The science of Soil Security and Food Security. Soil Security, 1, 100002. https://doi.org/10.1016/j.soisec.2020.100002

Quinton, J. N., & Fiener, P. (2024). Soil erosion on arable land: An unresolved global environmental threat. Progress in Physical Geography: Earth and Environment, 48(1), 136–161. https://doi.org/10.1177/03091333231216595

Raj, R., Saharia, M., & Chakma, S. (2023). Mapping soil erodibility over India. CATENA, 230, 107271. https://doi.org/10.1016/j.catena.2023.107271

Rajan, K., Natarajan, A., Kumar, K. S. A., Badrinath, M. S., & Gowda, R. C. (2010). Soil organic carbon – the most reliable indicator for monitoring land degradation by soil erosion. Current Science, 99(6), 823–827. JSTOR.

Raschka, S. (2020). Model Evaluation, Model Selection, and Algorithm Selection in Machine Learning (arXiv:1811.12808). arXiv. http://arxiv.org/abs/1811.12808

Rayburg, S., Neave, M., & Thompson-Laing, J. (2023). The Impact of Flood Frequency on the Heterogeneity of Floodplain Surface Soil Properties. Soil Systems, 7(3), 63. https://doi.org/10.3390/soilsystems7030063

Ricci, G. F., Jeong, J., De Girolamo, A. M., & Gentile, F. (2020). Effectiveness and feasibility of different management practices to reduce soil erosion in an agricultural watershed. Land Use Policy, 90, 104306. https://doi.org/10.1016/j.landusepol.2019.104306

Rolfe, M. I., Pit, S. W., McKenzie, J. W., Longman, J., Matthews, V., Bailie, R., & Morgan, G. G. (2020). Social vulnerability in a high-risk flood-affected rural region of NSW, Australia. Natural Hazards, 101(3), 631–650. https://doi.org/10.1007/s11069-020-03887-z

Román Dobarco, M., McBratney, A., Minasny, B., & Malone, B. (2021). A modelling framework for pedogenon mapping. Geoderma, 393, 115012. https://doi.org/10.1016/j.geoderma.2021.115012

Román Dobarco, M., Padarian Campusano, J., McBratney, A. B., Malone, B., & Minasny, B. (2023). Genosoil and phenosoil mapping in continental Australia is essential for soil security. Soil Security, 13, 100108. https://doi.org/10.1016/j.soisec.2023.100108

Sarkar, T., & Mishra, M. (2018). Soil Erosion Susceptibility Mapping with the Application of Logistic Regression and Artificial Neural Network. Journal of Geovisualization and Spatial Analysis, 2(1), 8. https://doi.org/10.1007/s41651-018-0015-9

Schumm, S. A., & Harvey, M. D. (2015). Natural Erosion in the USA. In B. L. Schmidt, R. R. Allmaras, J. V. Mannering, & R. I. Papendick (Eds.), ASA Special Publications (pp. 15–22). American Society of Agronomy and Soil Science Society of America. https://doi.org/10.2134/asaspecpub45.c2

Schrader, S., Graham, S., Campbell, R., Height, K., & Hawkes, G. (2024). Grower attitudes and practices toward area-wide management of cropping weeds in Australia. Land Use Policy, 137, 107001. https://doi.org/10.1016/j.landusepol.2023.107001

Senanayake, I. P., Hancock, G. R., & Welivitiya, W. D. D. P. (2024). Soil depth and catchment geomorphology: A field, vegetation and GIS based assessment. Geoderma Regional, 38, e00824. https://doi.org/10.1016/j.geodrs.2024.e00824

Senanayake, I. P., Yeo, I.-Y., Robinson, N. J., Dahlhaus, P. G., & Hancock, G. R. (2024). Identification of high-performing soil groups in grazing lands using a multivariate analysis method. Soil Security, 16, 100163. https://doi.org/10.1016/j.soisec.2024.100163

Sione, S. M. J., Wilson, M. G., Lado, M., & González, A. P. (2017). Evaluation of soil degradationproduced by rice crop systems in a Vertisol, using a soil quality index. CATENA, 150, 79–86. https://doi.org/10.1016/j.catena.2016.11.011.

Smith, D. R., Owens, P. R., Leytem, A. B., & Warnemuende, E. A. (2007). Nutrient losses from manure and fertilizer applications as impacted by time to first runoff event. Environmental Pollution, 147(1), 131–137. https://doi.org/10.1016/j.envpol.2006.08.021

Speer, M. S., & Leslie, L. M. (2000). A comparison of five flood rain events over the New South Wales north coast and a case study. International Journal of Climatology, 20(5), 543–563. https://doi.org/10.1002/(SICI)1097-0088(200004)20:5<543::AID-JOC498>3.0.CO;2-C

Styc, Q., Minasny, B., Jang, H. J., & McBratney, A. (2025). Modelling Soil Organic Carbon Dynamics atthe Continental Extent Using Pedogenon Mapping. European Journal of Soil Science, 76(2), e70070. https://doi.org/10.1111/ejss.70070.

Tan, Z. X., Lal, R., & Wiebe, K. D. (2005). Global Soil Nutrient Depletion and Yield Reduction. Journal of Sustainable Agriculture, 26(1), 123–146. https://doi.org/10.1300/J064v26n01_10

Tang, Y., Minasny, B., McBratney, A., & Jang, H. J. (2024). Assessing soil capacity and condition for “habitat of biodiversity” in the Lower Namoi Valley. Soil Security, 15, 100152. https://doi.org/10.1016/j.soisec.2024.100152

Tesfahunegn, G. B. (2014). Soil Quality Assessment Strategies for Evaluating Soil Degradation in NorthernEthiopia. Applied and Environmental Soil Science, 2014, 1–14. https://doi.org/10.1155/2014/646502

Toy, T. J., Foster, G. R., Renard, K. G., & Hardcover. (2002). Soil Erosion: Processes, Prediction, Measurement, and Control. https://api.semanticscholar.org/CorpusID:126981815

Turkelboom, F., Poesen, J., & Trébuil, G. (2008). The multiple land degradation effects caused by land-use intensification in tropical steeplands: A catchment study from northern Thailand. CATENA, 75(1), 102–116. https://doi.org/10.1016/j.catena.2008.04.012

Turner, B. L., Fuhrer, J., Wuellner, M., Menendez, H. M., Dunn, B. H., & Gates, R. (2018). Scientific case studies in land-use driven soil erosion in the central United States: Why soil potential and risk concepts should be included in the principles of soil health. International Soil and Water Conservation Research, 6(1), 63–78. https://doi.org/10.1016/j.iswcr.2017.12.004

Tuo, D., Xu, M., & Gao, G. (2018). Relative contributions of wind and water erosion to total soil loss and its effect on soil properties in sloping croplands of the Chinese Loess Plateau. Science of The Total Environment, 633, 1032–1040. https://doi.org/10.1016/j.scitotenv.2018.03.237

Vaca, R., Del Águila, P., Yañez-Ocampo, G., Lugo, J. A., & De La Portilla-López, N. (2023). Soil Quality Assessment in Response to Water Erosion and Mining Activity. Agriculture, 13(7), 1380. https://doi.org/10.3390/agriculture13071380

Vanwalleghem, T., Gómez, J. A., Infante Amate, J., González De Molina, M., Vanderlinden, K., Guzmán, G., Laguna, A., & Giráldez, J. V. (2017). Impact of historical land use and soil management change on soil erosion and agricultural sustainability during the Anthropocene. Anthropocene, 17, 13–29. https://doi.org/10.1016/j.ancene.2017.01.002

Verheijen, F. G. A., Jones, R. J. A., Rickson, R. J., & Smith, C. J. (2009). Tolerable versus actual soil erosion rates in Europe. Earth-Science Reviews, 94(1–4), 23–38. https://doi.org/10.1016/j.earscirev.2009.02.003

Viscarra Rossel, R. A., Chen, C., Grundy, M. J., Searle, R., Clifford, D., & Campbell, P. H. (2015). The Australian three-dimensional soil grid: Australia's contribution to the GlobalSoilMap project. Soil Research, 53(8), 845. https://doi.org/10.1071/SR14366

Volchko, Y., Norrman, J., Rosèn, L., & Norberg, T. (2014). A minimum data set for evaluating the ecological soil functions in remediation projects. Journal of Soils and Sediments, 14(11), 1850–1860. https://doi.org/10.1007/s11368-014-0939-8

Wadoux, A. M. J. -C. (2023). Interpretable spectroscopic modelling of soil with machine learning. European Journal of Soil Science, 74(3), e13370. https://doi.org/10.1111/ejss.13370

Wadoux, A. M. J.-C., Román Dobarco, M., Malone, B., Minasny, B., McBratney, A. B., & Searle, R. (2023). Baseline high-resolution maps of organic carbon content in Australian soils. Scientific Data, 10(1), 181. https://doi.org/10.1038/s41597-023-02056-8

Wadoux, A. M. J.-C., Román Dobarco, M., Ng, W., & McBratney, A. B. (2024). Spatial evaluation of the soils capacity and condition to store carbon across Australia. Geoderma, 442, 116805. https://doi.org/10.1016/j.geoderma.2024.116805

Wang, H., & Zhang, G. (2021). Temporal variation in soil erodibility indices for five typical land use types on the Loess Plateau of China. Geoderma, 381, 114695. https://doi.org/10.1016/j.geoderma.2020.114695

Wallbrink, P.J., Olley, J.M., Murray, A.S., & Olive, L.J. (1996). The contribution of subsoil to sediment yield in the Murrumbidgee River basin, New South Wales, Australia. IAHS-AISH Publication, 236, 347–356.

Wang, X., Qin, X., Tan, J., Yang, L., Ou, L., Duan, X., & Deng, Y. (2023). Effect of the moisture content and dry density on the shear strength parameters of collapsing wall in hilly granite areas of South China. International Soil and Water Conservation Research, S2095633923000874. https://doi.org/10.1016/j.iswcr.2023.09.006

Wang, Y., Qin, X., Kong, Y., Hou, D., & Ren, P. (2024). Temporal Variation in Soil Resistance to Rill Erosion in Cropland of the Dry—Hot Valley Region, Southwest China. Land, 13(4), 546. https://doi.org/10.3390/land13040546

Webb, N. P., Marshall, N. A., Stringer, L. C., Reed, M. S., Chappell, A., & Herrick, J. E. (2017). Land degradation and climate change: Building climate resilience in agriculture. Frontiers in Ecology and the Environment, 15(8), 450–459. https://doi.org/10.1002/fee.1530

Wei, Y., Wu, X., Xia, J., Miller, G. A., Cai, C., Guo, Z., & Hassanikhah, A. (2019). The effect of water content on the shear strength characteristics of granitic soils in South China. Soil and Tillage Research, 187, 50–59. https://doi.org/10.1016/j.still.2018.11.013

Whitbread, A. M., Lefroy, R. D. B., & Blair, G. J. (1998). A survey of the impact of cropping on soil physical and chemical properties in north-western New South Wales. Soil Research, 36(4), 669. https://doi.org/10.1071/S97031

Wischmeier, W. H., & Mannering, J. V. (1969). Relation of Soil Properties to its Erodibility. Soil Science Society of America Journal, 33(1), 131–137. https://doi.org/10.2136/sssaj1969.03615995003300010035x

Yamashita, N., Ohnuki, Y., Iwahashi, J., & Imaya, A. (2024). National-scale mapping of soil-thickness probability in hilly and mountainous areas of Japan using legacy and modern soil survey. Geoderma, 446, 116896. https://doi.org/10.1016/j.geoderma.2024.116896

Yan, X., Li, J., Yang, D., Li, J., Ma, T., Su, Y., Shao, J., & Zhang, R. (2022). A Random Forest Algorithm for Landsat Image Chromatic Aberration Restoration Based on GEE Cloud Platform A Case Study of Yucatán Peninsula, Mexico.

Yang, X., Leys, J., Zhang, M., & Gray, J. M. (2023). Estimating nutrient transport associated with water and wind erosion across New South Wales, Australia. Geoderma, 430, 116345. https://doi.org/10.1016/j.geoderma.2023.116345

Yang, T., Siddique, K. H. M., & Liu, K. (2020). Cropping systems in agriculture and their impact on soil health-A review. Global Ecology and Conservation, 23, e01118. https://doi.org/10.1016/j.gecco.2020.e01118

Yang, X., & Yu, B. (2015). Modelling and mapping rainfall erosivity in New South Wales, Australia. Soil Research, 53(2), 178. https://doi.org/10.1071/SR14188

Ye, Z., Sheng, Z., Liu, X., Ma, Y., Wang, R., Ding, S., Liu, M., Li, Z., & Wang, Q. (2021). Using Machine Learning Algorithms Based on GF-6 and Google Earth Engine to Predict and Map the Spatial Distribution of Soil Organic Matter Content. Sustainability, 13(24), 14055. https://doi.org/10.3390/su132414055

Zhang, L., Huang, Y., Rong, L., Duan, X., Zhang, R., Li, Y., & Guan, J. (2021). Effect of soil erosion depth on crop yield based on topsoil removal method: A meta-analysis.

Agronomy for Sustainable Development, 41(5), 63. https://doi.org/10.1007/s13593-021-00718-8

Zhang, J., Wang, S., Fu, Z., Wang, F., Wang, K., & Chen, H. (2024). Soil thickness influences the control effect of micro-topography on subsurface runoff generation in the karst hillslope critical zone. CATENA, 239, 107957. https://doi.org/10.1016/j.catena.2024.107957

Zhu, Q., Yang, X., Ji, F., & Du, Z. (2025). Rainfall Erosivity Projection in South-East Australia Using the Improved Regional Climate Simulations. International Journal of Climatology, 45(2), e8702. https://doi.org/10.1002/joc.8702

Zhao, G., Mu, X., Wen, Z., Wang, F., & Gao, P. (2013). SOIL EROSION, CONSERVATION, AND Eco-environment changes in the loess plateau of china. Land Degradation & Development, 24(5), 499–510. https://doi.org/10.1002/ldr.2246

Zhang, Y., Hartemink, A. E., Vanwalleghem, T., Bonfatti, B. R., & Moen, S. (2024). Climate and land use changes explain variation in the A horizon and soil thickness in the United States. Communications Earth & Environment, 5(1), 129. https://doi.org/10.1038/s43247-024-01299-6

Chapter 3: Towards Soil Security: Understanding Soil Erosion Footprints and Their Implications in NSW

This chapter is published at:

Anilkumar Hunakunti, Alex McBratney, Budiman Minasny (2025) Towards Soil security: Understanding Soil erosion footprint and their implications in NSW. Soil security, 19, 100184.

3.1 Abstract

A key challenge in maintaining soil security is assessing and mitigating soil degradation. The soil footprint is a promising indicator for quantifying degradation impacts, yet it remains underdeveloped, lacking a standardized definition and a comprehensive calculation framework. This study introduces a generalized soil footprint framework, integrating three key components: (1) Threat to soil, representing degradation processes such as soil water erosion or salinization; (2) Soil service ratio, which quantifies changes in soil services such as crop yield or Available Water Capacity relative to their natural state; and (3) Inherent mitigation capability, reflecting the soil's resilience to degradation. Applied in New South Wales (NSW), Australia, we calculated two soil erosion footprints using crop yield and Available Water Capacity (AWC) as indicators of soil services. In both cases, soil erosion rate, specifically water erosion, was used as the threat to soil, while erosion risk capability represented the soil's intrinsic mitigation capacity. Results show that oats had the highest soil erosion footprint due to lower yields, whereas wheat, barley, sorghum, and grain legumes had smaller footprints. An inverse relationship between soil erosion footprint and crop receipts (i.e., farm revenue from crop production) highlights the economic risks of soil erosion, particularly in high-revenue regions like the Northwest Slopes and Plains and the Riverina. AWC-based soil erosion footprints were highest in coastal and dryland cropping areas, indicating greater erosion stress, while irrigated systems, plantation forests, and managed resource protection areas showed lower footprints, reflecting better resilience. Modified pastures, native forests, nature conservation areas, and minimal-use lands had higher footprints. This study highlights the need to integrate soil service ratios and erosion risk capability alongside erosion rates for a more comprehensive approach to soil sustainability and mitigation strategies. The proposed soil footprint framework provides a valuable tool for evaluating human impacts on soil services, guiding targeted soil conservation efforts.

Keywords: Sustainability; Soil Erosion; Soil Security; Soil Erosion Footprint; Soil Degradation; Crop Yield; Available Water Capacity

3.2 . Introduction

Soil is a fundamental component of Earth's biophysical system, influenced by key processes such as nutrient cycling, erosion, climate regulation, and geophysical forces like gravity. However, human activities, particularly since the Industrial Revolution, have intensified pressures on soil through increased greenhouse gas (GHG) emissions (Mitchell, 1989) and accelerated degradation (Ahuti, 2015). At the same time, growing global populations and consumption are placing greater demands on soils to support intensified agricultural productivity (Lal, 2008; Kopittke et al., 2019). Current crop yield growth rates are insufficient to meet projected food needs by 2050 (Ray et al., 2013), further intensifying pressure on soil resources. Expanding agricultural land to meet these demands would exacerbate existing environmental challenges; thus, enhancing cropping efficiency on existing soils is imperative for sustainably addressing future food requirements (Foley et al., 2011).

In recent decades, environmental footprints such as carbon and water footprints have emerged as critical metrics for evaluating the environmental impacts of human activities (Wackernagel & Yount, 1998; Hoekstra & Wiedmann, 2014; Čuček et al., 2015; Lovarelli et al., 2016). These frameworks have significantly advanced understanding of resource use, environmental pressures, and the sustainability of production systems, drawing attention from policymakers and industries committed to reducing ecological impacts (Čuček et al., 2015). However, despite soil's vital role in sustaining planetary functions, threats to soil sustainability are still insufficiently represented in current discourse, highlighting the need for soil-specific footprints to address the gap.

The soil footprint concept is still evolving but has gained momentum through initiatives like the Soil Deal for Europe, which aims to reduce the European Union’s global soil footprint by 2030 (European Commission, 2021). A recent study in Spain focusing on agricultural systems defined the soil footprint as the ratio of soil loss rate to crop yield, using it as a proxy for soil services to identify regions with the highest footprints and the least sustainable agricultural practices (García-Gamero et al., 2024). While this definition captures the impact of erosion on crop productivity, it addresses only one aspect of soil degradation, excluding processes such as salinization and contamination. Moreover, it does not consider the full range of essential soil services, including carbon

storage, water filtration, nutrient cycling, and biodiversity support, all of which are critical for maintaining ecosystem resilience under increasing environmental pressures (Smith et al., 2016).

Furthermore, soil degradation not only reduces the ability of soil to support essential services but also weakens its inherent mitigation capacity, which is critical for resisting and recovering from degradation (Lal, 1997; Abdel Kawy & Ali, 2012). A comprehensive soil footprint framework should integrate mitigation capability to better reflect soil's resilience and capacity to counteract degradation over time.

Soil degradation is a cumulative process driven by both natural and anthropogenic influences across space and time, altering soil properties and affecting its ability to provide essential services (Gachene et al., 1997; Lal, 2015). The aspect of space for time is lacking in previous soil footprint definitions, which inadequately incorporate the temporal dimension necessary to assess progressive changes in soil services. By integrating the space-for-time substitution approach, the soil footprint framework can provide a more dynamic representation of soil degradation, accounting for long-term shifts in soil services and resilience. To assess these changes, the space-for-time substitution concept is employed (Damgaard, 2019), allowing soil service variations to be studied across different timeframes. This approach compares Genosoils primarily influenced by natural degradation processes to Phenosoils, where both natural and human-induced degradation have altered soil properties over time (Evangelista et al., 2024; Francos et al., 2024). Since Genosoils and Phenosoils represent different stages in soil evolution, the soil service ratio, defined as the ratio of Phenosoil to Genosoil services, provides a relative measure of how much soil services have changed due to human intervention. By integrating this ratio, the soil footprint framework can quantify deviations from natural soil conditions, offering a dynamic representation of soil degradation and resilience over time.

Building upon these identified gaps, this study aims to introduce a new, generalized soil footprint concept with a more comprehensive definition that integrates key components: threat to soil, soil service ratio, and inherent soil threat mitigation capability. This comprehensive approach accounts for multiple degradation processes, diverse soil services, and varying mitigation capacities, enabling a more adaptable framework

applicable across different land uses and soil services. By refining the soil footprint concept, this study enhances the understanding of soil security and long-term sustainability.

In this study, we demonstrate the calculation of the soil footprint using the proposed new soil footprint framework by considering soil erosion as a specific example of a threat to soil. We calculate two different soil erosion footprints based on two distinct soil services: crop productivity (short-term service) and Available Water Capacity (AWC) (long-term service) (Lal, 2001).

To account for threat mitigation capability, we use Erosion Risk Capability, which represents the inherent capacity of soil to resist erosion. It is defined as the difference between the soil's natural resistance to erosion and its current condition, highlighting both its vulnerability and its ability to mitigate future erosion risks. This serves as the mitigation capacity in both soil erosion footprint calculations. While indicators like the K-factor (soil erodibility) or soil shear strength could assess erosion vulnerability, we use soil erosion rate from the RUSLE model as the threat to soil. The K-factor, already part of RUSLE, is influenced by land use and external factors, making it less suitable for assessing long-term, intrinsic soil properties (Ferreira et al., 2015; H. Wang & Zhang, 2021 ;Baskan, 2022). Similarly, soil shear strength is affected by moisture and land use changes, reducing its reliability for long-term assessments (Havaee et al., 2015; Wei et al., 2019).

The Erosion Risk Capability Map captures the soil's intrinsic resistance to erosion, derived from key indicators: clay ratio and topsoil thickness measured in Genosoils. Soil condition is assessed by the deviation of these indicators in Phenosoils relative to their corresponding Genosoils. The difference between capacity (inherent resistance) and condition (current state) determines the ERC, ranging from 0 to 1, where higher values indicate a greater natural ability to resist erosion.

Given the importance of assessing soil threats relative to soil services and mitigation capacities, this study aims to develop a comprehensive framework for quantifying the Soil Footprint. Specifically, the objectives of this study are:

1. To define the Soil Footprint as a metric for measuring soil threats relative to soil services and mitigation capacities (Section 3.3.2).

2. To apply this framework by calculating the soil erosion footprint based on soil services, erosion risk capability, and soil erosion as a threat, using crop yield and the soil service ratio (phenosoil/genosoil) for Available Water Capacity (AWC) as indicators. This objective includes estimating crop yield across Bureau of Agricultural and Resource Economics and Sciences (ABARES) regions, calculating soil service ratios within each land-use class in NSW, and assessing soil erosion rate and erosion risk capability across ABARES regions. Crop-specific soil erosion footprint rankings are provided for NSW regions, with AWC and soil service ratio variation assessed spatially across NSW to capture differences across land-use (Sections 3.3.3, 3.3.4, 3.3.5, 3.3.6, 3.4.2, 3.4.1, 3.4.6).

3. To assess the soil erosion footprint by integrating erosion rate, erosion risk capability, and the soil service ratio (phenosoil to genosoil) across different land use systems in NSW (Sections 3.4.7).

4. To evaluate the relationship between the soil erosion footprint and crop receipts as an economic indicator across different regions of ABARES for various crops (Section 3.3.7, 3.4.3, 3.4.4).

3.3. Materials and methods

The flowchart (Fig. 16) outlines the general workflow of this study and presents the framework for quantifying soil erosion footprints. This framework begins with a broad definition of the soil footprint, incorporating threats to soil (erosion rate), soil services, and mitigation capacity into a calculation equation. It is applied to two types of soil erosion footprint calculations: one using crop yield as the soil service and the other using Available Water Capacity (AWC), where the soil service ratio (phenosoil/genosoil AWC) captures changes due to human activities. Erosion Risk Capability (ERC), defined as the difference between the soil's inherent resistance to erosion and its current condition, represents the mitigation capacity in both cases.

In the first pathway, the soil erosion footprint (SEP) is calculated by integrating soil erosion rate (SER), crop yield, and Erosion Risk Capability (ERC). A functional relationship, denoted as f(x), represents the SEP formula, allowing quantification of SEP for each region and crop. SEP values are then ranked across different crops and regions, where lower SEP values receive higher ranks. This pathway also involves analysing the relationship between SER, crop yield, and ERC across various regions and crops. Additionally, an economic analysis using f(x) is performed to examine the relationship between SEP and crop receipts (farm revenue from crop production), providing insights into the economic implications of changes in SEP.

The second pathway focuses on Available Water Capacity (AWC) as an indicator of soil services. Genosoil AWC (natural soil) and phenosoil AWC (corresponding human-affected soil) are mapped using a machine learning model (e.g., Random Forest) with relevant covariates. The soil service ratio (SSR), calculated as the ratio of phenosoil AWC to genosoil AWC, represents changes in AWC due to human activities. The SEP formula, denoted as f(x), integrates SER, SSR, and ERC to generate soil erosion footprint (SEP) values, capturing the combined effects of soil erosion threats, soil services, and mitigation capacities.

The workflow produces a SEP map, followed by the calculation of mean SER, SSR, ERC, and SEP values for each land use class using land cover maps, with f(x) applied to compute these mean values. Additionally, SEP values are analysed and ranked across different land use categories to identify regions most affected by erosion. The analysis further explores the interactions between SER, SSR, and ERC, while providing insights into the spatial distribution of SEP, AWC, and SSR. The following sections will elaborate on the first and second pathways, along with their implications.

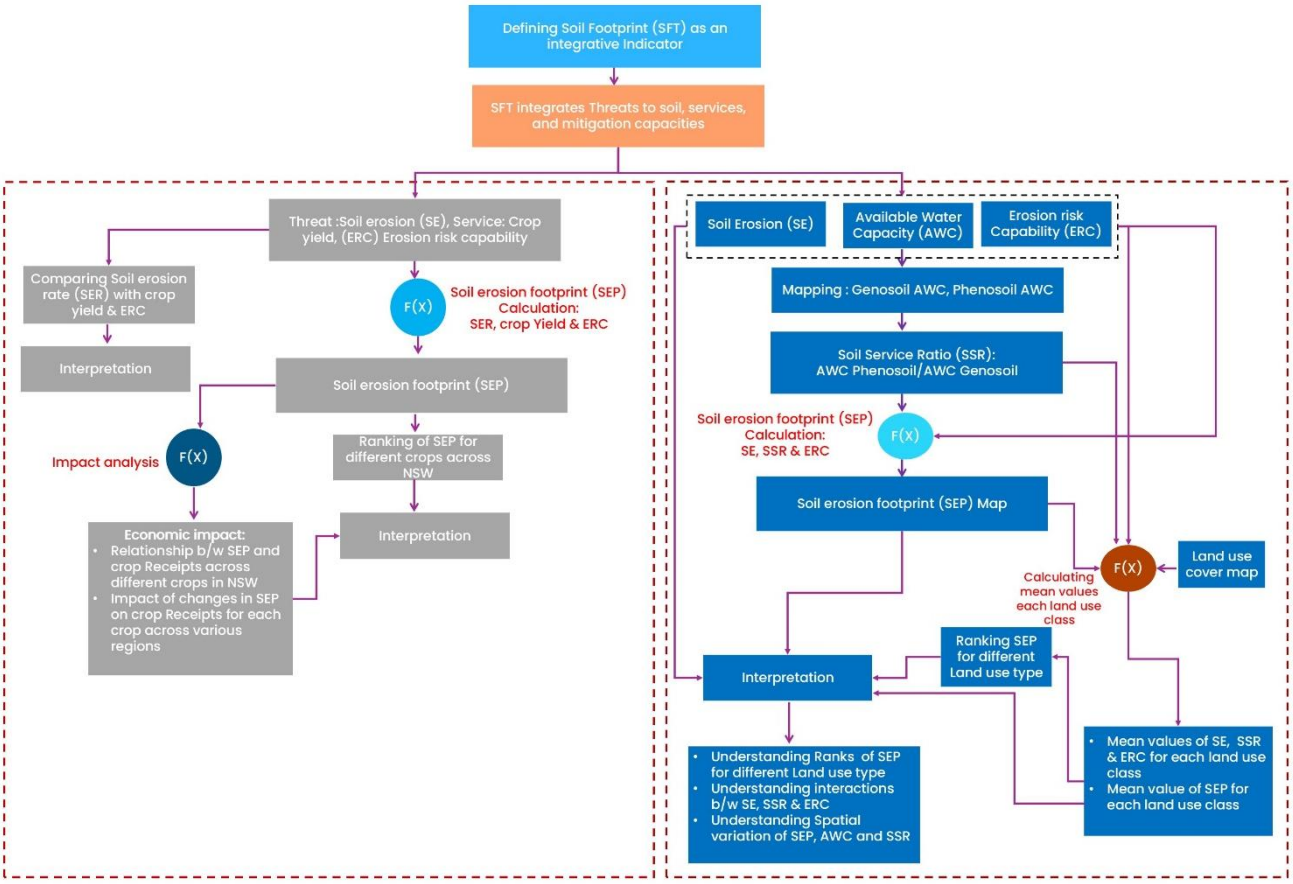

Fig. 16. General workflow for calculating the soil erosion footprint

3.3.1 Study area

New South Wales (NSW) encompasses an area of 808,444 square kilometres. This study focused on regions characterized and classified by the Australian Bureau of Agricultural and Resource Economics and Sciences (ABARES) based on their geographical and agricultural attributes. The regions included in this analysis are the Central West, Coastal, Far West, Northwest Slopes and Plains, Riverina, and Tablelands (see Fig. 17). These regions are systematically monitored for crop productivity and other economically relevant data. Within these areas, a variety of cropping practices are observed, influenced by geographical variations, climate, weather patterns, and a diverse range of soil types, including podzols and vertisols. Agricultural production is dominated by crops such as oats, wheat, barley, canola, grain legumes, cotton, and sorghum.

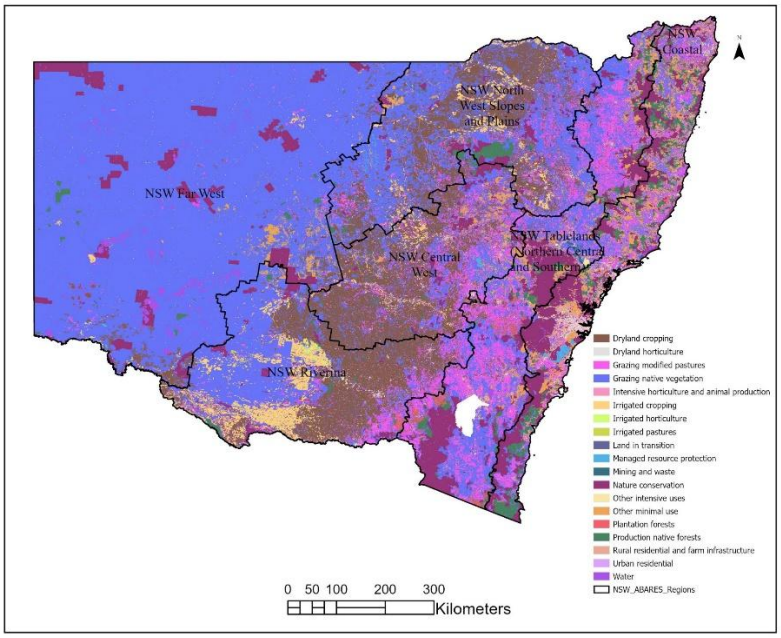

Fig. 17. Study area map, showing ABARES regions with different land use cover across NSW, Sourced from the Department of Agriculture, Fisheries and Forestry

3.3.2 Soil Footprint

Our definition characterizes the soil footprint as a "*unitless quantitative measure that evaluates the balance between threats to soil and the soil's capacity to provide essential services while resisting or mitigating these threats*." This metric is calculated using the following general equation:

$$\text{Soil Footprint} = \frac{\text{Threat to Soil}}{\text{Soil Service} \times \text{Threat Mitigation Capability}} \quad (1)$$

Key Components of the Soil Footprint Equation

1. Threat to Soil

Threats to soil represent degradation processes such as erosion, compaction, salinity, and organic carbon loss. To enable comparability across different degradation factors, each threat is normalized into a unitless value (0–1) using empirical data transformations. For example, soil erosion rate (t/ha/year) is normalized using a function (e.g.,

exponential). This ensures that threats measured in different units can be consistently integrated within the framework.

Threats can be evaluated individually or aggregated into a Composite Threat Index (CTI):

$$\mathrm{CTI} = \sum_{i=1}^{n} W_i \,.\, \mathrm{Normalized\ Parameter}_i$$

where W_i represents the weight assigned to each parameter based on its influence on soil degradation.

Multiple Parameters for a Single Threat: Since some threats cannot be fully captured by a single parameter, multiple indicators are often required to represent their impact comprehensively. For instance, soil compaction is commonly assessed using bulk density (Håkansson & Lipiec, 2000), texture, and also penetration resistance (Vomocil, 1957; Tian et al., 2022). Depending on the study's objectives, either a single dominant parameter or a combined index may be used in the calculation. When uncertainty exists regarding the relative importance of parameters, sensitivity analysis and minimum data selection approaches can help identify the most influential factor or determine whether multiple indicators should be integrated for a more comprehensive representation of the threat (Evangelista et al., 2023).

2. Soil services

Soil services are measured as unitless values and represent the soil's capacity to support a range of ecosystem functions. These may include, Water securing (e.g., soil water holding capacity), Food securing (e.g., yield, biomass), Carbon sequestration, etc (Evangelista et al., 2023).

Soil services can be assessed individually or aggregated into a composite value that reflects the overall service capacity of the soil. For instance, when evaluating food securing, crop yield may be the primary soil service, while in water securing, AWC may take precedence.

*Multiple Parameters for a Single Service***:** In many cases, a single soil service is characterized by multiple parameters. For example, water securing may include both field capacity and available water content, while food securing could involve grain yield

and biomass (Agegnehu et al., 2014). These parameters can be combined into a composite service index or used individually, depending on the objective of the assessment.

3. Threat Mitigation Capability:

Threat mitigation capability represents the soil's inherent ability to resist and mitigate degradation, determined by its physical, chemical, and biological properties. For example, erosion resistance is influenced by topsoil thickness, clay content, and organic matter, while compaction resistance depends on aggregate stability and soil moisture content (B. Wang et al., 2018; Moragoda et al., 2022; Xing et al., 2023; Gan et al., 2024). Like threats and soil services, mitigation capability can be evaluated individually for each parameter or combined into a composite index, depending on the degradation process being assessed.

Multiple Parameters for Mitigation Capability: Similar to threats and services, mitigation capability may also involve multiple parameters. For instance, erosion mitigation capability may integrate vegetative cover (Z.-J. Wang et al., 2016) and soil structural stability (Lal, 2015), while compaction resistance could involve both aggregate stability and soil porosity (Shah et al., 2017). These factors can either be analysed separately or aggregated into a single mitigation index, depending on the study objectives.

Since threats to soil, soil services, and mitigation capabilities are dynamic and interdependent, ongoing human activities and extreme events (Sivakumar, 2011), alter soil properties and processes. In some cases, human interventions such as liming, fertilization, or organic amendments may modify soil services (Larney & Angers, 2012; Mahmud & Chong, 2022), in phenosoils compared to their genosoil counterparts, sometimes leading to improvements in certain functions. To quantify these changes in soil services, we use the soil service ratio, defined as the ratio of soil services in phenosoil to those in genosoil:

$$Q = \frac{Soil\ service_{phenosoil}}{Soil\ service_{genosoil}} \quad (2)$$

By substituting equation (2) into equation (1), the Soil Footprint can be expressed as:

$$\text{Soil Footprint} = \frac{\text{Threat to Soil}}{\frac{Soil\ service_{phenosoil}}{Soil\ service_{genosoil}} \times \text{Threat Mitigation Capability}} \quad (3)$$

Special Case: Focus on Agricultural production

In contexts where agricultural production is the primary soil service, and where soils have been extensively modified by human activities (phenosoil), the distinction between phenosoil and genosoil becomes less relevant. This is because the act of cultivating crops inherently transitions soils into phenosoil due to anthropogenic inputs like tilling, fertilization, and irrigation. Consequently, soil service assessments in these systems focus primarily on phenosoil productivity. Thus, the soil service ratio simplifies to:

$$\text{Soil footprint} = \frac{\text{Threat to soil}}{Soil\ service_{phenosoil} \times \text{Threat mitigation capability}} \quad (4)$$

This special case highlights the soil footprint's relevance in intensively managed agricultural landscapes, where the focus is on sustaining productivity while minimizing degradation.

3.3.3 Soil erosion footprint

In this study, we calculated the Soil Erosion Footprint as a specific example of the Soil Footprint, where soil erosion represents the threat and Available Water Capacity (AWC) represents the soil service. We also illustrate the special case using agricultural production yield, as in equation (4).

The general Soil Footprint equation (3) can be modified for soil erosion and AWC as follows:

$$\text{Soil Footprint}_{(\text{erosion})} = \frac{\text{K}_\text{n}}{\text{Q}_\text{n} \times \text{Soil Erosion Risk Capability}} \quad (5)$$

where:

- $K_n = f(K)$: K_n is the normalized erosion rate, which converts the actual erosion rate K at a location into a unitless value (0 to 1) using (Fig. 18):

$$K_n = 1 - \exp(-0.099 \times K^{0.92}) \quad (6)$$

Here, K is the modelled erosion rate (t/ha/year), averaged from 2001 to 2022.

- $Q_n = f(Q)$: Q_n is the normalized soil service ratio, transforming the Q deviation between AWC in phenosoil and genosoil into a unitless value (0 to 1) using (Fig. 19):

$$Q_n = 1 - \exp(-0.89 \times Q^{12.92}) \quad (7)$$

The deviation Q is calculated as:

$$Q = \frac{AWC_{phenosoil}}{AWC_{Genosoil}}$$

While maximum value normalization is commonly used to scale data, it assumes a linear relationship, which may not accurately reflect the complex, nonlinear nature of soil threats and services. In this study, we employed exponential functions for normalization because they better capture the observed variability in soil erosion rates and soil service ratios. This approach ensures that the normalized values align more closely with empirical data. The constants in equations (6) and (7) were determined by curve fitting to empirical data.

Special Case: Focus on Agricultural production

When agricultural yield is the primary soil service, equation (4) can be adapted to focus on crop yield as follows:

$$\text{soil Footprint}_{erosion} = \frac{K}{\text{Crop Yield} \times \text{Soil Erosion Risk Capability}} \quad (8)$$

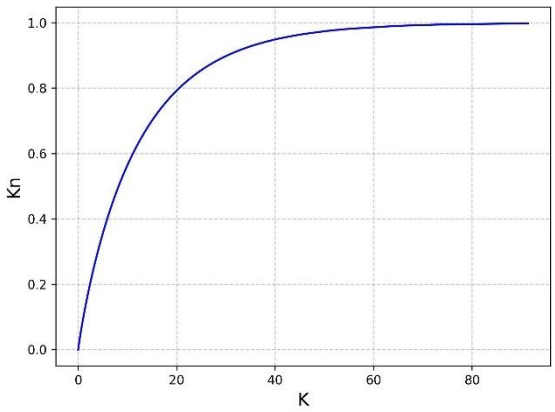

Fig. 18. Relationship between the normalized erosion rate (K_n) and the actual erosion rate (K, in ton/ha/year). The plot demonstrates how K_n increases with K following transformation $K_n = 1 - \exp(-0.099 \times k^{0.92})$

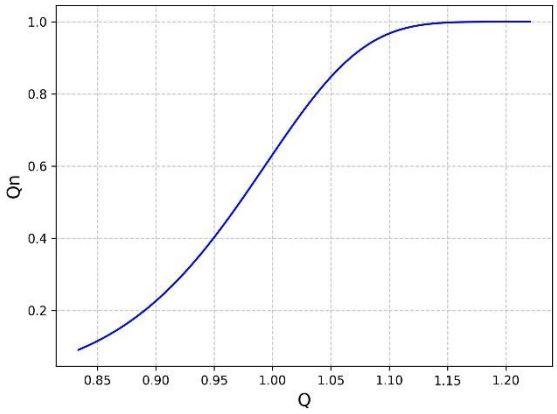

Fig. 19. Relationship between the normalized soil service ratio (Q_n) and the actual soil service ratio (Q, dimensionless). The plot demonstrates how Q_n increases with Q following transformation $Q_n = 1 - exp(-0.89 \times Q^{12.92})$

3.3.4. Soil Erosion Rate and Soil Erosion Risk Capability Estimation in ABARES Regions

Soil erosion rate data were obtained from the New South Wales Department of Climate Change, Energy, the Environment, and Water, calculated using the Revised Universal Soil Loss Equation (RUSLE) model (https: //datasets. seed.nsw. gov.au/dataset/modelled-hillslope-erosion-over-new-south-wales). This dataset provides annual soil erosion rates (t/ha/year) spanning the period from 2001 to 2021. We used this data to calculate the average soil erosion rate across the ABARES regions.

Furthermore, we estimated the average erosion risk capability for the same ABARES regions and land use classes based on the erosion risk capability map developed in our study (Chapter 2). This map calculates erosion risk capability as the difference between the soil's capacity, estimated from genosoil characteristics, and its condition, derived from the phenosoil-to-genosoil ratio. Key indicators include topsoil thickness and the clay ratio, with higher erosion risk capability values indicating a higher potential to resist erosion.

3.3.5. Estimation of Crop yield in ABARES Regions

Crop yield, a measure of agricultural productivity, is defined as the amount of crop produced per unit area (Bandyopadhyay et al., 2001), typically expressed in tons per hectare (t/ha). It is calculated as:

$$\text{Yield } (t\ ha^{-1}yr^{-1}) = \frac{Total\ Crop\ Produced\ (t)}{Total\ Area\ Sown(ha)} \quad (9)$$

where:

Yield (t/ha): Crop yield, in tonnes (t) per hectare per year.

Total Crop Production (t): Total crop quantity produced, in tonnes (t).

Total Area Sown (ha): Area of land sown with the crop, in hectares.

Data on crop production and area sown were sourced from the ABARES Farm Data Portal (https://www.agriculture.gov.au/abares/data/farm-data-portal#data-download), encompassing annual statistics from 1990 to 2022 for six regions in New South Wales: Central West, Far West, Northwest Slopes and Plains, Riverina, and Tablelands (Northern, Central, Southern). The Coastal region was excluded from the analysis due to its low levels of crop production. Using these data, we calculated annual crop yields for various crops across the remaining regions, along with their average crop yields from 1990 to 2022.

3.3.6. Estimation of Soil Service Ratio

This study utilized topsoil (0–5 cm depth) Available Water Capacity (AWC) data at a 90 m resolution from the TERN Soil and Landscape Grid of Australia dataset (https://data.csiro.au/), with AWC values expressed as percentages. Genosoil-AWC and Phenosoil-AWC were mapped using a Random Forest (RF) model. The covariates used in the modeling are listed in (Supplementary Materials, Table 3). Pre-European vegetation data were employed for genosoil mapping, while current vegetation data were utilized for phenosoil mapping, as detailed in Tang et al. 2024. Training data for both genosoil and phenosoil were sourced from locations identified in the maps produced by Román

Dobarco et al. 2023. Finally, we calculated the ratio of phenosoil to genosoil Available Water Capacity (AWC).

3.3.7. Soil Erosion Footprint Analysis Based on Land Use Classification

This study evaluated soil erosion footprints using Available Water Capacity (AWC) as a soil service across five representative land use systems in New South Wales (NSW): Irrigated and Dryland Systems (IDS), Grazing Ecosystem (GE), Forest Production System (FPS), Protected Land System (PLS), and Transitional and Minimal Use Land (TMUK). These systems were chosen based on their diverse landscapes and their relevance for understanding soil erosion dynamics under varying levels of human influence. The land use systems were derived from Department of Agriculture, Fisheries, and Forestry.

The IDS system includes both irrigated and dryland cropping and horticultural practices, subdivided into dryland cropping (DC), dryland horticulture (DH), irrigated cropping (IC), irrigated horticulture (IH), and intensive horticulture and animal production (IHP). The GE system represents grazing lands, categorized into grazing modified pastures (GMP), grazing native vegetation (GNV), and irrigated pastures (IP). The FPS system comprises forested areas managed for timber production, divided into plantation forests (PF) and production native forests (PNF). The PLS system includes conservation areas with nature conservation (NC) and managed resource protection (MRP). Finally, the TMUK system encompasses minimally disturbed or transitioning areas, classified into land in transition (LIT) and other minimal use (OMU).

For each land use subclass, the average soil erosion footprint was calculated using Equation 5, which integrates average soil erosion rate (SER), soil service ratio (SSR), and erosion risk capability (ERC). These footprints were then ranked within each system. A higher rank indicates a lower soil erosion footprint, suggesting reduced soil erosion stress and potentially better soil resilience and sustainability. Conversely, a lower rank reflects a higher soil erosion footprint, highlighting areas with increased erosion stress and a greater need for targeted management interventions to mitigate soil degradation.

3.3.8. Impact on crop receipts change in Soil Footprint

Soil, particularly when expressed as "soil capital" (McBratney et al., 2014; Belcher et al., 2003), plays a critical role in agricultural productivity and economic returns (Knowler, 2004). Healthier or better conditioned soils enhance crop yields and increase farmer income, establishing soil as a vital agricultural asset (Shah & Wu, 2019; Pozza & Field, 2020). Conversely, increasing soil erosion leads to declines in productivity, resulting in reduced yields and lower farmer income (Colacicco et al., 1989; Amann et al., 2021).

The soil erosion footprint is related to the economic impact of soil degradation. A larger footprint indicates greater soil loss relative to yield, thereby reflecting more significant economic losses due to decreased agricultural output and income. To assess the economic implications of soil degradation, it is essential to evaluate its effect on total income derived from crop sales. This study employed crop receipts (in dollars) as an economic indicator, capturing fluctuations in yield and market conditions to analyse the financial impact of soil degradation. By investigating how variations in the soil erosion footprint affect crop receipts, we can elucidate the economic consequences of soil erosion on agricultural productivity. It is important to note that this metric reflects only one dimension of the economic impact, as it does not account for other costs associated with soil degradation, such as increased expenditure on fertilizers, soil amendments, or other remedial measures.

Crop receipts data obtained from the ABARES Farm Data Portal (https://www.agriculture.gov.au/abares/data/farm-data-portal#data-download) encompass multiple crops across the ABARES regions of New South Wales from 1990 to 2022, reflecting average revenue per farm for each crop and year. To analyse the effect of changes in the soil erosion footprint on crop receipts, we employed a logarithmic model to effectively capture the non-linear impacts. We calculated the soil erosion footprint annually from 1990 to 2022, utilizing crop yield data (as detailed in section 3.3.5), erosion risk capability, and soil erosion rate data (as discussed in section 3.3.4).

The relationship between the soil erosion footprint (x) and crop receipts (y) for the period from 1990 to 2022 was modelled as follows:

$$y = a.In(x) + b \quad (10)$$

where x and y represent the soil erosion footprint and crop receipts ($) for each year, and a and b are regression coefficients estimated using ordinary least squares fitting to the annual data from 1990 to 2022. Once the logarithmic model was established, we analyzed the impact of the change in soil erosion footprint ($\Delta\%$) at 20%, 50%, and 100% levels on receipts. The adjected soil erosion footprint (x') was calculated as:

$$x' = x.\left(1 + \frac{\Delta\%}{100}\right) \quad (11)$$

The impact on receipts, due to the change in soil erosion footprint, was determined by difference between the new receipts y' and the original receipts y:

$$\text{Impact} = y' - y = (a.In\,(x') + b - (a.In\,(x) + b)) \quad (12)$$

Simplifying this becomes:

$$\text{Impact} = \text{a. ln}\left(\frac{x'}{x}\right) \quad (13)$$

This expression highlights how changes in soil erosion footprint affect economic outcomes. To enable cross-region comparisons, we calculated the percentage deviation of the impact relative to the mean receipts for each region different crops. The mean receipts M for each region were calculated as:

$$\text{M} = \frac{1}{N}\sum_{i=1}^{N} M_i \quad (14)$$

where N is the total crop receipts data points from 1990 to 2022, and M_i individual crop receipts values. The percentage deviation was computed by:

$$\text{Percentage Deviation} = \left(\frac{Impact}{M}\right).100 \quad (15)$$

Equation 15 quantifies the deviations in crop receipts attributable to changes in the soil erosion footprint relative to the mean receipts of the region. This approach provides a standardized metric for evaluating the economic impact of soil erosion-induced degradation, facilitating comparisons across various regions and crops.

3.4 Results and discussion

3.4.1 Crop-Specific Soil Erosion Footprint Rankings Across NSW Regions

The soil erosion footprint was calculated using Equation 8 , incorporating average crop yield data from 1990 to 2022, soil erosion rates from 2001 to 2021, and erosion risk capability across five regions in New South Wales (NSW), as detailed in Sections 2.4 and 2.5. Rankings were assigned based on footprint values, with lower values receiving higher ranks. Oats consistently exhibit the largest soil footprint, particularly in the Central West (CW), Far West (FW), Northwest Slopes and Plains (NWSP), and Tablelands (T) regions (Fig. 20). In contrast, grain legumes, sorghum, barley, wheat, and canola generally display smaller to moderate footprints.

In the Far West, oats exhibit a large soil footprint, while wheat and barley show comparatively lower values. In the Tablelands, wheat has the lowest soil footprint, closely followed by oats. In the Riverina, footprints across all crop's wheat, barley, canola, grain legumes, and oats are generally small to moderate.

The high soil erosion footprint values associated with oats are primarily driven by their low yields, as erosion rates are likely relatively similar across crops. Oats' lower productivity is likely due to a combination of factors, including greater sensitivity to environmental conditions such as nutrient deficiencies, water availability, and temperature fluctuations (Ma et al., 2021), as well as potentially lower agronomic input compared to higher-value crops like wheat (Marshall et al., 2013). Therefore, strategies aimed at improving oat yields, such as optimizing fertilization, irrigation, and crop variety selection, may prove more effective in reducing soil erosion footprints than soil conservation measures alone.

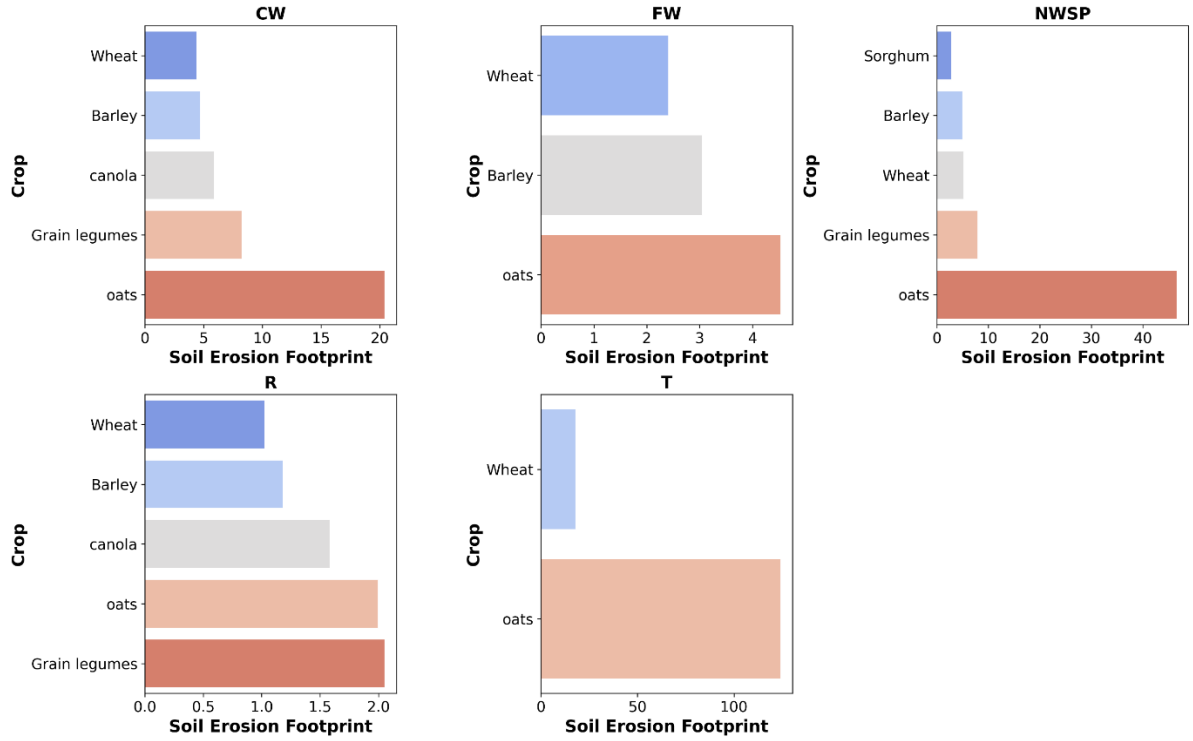

Fig. 20. Footprint ranking is based on soil footprint values, soil erosion risk capability, and crop yield. The plot presents various crop types ranked by their soil footprint, where lower footprint values indicate higher ranks. The analysis includes five regions: Central West (CW), Far West (FW), Northwest Slopes and Plains (NWSP), Riverina (R), and Tablelands (T).

3.4.2 Crop Yield, Erosion Rate, and Risk capabilities across ABARES regions

The 32-year average crop yield (1990–2022), 20-year average soil erosion rate (2001–2021), and average erosion risk capability across ABARES regions in New South Wales (NSW) are presented in Fig. 21 and 22 for key crops, including oats, barley, grain legumes, wheat, and sorghum. Erosion rate and erosion risk capability are calculated as regional averages, capturing topographical, soil, and climatic conditions independent of crop-specific management practices. These values remain consistent across all crops within each region.

In the Riverina region of NSW, the highest yields were recorded for wheat (2.41 t/ha/year), barley (2.07 t/ha/year), canola (1.43 t/ha/year), and grain legumes (1.30 t/ha/year). This is accompanied by a low erosion rate of 0.23 t/ha/year and a high erosion risk capability of 0.125. These findings indicate a potential correlation between low erosion rates, high mitigation capacity, and increased productivity, likely

attributable to effective soil management practices and favourable environmental conditions (Schrader et al., 2024). Supporting this observation, prior studies have demonstrated that regions characterised by well-managed soils and low erosion rates tend to achieve higher agricultural productivity (Koch et al., 2015; Thomas et al., 2018; Nordblom et al., 2023).

Similarly, the Central West region exhibited an erosion rate of 0.52 t/ha/year and an erosion risk capability of 0.09, which correlate with yields for oats (0.85 t/ha/year), wheat (1.88 t/ha/year), barley (1.77 t/ha/year), canola (1.31 t/ha/year), and grain legumes (1.05 t/ha/year). Although this erosion rate was higher than that in the Riverina, both values fell within the low range when considering the broader spectrum of erosion rates observed globally (Wuepper et al., 2019).

In contrast, the Far West region of New South Wales (NSW), characterized by the lowest water erosion rate of 0.18 t/ha/year and a low erosion risk capability of 0.11, exhibits only moderate crop yields. Specifically, oats yield 0.86 t/ha/year, wheat yields 1.08 t/ha/year, and barley yields 1.26 t/ha/year. This moderate productivity is likely influenced by the region's low rainfall (NSW Office of Environment and Heritage 2014), which limits water availability for crops, despite low erosion rates. Additionally, significant wind erosion and adverse weather conditions further exacerbate soil degradation and constrain agricultural productivity in this dry cropland area (Yang et al., 2023; Dregne, 1995).

In the Northwest Slopes and Plains region of New South Wales (NSW), an erosion rate of 0.52 t/ha/year, coupled with an erosion risk capability of 0.075, results in variable crop performance. Sorghum thrives in this environment, yielding 3.04 t/ha/year, attributed to the region's warmer climate and adequate rainfall. Barley (1.93 t/ha/year) and wheat (1.89 t/ha/year) also demonstrated strong performance. In contrast, oats (0.30 t/ha/year) and grain legumes (1.05 t/ha/year) yielded less, indicating a higher sensitivity to erosion and environmental conditions. Sorghum's resilience in dry

conditions enhances its value as a summer crop, while wheat remains a crucial staple during the winter months (Potgieter et al., 2016).

In the Tablelands region of NSW, where the erosion rate was notably higher at 2.34 t/ha/year and the erosion risk capability was 0.086, wheat achieved favourable yields of 2.31 t/ha/year. However, oats underperformed, yielding only 0.39 t/ha/year, suggesting that increased erosion rates negatively impacted their productivity.

Erosion rates provide valuable insights into soil degradation; however, integrating these rates with erosion risk capability offers a more comprehensive understanding of soil resilience and its implications for crop yields. For example, in the Riverina region of New South Wales (NSW), where both erosion rates and risk capability were favorable, crop performance was robust. Conversely, in the Tablelands region, despite higher erosion rates, certain crops still achieve satisfactory yields, attributable to the moderate erosion risk capability. This emphasises the importance of considering both erosion rates and risk capability when developing effective soil management strategies tailored to the unique conditions of each region.

It is also important to acknowledge that crop yield variability is influenced not solely by soil erosion rates and erosion risk capabilities but also by climatic factors such as rainfall distribution, temperature fluctuations, and extreme weather events (Beillouin et al., 2020). For example, in the Far West region, where water erosion rates are low, but yields remain moderate, limited rainfall and high temperatures act as limiting factors. Similarly, in the Northwest Slopes and Plains, sorghum thrived due to its resilience to warm and dry climates, illustrating the interplay between crop-specific climatic adaptability and soil conditions (Khalifa & Eltahir, 2023; Mwamahonje et al., 2024). Thus, while soil-related metrics like erosion rates and mitigation capacity provide essential insights into soil degradation and resilience, their influence on yield must be interpreted alongside climatic and other environmental factors.

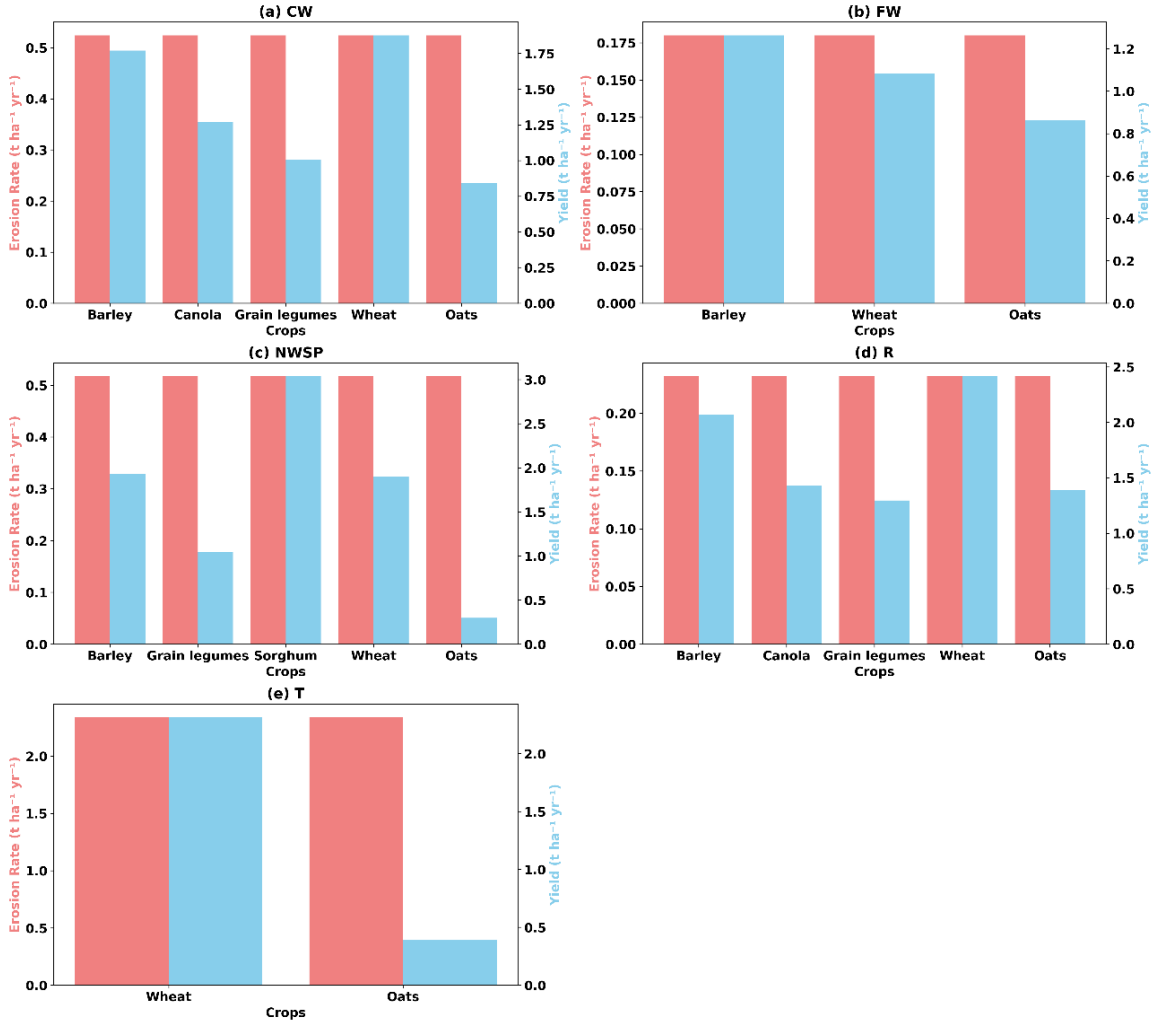

Fig. 21. Crop Yield and Erosion Rate Across NSW Regions. This figure compares crop yield (blue bars) across five NSW regions: (a) Central West (CW), (b) Far West (FW), (c) Northwest Slopes and Plains (NWSP), (d) Riverina (R), and (e) Tablelands (T). The red bars indicate the regional average erosion rate, which remains the same for all crops within each region.

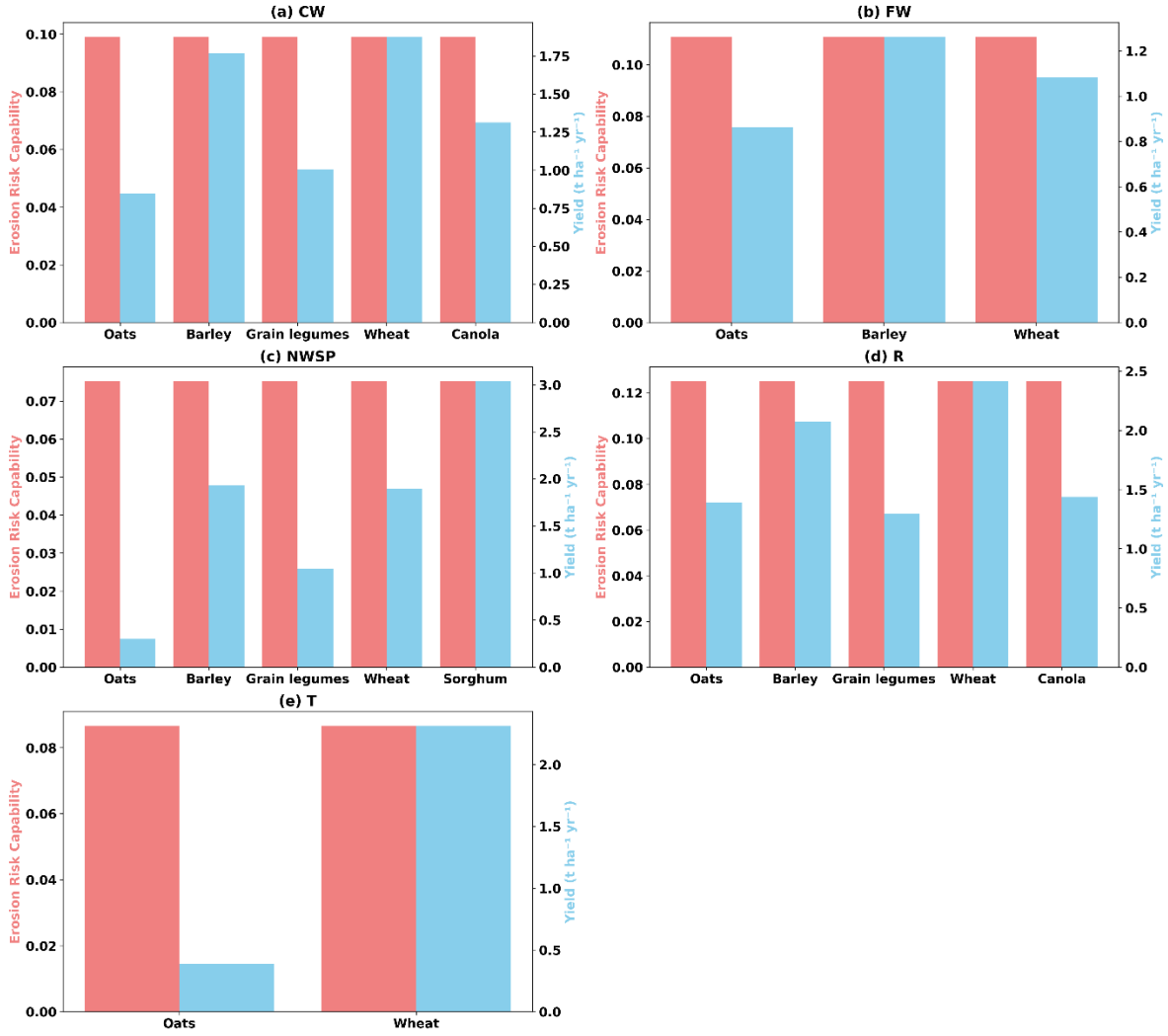

Fig. 22. Crop Yield and Erosion Risk Capability Across NSW Regions. This figure compares crop yield (blue bars) across five NSW regions: Central West (CW), Far West (FW), Northwest Slopes and Plains (NWSP), Riverina (R), and Tablelands (T). The red bars indicate the regional average erosion risk capability, which remains the same for all crops within each region.

3.4.3 Relationship between soil erosion footprint and Crop receipts in NSW

The analysis revealed an inverse relationship between the soil erosion footprint and crop receipts across various crops and regions in New South Wales (NSW), based on a logarithmic regression model of the form $y = a\ln(x) + b$ relating average farm revenue per crop to soil erosion footprint values from 1990 to 2022 (Section 3.3.7). Representative relationships for selected crops and regions are shown in Fig. 23, while additional crop- and region-specific results are provided in the Appendix (Fig 2). This relationship likely reflects the cumulative effects of soil degradation, as the soil erosion footprint integrates erosion rates, soil service metrics, and erosion risk capability, providing a broader perspective on the economic impacts of soil erosion beyond short-term fluctuations.

While crop yield influences both soil erosion footprint (as a measure of soil service) and crop receipts (as economic output), these metrics represent different aspects. The soil erosion footprint reflects the soil's ability to sustain productivity under erosion pressures, whereas crop receipts capture economic returns. The absence of a linear relationship further suggests that the observed trends reflect broader degradation patterns rather than a direct dependency between these two variables.

Regional variations in crop receipts are influenced by differences in soil properties, crop-specific yield potential, management practices, and climatic conditions. While annual data may not fully capture medium- to long-term erosion effects, the soil erosion footprint accounts for ongoing and cumulative soil degradation impacts. This aligns with prior studies highlighting the gradual decline in productivity in regions experiencing persistent soil erosion (Vanwalleghem et al., 2011). Incorporating longer-term datasets in future research could refine the temporal dynamics of soil degradation and its economic consequences. Additionally, farm-level data could enhance the analysis by directly comparing soil footprint values against crop receipts, offering a more granular understanding of how soil degradation affects economic returns at the farm scale.

The logarithmic model showed moderate to low R^2 values, indicating variability in the strength of the inverse correlation across different crops and regions. Selected relationships illustrating this variability are presented in Fig. 23, whereas the full set of crop-and region-specific regression results is shown in the Appendix (Fig 1).

For wheat, R^2 values ranged from 0.26 to 0.52, suggesting a moderate fit, while canola exhibited R^2 values between 0.18 and 0.22. Barley had R^2 values from 0.28 to 0.30, oats ranged from 0.13 to 0.23, sorghum had an R^2 of 0.28, and grain legumes showed values between 0.17 and 0.30 (Appendix Fig 1). The FW region for oats ($p = 0.093$) was excluded from the percentage deviation analysis due to limited data points and high variability, resulting in a non-significant relationship between soil erosion footprint and receipts.

The results highlight that, while an overall inverse trend exists, the strength of the relationship between soil erosion footprint and crop receipts varies depending on crop type and regional conditions. This variability could arise from differences in soil properties, crop characteristics, and management practices (Lal & Moldenhauer, 1987). Additionally, Regional factors such as topography and climate, particularly rainfall erosivity, influence erosion in New South Wales (Yang et al., 2022), which may have implications for economic outcomes. For instance, steeper slopes in the Tablelands may contribute to higher erosion rates despite similar management practices, leading to variability in crop receipts.

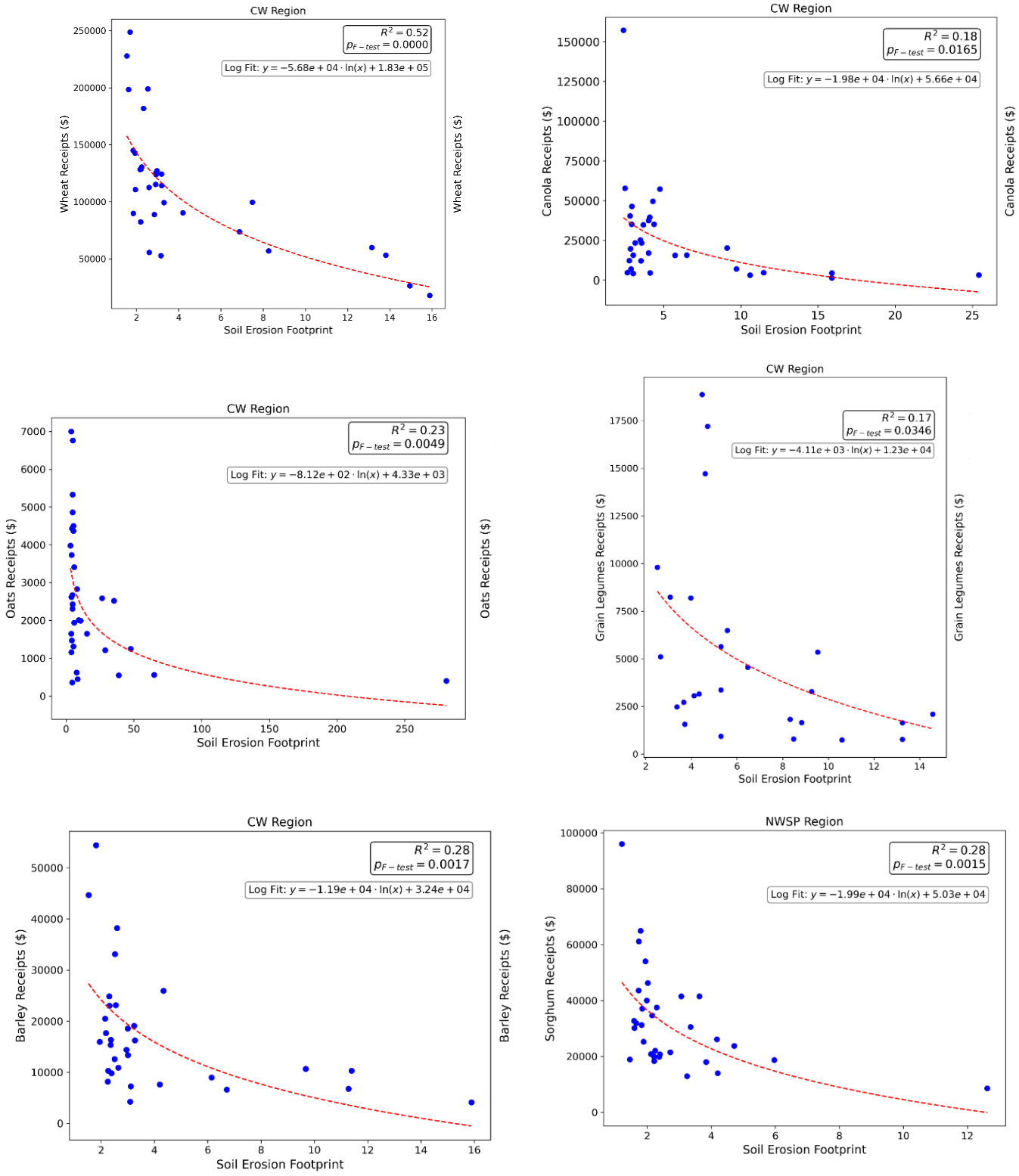

Fig. 23. Logarithmic relationship between soil erosion footprint and crop receipts for selected crops in the Central West (CW) and Northwest Slopes and Plains (NWSP) regions of New South Wales (NSW). Each panel shows average farm revenue (in dollars) plotted against soil erosion footprint values over the period 1990–2022. The fitted curves represent logarithmic regression models (Eq.

10), with R^2 and p-values indicating the strength and significance of the relationships. Results for additional regions and crops are provided in the Appendix.

3.4.4 Impact of Soil Footprint on Crop Receipts Across Different Regions

The analysis, based on Equation 15 in Section 3.3.7, reveals significant regional variability in the impact of an increased soil erosion footprint on crop receipts across New South Wales (NSW). Representative results for wheat and oats are shown in Fig.24, while crops and regions specific results for other crops are presented in the Appendix (Fig.2). The percentage deviation calculated using Percentage Deviation = $\left(\frac{Impact}{M}\right).100$, quantifies the relative change in crop receipts due to changes in the soil erosion footprint, where "Impact" refers to the absolute difference in receipts under increased erosion scenarios, and M represents the mean receipts for the region.

The Northwest Slopes and Plains (NWSP) region consistently demonstrated the highest percentage deviations for several crops, as shown for wheat in Fig.24 and for other crops in the Appendix (Fig 2). For instance, grain legumes showed nearly -80% deviation at a 100% increase in soil erosion footprint, -48% at a 50% increase, and -22% at a 20% increase. Wheat exhibited deviations of up to -48%, -28%, and -12% at the corresponding footprint levels, while sorghum shows approximately -40%, -25%, and -11%. This heightened sensitivity to soil degradation is particularly concerning given the region's high mean receipts, approximately $172,452.42 for wheat and $43,065.76 for grain legumes.

Similarly, the Riverina (R) region exhibited notable deviations, particularly for barley (-48% at a 100% increase, -25% at a 50% increase, and -12% at a 20% increase), canola (-68%, -40%, and -18%), and wheat (-33%, -18%, and -10%), with these results shown in the Appendix (Fig 2) except for wheat, which is illustrated in Fig 24. This is noteworthy given the region's high mean receipts for several crops, such as $43,994.38 for canola and $131,828.79 for wheat, highlighting significant financial sensitivity to soil erosion footprint.

In contrast, the Central West (CW) and Far West (FW) regions showed moderate deviations, with CW reaching up to -55% at a 100% increase, -30% at a 50% increase, and -16% at a 20% increase for grain legumes. The FW region displays deviations of approximately -37%, -20%, and -10% for wheat. These patterns are illustrated for wheat in Fig.24 and for other crops in the Appendix (Fig 2). The lower absolute impacts in these regions align with their comparatively lower mean receipts, exemplified by $26,089.38 for canola in CW and $66,426.97 for wheat in FW. The Northern Central Slopes (T) region also demonstrates significant deviations for oats (-35% at a 100% increase, -23% at a 50% increase, and -10% at a 20% increase) and wheat (-44%, -25%, and -12%). However, the lower mean receipts in this region result in a less pronounced absolute impact.

The results indicate that the economic impact of soil erosion footprint is influenced not only by the magnitude of changes in the soil erosion footprint but also by the mean crop receipts within each region. Regions with higher mean receipts, such as the Northwest Slopes and Plains (NWSP) and the Riverina, experience greater absolute financial losses with increases in soil erosion footprint, underscoring their vulnerability to soil degradation. However, it is important to note that this trend is not observed in all crops. For instance, barely exhibits relatively smaller deviations, indicating that factors other than soil degradation, such as climate adaptability and crop management practices, may play a more significant role in determining their economic impact. Similarly, sorghum's performance, particularly in NWSP, may reflect resilience to drier conditions rather than direct sensitivity to soil erosion, though limited data restricts a full assessment of its vulnerability.

These findings highlight the importance of assessing production losses due to soil erosion on a per-unit area basis while considering crop-specific responses and external influencing factors to identify areas most significantly affected economically (Sharda & Dogra, 2013). Additionally, they emphasize the need for region- and crop-specific management strategies that integrate soil conservation with optimized fertilization, irrigation, and crop diversification to mitigate economic risks and enhance long-term agricultural sustainability.

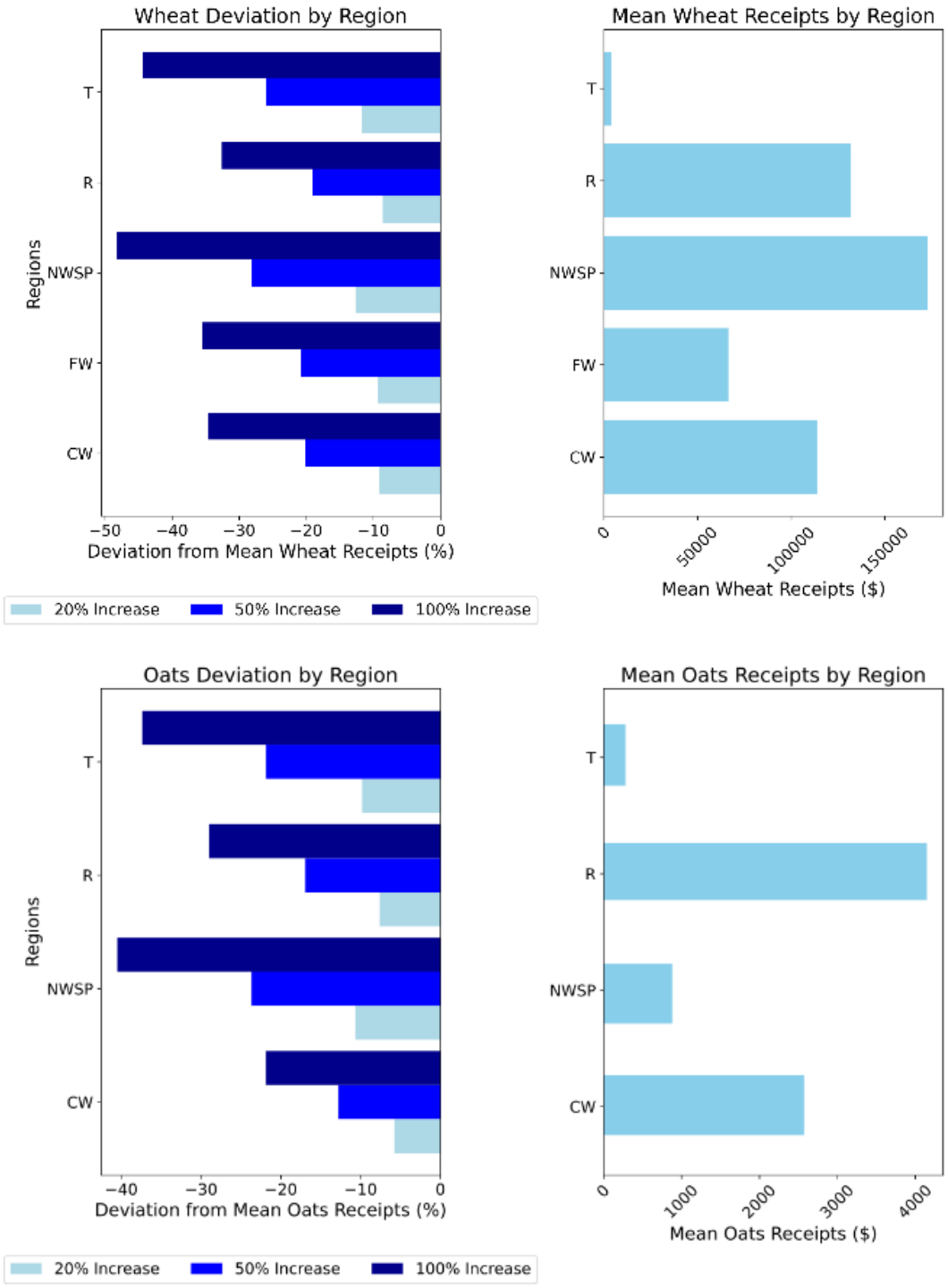

Fig. 24. Impact of Soil Erosion Footprint Increases on Crop Receipts Across NSW Regions. The fig shows the percentage deviation in crop receipts for various crops under 20%, 50%, and 100% increases in soil erosion footprint across regions relative to the mean crop receipts. The left panels display the percentage deviations, while the right panels show the mean crop receipts ($) per region. Results for additional regions are provided in the Appendix.

3.4.5 Variation of AWC and Soil Service Ratio Mapping Across NSW

Fig. 25A illustrates the spatial distribution of Available Water Capacity (AWC) across New South Wales (NSW), based on topsoil data (0–5 cm) from the TERN/CSIRO dataset, with AWC values ranging from 6.53% to 23.55%. The highest AWC levels, between 16% and 23.55%, are predominantly concentrated in the Northwest Slopes and Plains region, with notable pockets in the Far West and certain Coastal areas. Moderate AWC values, ranging from 10% to 14.79%, are distributed across various regions of NSW. In contrast, the lowest AWC levels, between 6% and 10.59%, are primarily found in the Riverina, Central West, and Coastal regions, indicating reduced AWC in these areas.

Fig. 25E presents the soil service ratio map, calculated as the ratio of AWC between genosoil and phenosoil, as described in Section 2.6 and illustrated in Fig. 25B and 25C. These ratio values are normalized to a scale of 0 to 1 (see Fig. 18 and 19 and Section 2.3, Equations 6 and 7). Across NSW, the phenosoil/genosoil AWC ratio varies from 0.760 to 1.25. Higher deviations, shown in yellow, are primarily located in the Far West, Riverina, and Central West regions, indicating significant discrepancies between the AWC of phenosoil and genosoil. In contrast, the Northwest Slopes and Plains exhibit the lowest deviations, with ratios ranging from 1.0 to 1.22, suggesting that the AWC of phenosoil in this region is similar to that of genosoil. Medium deviations, with ratios between 0.8 and 1.0, are observed in other areas of NSW, reflecting an intermediate level of alteration in soil properties.

3.4.6 Soil erosion footprint based on AWC as a soil service

Fig. 25, comprising sub–Fig. A to H, illustrates the intermediate maps used to calculate the spatial soil erosion footprint according to Equation 5, with Available Water Capacity (AWC) as the soil service. Fig. 25I presents the final soil erosion footprint map for NSW. Dark red areas indicate larger footprint values, reflecting a higher erosion impact relative to the soil's capacity to provide essential services and mitigate degradation. In contrast,

light blue areas represent smaller footprint values, suggesting minimal erosion impact and a greater ability to sustain soil services.

The coastal regions exhibit the highest soil erosion footprint values (dark red), with values reaching approximately 4761.90, likely due to elevated erosion rates compared to other regions of NSW (Yang et al., 2023). Moderate footprint values (lighter red) are observed in other parts of the coastal and adjacent regions, with wind erosion identified as a contributing factor in the western areas (Yang et al., 2023). Additionally, high to moderately high footprint values are observed in the dryland cropping areas of the wheat belt, indicating increased erosion vulnerability and the need for targeted erosion management to support productivity in these regions (Thomas et al., 2018).

Lower soil erosion footprint values, shown in light blue, are scattered across NSW, especially in parts of the wheat belt, with more consistent lower values observed in the Riverina region. Moderately low soil erosion footprint values are present across much of NSW, with fewer instances in coastal areas and the Tablelands. This distribution pattern suggests that moderate soil service ratios combined with erosion risk capability influence the spatial variation of soil erosion footprints across NSW, as illustrated in sub - Fig. E and F of Fig. 25.

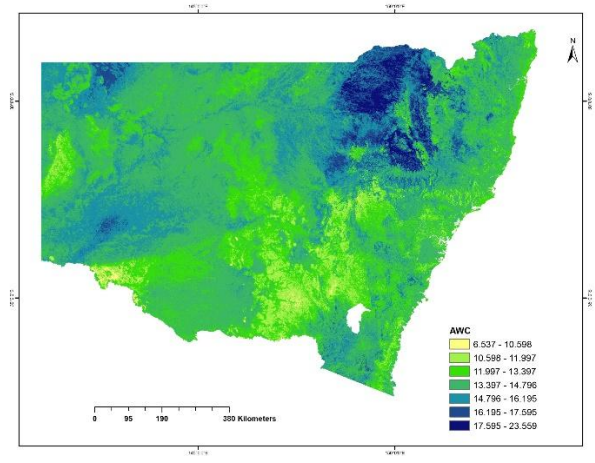

Fig. A. Available water Capacity

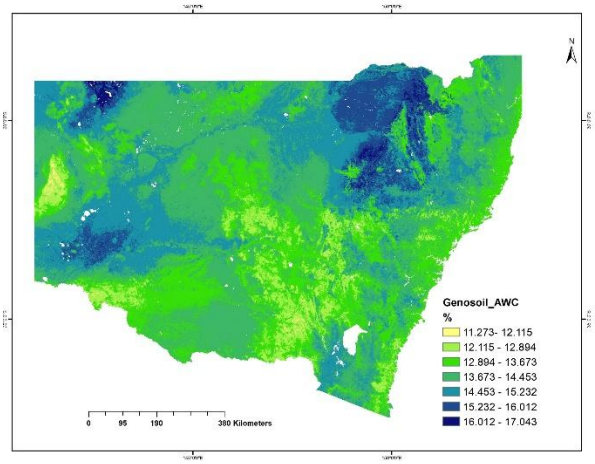

Fig.B. Genosoil-Available water Capacity

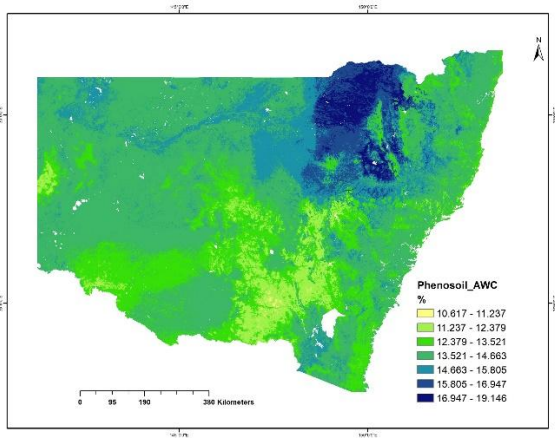

Fig. C. Phenosoil-Available water Capacity

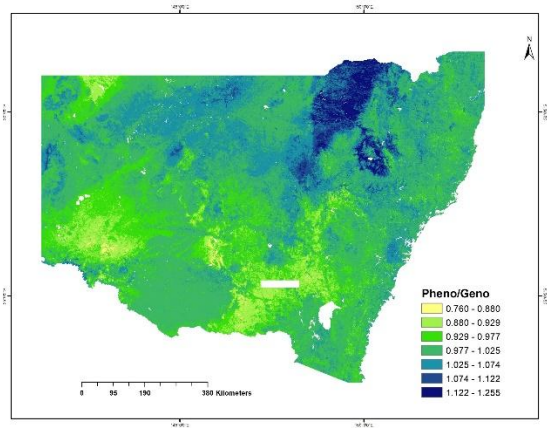

Fig. D. Ratio between Pheno/Geno soil - Available water Capacity

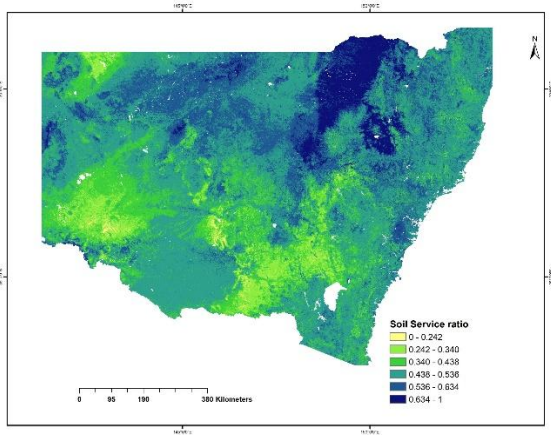

Fig. E. (Q_n) normalized Soil Service ratio

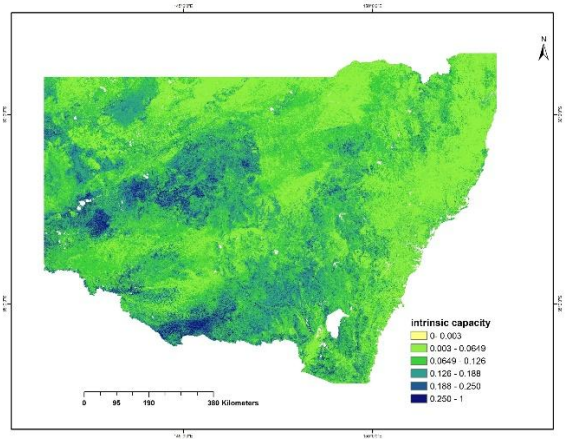

Fig. F. Erosion risk capability map

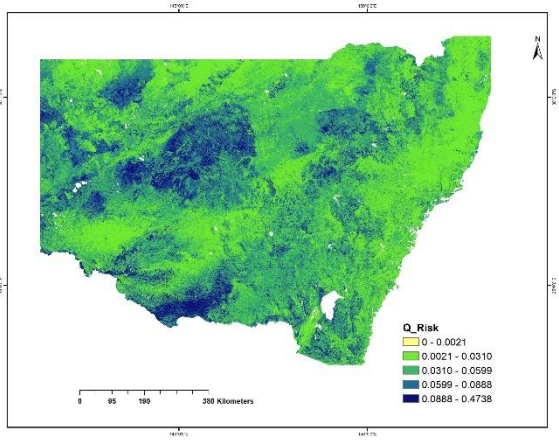

Fig. G. Map showing the product of intrinsic capacity and normalized soil service ratio

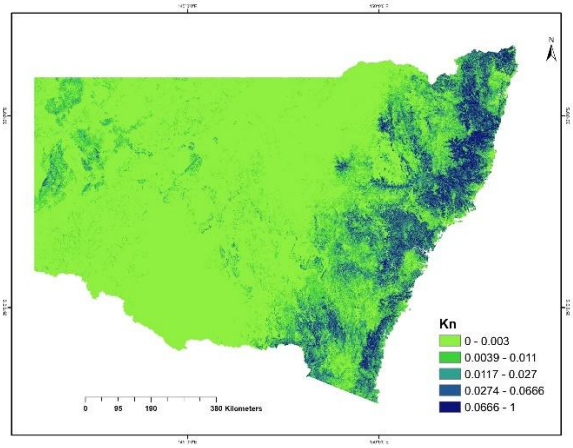

Fig. H. (K_n) normalized Erosion rate

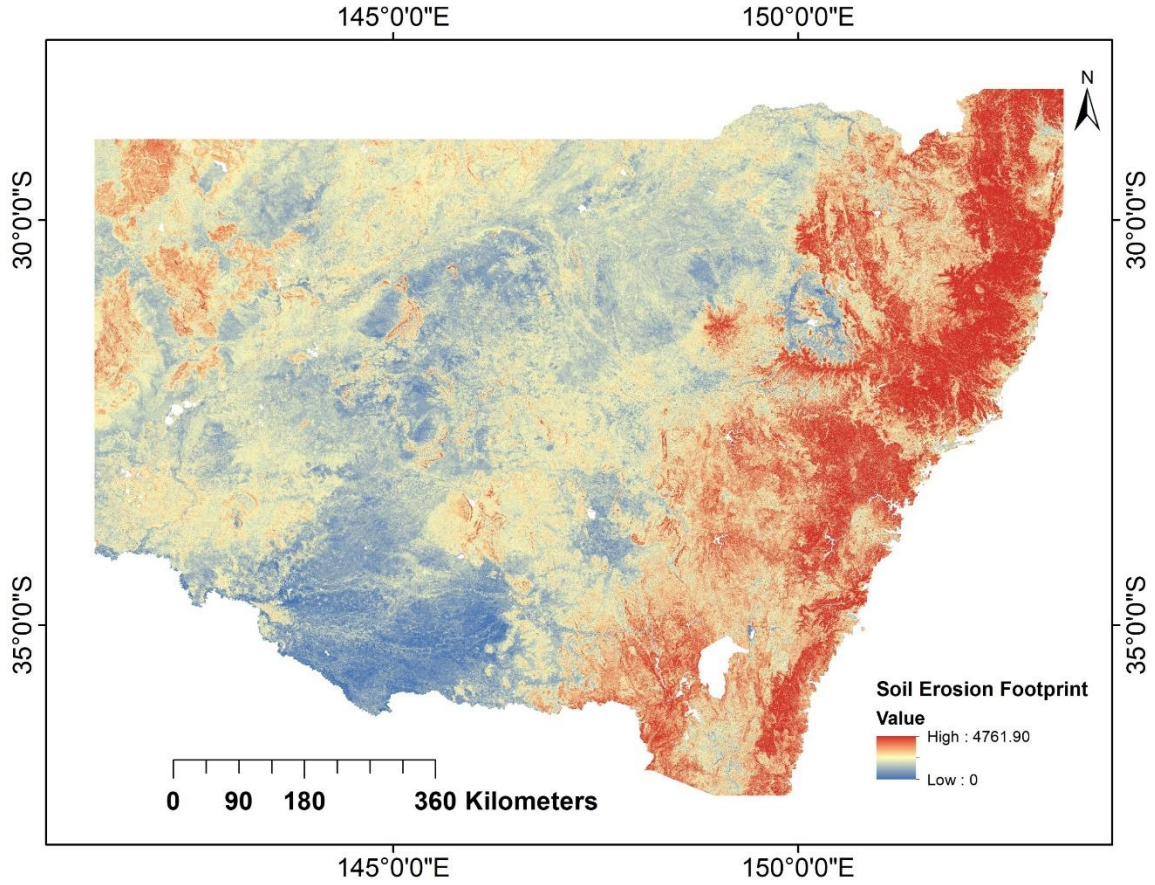

Fig. I. Soil Erosion Footprint Map

Fig. 25. Intermediate Output and Final Soil Erosion Footprint Map. The fig displays the intermediate outputs and the final soil erosion footprint map based on Equation 5, where AWC is used as the soil service measure.

3.4.7. Integrating assessment of soil erosion across land use systems

This section evaluates soil erosion footprints across various land use systems by integrating erosion rate, erosion risk capability, and soil service ratio. Land use classes were categorised into five systems, each with subclasses as described in Section 2.7. The average soil erosion footprint for each subclass was calculated using the spatial footprint map (Fig. 25I). Fig. 26 presents the ranking of land use types based on their mean soil erosion footprint values. Additionally, Fig. 27 examines the relationships between soil erosion rate, soil service ratio, and erosion risk capability across different land uses in NSW.

In the IDS, dryland systems, including cropping and horticultural practices, exhibited a broader range of soil erosion footprints compared to irrigated systems, reflecting differences in erosion susceptibility Fig.26. This variability is evident in soil service ratios

(SSR), erosion risk capabilities (ERC), and soil erosion rates (SER), as shown in Fig.27. Dryland cropping and horticulture collectively showed erosion footprints ranging from 0.1 to 0.9, compared to irrigated systems, which exhibited a narrower range of 0.08 (IC) to 0.2 (IHP) (Fig. 26). This highlights the greater vulnerability of certain dryland practices, particularly horticulture, to erosion. The higher erosion footprints in dryland systems can be attributed to reduced AWC, which limits the soil's ability to retain moisture and buffer against erosion. Decreasing AWC, driven by factors such as soil erosion, compaction, and organic matter loss, significantly affects soil stability and increases erosion risks (Trnka et al., 2022).

Fig. 27 illustrates the contrasting characteristics of irrigated and dryland systems regarding soil erosion dynamics. These results should be interpreted within the context of comparisons made within the same system, such as dryland cropping to irrigated cropping or dryland horticulture to irrigated horticulture, as each subclass possesses distinct characteristics that influence soil erosion dynamics. Irrigated systems are associated with lower erosion rates, higher erosion risk capabilities, and elevated soil service ratios, indicating a more robust capacity for erosion management and mitigation. Erosion Risk Capability represents the gap between the soil's natural resistance to erosion and its current state, emphasizing its susceptibility to erosion and potential to mitigate future risks. Higher erosion risk capability values reflect soils with a greater capacity to resist erosion pressures.

Conversely, dryland systems exhibit higher erosion rates, reduced erosion risk capabilities, and reduced soil service ratios, rendering them more susceptible to erosion. This observed pattern is consistent with both local surveys and global research, which identify soil erosion as a critical challenge in dryland agriculture (Dregne, 1995; Graham, 1992; Farooq & Siddique, 2016). For instance, dryland cropping (DC) is characterized by an erosion rate of approximately 0.171 t/ha/year, an erosion risk capability of 0.097, and a soil service ratio of 0.494, indicating higher vulnerability. In contrast, irrigated cropping (IC) demonstrates a significantly lower erosion rate (~0.04 t/ha/year), the highest erosion risk capability (0.114), and an enhanced soil service ratio (0.550), collectively contributing to a reduced erosion vulnerability.

This interaction highlights the importance of integrating erosion risk capability and soil service ratios alongside erosion rates to achieve a comprehensive understanding of soil services under stress. An exclusive focus on erosion rates may insufficiently capture the potential for erosion mitigation. This perspective aligns with studies advocating holistic assessments of soil health and security (Lal, 1993; Evangelista et al., 2024). Such comprehensive evaluations are vital for informing soil management strategies that promote sustainability and enhance agricultural productivity.

In the Grazing Ecosystem (GE), analysis indicates that grazing modified pastures (GMP) exhibit the highest soil erosion footprint, quantified at 0.32, followed by grazing native vegetation (GNV) at 0.20. In contrast, irrigated pastures (IP) display the lowest recorded erosion footprint, at 0.04. Specifically, GNV is characterized by an erosion rate of 0.55 t/ha/year, an erosion risk capability of 0.103, and a soil service ratio of 0.487, resulting in a moderate erosion footprint. Comparatively, GMP demonstrates a slightly lower erosion risk capability (0.093) but a significantly higher erosion rate (0.87 t/ha/year) and a soil service ratio of 0.484, indicating increased vulnerability to erosion. Conversely, irrigated pastures exhibit the strongest erosion mitigation capacity, with the lowest erosion rate (0.099 t/ha/year), a higher erosion risk capability (0.093), and a soil service ratio of 0.489. These results underscore the substantial influence of varied grazing management practices on soil erosion outcomes and overall soil health, emphasizing the importance of effective land management strategies for enhancing soil sustainability (Byrnes et al., 2018).

In the Forest Production System (FPS), Plantation Forests (PF) demonstrate a lower soil erosion footprint compared to Production Native Forests (PNF). The erosion rate for PF is approximately 1.67 t/ha/year, coupled with a higher erosion risk capability of around 0.082 and a slightly lower soil service ratio of about 0.486. The higher ERC observed in PF can be attributed to the intensive management practices typically associated with plantation forests. These practices, such as controlled tree spacing, periodic thinning, and soil amendments, contribute to improved soil structure, reduced surface runoff, and enhanced root stabilization, collectively mitigating erosion risks (Knoepp & Swank, 1997). In contrast, PNF exhibits a higher erosion rate of approximately 4.02 t/ha/year, a marginally elevated soil service ratio of about 0.490, and a lower erosion risk capability

of approximately 0.078, indicating greater susceptibility to erosion. These findings underscore the critical role of erosion risk capability in enhancing resilience against erosion within the FPS.

In the Protected Land System (PLS), Nature Conservation (NC) areas present a higher soil erosion footprint (2.3) compared to Managed Resource Protection (MRP) areas (0.60). Despite both categories exhibiting similar erosion risk capabilities (approximately 0.083), the disparity arises primarily from NC's higher erosion rate of approximately 3.95 t/ha/year versus MRP's lower rate of about 1.43 t/ha/year. Although NC has a slightly higher soil service ratio (~0.487), suggesting some mitigation potential, MRP's lower erosion rate combined with a less favourable soil service ratio (~0.476) indicates reduced vulnerability to erosion.

The lower erosion rates in MRP compared to NC may be influenced by differences in land management and vegetation cover. Managed areas often incorporate practices like adaptive grazing strategies (e.g., rotational grazing) and reforestation, which enhance soil stability (Xu et al., 2018; Teague & Kreuter, 2020). In contrast, NC areas, despite protection, may have naturally higher erosion rate due to steep slopes or degraded soils, with the lack of active management potentially contributing to erosion (Gager & Conacher, 2001 ;Yang, 2020). However, direct comparisons between MRP and NC areas remain limited, and further research is needed to assess how different management strategies impact erosion over time.

In the Transitional and Minimal Use Land (TMUK) ecosystem, Other Minimal Use (OMU) areas exhibit a significantly higher soil erosion footprint (2.7) than Land in Transition (LIT) areas (1.2), predominantly due to OMU's elevated erosion rate of approximately 4.61 t/ha/year. Despite comparable erosion risk capabilities (approximately 0.080 for OMU and 0.078 for LIT), LIT's slightly higher soil service ratio (~0.541) relative to OMU's (~0.498) suggests a greater erosion mitigation potential, emphasizing how even minor differences in soil properties can substantially influence erosion risk.

Across the five ecosystems, greater deviations between phenosoil and genosoil AWC, reflected by the soil service ratio, generally correspond to higher erosion rates (Frye et al., 1982). However, Fig. 27 demonstrates that this relationship is not strictly linear across all

land use subclasses, as higher soil service ratios do not always correspond to lower erosion rates. This variability can be influenced by additional factors such as topography (LS factor), vegetation cover, and land management practices. Notably, native forests and conservation areas, often on steep, uncultivated terrain with high LS factors, experience elevated erosion (Yang, 2020). These findings highlight the need to consider multiple landscape attributes beyond soil properties when assessing erosion and developing strategies for soil stability.

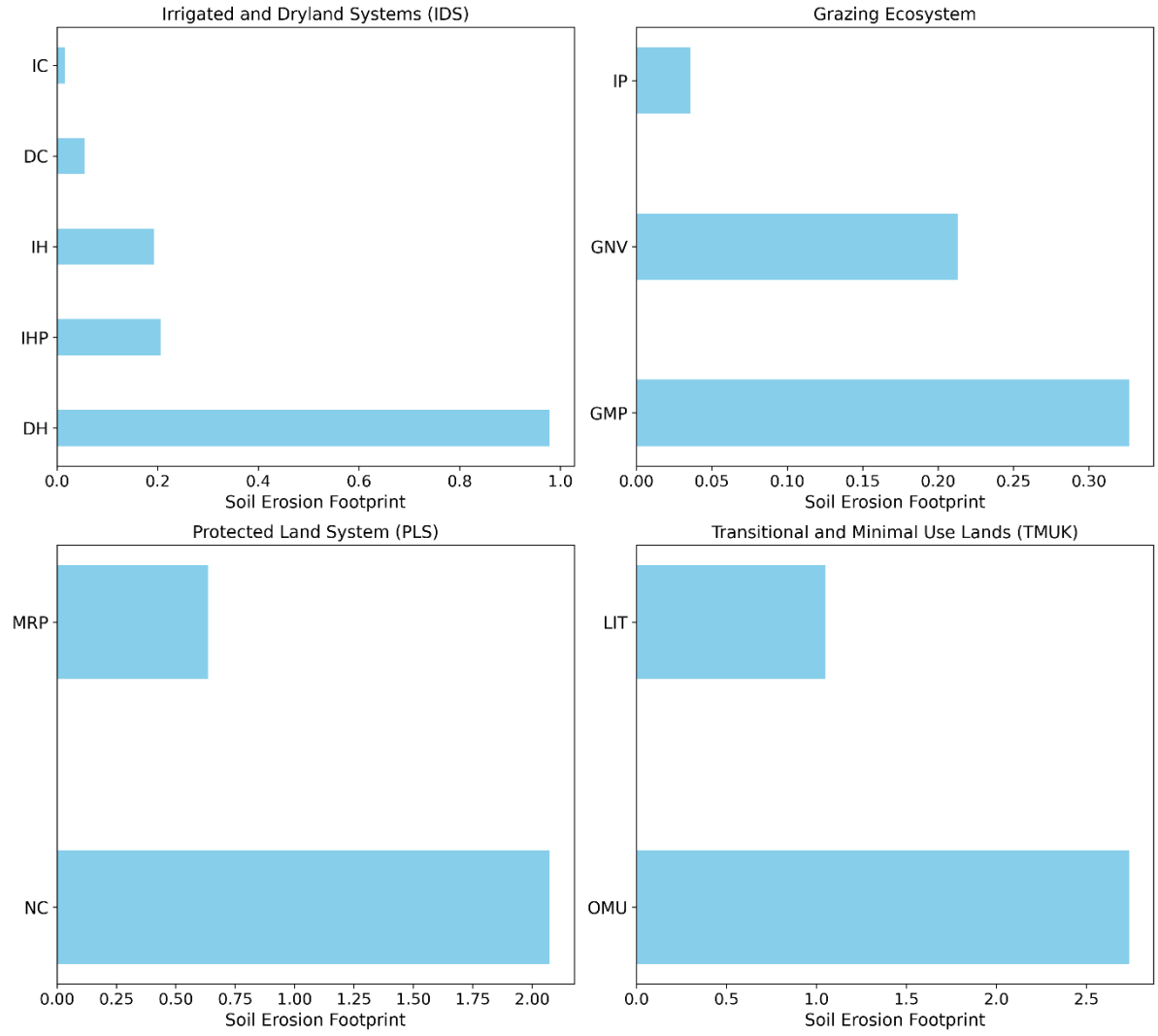

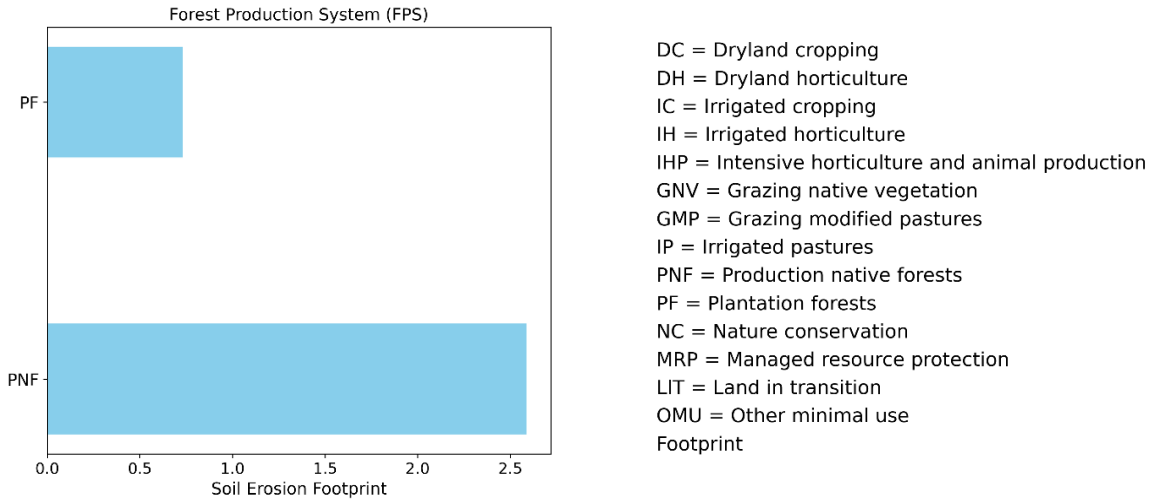

Fig. 26. Land Use Footprint Ranking Based on Mean Soil Footprint Values. The plot ranks various land use types by their soil footprint, with lower footprint values corresponding to higher ranks

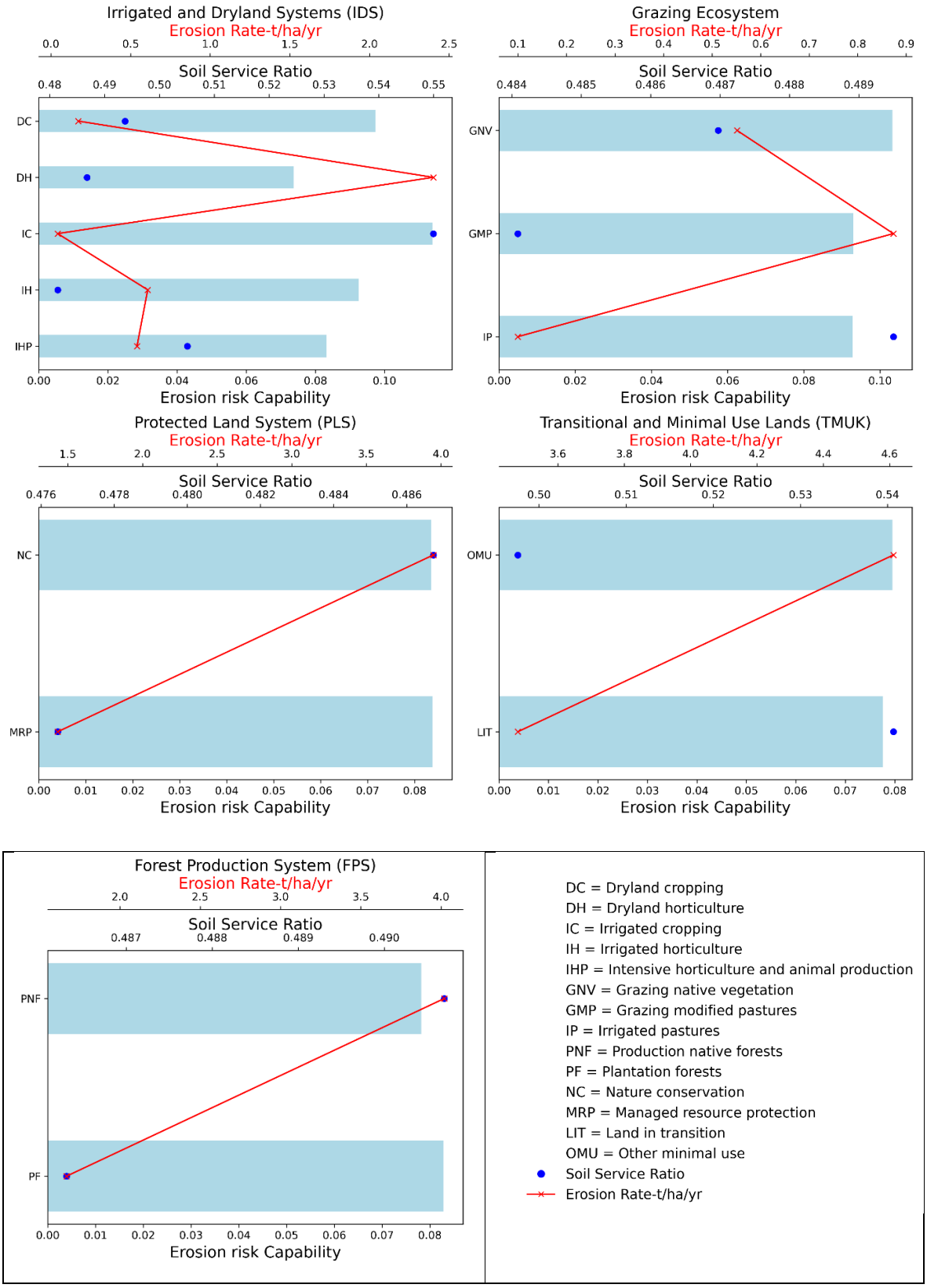

Fig. 27. Relationship Between Soil Erosion Rate, Soil Service Ratio, and Erosion Risk Capability Across Different Land Uses in NSW.

3.5. Conclusion and future work

This study generalized the concept of the soil footprint, developing a framework to quantify different degradation processes and soil services (e.g. yield and AWC), serving as a key indicator of soil security. Soil erosion was analysed as a primary degradation process, with two distinct soil erosion footprints calculated across NSW based on yield and AWC.

Oats exhibited the highest soil erosion footprint due to low yields, while other crops showed smaller footprints. Enhancing oat yields through improved agronomic practices may reduce footprints more effectively than conservation alone, highlighting the importance of integrating yield optimization with soil management.

By incorporating soil erosion rate, erosion risk capability, and soil service ratio, this study examined the influence of soil degradation on agricultural sustainability and economic resilience. Results indicate that soil erosion metrics alone do not fully determine crop productivity; climatic conditions, crop adaptability, and management practices also play crucial roles. Regions like Riverina and Central West, with lower erosion rates and higher erosion risk capabilities, achieved higher yields, while the Tablelands and Northwest Slopes and Plains maintained productivity despite higher erosion rates due to crop adaptability. Economic analysis revealed an inverse relationship between soil erosion footprint and crop receipts, underscoring the financial risks of soil degradation, particularly in high-revenue regions like the Northwest Slopes and Plains and the Riverina.

Soil erosion footprints based on AWC varied significantly across NSW, with coastal and dryland cropping areas showing the highest values, indicating greater vulnerability, while regions like Riverina had lower footprints, suggesting better soil resilience. Across land use systems, dryland cropping, grazing modified pastures, and nature conservation areas had the highest footprints, whereas irrigated systems, plantation forests, and managed resource protection areas exhibited lower footprints. While deviations between phenosoil and genosoil AWC generally correlated with higher erosion rates, factors such as topography, vegetation cover, and land management practices also influenced erosion dynamics.

While simpler indicators, such as the initial approach by Garcia-Gamero et al. (2024), provide a straightforward assessment, the soil footprint framework expanded in this study is flexible, allowing both simplified and more detailed evaluations depending on the application. This adaptability ensures that the framework can be tailored to different stakeholder needs, providing either a high-level assessment or a more comprehensive analysis of multiple degradation processes and soil services.

The concept of the Soil Service Ratio enables comparison between altered soil (phenosoil) and its natural state (genosoil), providing a metric for evaluating human impacts on soil services. This expanded soil footprint framework allows for application across diverse land uses and ecosystems, offering a comprehensive perspective on soil security.

By integrating soil threats, services, and mitigation capacities, the framework serves as a valuable tool for policymakers, stakeholders, and farmers in developing sustainable soil management strategies. Future research should expand this framework to include additional soil threats and services, along with their respective mitigation capabilities, to capture the cumulative impacts on soil health. Standardizing the soil footprint indicator will facilitate informed decision-making, enable cross-regional comparisons, and guide efforts to protect soil resources for the benefit of future generations.

Appendix

Fig.1. Logarithmic relationships between soil erosion footprint and crop receipts across additional crops and regions of New South Wales (NSW).

Wheat crop

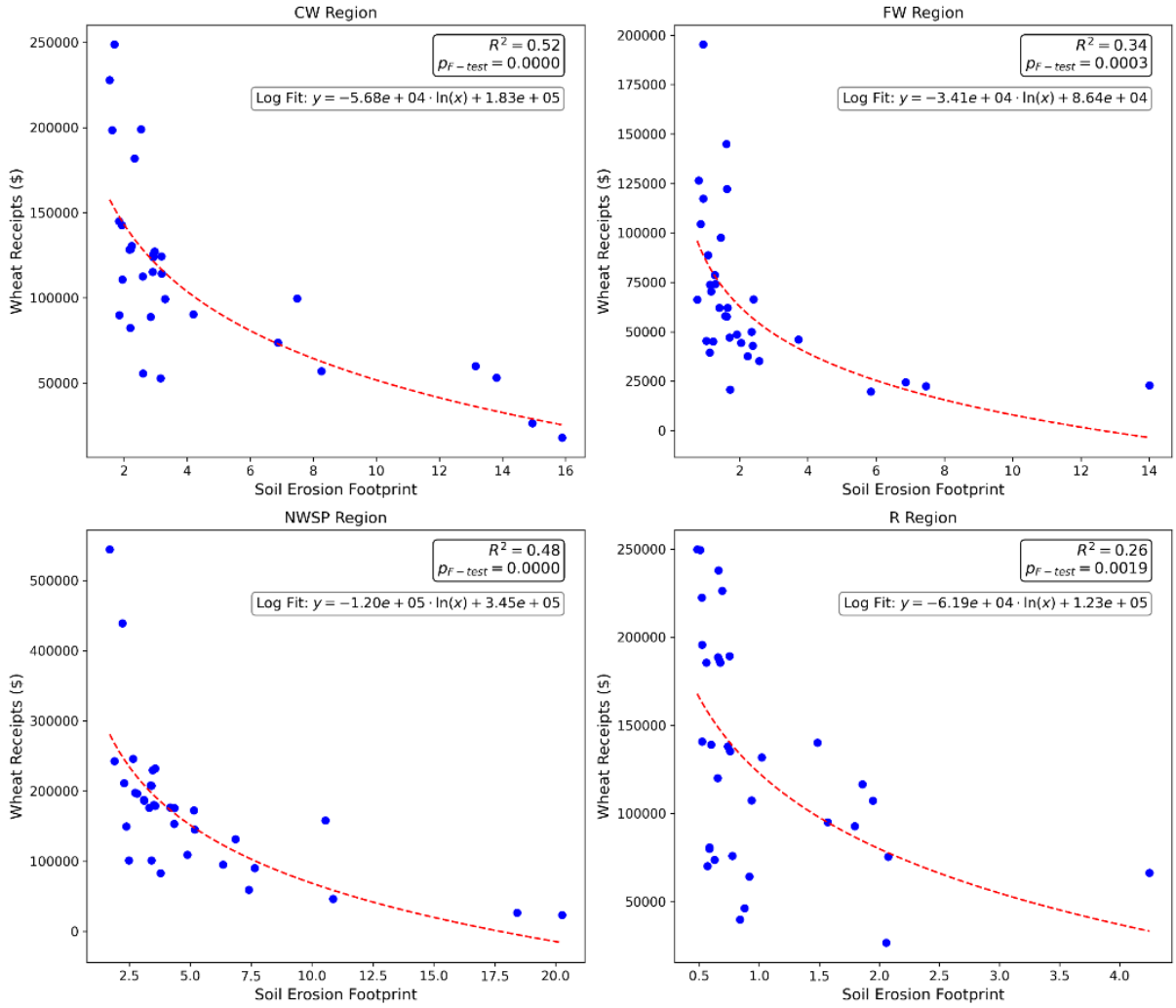

Canola Crop

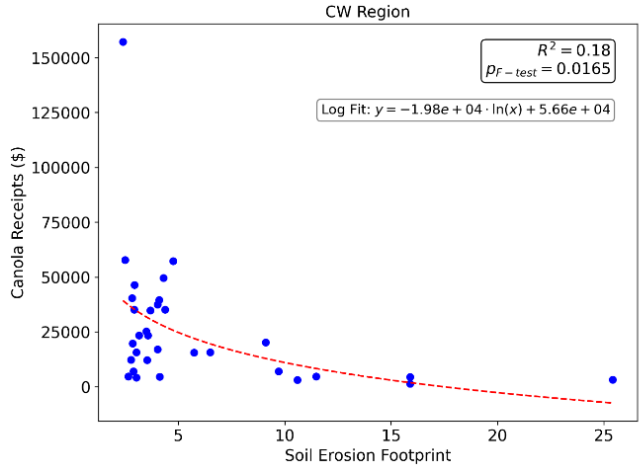

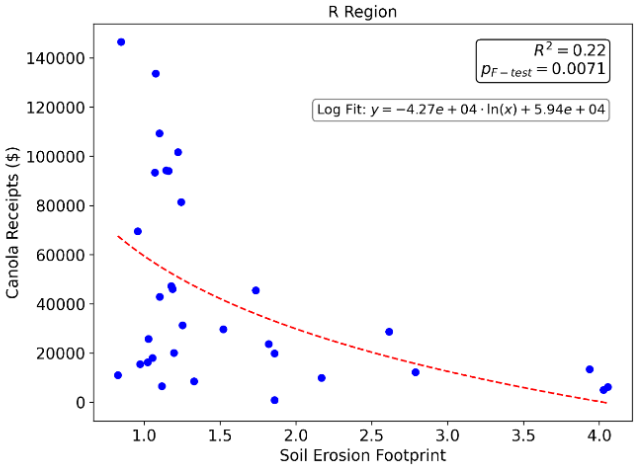

Oats Crop

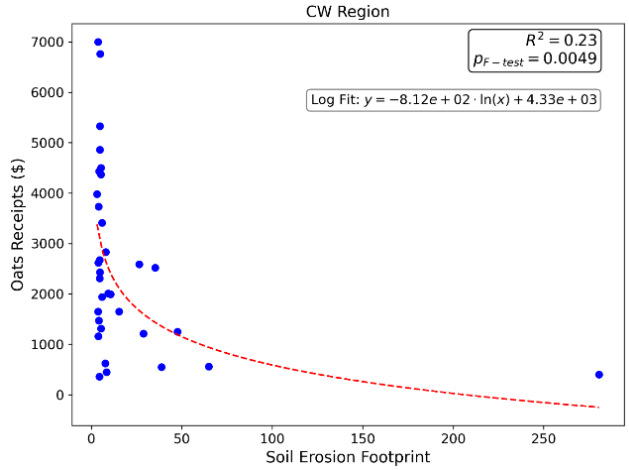

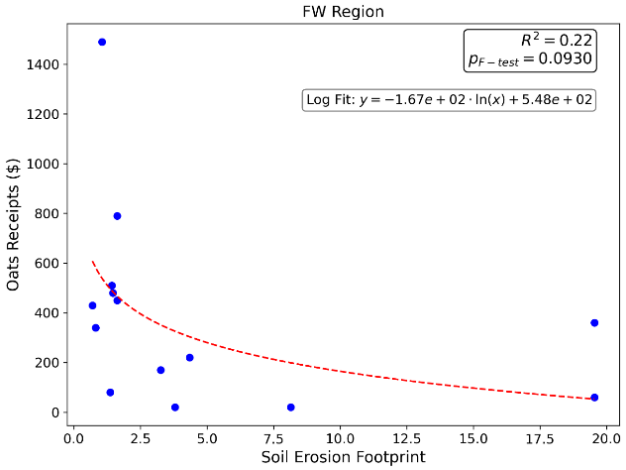

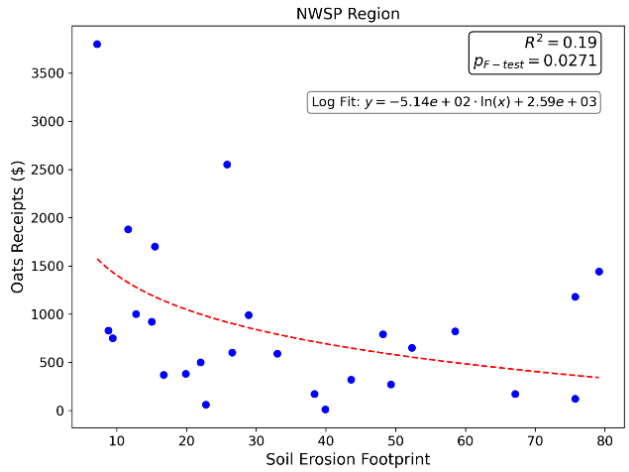

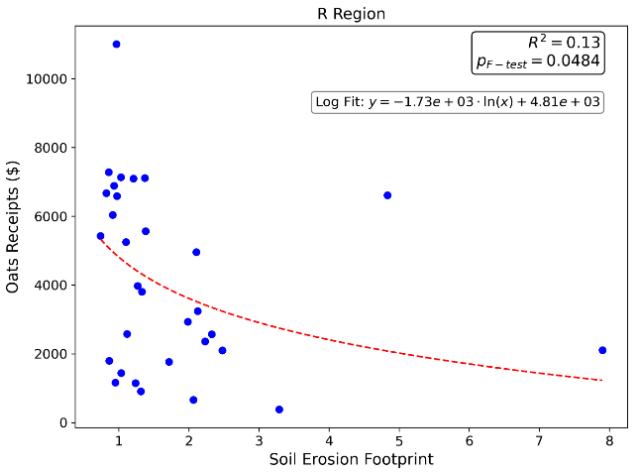

Grain Legumes Crop

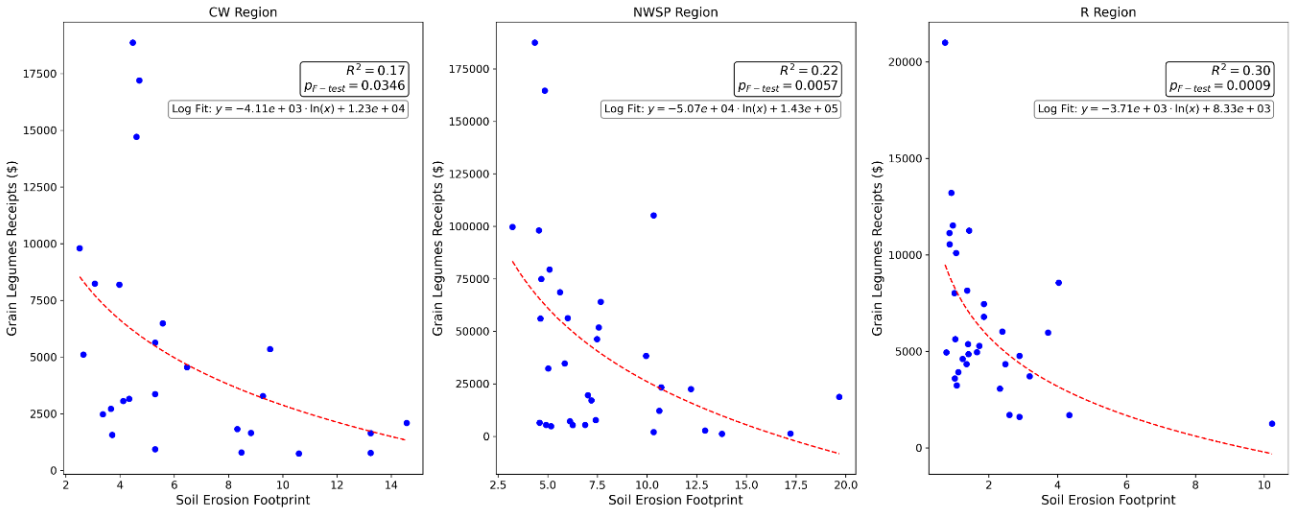

Barley crop

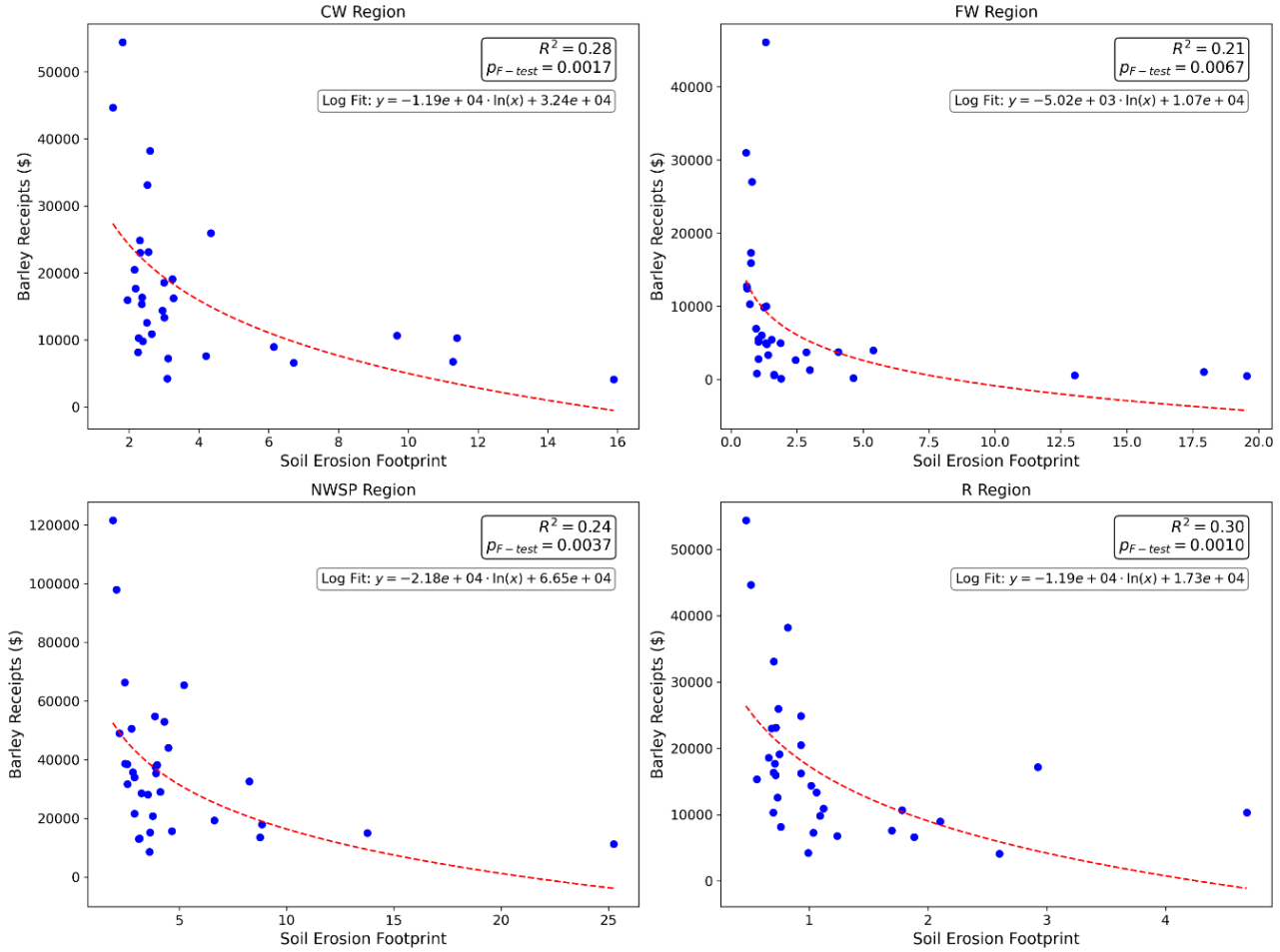

Sorghum Crop

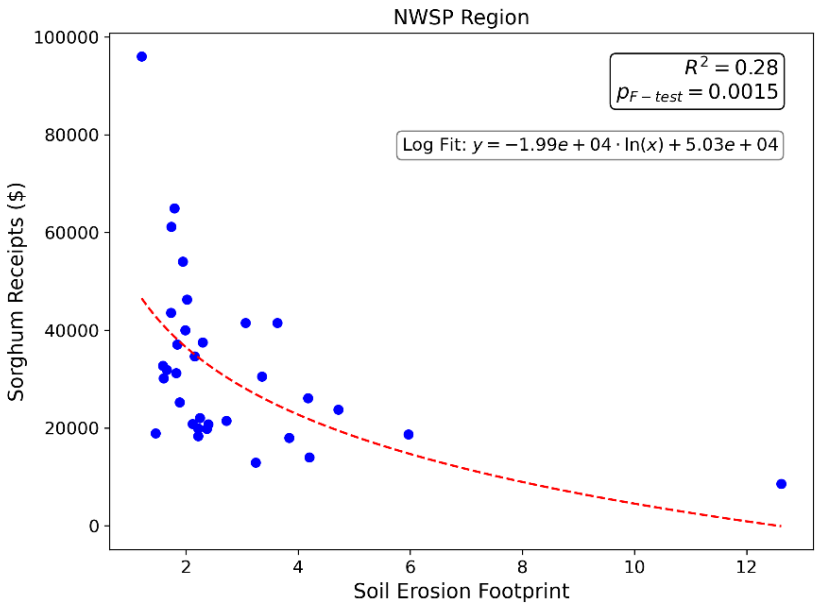

Fig. 2. Impact of Soil Erosion Footprint Increases on Crop Receipts Across NSW Regions. The fig shows the percentage deviation in crop receipts for various crops under 20%, 50%, and 100% increases in soil erosion footprint across regions relative to the mean crop receipts.

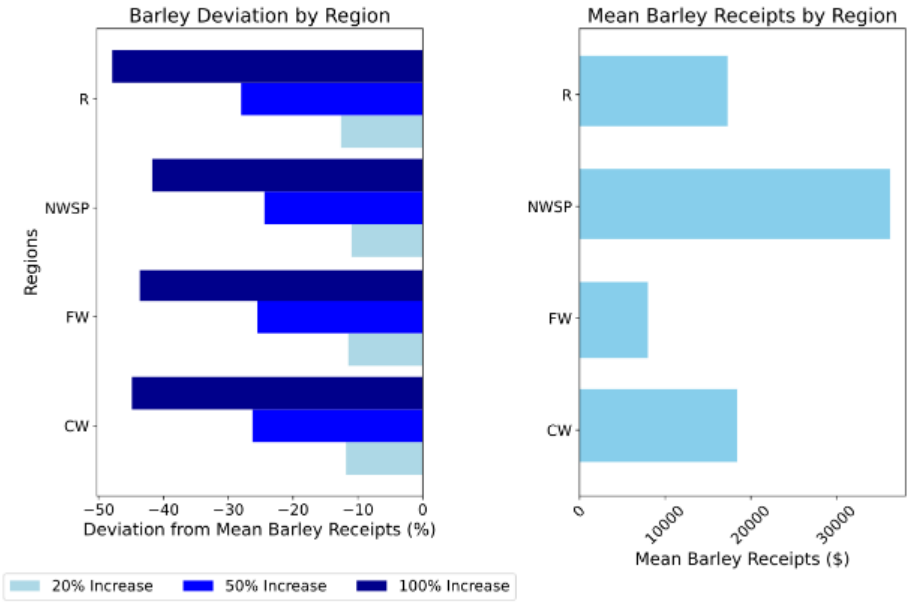

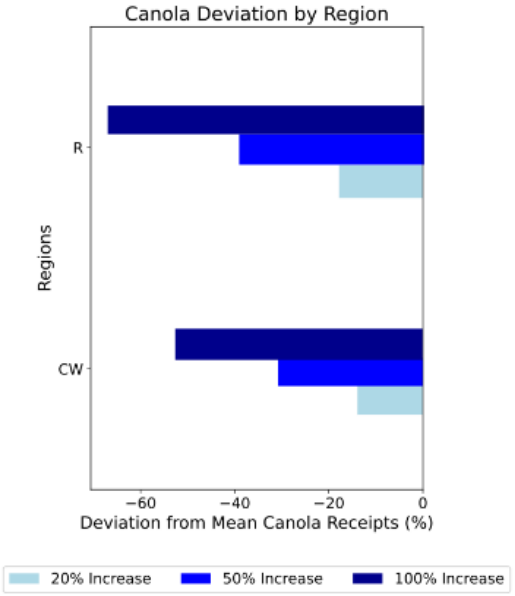
Canola Deviation by Region
Regions
R
CW
−60
−40
−20
0
Deviation from Mean Canola Receipts (%)
20% Increase
50% Increase
100% Increase

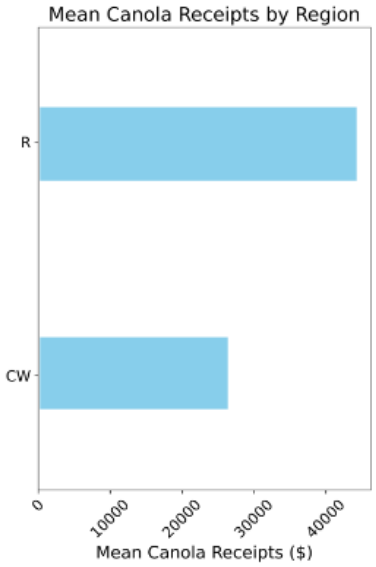
Mean Canola Receipts by Region
R
CW
0
10000
20000
30000
40000
Mean Canola Receipts ($)

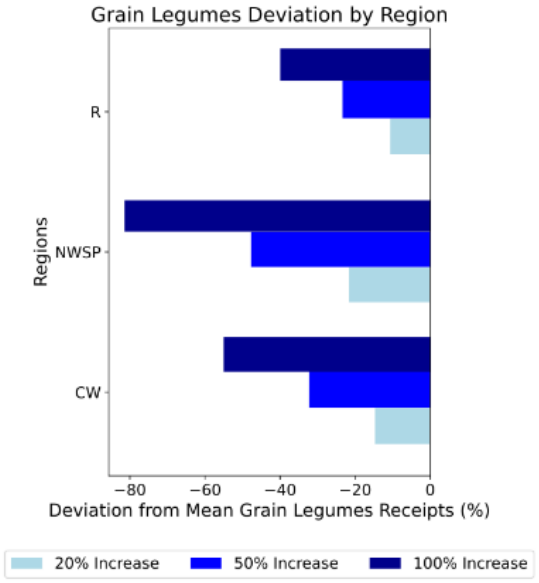
Grain Legumes Deviation by Region
Regions
R
NWSP
CW
−80
−60
−40
−20
0
Deviation from Mean Grain Legumes Receipts (%)
20% Increase
50% Increase
100% Increase

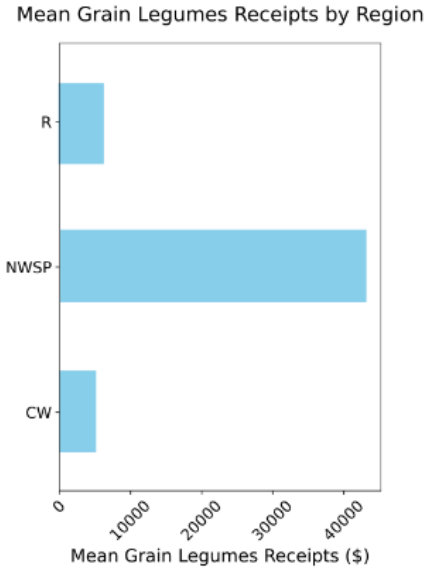
Mean Grain Legumes Receipts by Region
R
NWSP
CW
0
10000
20000
30000
40000
Mean Grain Legumes Receipts ($)

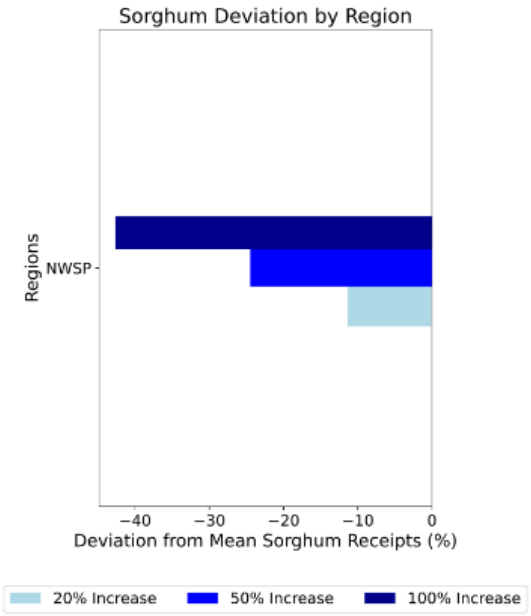
Sorghum Deviation by Region
Regions
NWSP
−40
−30
−20
−10
0
Deviation from Mean Sorghum Receipts (%)
20% Increase
50% Increase
100% Increase

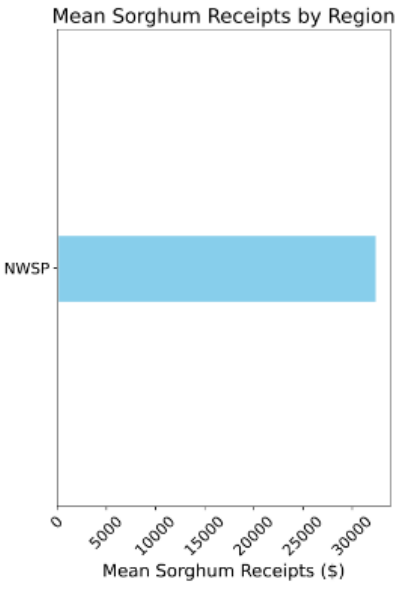
Mean Sorghum Receipts by Region
NWSP
0
5000
10000
15000
20000
25000
30000
Mean Sorghum Receipts ($)

3.6 References

Agegnehu, G., vanBeek, C., & Bird, M. I. (2014). Influence of integrated soil fertility management in wheat and tef productivity and soil chemical properties in the highland tropical environment. Journal of Soil Science and Plant Nutrition, ahead, 0–0. https://doi.org/10.4067/S0718-95162014005000042

Álvarez Torres, B., Sotomayor Ramírez, D. R., Castro Chacón, J. P., Martínez Rodríguez, G., Pérez Alegría, L. R., & DeSutter, T. M. (2023). An alternative method to measure electrical conductivity (EC) and sodium adsorption ratio (SAR) in salt-affected soil extracts. Frontiers in Environmental Science, 11, 1108272. https://doi.org/10.3389/fenvs.2023.1108272

Abdel Kawy, W. A. M., & Ali, R. R. (2012). Assessment of soil degradation and resilience at northeast Nile Delta, Egypt: The impact on soil productivity. The Egyptian Journal of Remote Sensing and Space Science, 15(1), 19–30. https://doi.org/10.1016/j.ejrs.2012.01.001

Ahuti, d. s. (2015). industrial_growth_and_environmental degradation.

Amann, A., Herrnegger, M., Karungi, J., Komakech, A. J., Mwanake, H., Schneider, L., Schürz, C., Stecher, G., Turinawe, A., Zessner, M., & Lederer, J. (2021). Can local nutrient-circularity and erosion control increase yields of resource-constraint smallholder farmers? A case study in Kenya and Uganda. Journal of Cleaner Production, 318, 128510. https://doi.org/10.1016/j.jclepro.2021.128510

Bandyopadhyay, S. K., Pathak, H., Kalra, N., Aggarwal, P. K., Kaur, R., Joshi, H. C., Choudhary, R., & Roetter, R. P. (2001). Yield estimation and agro-technical description of production systems. In P. K. Aggarwal, R. P. Roetter, N. Kalra, H. van Keulen, C. T. Hoanh, & H. H. van Laar (Eds.), Land use analysis and planning for sustainable food security: With an illustration for the state of Haryana, India (pp. 61–89). IARI.

Baskan, O. (2022). Analysis of spatial and temporal changes of RUSLE-K soil erodibility factor in semi-arid areas in two different periods by conditional simulation. Archives of Agronomy and Soil Science, 68(12), 1698–1710. https://doi.org/10.1080/03650340.2021.1922673

Belcher, K. W., Boehm, M. M., & Zentner, R. P. (2003). The Economic Value of Soil Quality under Alternative Management in the Canadian Prairies. Canadian Journal of Agricultural Economics/Revue Canadienne d'agroeconomie, 51(2), 175–196. https://doi.org/10.1111/j.1744-7976.2003.tb00172.x

Bescansa, P., Imaz, M. J., Virto, I., Enrique, A., & Hoogmoed, W. B. (2006). Soil water retention as affected by tillage and residue management in semiarid Spain. Soil and Tillage Research, 87(1), 19–27. https://doi.org/10.1016/j.still.2005.02.028

Beillouin, D., Schauberger, B., Bastos, A., Ciais, P., & Makowski, D. (2020). Impact of extreme weather conditions on European crop production in 2018. Philosophical Transactions of the Royal Society B: Biological Sciences, 375(1810), 20190510. https://doi.org/10.1098/rstb.2019.0510

Byrnes, R. C., Eastburn, D. J., Tate, K. W., & Roche, L. M. (2018). A Global Meta-Analysis of Grazing Impacts on Soil Health Indicators. Journal of Environmental Quality, 47(4), 758–765. https://doi.org/10.2134/jeq2017.08.0313

Colacicco, D., Osborn, T., & Alt, K. (1989). Economic damage from soil erosion. Journal of Soil and Water Conservation, 44(1), 35–39.

Čuček, L., Klemeš, J. J., & Kravanja, Z. (2015). Overview of environmental footprints. In Assessing and Measuring Environmental Impact and Sustainability (pp. 131–193). Elsevier. https://doi.org/10.1016/B978-0-12-799968-5.00005-1

Damgaard, C. (2019). A Critique of the Space-for-Time Substitution Practice in Community Ecology. Trends in Ecology & Evolution, 34(5), 416–421. https://doi.org/10.1016/j.tree.2019.01.013

Dregne, H. E. (1995). Erosion and soil productivity in Australia and New Zealand. Land Degradation & Development, 6(2), 71–78. https://doi.org/10.1002/ldr.3400060202

Evangelista, S. J., Field, D. J., McBratney, A. B., Minasny, B., Ng, W., Padarian, J., Román Dobarco, M., & Wadoux, A. M. J.-C. (2023). A proposal for the assessment of soil security: Soil functions, soil services and threats to soil. Soil Security, 10, 100086. https://doi.org/10.1016/j.soisec.2023.100086

Evangelista, S. J., Field, D. J., McBratney, A. B., Minasny, B., Ng, W., Padarian, J., Román Dobarco, M., & Wadoux, A. M. J.-C. (2024). Soil security—Strategizing a sustainable future for soil. In Advances in Agronomy (Vol. 183, pp. 1–70). Elsevier. https://doi.org/10.1016/bs.agron.2023.10.001

Farooq, M., & Siddique, K. H. M. (2016). Research and Developmental Issues in Dryland Agriculture. In M. Farooq & K. H. M. Siddique (Eds.), Innovations in Dryland Agriculture (pp. 31–46). Springer International Publishing. https://doi.org/10.1007/978-3-319-47928-6_2

Ferreira, V., Panagopoulos, T., Andrade, R., Guerrero, C., & Loures, L. (2015). Spatial variability of soil properties and soil erodibility in the Alqueva reservoir watershed. Solid Earth, 6(2), 383–392. https://doi.org/10.5194/se-6-383-2015

Foley, J. A., Ramankutty, N., Brauman, K. A., Cassidy, E. S., Gerber, J. S., Johnston, M., Mueller, N. D., O'Connell, C., Ray, D. K., West, P. C., Balzer, C., Bennett, E. M., Carpenter, S. R., Hill, J., Monfreda, C., Polasky, S., Rockström, J., Sheehan, J., Siebert, S., … Zaks, D. P. M. (2011). Solutions for a cultivated planet. Nature, 478(7369), 337–342. https://doi.org/10.1038/nature10452

Francos, N., McBratney, A. B., Field, D. J., Minasny, B., Pachon, J. C., Padarian, J., Hunakunti, A., Ng, W., Evangelista, S. J., & O'Donoghue, T. (2024). Valuing and integrating soil roles in assessing the capital dimension of soil security: An Australian case study. Soil Security, 16, 100141. https://doi.org/10.1016/j.soisec.2024.100141

Frye, W. W., Ebelhar, S. A., Murdock, L. W., & Blevins, R. L. (1982). Soil Erosion Effects on Properties and Productivity of Two Kentucky Soils. Soil Science Society of America Journal, 46(5), 1051–1055. https://doi.org/10.2136/sssaj1982.03615995004600050033x

Gachene, C. K. K., Mbuvi, J. P., Jarvis, N. J., & Linner, H. (1997). Soil Erosion Effects on Soil Properties in a Highland Area of Central Kenya. Soil Science Society of America Journal, 61(2), 559–564. https://doi.org/10.2136/sssaj1997.03615995006100020027x

Gager, P., & Conacher, A. (2001). Erosion of Access Tracks in Kalamunda National Park, Western Australia: Causes and management implications. Australian Geographer, 32(3), 343–357. https://doi.org/10.1080/00049180120100068

Gan, F., Shi, H., Gou, J., Zhang, L., Dai, Q., & Yan, Y. (2024). Responses of soil aggregate stability and soil erosion resistance to different bedrock strata dip and land use types in the karst trough valley of Southwest China. International Soil and Water Conservation Research, 12(3), 684–696. https://doi.org/10.1016/j.iswcr.2023.09.002

García-Gamero, V., Vanwalleghem, T., & Peñuela, A. (2024). Soil footprint: A simple indicator to communicate and quantify soil security. Soil Security, 16, 100156. https://doi.org/10.1016/j.soisec.2024.100156

Graham, O. P. (1992). Survey of land degradation in New South Wales, Australia. Environmental Management, 16(2), 205–223. https://doi.org/10.1007/BF02393826

Håkansson, I., & Lipiec, J. (2000). A review of the usefulness of relative bulk density values in studies of soil structure and compaction. Soil and Tillage Research, 53(2), 71–85. https://doi.org/10.1016/S0167-1987(99)00095-1

Havaee, S., Mosaddeghi, M. R., & Ayoubi, S. (2015). In situ surface shear strength as affected by soil characteristics and land use in calcareous soils of central Iran. Geoderma, 237–238, 137–148. https://doi.org/10.1016/j.geoderma.2014.08.016

Hoekstra, A. Y., & Wiedmann, T. O. (2014). Humanity's unsustainable environmental footprint. Science, 344(6188), 1114–1117. https://doi.org/10.1126/science.1248365

Knoepp, J. D., & Swank, W. T. (1997). Forest Management Effects on Surface Soil Carbon and Nitrogen. Soil Science Society of America Journal, 61(3), 928–935. https://doi.org/10.2136/sssaj1997.03615995006100030031x

Knowler, D. J. (2004). The economics of soil productivity: Local, national and global perspectives. Land Degradation & Development, 15(6), 543–561. https://doi.org/10.1002/ldr.635

Koch, A., Chappell, A., Eyres, M., & Scott, E. (2015). Monitor Soil Degradation or Triage for Soil Security? An Australian Challenge. Sustainability, 7(5), 4870–4892. https://doi.org/10.3390/su7054870

Kopittke, P. M., Menzies, N. W., Wang, P., McKenna, B. A., & Lombi, E. (2019). Soil and the intensification of agriculture for global food security. Environment International, 132, 105078. https://doi.org/10.1016/j.envint.2019.105078

Khalifa, M., & Eltahir, E. A. B. (2023). Assessment of global sorghum production, tolerance, and climate risk. Frontiers in Sustainable Food Systems, 7, 1184373. https://doi.org/10.3389/fsufs.2023.1184373

Lal, R. (1993). Tillage effects on soil degradation, soil resilience, soil quality, and sustainability. Soil and Tillage Research, 27(1–4), 1–8. https://doi.org/10.1016/0167-1987(93)90059-X

Lal, R. (1997). Degradation and resilience of soils. Philosophical Transactions of the Royal Society of London. Series B: Biological Sciences, 352(1356), 997–1010. https://doi.org/10.1098/rstb.1997.0078

Lal, R. (2001). Soil degradation by erosion. Land Degradation & Development, 12(6), 519–539. https://doi.org/10.1002/ldr.472

Lal, R. (2008). Soils and sustainable agriculture. A review. Agronomy for Sustainable Development, 28(1), 57–64. https://doi.org/10.1051/agro:2007025

Lal, R. (2015). Restoring Soil Quality to Mitigate Soil Degradation. Sustainability, 7(5), 5875–5895. https://doi.org/10.3390/su7055875

Lal, R., & Moldenhauer, W. C. (1987). Effects of soil erosion on crop productivity. Critical Reviews in Plant Sciences, 5(4), 303–367. https://doi.org/10.1080/07352688709382244

Larney, F. J., & Angers, D. A. (2012). The role of organic amendments in soil reclamation: A review. Canadian Journal of Soil Science, 92(1), 19–38. https://doi.org/10.4141/cjss2010-064

Lovarelli, D., Bacenetti, J., & Fiala, M. (2016). Water Footprint of crop productions: A review. Science of The Total Environment, 548–549, 236–251. https://doi.org/10.1016/j.scitotenv.2016.01.022

Ma, B.-L., Zheng, Z., & Ren, C. (2021). Oat. In Crop Physiology Case Histories for Major Crops (pp. 222–248). Elsevier. https://doi.org/10.1016/B978-0-12-819194-1.00006-2

Maharjan, B., Das, S., & Acharya, B. S. (2020). Soil Health Gap: A concept to establish a benchmark for soil health management. Global Ecology and Conservation, 23, e01116. https://doi.org/10.1016/j.gecco.2020.e01116

Mahmud, M. S., & Chong, K. P. (2022). Effects of Liming on Soil Properties and Its Roles in Increasing the Productivity and Profitability of the Oil Palm Industry in Malaysia. Agriculture, 12(3), 322. https://doi.org/10.3390/agriculture12030322

Marshall, A., Cowan, S., Edwards, S., Griffiths, I., Howarth, C., Langdon, T., & White, E. (2013). Crops that feed the world 9. Oats- a cereal crop for human and livestock feed with industrial applications. Food Security, 5(1), 13–33. https://doi.org/10.1007/s12571-012-0232-x

Moragoda, N., Kumar, M., & Cohen, S. (2022). Representing the role of soil moisture on erosion resistance in sediment models: Challenges and opportunities. Earth-Science Reviews, 229, 104032. https://doi.org/10.1016/j.earscirev.2022.104032

Mwamahonje, A., Mdindikasi, Z., Mchau, D., Mwenda, E., Sanga, D., Garcia-Oliveira, A. L., & Ojiewo, C. O. (2024). Advances in Sorghum Improvement for Climate Resilience in the Global Arid and Semi-Arid Tropics: A Review. Agronomy, 14(12), 3025. https://doi.org/10.3390/agronomy14123025

Mc Carthy, U., Uysal, I., Badia-Melis, R., Mercier, S., O'Donnell, C., & Ktenioudaki, A. (2018). Global food security – Issues, challenges and technological solutions. Trends in Food Science & Technology, 77, 11–20. https://doi.org/10.1016/j.tifs.2018.05.002

McBratney, A., & Field, D. (2015). Securing our soil. Soil Science and Plant Nutrition, 61(4), 587–591. https://doi.org/10.1080/00380768.2015.1071060

McBratney, A., Field, D. J., & Koch, A. (2014). The dimensions of soil security. Geoderma, 213, 203–213. https://doi.org/10.1016/j.geoderma.2013.08.013

Mitchell, J. F. B. (1989). The "Greenhouse" effect and climate change. Reviews of Geophysics, 27(1), 115–139. https://doi.org/10.1029/RG027i001p00115

Montgomery, D. R. (2007). Soil erosion and agricultural sustainability. Proceedings of the National Academy of Sciences, 104(33), 13268–13272. https://doi.org/10.1073/pnas.0611508104

Nordblom, T., Gurusinghe, S., Erbacher, A., & Weston, L. A. (2023). Opportunities and Challenges for Cover Cropping in Sustainable Agriculture Systems in Southern Australia. Agriculture, 13(3), 688. https://doi.org/10.3390/agriculture13030688

NSW Office of Environment and Heritage, 2014. Far West Climate Change Snapshot. NSW Government. Available at: climatechange.environment.nsw.gov.au

Pappalardo, S. E., Gislimberti, L., Ferrarese, F., De Marchi, M., & Mozzi, P. (2019). Estimation of potential soil erosion in the Prosecco DOCG area (NE Italy), toward a soil footprint of bottled sparkling wine production in different land-management scenarios. Plos one, 14(5), e0210922. https://doi.org/10.1371/journal.pone.0210922

Potgieter, A. B., Lobell, D. B., Hammer, G. L., Jordan, D. R., Davis, P., & Brider, J. (2016). Yield trends under varying environmental conditions for sorghum and wheat across Australia. Agricultural and Forest Meteorology, 228–229, 276–285. https://doi.org/10.1016/j.agrformet.2016.07.004

Pozza, L. E., & Field, D. J. (2020). The science of Soil Security and Food Security. Soil Security, 1, 100002. https://doi.org/10.1016/j.soisec.2020.100002

Ray, D. K., Mueller, N. D., West, P. C., & Foley, J. A. (2013). Yield Trends Are Insufficient to Double Global Crop Production by 2050. PLoS ONE, 8(6), e66428. https://doi.org/10.1371/journal.pone.0066428

Román Dobarco, M., Padarian Campusano, J., McBratney, A. B., Malone, B., & Minasny, B. (2023). Genosoil and phenosoil mapping in continental Australia is essential for soil security. Soil Security, 13, 100108. https://doi.org/10.1016/j.soisec.2023.100108

Schrader, S., Graham, S., Campbell, R., Height, K., & Hawkes, G. (2024). Grower attitudes and practices toward area-wide management of cropping weeds in Australia. Land Use Policy, 137, 107001. https://doi.org/10.1016/j.landusepol.2023.107001

Shah, F., & Wu, W. (2019). Soil and Crop Management Strategies to Ensure Higher Crop Productivity within Sustainable Environments. Sustainability, 11(5), 1485. https://doi.org/10.3390/su11051485

Sharda, V. N., & Dogra, P. (2013). Assessment of Productivity and Monetary Losses Due to Water Erosion in Rainfed Crops Across Different States of India for Prioritization and Conservation Planning. Agricultural Research, 2(4), 382–392. https://doi.org/10.1007/s40003-013-0087-1

Status of the world's soil resources: Main report. (2015). FAO : ITPS.

Shah, A. N., Tanveer, M., Shahzad, B., Yang, G., Fahad, S., Ali, S., Bukhari, M. A., Tung, S. A., Hafeez, A., & Souliyanonh, B. (2017). Soil compaction effects on soil health and cropproductivity: An overview. Environmental Science and Pollution Research, 24(11), 10056–10067. https://doi.org/10.1007/s11356-017-8421-y

Sivakumar, M. V. K. (2011). Climate and Land Degradation. In T. J. Sauer, J. M. Norman, & M. V. K. Sivakumar (Eds.), Sustaining Soil Productivity in Response to Global Climate Change (1st ed., pp. 141–154). Wiley. https://doi.org/10.1002/9780470960257.ch10

Smith, P., House, J. I., Bustamante, M., Sobocká, J., Harper, R., Pan, G., West, P. C., Clark, J. M., Adhya, T., Rumpel, C., Paustian, K., Kuikman, P., Cotrufo, M. F., Elliott, J. A., McDowell, R., Griffiths, R. I., Asakawa, S., Bondeau, A., Jain, A. K., … Pugh, T. A.

M. (2016). Global change pressures on soils from land use and management. Global Change Biology, 22(3), 1008–1028. https://doi.org/10.1111/gcb.13068

Teague, R., & Kreuter, U. (2020). Managing Grazing to Restore Soil Health, Ecosystem Function, and Ecosystem Services. Frontiers in Sustainable Food Systems, 4, 534187. https://doi.org/10.3389/fsufs.2020.534187

Tian, M., Qin, S., Whalley, W. R., Zhou, H., Ren, T., & Gao, W. (2022). Changes of soil structure under different tillage management assessed by bulk density, penetrometer resistance, water retention curve, least limiting water range and X-ray computed tomography. Soil and Tillage Research, 221, 105420. https://doi.org/10.1016/j.still.2022.105420

Trnka, M., Vizina, A., Hanel, M., Balek, J., Fischer, M., Hlavinka, P., Semerádová, D., Štěpánek, P., Zahradníček, P., Skalák, P., Eitzinger, J., Dubrovský, M., Máca, P., Bělínová, M., Zeman, E., & Brázdil, R. (2022). Increasing available water capacity as a factor for increasing drought resilience or potential conflict over water resources under present and future climate conditions. Agricultural Water Management, 264, 107460. https://doi.org/10.1016/j.agwat.2022.107460

Thomas, D. T., Moore, A. D., Bell, L. W., & Webb, N. P. (2018). Ground cover, erosion risk and production implications of targeted management practices in Australian mixed farming systems: Lessons from the Grain and Graze program. Agricultural Systems, 162, 123–135. https://doi.org/10.1016/j.agsy.2018.02.001

Vanwalleghem, T., Amate, J. I., De Molina, M. G., Fernández, D. S., & Gómez, J. A. (2011). Quantifying the effect of historical soil management on soil erosion rates in Mediterranean olive orchards. Agriculture, Ecosystems & Environment, 142(3–4), 341–351. https://doi.org/10.1016/j.agee.2011.06.003

Vomocil, J. A. (1957). Measurement of Soil Bulk Density and Penetrability: A Review of Methods. In Advances in Agronomy (Vol. 9, pp. 159–175). Elsevier. https://doi.org/10.1016/S0065-2113(08)60112-1

Wackernagel, M., & Yount, J. D. (1998). The Ecological Footprint: An Indicator of Progress Toward Regional Sustainability. Environmental Monitoring and Assessment, 51(1/2), 511–529. https://doi.org/10.1023/A:1006094904277

Wang, B., Zhang, G.-H., Yang, Y.-F., Li, P.-P., & Liu, J.-X. (2018). The effects of varied soil properties induced by natural grassland succession on the process of soil detachment. Catena, 166, 192–199. https://doi.org/10.1016/j.catena.2018.04.007

Wang, H., & Zhang, G. (2021). Temporal variation in soil erodibility indices for five typical land use types on the Loess Plateau of China. Geoderma, 381, 114695. https://doi.org/10.1016/j.geoderma.2020.114695

Wang, Z.-J., Jiao, J.-Y., Rayburg, S., Wang, Q.-L., & Su, Y. (2016). Soil erosion resistance of "Grain for Green" vegetation types under extreme rainfall conditions on the Loess Plateau, China. Catena, 141, 109–116. https://doi.org/10.1016/j.catena.2016.02.025

Wei, Y., Wu, X., Xia, J., Miller, G. A., Cai, C., Guo, Z., & Hassanikhah, A. (2019). The effect of water content on the shear strength characteristics of granitic soils in South China. Soil and Tillage Research, 187, 50–59. https://doi.org/10.1016/j.still.2018.11.013

Wuepper, D., Borrelli, P., & Finger, R. (2019). Countries and the global rate of soil erosion. Nature Sustainability, 3(1), 51–55. https://doi.org/10.1038/s41893-019-0438-4

Xing, S., Zhang, G., Wang, C., Zhang, N., & Chen, S. (2023). Effects of straw incorporation on soil erosion resistance along a land degradation gradient in the black soil region of China. Catena, 231, 107365. https://doi.org/10.1016/j.catena.2023.107365

Xu, S., Jagadamma, S., & Rowntree, J. (2018). Response of Grazing Land Soil Health to Management Strategies: A Summary Review. Sustainability, 10(12), 4769. https://doi.org/10.3390/su10124769

Yang, X. (2020). State and trends of hillslope erosion across New South Wales, Australia. Catena, 186, 104361. https://doi.org/10.1016/j.catena.2019.104361

Yang, X., Leys, J., Gray, J., & Zhang, M. (2022). Hillslope erosion improvement targets: Towards sustainable land management across New South Wales, Australia. Catena, 211, 105956. https://doi.org/10.1016/j.catena.2021.105956

Yang, X., Leys, J., Zhang, M., & Gray, J. M. (2023). Estimating nutrient transport associated with water and wind erosion across New South Wales, Australia. Geoderma, 430, 116345. https://doi.org/10.1016/j.geoderma.2023.116345

Chapter 4: Introducing an Exergy-Based Model for Soil Restoration - Quantifying Energy Demands for SOC Rebuilding

This chapter is published at:

Anilkumar Hunakunti, Alex McBratney, Budiman Minasny (2025) Introducing an exergy-based model for soil restoration: quantifying energy demands for SOC rebuilding, Geoderma, 461, 117474.

4.1. Abstract

Soil degradation driven by human activities threatens ecosystem stability and agricultural productivity. This study introduces an exergy-based model to quantify the energy required to restore degraded soils (phenosoils) to their natural reference state (genosoils), focusing on Soil Organic Carbon (SOC) as a key indicator of restoration progress. SOC plays a crucial role in carbon storage, nutrient cycling, and soil functionality, making its recovery essential for sustainable land management. A mathematical model was developed to calculate the exergy required to restore SOC in degraded soils to levels characteristic of genosoils. Results reveal significant variability in energy demands across management practices and soil types. Pedogenons with large SOC gaps and low recovery rates exhibited the highest exergy demands, highlighting the need for long-term, energy-efficient management strategies. Compost application demonstrated lower exergy requirements compared to irrigated cotton-to-wheat rotations, while wheat-to-sorghum rotations in dry areas showed the highest energy efficiency. Sensitivity analysis identified recovery rates (k) as the dominant parameter influencing total exergy, followed by SOC gaps (ΔSOC), with energy cost per unit SOC increase (α) playing a secondary role. Optimizing k and managing ΔSOC are essential for achieving energy-efficient SOC restoration, while enhancements in α offer secondary benefits. The proposed model provides a robust tool for evaluating the energy demands of SOC restoration, offering actionable insights to optimize restoration efforts. By linking SOC dynamics to energy requirements, this study supports the development of sustainable soil management strategies and advances our understanding of energy-efficient approaches to soil restoration.

Keywords: Soil security; Sustainability; Exergy; Soil degradation; Soil restoration; soil health; Soil Organic Carbon

4.2. Introduction

Soil faces significant threats from various degradation processes, undermining its vital functions and services, and consequently posing a significant risk to soil security, ecosystem health, and agricultural sustainability. Human activities, particularly intensive agricultural practices, deforestation, and overgrazing, have significantly accelerated these degradation processes (Lal, 2004; FAO, 2015; Pimentel & Burgess, 2013). These practices lead to reduced fertility, compromised soil structure, and increased susceptibility to erosion (Montgomery, 2007; Baumhardt et al., 2015). Among these, soil erosion plays a critical role by depleting nutrient-rich topsoil and Soil Organic Carbon (SOC), directly impacting soil functions and ultimately reducing crop productivity (Pimentel, 2006).

SOC is a crucial indicator of soil condition and health, playing a vital role in supporting soil aggregation, water, and nutrient cycling (Lehmann & Kleber, 2015). These functions are essential for long-term agricultural productivity and ecosystem health. Restoring SOC is critical not only for reversing degradation, mitigating erosion, and sustaining agricultural practices but also for addressing climate change by sequestering carbon dioxide and reducing greenhouse gas emissions (Powlson et al., 2011). Unlike other soil conditions and health indicators, SOC restoration has a cascading effect, improving multiple soil functions while contributing to climate change mitigation(Ros, 2003; Murphy, 2015; Lal, 2015; Bieluczyk et al., 2023). However, restoring SOC is energy-intensive and requires external inputs such as management, biomass incorporation, organic amendments, and fertilizers (Larney & Angers, 2012; Cao et al., 2024).

Research on SOC has largely focused on its dynamics, prediction, and spatial estimation through approaches like remote sensing, spectroscopy, digital soil mapping, and accounting methods (Post et al., 2001; Wendt & Hauser, 2013; Jandl et al., 2014; Angelopoulou et al., 2019; Román Dobarco et al., 2023; Jang et al., 2023 Minasny et al.,2024). While frameworks like the UNFCCC underscore the importance of SOC sequestration as a vital carbon sink (Saby et al., 2008), much of the current focus remains on understanding SOC variability and loss. However, there is limited emphasis on the energy requirements for restoring SOC. Process-based models (e.g., CENTURY, RothC) simulate SOC changes over time by incorporating soil, climate, and management

parameters, but do not quantify the energy required for restoration. Life Cycle Assessment (LCA) provides a comprehensive evaluation of environmental impacts but often simplifies soil as a "black box"(Van Der Werf et al., 2020), overlooking interactions and temporal dynamics essential for SOC restoration.

Thermodynamic concepts provide an alternative perspective for understanding energy dynamics in soil restoration. Concepts such as Gibbs free energy, enthalpy, and entropy offer insights into energy transformations, but their traditional applications are often confined to specific conditions, such as reaction spontaneity or total system energy (Stoner, 2000). However, exergy provides a broader perspective by quantifying the work potential of energy when interacting with reference substances in the environment (Sato, 2004). By accounting for these interactions and the thermodynamic state of both the system and its surroundings, exergy serves as a key parameter for understanding energy requirements in processes like soil restoration. Unlike energy already present in the soil, exergy represents the usable energy supplied to close the SOC gap, offering a practical framework for addressing the energy requirements of SOC recovery in a more integrated and dynamic manner.

A recent study utilized the concept of exergy to assess soil degradation and restoration costs, focusing primarily on static energy costs required to return soils to an idealized "OptSOIL" or pristine state (Palacino et al., 2024). This approach emphasized energy inputs for processes such as nutrient amendments, organic matter addition, salinity correction, and acidification. While valuable for understanding general restoration energy costs, the study did not specifically address the restoration of SOC as a dynamic process. Instead, SOC was treated indirectly as part of broader soil amendments, without consideration of its temporal energy demands or the dynamic changes involved in its recovery. The reliance on idealized conditions overlooked real-world spatial variability and site-specific SOC dynamics, limiting the applicability of the findings to practical soil restoration efforts. To the best of our knowledge, no SOC restoration model based on exergy currently exists.

Given this gap, we propose a dynamic framework for modelling SOC restoration based on the exergy concept. This framework operates within a unique spatial context called the pedogenon, where soil-forming processes are operating comparably (Jang et al., 2023).

Within this space, the genosoil represents minimally human-impacted soils, while the phenosoil refers to altered soils affected by human activities (Chapter 2). This framework explicitly accounts for spatial variability and site-specific SOC dynamics, and thus links SOC recovery dynamics to energy requirements over time.

The specific objectives of this study include using a first-order differential equation to model temporal SOC recovery, deriving a mathematical expression for total exergy, and evaluating energy demands under various management practices. Furthermore, the study seeks to identify key factors influencing restoration efficiency, simulate scenario-based recovery trajectories, and explore the potential for integrating the framework into soil monitoring tools to support sustainable soil management strategies.

4.3. Methodology

4.3.1. Exergy-Based Soil Restoration: Conceptual Framework

Exergy is a thermodynamic concept that measures the maximum useful work obtainable as a system moves toward equilibrium with a defined reference state (Rosen & Dincer, 2001). Unlike energy, which simply represents the capacity to do work, exergy specifically quantifies the potential for a system to achieve balance with its surroundings. In this context, exergy can measure the energy required to reverse degradation and restore a system to an optimal state (Palacino et al., 2024).

Fig.28 depicts an exergy-based model for restoring phenosoil (human-affected soil) to genosoil (natural or less-disturbed soil) within a conceptual pedogenon (soil type). Genosoil serves as the reference state for soil organic carbon (SOC). Phenosoil, usually depleted in SOC due to human activities, requires energy inputs to close the SOC gap and restore its carbon levels similar to those of genosoil. Exergy in this model represents the total energy needed to achieve this restoration.

The exergy required for this restoration is calculated by integrating the energy input (or exergy rate) needed to close the SOC gap over time. Initially, a significant amount of energy is required to address the large SOC difference between phenosoil and genosoil. As phenosoil's SOC approaches that of genosoil, the exergy requirement naturally

decreases, eventually reaching zero when equilibrium is achieved, meaning no further energy is needed once phenosoil's SOC equals genosoil's.

This model outlines a conceptual framework for assessing the energy demands of SOC restoration in phenosoil, emphasizing the key components and principles necessary for evaluating restoration dynamics. The following section derives the mathematical expression for total exergy.

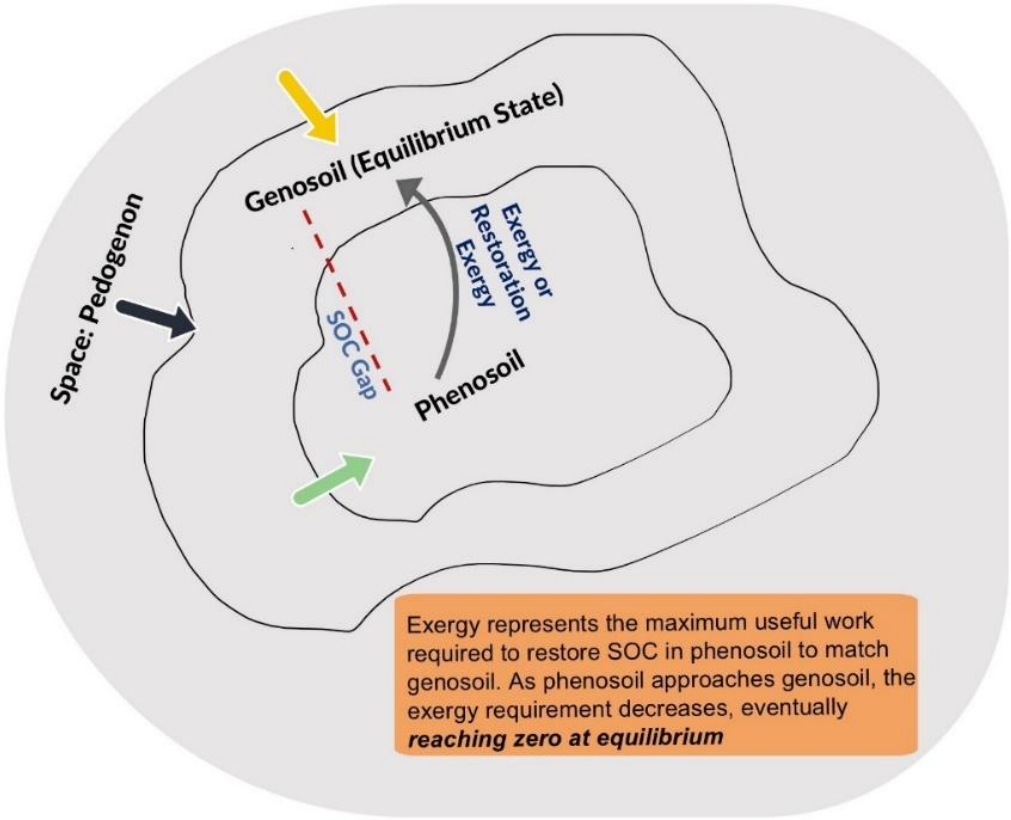

Fig.28. This figure encapsulates the exergy concept: it represents the cumulative energy required to bring phenosoil to equilibrium with genosoil, capturing the dynamics of SOC restoration until the system reaches its stable, natural state.

4.3.2. Mathematical Framework

4.3.2.1. Modeling SOC Changes Over Time

Building on the conceptual framework, the mathematical model quantifies the dynamic change in SOC within a phenosoil over time. This change is modelled using a first-order differential equation, which describes how the SOC level in phenosoil ($\mathrm{SOC_{pheno}}$) evolves toward the target SOC level in genosoil ($\mathrm{SOC_{geno}}$), consistent with the use of first-order models in SOC dynamics (Minasny et al., 2024; Parton et al., 1987; Stepanchenko et al., 2023; Zhou et al., 2025) :

$$\frac{\mathrm{d(SOC_{pheno})}}{\mathrm{dt}} = \mathrm{k} \times \left(\mathrm{SOC_{geno}} - \mathrm{SOC_{pheno}}\right) \qquad (1)$$

$\mathrm{SOC_{geno}}$ The target SOC level in genosoil represents the natural, undisturbed soil.

$\mathrm{SOC_{pheno}}$(t)The SOC level in phenosoil (human-affected soil) at time t

k: the rate constant, determining how quickly SOC in phenosoil approaches the SOC level of genosoil.

This equation assumes that the rate of change of SOC in phenosoil $\frac{\mathrm{d(SOC_{pheno})}}{\mathrm{dt}}$ is proportional to the difference between the current SOC in phenosoil ($\mathrm{SOC_{pheno}}$) and the target SOC in genosoil ($\mathrm{SOC_{geno}}$).

Rearranging the Equation

To solve Equation (1), the variables are separated:

$$\frac{\mathrm{d(SOC_{pheno})}}{\mathrm{SOC_{geno} - SOC_{pheno}}} = \mathrm{k\ dt} \qquad (2)$$

This form expresses the SOC dynamics as a relationship between the relative change in SOC and time.

Equation (2) is integrated to obtain the explicit relationship between SOC and time:

$$\int_{\mathrm{SOC_0}}^{\mathrm{SOC_{pheno}(t)}} \frac{1}{\mathrm{SOC_{geno} - SOC_{pheno}}}\ \mathrm{d\left(SOC_{pheno}\right)} = \int_0^{\mathrm{t}} \mathrm{k\ dt} \qquad (3)$$

The integration is carried out under the following initial conditions:

At t = 0, $SOC_{pheno}(0) = SOC_0$, where SOC_0 is the initial SOC level in phenosoil.

At time t, $SOC_{pheno}(t)$ is the SOC level in phenosoil at that time.

The result of the integration is:

$$-\ln \left| SOC_{geno} - SOC_{pheno} \right| = k\,t + C$$

Where C is the integration constant, determined using the initial condition.

Solution for $SOC_{pheno}(t)$

By applying the initial condition $SOC_{pheno}(0) = SOC_0$, the constant of integration is determined. The final solution for $SOC_{pheno}(t)$ is :

$$SOC_{pheno}(t) = SOC_{geno} - e^{-kt} \times (SOC_{geno} - SOC_0) \qquad (4)$$

This solution describes the change in SOC within phenosoil over time:

Initial SOC Gap: At t=0, the SOC gap is $SOC_{geno} - SOC_0$, representing the starting gap between phenosoil and genosoil.

Exponential Decay: The term e^{-kt} reflects the exponential decay of the SOC gap. As t increases, e^{-kt} approaches zero, and $SOC_{pheno}(t)$ asymptotically approaches SOC_{geno} Fig.29.

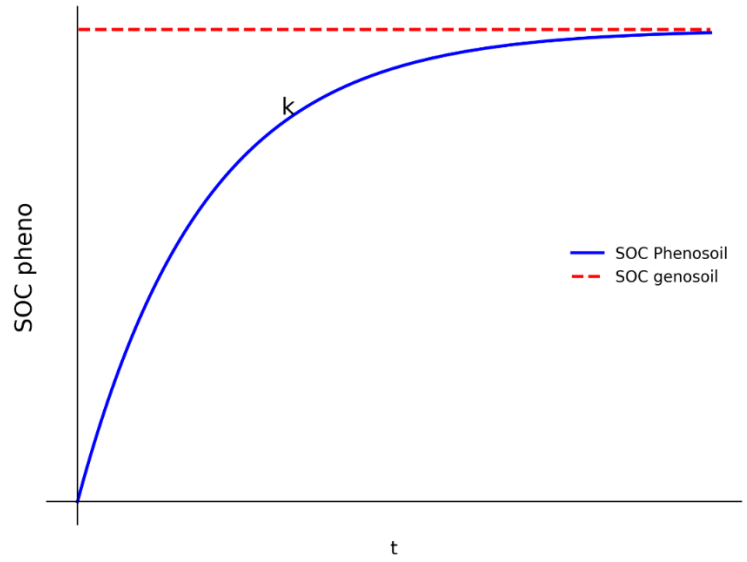

Fig.29. SOC recovery dynamics show the exponential approach of phenosoil SOC toward genosoil equilibrium over time.

4.3.3. Exergy Calculation for Restoration

The total energy required to restore the SOC level in phenosoil (SOC_{pheno}) to match that of genosoil (SOC_{geno}) is quantified using the exergy rate. The exergy rate represents the energy needed per unit increase in SOC and is expressed as:

$$\text{Exergy rate} = \alpha \times \left(SOC_{geno} - SOC_{pheno}(t)\right) \quad (5)$$

where α represents the energy cost per unit SOC increase.

Expression for Total Exergy

To compute the total exergy required for restoration, the exergy rate is integrated over time from t =0 to t =∞

$$\text{Total Exergy} = \int_0^{\infty} \alpha \times \left(SOC_{geno} - SOC_{pheno}(t)\right)dt \quad (6)$$

Substituting the equation for SOC change over time

$$SOC_{pheno}(t) = SOC_{geno} - (SOC_{geno} - SOC_{pheno}(0))\, e^{-kt} \quad (7)$$

The total exergy equation becomes:

$$\text{Total Exergy} = \int_0^{\infty} \alpha \times \left(SOC_{geno} - [SOC_{geno} - (SOC_{geno} - SOC_{pheno}(0))\, e^{-kt}]\right)dt \quad .....(8)$$

Simplifying:

$$\text{Total Exergy} = \int_0^{\infty} \alpha \times \left(SOC_{geno} - SOC_{pheno}(0)\right)e^{-kt}dt \quad (9)$$

Solution for the integral:

$$\text{Total Exergy} = \alpha \times \left(SOC_{geno} - SOC_{pheno}(0)\right) \int_0^{\infty} e^{-kt}\, dt \quad (10)$$

$$\therefore \int_0^{\infty} e^{-kt}\, dt = \frac{1}{k}$$

$$\text{Total Exergy} = \frac{\alpha \times \left(SOC_{geno} - SOC_{pheno}(0)\right)}{k} \quad (11)$$

Eq. (11) represents the total exergy required to restore the phenosoil SOC to the level of the genosoil. It depends on the initial SOC gap, the energy cost per unit SOC increase (α),

and the recovery rate (k). This formulation aligns with the broader ecological interpretation of exergy as a measure of system deviation from a reference equilibrium state, in this case, the genosoil condition and the energy needed to reduce that deviation over time (Jørgensen et al., 1995; Jorgensen & Norsnielsen, 2007).

α : Represents the energy cost per unit increase in SOC, reflecting the maximum energy needed to raise SOC in phenosoil.

$\left(\mathrm{SOC_{geno}} - \mathrm{SOC_{pheno}}(0)\right)$: Denotes the initial SOC difference, indicating how far phenosoil is from the reference state (genosoil) at the start of restoration.

$\frac{1}{\mathrm{k}}$: Represents the rate constant, which controls the speed at which SOC in phenosoil approaches that in genosoil. It scales the total energy over time, with smaller k values indicating slower SOC recovery and thus a larger exergy requirement.

4.3.4. Thermodynamic Principles in SOC Restoration

The total exergy equation is derived by integrating the exergy rate over time, which decreases as the SOC in phenosoil gradually approaches that of genosoil. Initially, the expression $\left(\mathrm{SOC_{geno}} - \mathrm{SOC_{pheno}}(0)\right)$ represents the SOC gap between genosoil and phenosoil. Over time, as the phenosoil's SOC level increases and approaches that of the genosoil, this gap narrows and eventually approaches zero.

From the SOC change (Equation 4), as $\mathrm{t} \to \infty$, the term $\mathrm{e}^{-\mathrm{kt}}$ approaches zero. This leads to $\mathrm{SOC_{pheno}}(\mathrm{t}) \to \mathrm{SOC_{geno}}$, and consequently, $(\mathrm{SOC_{geno}} - \mathrm{SOC_{pheno}}(\mathrm{t})) \to 0$. This exponential form is widely used in soil science to represent organic matter decomposition and stabilization dynamics (Alvarez & Alvarez, 2000; Lascalajr et al., 2008; Murindangabo et al., 2023).

As a result, the exergy rate also asymptotically approaches zero over time. This dynamic reflects the core concept of exergy: as the phenosoil's SOC level converges with that of the genosoil, the total exergy requirement decreases over time. At equilibrium, when the phenosoil's SOC equals the genosoil's SOC, no further energy is required, aligning with

thermodynamic principles that indicate the total exergy demand approaches zero at the stable reference state (Rosen & Dincer, 2001).

4.3.5 Unit for Total Exergy

The unit for total exergy can be derived from the components of the total exergy equation:

Total Exergy = (α×(SOC_geno- SOC_pheno (0)))/k

Where:

α is the energy cost per unit increase in SOC, measured in kJ/g of SOC

(SOC_geno- SOC_pheno (0)) is the initial SOC difference between genosoil and phenosoil, measured in g/kg.

k is the rate constant, which unit of year^(-1), which controls how quickly SOC in phenosoil approaches the SOC level in genosoil over time.

Substituting the units of each component into the equation, we get:

$$\text{Total Exergy} = \frac{(\frac{\text{kJ}}{\text{g}})\times(\frac{\text{g}}{\text{kg}})}{\text{year}^{-1}} = \frac{\text{kJ.year}}{\text{kg}}$$

This unit, kJ·year/kg, represents the cumulative energy input (in kilojoules) required over a given time period (in years) to restore SOC in phenosoil to match the SOC level in genosoil, capturing both spatial (mass of soil) and temporal (time) dimensions.

4.3.6. Pedogenon and Management-Specific Model Calculations

The developed model (Eq.11) was applied in the Lower Namoi Valley, a 1700 km^2 region in the Edgeroi district of New South Wales (NSW), Australia. This area has undergone substantial soil alterations. Adjacent national parks provided undisturbed genosoil references, serving as benchmarks for comparison with human-affected soils. For additional details, refer to (Jang et al., 2023).

The SOC data used in the analysis included mean SOC values (g/kg) measured at a depth of 0–30 cm (Table 3) (Jang et al., 2023). These data were collected across 13 distinct

pedogenons (A to M), representing various soil types and land uses. Pedogenons A to D were dominated by irrigated systems, with cotton as the primary crop, while pedogenons E to M comprised non-irrigated areas primarily cultivating wheat. Each pedogenon was further classified into phenosoil (croplands or other human-affected soils) and genosoil (woodlands or less-disturbed soils).

To apply the model, three key components are required: (1) the SOC gap between phenosoil and genosoil, (2) the rate constant (k), and (3) the energy cost per unit SOC increase (α). These parameters were calculated separately for each pedogenon, based on representative management practices (e.g., compost application, cover cropping) and the unique SOC gap observed across the study area.

The following sections provide detailed descriptions of how each parameter was calculated for the study area. This approach was then applied to each pedogenon, using the respective SOC gap between genosoil and phenosoil in that pedogenon, along with the relevant management practices.

Table 3. Mean soil organic carbon (SOC) content (g/kg) at 0–30 cm depth across different pedogenons (A–M) and land uses. C, P & W represent cropland, pasture, and woodland, respectively (Jang et al., 2023).

Soil Type/pedogenons	Land use	0–30 cm
		Mean
A	C	8.55
A	W	14.04
B	C	9.73
B	W	14.12
C	C	6.88
C	W	9.49
D	C	6.85
D	W	8.86
E	C	4.52
E	W	6.66
F	C	5.29
F	P	8.22
G	C	5.31
G	P	9.11
H	C	7.44
H	P	10.58
H	W	10.17
I	C	5.80
I	W	20.27
J	C	7.96
J	W	14.30
K	C	6.41
K	W	9.33
L	C	9.68
L	W	15.52
M	C	12.61
M	W	14.46

4.3.7. Calculating k: The Rate Constant for SOC Recovery

The rate constant k quantifies the speed at which SOC in phenosoil SOC_{pheno} approaches the SOC level of genosoil SOC_{geno} when the initial SOC level of phenosoil $SOC_{pheno}(0)$ is not directly known, k can be estimated using SOC measurements at two distinct time points, t_1 & t_2 . In this context, genosoil represents a past reference state (t_1), while phenosoil corresponds to the current observation (t_2), reflecting its modification by human activities.

Using Equation (4), the relationship can be expressed for the recovery period (t = t_2- t_1 as:

$$SOC_{pheno}(t_2) = SOC_{geno} - e^{-k(t_2-t_1)} \times (SOC_{geno} - SOC_{pheno}(t_1)) \quad (12)$$

By dividing the SOC gap at t_2 by the SOC gap at t_1 we derived:

$$\frac{SOC_{geno} - SOC_{pheno}(t_2)}{SOC_{geno} - SOC_{pheno}(t_1)} = e^{-k(t_2-t_1)} \quad (13)$$

This ratio captures the fraction of the initial SOC gap that remains over time as phenosoil SOC approaches genosoil SOC. Assuming the SOC level in phenosoil at t_1 negligible compared to that in genosoil, the SOC gap at t_1 can be approximated as SOCgeno. This simplifies the equation to:

$$\frac{SOC_{geno} - SOC_{pheno}(t_2)}{SOC_{geno}} = e^{-k(t_2-t_1)} \quad (14)$$

Taking the natural logarithm and solving for k we get:

$$k = -\frac{\ln\left(\frac{SOC_{geno} - SOC_{pheno}(t_2)}{SOC_{geno}}\right)}{t_2 - t_1} \quad (15)$$

In this study, the recovery time ($t_2 - t_1$) the period during which SOC in phenosoil approaches SOC in genosoil is assumed to be 50 years, based on the following considerations:

Long-term SOC Dynamics: SOC restoration processes are inherently slow, requiring decades to observe significant changes.

Practical Timeframe: A 50-year interval aligns with the timescales used in soil management and policy planning, providing a realistic perspective.

Equilibrium: A 50-year recovery period allows meaningful progress toward equilibrium, reflecting the natural decay rate of SOC gaps.

To assess the sensitivity of the exergy calculations, the analysis was extended to include recovery times ranging from 5 to 50 years in 5-year intervals.

4.3.8. Calculating α : Energy Cost per unit increase in SOC

The energy cost per unit increase in SOC (α) quantifies the external energy required to increase SOC by one unit (e.g., kJ per gram of SOC). This measure reflects the energy investment associated with SOC restoration in phenosoil, capturing the demands of approaches such as compost application and crop cover practices.

In this study, SOC values for phenosoil were obtained from irrigated cotton and non-irrigated wheat fields in the Lower Namoi Valley, NSW, Australia. Two example methods for enhancing SOC are explored: compost application and crop cover methods. Compost application is less common in Australia but offers a theoretical benchmark for energy requirements, while crop cover practices, particularly crop rotations, are widely adopted and serve as a practical approach for improving SOC.

4.3.8.1. Energy Requirements for Compost-Based SOC Restoration

Restoring SOC levels in phenosoil to match those in genosoil requires the application of organic matter (OM). In this study, we assume a single application event to simplify the estimation of energy costs, recognizing that in practice, multiple or periodic applications may occur.

However, due to decomposition losses, only a fraction of the applied OM is retained in the soil over the long term. Studies suggest that approximately 10% of the applied OM remains in the soil, necessitating larger inputs to achieve the desired SOC increase (Kong et al., 2005; Lützow et al., 2006; Palacino et al., 2024). This relationship is expressed using the soil incorporation factor (SIF = 0.10), which includes both the conversion rate of OM to carbon and the assumed carbon content of OM (typically around 50%). Thus, the total OM required to achieve a given SOC increase (ΔSOC, expressed in g C/kg soil) is:

$$\text{OM Required } \left(\frac{\text{kg}}{\text{g soil}}\right) = \Delta\text{SOC} \times \frac{1}{\text{Soil Incorporation Fator}} \quad (16)$$

The energy required for compost production and application is included in the calculation of α. Windrow composting, a commonly used method, has a relatively low energy demand of 0.076 kJ/g due to minimal machinery requirements (Palacino et al., 2024). This value excludes transport or additional treatments, as OM is typically applied close to its production site. The total energy required to achieve a given SOC increase is calculated as:

$$\text{Total energy } \left(\frac{\text{kJ}}{\text{kg soil}}\right) = \left(\frac{\Delta\text{SOC}}{\text{SIF}}\right) \times \text{Composite energy} \quad (17)$$

The exergy cost per unit SOC increase (α) is then calculated as:

$$\alpha = \frac{\text{Total Energy}}{\Delta\text{SOC}} \quad (18)$$

By substituting the energy relationship, α is simplified to:

$$\alpha = \frac{\text{Composite energy}}{\text{soil Incorporation Fator}} \quad (19)$$

This equation demonstrates that α is inversely proportional to the soil incorporation factor; higher decomposition losses (lower SIF values) require greater OM inputs and increase the energy cost per unit SOC gain.

4.3.8.2. Energy Requirements for Crop Cover Practices

Crop cover methods are recognised as effective strategies for restoring SOC in agricultural systems (Zhou et al., 2012; Zhou et al., 2016; Jian et al., 2020). This study focuses on SOC restoration in irrigated cotton and non-irrigated wheat systems within the Lower Namoi Valley, Australia. Cotton cultivation is associated with lower SOC levels due to intensive management and irrigation practices (Rochester, 2011). To address this, crop rotation from cotton to wheat is evaluated as a strategy to enhance SOC levels by reducing soil disturbance and increasing organic matter inputs through biomass incorporation (Hulugalle et al., 2006; Hulugalle & Scott, 2008).

The energy cost per unit increase in SOC (α) was calculated using the total energy input for wheat production, reported as 3028 kWh/ha/year in an irrigated wheat system in New South Wales (NSW), Australia (Khan et al., 2010). Among the components, fertilizer

application accounted for 47.32% of the total energy input, followed by seeding operations (22.64%) and irrigation (6.37%). Nitrogen fertilization, in particular, plays a critical role in biomass production and supports SOC restoration by enhancing crop residue returns to the soil (Kuesters & Lammel, 1999). The total energy value was then converted to kilojoules for subsequent calculations:

Energy input for wheat = 3,028 kWh/ha/year × 3,600 kJ/kWh = 10,900,800 kJ/ha/year (20)

To quantify the energy cost per unit SOC increase (α), the SOC sequestration rate is required. It represents the accumulation of organic carbon in the soil through biomass inputs and reduced decomposition under specific management practices, such as cover cropping. The average SOC sequestration rate of 0.56 Mg SOC/ha/year, derived from meta-analyses comparing systems with and without cover crops (Jian et al., 2020), serves as a useful benchmark for estimating α. This rate links biomass production with SOC gains, providing a standardized measure of carbon accumulation over time. While site-specific variability in the Lower Namoi Valley may exist due to unique soil and climatic conditions, this benchmark remains applicable for evaluating biomass-based SOC restoration strategies.

To apply the SOC sequestration rate to our study, the rate was standardized to grams of SOC per kilogram of soil per year. Using a bulk density of 1.3 g/cm^3 and a sampling depth of 0.3 m, the total soil mass per hectare was calculated as 3,900,000 kg soil/ha. Given an SOC sequestration rate of 0.56 Mg SOC/ha/year (or 560,000 g SOC/ha/year), the standardized rate is:

$$\text{SOC sequestration rate} = \frac{560{,}000\ \text{g SOC/ha/year}}{3{,}900{,}000\text{kgsoil/ha}} = 0.143\text{g SOC/kg soil/year} \quad (21)$$

The total energy input for wheat production, 10,900,800 kJ/ha/year, was first normalized to energy input per kilogram of soil:

$$\text{Energy kg per soil} = \frac{10{,}900{,}800\ \text{kJ/ha/year}}{3{,}900{,}000\text{kgsoil/ha}} = 2.79\ \text{kJ/kg soil/year} \quad (22)$$

To calculate the exergy cost per unit SOC increase (α), the energy input per kilogram of soil was divided by the SOC sequestration rate (0.143 g SOC/kg soil/year):

$$\alpha = \frac{2.79\ \text{kJ/kg soil/year}}{0.143\text{gSOC/kg soil/year}} = 19.51\ \text{kJ/g SOC} \quad (23)$$

For non-irrigated systems, crop rotation with sorghum can help enhance SOC levels (Halvorson & Schlegel, 2012). Sorghum's suitability for dryland farming stems from its high biomass production and compatibility with reduced tillage systems, as demonstrated in wheat-sorghum-fallow rotations (Ghimire & Khanal, 2020).

To calculate α for sorghum, the total direct energy input for sorghum production was obtained from the Northern Grain Region of Australia. Reported values indicate an energy input of 0.85 GJ/ha/year (850,000 kJ/ha/year; Maraseni et al., 2015). Since indirect energy data were unavailable for this region, only direct energy inputs were considered. Following the same process as described earlier for wheat, the energy input was normalized to energy per kilogram of soil and divided by the SOC sequestration rate (0.143 g SOC/kg soil/year). This resulted in an exergy cost per unit SOC increase (α) of 1.52 kJ/g SOC.

4.3.9. Variance Decomposition of Exergy Via Sobol Indices

Sobol sensitivity analysis was conducted to quantify the contribution of three parameters (k, ΔSOC, and α) to total exergy (Sobol, 2001), using the sampling approach developed by Saltelli (Saltelli, 2002).

The Sobol sensitivity analysis was implemented in Python using the SALib library (Herman & Usher, 2017). Parameter sampling was conducted using Saltelli's method (Saltelli.sample), and total exergy was computed based on Equation (11). The analysis was performed using sobol.analyze, with first-order, total-order, and second-order indices calculated for the parameters k, ΔSOC, and α.

Parameter values were sampled within defined bounds k ∈ [0.01,0.1], ΔSOC ∈ [1,20], and α ∈ [0.1,20] to generate 1000 samples. Total exergy was computed for each sample, and Sobol indices were subsequently calculated to decompose the variance of total exergy into contributions from individual parameters and their interactions.

First-order indices (S1) quantified the direct contribution of each parameter to the variance of total exergy, while total-order indices (ST) captured both direct effects and higher-order interactions. Additionally, second-order indices (S2) provided insights into interactions between parameter pairs.

4.4. Results

4.4.1. SOC Dynamics and Recovery Model

The SOC recovery dynamics for 13 pedogenons (A to M) over a 50-year period, modelled using Equation 4, illustrate temporal trends in SOC restoration (Fig. 30 and 31). These pedogenons represent diverse soil types and land uses, which influence their SOC recovery potential. Pedogenons A to D correspond primarily to irrigated systems, with cotton as the dominant crop, while pedogenons E to M represent non-irrigated systems, mainly cultivating wheat. The corresponding genosoils for these pedogenons are woodlands, serving as reference soils with minimal human disturbance.

Fig. 31 presents two components: the left-hand plots show the progressive increase in SOC levels in phenosoil over time, while the right-hand plots depict the exponential decay of the SOC gap between phenosoil and genosoil. Pedogenons with higher recovery rate constants (k), such as D and M, exhibit steeper recovery curves, achieving faster SOC gap closure due to their favorable conditions for organic carbon accumulation. Conversely, pedogenons like I, with lower k values, show slower recovery trends and prolonged timescales for SOC restoration, indicating the challenges posed by larger SOC gaps or less favourable soil and management conditions.

Fig.30 highlights the temporal behaviour of the recovery rate constant (k) for each pedogenon over time. The initial k values were high, reflecting rapid SOC recovery shortly after implementing restoration practices, but they decline over time as the phenosoil approaches the genosoil SOC levels. Pedogenons with initially higher k values, such as D and M, sustain relatively efficient recovery rates for longer periods compared to pedogenons like I and J, where recovery slows significantly over time. These trends highlight the variability in recovery dynamics across pedogenons, influenced not only by the size of the initial SOC gaps but also by inherent soil properties such as texture, mineralogy, and structure.

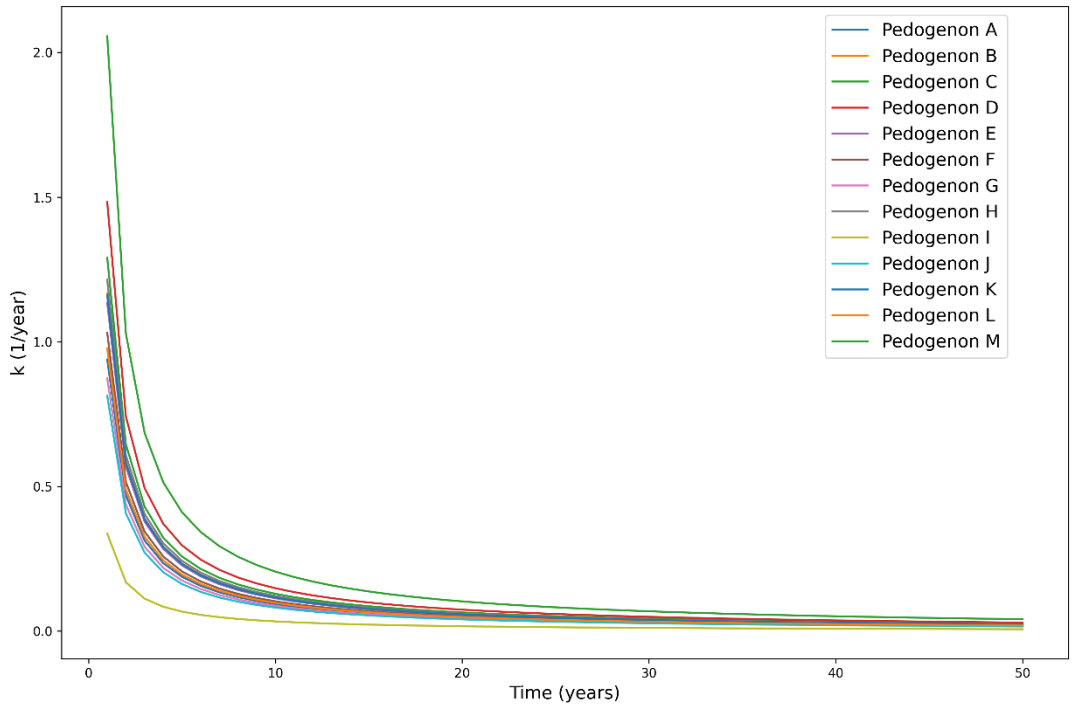

Fig.30. Temporal variation of the recovery rate constant (k) for pedogenons (A–M) over 50 years, showing declining recovery rates as SOC accumulation slows through time.

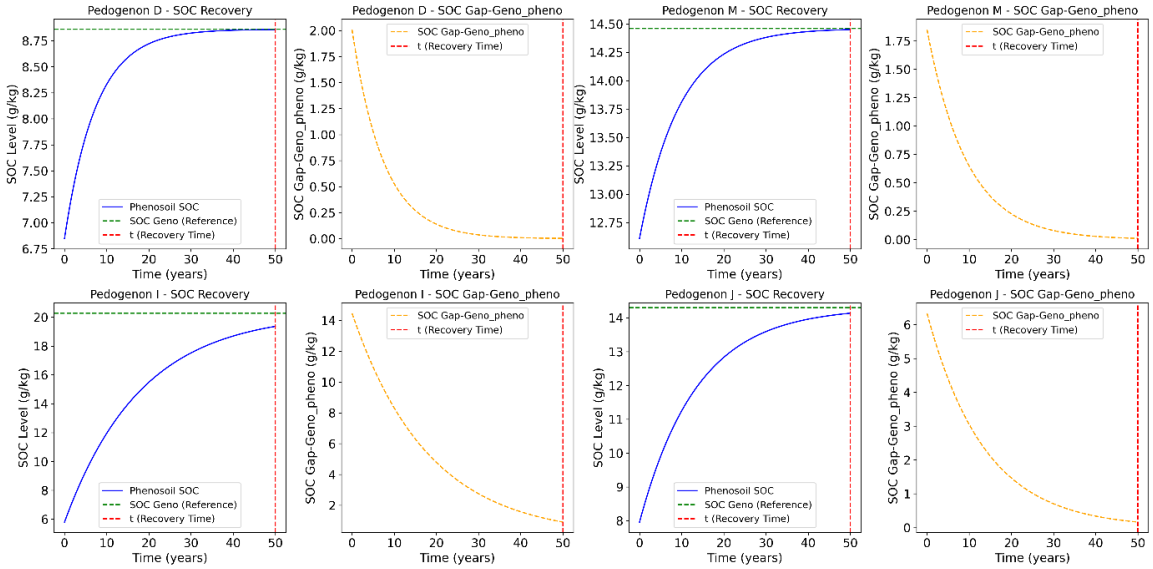

Fig. 31. Modeled SOC recovery dynamics (left) and SOC gap decay (right) for selected pedogenons (D-M, I-J) over 50 years, illustrating temporal trends in SOC restoration. The remaining pedogenons are provided in the supplementary materials, S1 Fig 32.

4. 4.2. Understanding Exergy Demands and Recovery Efficiency

The total exergy values across various time intervals and pedogenons were analysed under three management strategies: compost application, cotton rotation to wheat, and

wheat rotation to sorghum (Fig.33, 34, and 35). The exergy values at 50 years under different management systems compost, cotton, and wheat–sorghum are compared across soil types in Table 4, highlighting the variation in exergy values driven by both soil type and management strategy.

Fig.33 illustrates exergy demands for restoring SOC in phenosoil using compost across all pedogenons (A–M) over time intervals ranging from 5 to 50 years. Pedogenon I demonstratesthe highest exergy demands, increasing from 163.1 kJ/kg at 5 years to 1631.3 kJ/kg at 50 years, driven by its low recovery rate (k=0.0531/year), indicating inefficient SOC recovery. This highlights the substantial energy required to restore phenosoil to genosoil equilibrium for pedogenons with large SOC gaps. In contrast, Pedogenons M and D exhibit the lowest exergy demands, ranging from 3.4–34.2 kJ/kg and 5.1–51.5 kJ/kg, respectively, supported by higher recovery rates (k = 0.105 and 0.1331/year).

Fig.34 presents exergy demands for SOC restoration under cotton rotation to wheat in irrigated systems, focusing on Pedogenons A, B, C, and D. Pedogenon A shows the highest exergy demands, exceeding 5703 kJ/kg at longer intervals, attributed to its moderate recovery rate (k=0.0841/year). Conversely, Pedogenon D demonstrates lower exergy demands, ranging from 5–1321 kJ/kg, supported by its higher recovery rate (k=0.1331/year). These variations emphasize the need for strategies tailored to optimize energy efficiency across different pedogenons.

Fig.35 displays exergy demands for SOC restoration under wheat rotation to sorghum, focusing on Pedogenons E through M. Pedogenon I shows the highest exergy demands, ranging from 350–3262 kJ/kg, due to its low recovery rate (k=0.1091/year). In contrast, Pedogenons M and E exhibited lower exergy demands, reflecting their relatively higher recovery rates.

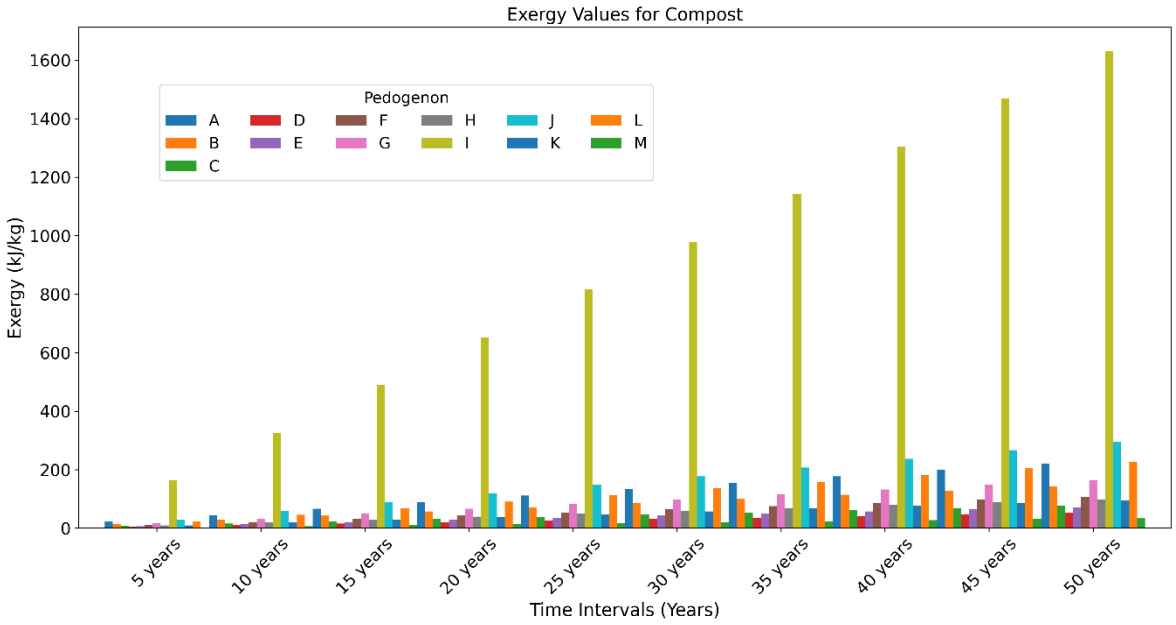

Fig.33. Exergy requirements (kJ/kg) for SOC restoration using compost across pedogenons (A–M) over 50-year intervals. The highest energy demands observed for pedogenon I, highlighting variations in energy demand across time and soil types.

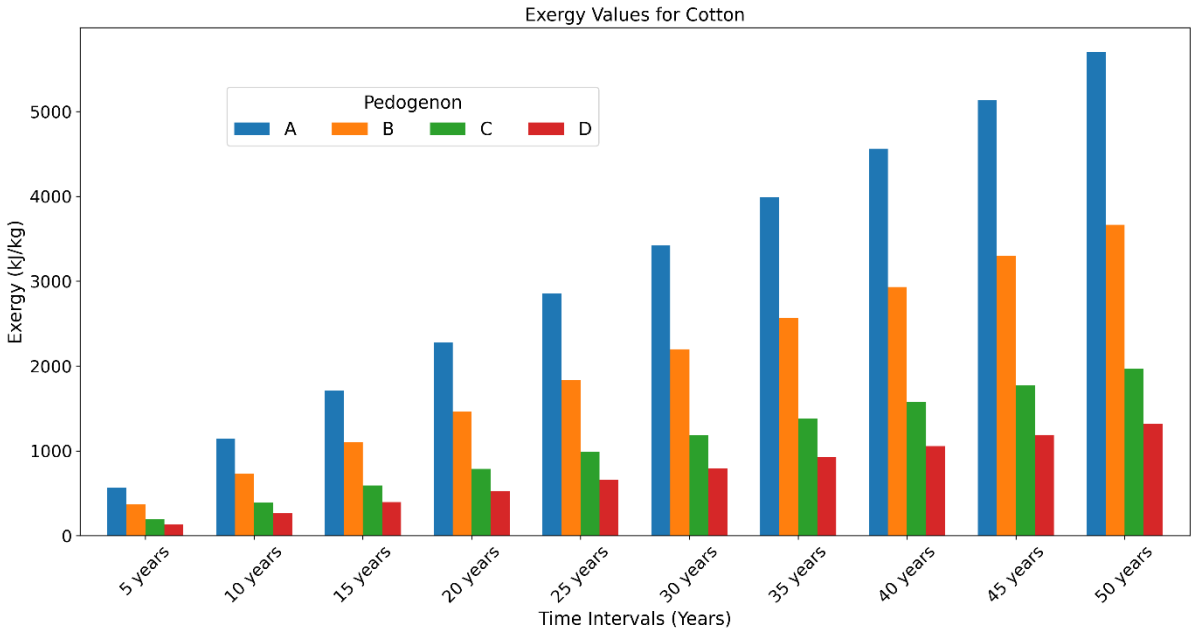

Fig.34. Exergy requirements (kJ/kg) for SOC restoration using cotton-to-wheat rotation across pedogenons (A–D) over 50-year intervals. The highest energy demand observed for pedogenon A, illustrating energy demands in irrigated systems.

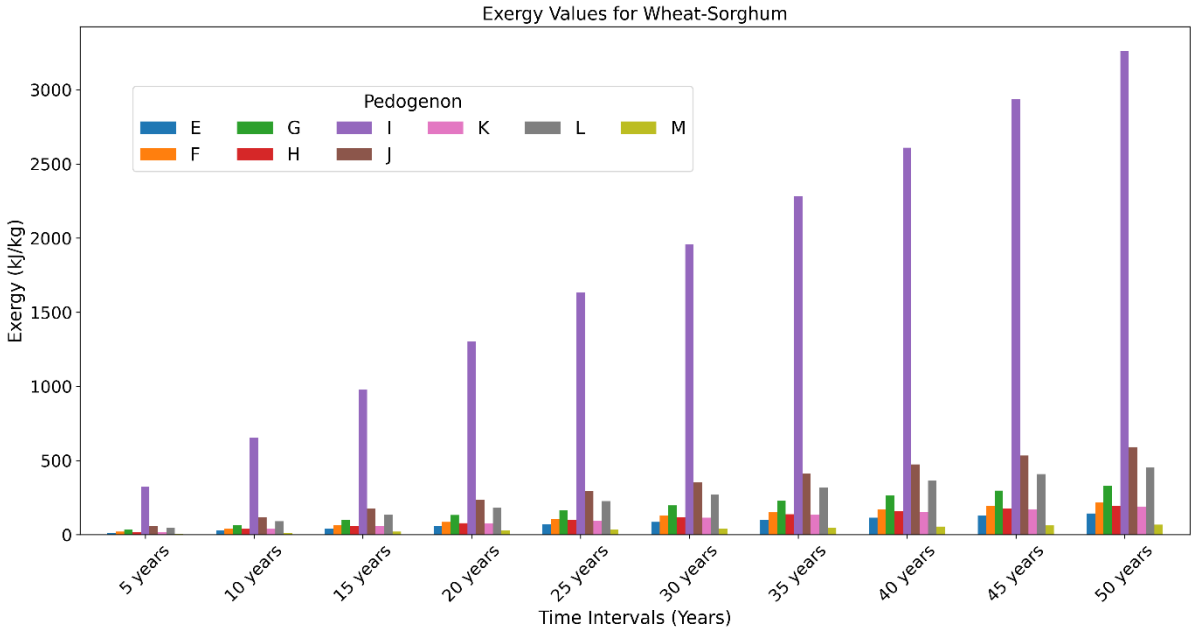

Fig.35. Exergy requirements (kJ/kg) for SOC restoration using wheat-to-sorghum rotation across pedogenons (E–M) over 50-year intervals. The highest energy demands observed for pedogenon I, highlighting energy demands in dryland systems.

Table 4. Exergy values (kJ/kg) at 50 years for different soil types (pedogenons) under three management systems: compost, cotton, and wheat–sorghum

Soil Type	Compost (kJ/kg)	Cotton (kJ/kg)	Wheat-Sorghum (kJ/kg)
A	222.17	5703.51	-
B	142.79	3665.65	-
C	76.83	1972.32	-
D	51.48	1321.78	-
E	71.62	-	143.25
F	107.93	-	215.86
G	165.14	-	330.29
H	98.22	-	196.45
I	1631.32	-	3262.64
J	296.19	-	592.39
K	95.51	-	191.03
L	227.05	-	454.10
M	34.18	-	68.37

4.4.3. Pedogenon-Specific Exergy Cost Per Unit SOC Increase

To understand the exergy cost per unit SOC increase (α), Equation 19 was applied, considering the actual SOC gaps (ΔSOC) for each pedogenon to reflect specific conditions. α is expressed as $\alpha = \frac{E}{SIF \times \Delta SOC}$, where E represents the energy cost of compost application, ΔSOC is the SOC gap between genosoil and phenosoil, and the (SIF) soil incorporation factor. This analysis was conducted specifically for compost application, as the primary aim was to understand the behaviour of α under varying SIF and SOC gaps.

This efficiency is expressed through the SIF, which ranges from 0.10 (10%) to 1 (100%), and is defined as SIF $\in [0.1,1.0]$. Larger SOC gaps, as observed in Pedogenon I, correspond to lower α values (Fig.36), consistent with thermodynamic principles that systems further from equilibrium possess higher recovery potential due to the larger gradient driving restoration. Conversely, pedogenons with smaller SOC gaps, such as M and D, exhibit higher α values, particularly at lower SIF levels, reflecting constrained SOC filling dynamics where phenosoil is closer to equilibrium with genosoil, requiring proportionally higher energy inputs for incremental SOC increases.

As SIF values increase, α values converge across pedogenons, irrespective of initial SOC gaps. This convergence underscores the role of SIF in scaling organic matter requirements and achieving more uniform energy efficiency across systems. The findings suggest that pedogenons with large SOC gaps, such as Pedogenon I, are more energy-efficient for SOC recovery, requiring long-term management practices that leverage their inherent recovery potential, while pedogenons with smaller SOC gaps require targeted improvements in soil incorporation to mitigate energy costs and achieve sustainable SOC recovery. This emphasizes the importance of scenario-based management strategies that are tailored to pedogenon-specific conditions, providing a basis for maximizing SOC recovery with minimal energy expenditure.

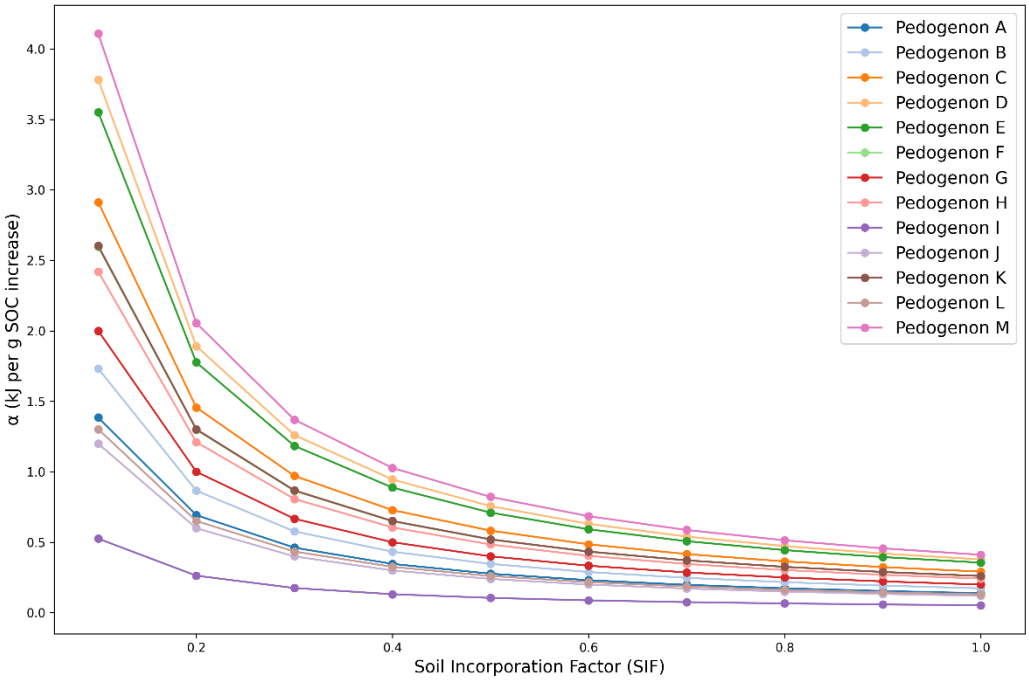

Fig.36. Relationship between the energy cost per unit SOC increase (α) and the Soil Incorporation Factor (SIF) across different pedogenons, illustrating how higher SIF values correspond to lower energy costs.

4.4.4. Role of k, ΔSOC and α in SOC Restoration

The Sobol sensitivity analysis reveals the contributions of k, ΔSOC, and α to the variability in total exergy. Fig.37 illustrates that k is the most influential parameter, with first order (S1) and total-order (ST) Sobol indices of 0.55 and 0.70, respectively. This indicates that variations in k directly and interactively contribute the most to the variance in total exergy. ΔSOC exhibits a moderate influence, with S1 around 0.22 and ST close to 0.37, indicating that the SOC gap not only directly impacts exergy but also interacts with other parameters to contribute to variability. In contrast, α has the lowest influence, with S1 and ST values of 0.09 and 0.15, respectively, indicating a relatively minor role compared to k and ΔSOC.

The heatmap of second-order indices (S2) provides additional insights into parameter interactions. The strongest interaction is observed between k and ΔSOC with an S2 value of 0.06 (Fig.38), indicating a synergistic relationship where changes in k rates and ΔSOC

jointly influence exergy outcomes. A weaker interaction is observed between ΔSOC and α, with an S2 value of 0.02, reflecting a limited but measurable interaction. The interaction between k and α is negligible, with an S2 value of -0.01, suggesting that (α) has a minimal combined effect with k rates.

This analysis underscores k as the dominant parameter influencing total exergy, followed by ΔSOC, which makes a moderate but significant contribution. Optimizing k and managing ΔSOC are essential for achieving energy-efficient SOC restoration, while enhancements in α offer secondary benefits. Moreover, the strong interaction between k and ΔSOC emphasizes the need for integrated interventions targeting these parameters to maximize restoration efficiency and effectiveness.

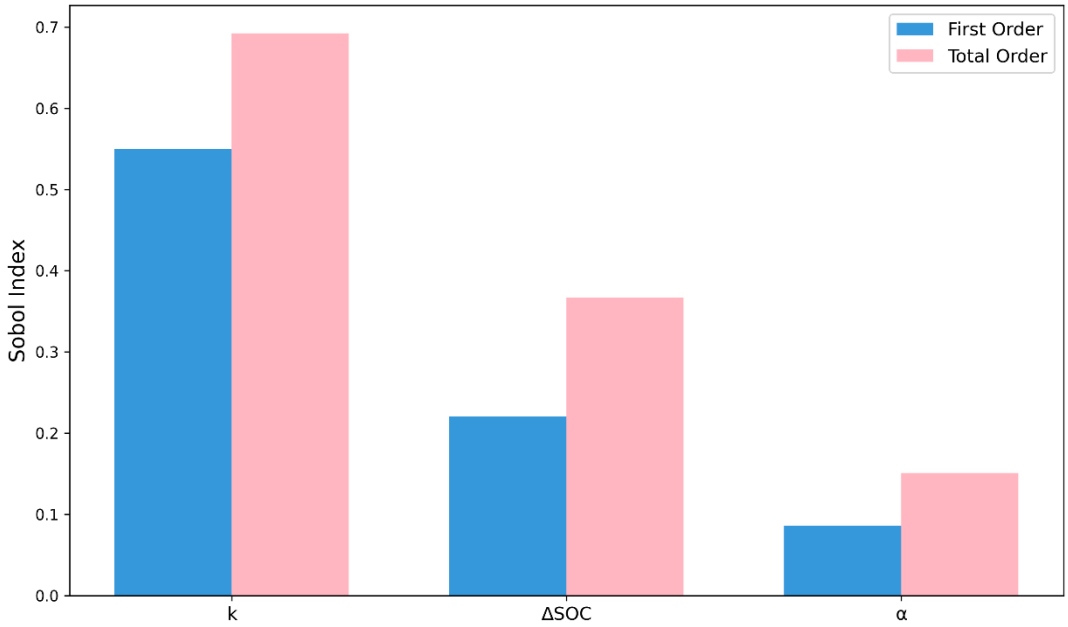

Fig.37. First-order and total-order Sobol sensitivity indices for parameters k, ΔSOC, and α, illustrating the relative influence of each parameter on total exergy variability.

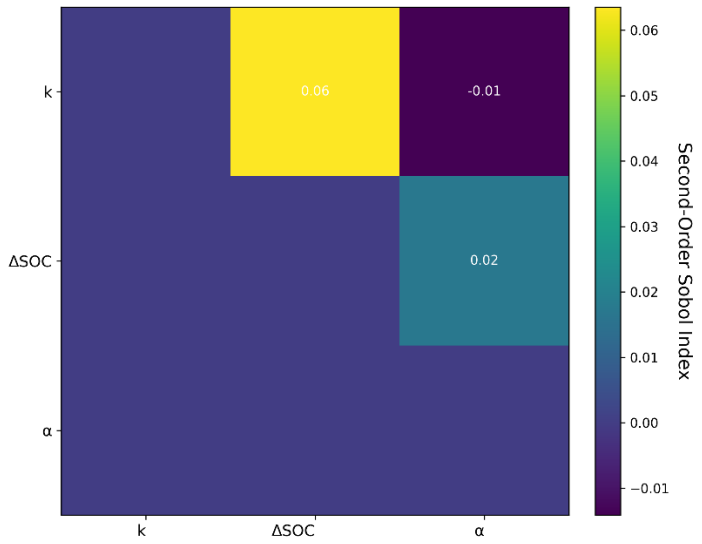

Fig.38. Second-order Sobol sensitivity indices showing the interactions among parameters k, ΔSOC, and α in driving total exergy variability.

4.5 Discussion

4.5.1. Establishing an Exergy Framework for SOC Restoration

This section establishes the theoretical basis and methodological robustness of the proposed exergy-based framework for SOC restoration. By quantifying energy demands associated with closing the SOC gap, the model offers a physically grounded approach to soil recovery. The concept of exergy, applied here for the first time in this context, links thermodynamic principles with carbon recovery modelling, enabling both theoretical coherence and cross-system comparison. By integrating exergy as a metric, this study highlights the need to balance SOC recovery rates (k) with energy demands, aligning with established principles in sustainable soil management and restoration strategies (R. Lal et al., 1990; L. G. Smith et al., 2015; Pratibha et al., 2019).

This focus on exergy seamlessly connects to the robust modelling framework provided by Equation 4, which captures the dynamics of SOC recovery across diverse pedogenons. Exponential models, as demonstrated in previous studies on organic matter decomposition and soil carbon dynamics (Yang et al., 2006; Manzoni et al., 2012; Morais et al., 2019b; Padarian et al., 2022), provide a theoretical foundation for applying Equation 4 to model SOC recovery processes. Within this framework, the rate constant (k) effectively captures variations in SOC recovery rates, reflecting distinct trajectories

among pedogenons based on their initial SOC gaps and inherent soil properties (Fig.31). For instance, pedogenons D and M, with higher k values, exhibit steeper recovery curves, indicating a greater capacity for rapid SOC restoration. In contrast, pedogenons like I, with lower k values, show slower recovery trends and require extended timeframes to approach genosoil equilibrium (Fig.30&31). The model's ability to asymptotically describe SOC recovery toward equilibrium further validates its applicability across diverse pedogenon conditions and aligns with theoretical insights into soil carbon stabilization (Stewart et al., 2007).

The derivation and application of the total exergy equation (Equation 11) demonstrate its utility in enabling scenario-specific calculations by adjusting parameters such as α, k, or the SOC gap (ΔSOC). This facilitates comparisons of energy demands across different pedogenon conditions. Sensitivity-based validation of conceptual models is well supported in systems modeling literature (Borgonovo & Plischke, 2016; Iwanaga et al., 2021), and in this context, it reinforces the relative influence of k in shaping exergy outcomes. Sensitivity analysis identifies k as the important parameter influencing total exergy, shaping restoration dynamics through its interaction with ΔSOC, while α plays a complementary role in fine-tuning energy efficiency (Fig.37&38). These findings underscore the importance of integrated strategies that optimize k and ΔSOC to minimize energy costs and maximize recovery efficiency.

Importantly, the model is not only consistent with theoretical expectations but also facilitates cross-system comparison by quantifying how soil carbon recovery effort scales with initial degradation severity. The results emphasize that exergy increases with larger SOC gaps (Fig.33, 34 & 35), as observed in pedogenons such as I, due to greater SOC losses in phenosoil compared to genosoil (Jang et al., 2023). These pedogenons exhibit higher exergy demands because larger energy gradients are required for SOC recovery, consistent with the thermodynamic principle that systems further from equilibrium need greater energy inputs to restore balance (Caruso et al., 2018). This emphasizes the strength of the framework, as it reflects well-established physical principles underlying ecological restoration. In contrast, pedogenons such as M and D,

with smaller SOC gaps (Jang et al., 2023), have lower exergy requirements, reflecting the reduced energy demand for soils closer to equilibrium.

The interplay between k and α is further illustrated across different management strategies. For compost application, exergy values remain relatively low over 50 years compared to other methods in both irrigated and non-irrigated systems (Fig.33). This is attributed to the lower energy demand of compost application (Palacino et al., 2024) and its reduced unit cost per SOC increase, as reflected in the α values. The observed exergy values, ranging from ~34 kJ/kg in pedogenons closer to equilibrium to over 1200 kJ/kg in pedogenons with large SOC gaps, highlight the proportional relationship between SOC gap size and energy requirements.

This proportionality is also evident in the modeled recovery rates (k), where pedogenons with higher k values demonstrate more efficient SOC recovery and lower energy costs, while those with lower k values exhibit slower recovery and heightened exergy demands. Similar patterns are observed in other methods, such as cotton-to-wheat and wheat-to-sorghum rotations (Fig.34 & 35). In irrigated systems, phenosoil exhibits significantly higher exergy values than non-irrigated systems due to the high energy demands of irrigation and fertilizer (Khan et al., 2010).

This distinction further illustrates how management intensity amplifies energy requirements, emphasizing the role of system inputs in influencing the thermodynamic cost of SOC restoration. For example, crop rotations from wheat to sorghum show lower energy costs due to the inherently lower production energy requirements of sorghum (Hossain et al., 2022). These patterns align with the framework's principles, demonstrating how both biophysical and management factors affect the energy expenditure required for SOC recovery (Monti & Venturi, 2003).

4.5.2 Towards Data-Driven Soil restoration

The results suggest that the recovery rate (k) varies across different pedogenons due to differences in the SOC concentrations of genosoil and phenosoil, reflecting their initial SOC gaps and inherent soil properties. These variations in k provide a foundation for developing a soil monitoring system by modeling scenario-based SOC recovery dynamics. For example, pedogenon I was analyzed under various management

practices, where initial SOC concentrations in phenosoil were combined with plausible k values to evaluate different scenarios: baseline (k=0.1), improved (k=0.2), degraded (k=0.05), and adverse (k=0.02) (Fig. 39). This scenario modeling allows us to systematically assess how changes in management affect long-term recovery trajectories. Such comparative insights help prioritize management interventions in high-risk areas and reinforce the model's capacity for scenario-based strategic planning.

The scenario results reveal distinct SOC recovery trajectories over a 50-year period. Improved management demonstrates the most efficient recovery, approaching the genosoil threshold of 20 g/kg, while baseline management achieves moderate recovery. In contrast, degraded and adverse scenarios show prolonged recovery timelines, with SOC levels plateauing well below optimal thresholds, highlighting the challenges of reversing degradation under suboptimal practices.

This scenario-based approach highlights the role of soil monitoring systems in addressing degradation and prioritizing interventions in degraded areas. By linking SOC recovery rates to management strategies, it could provide actionable insights for enhancing soil resilience and informing data-driven frameworks for sustainable soil management.

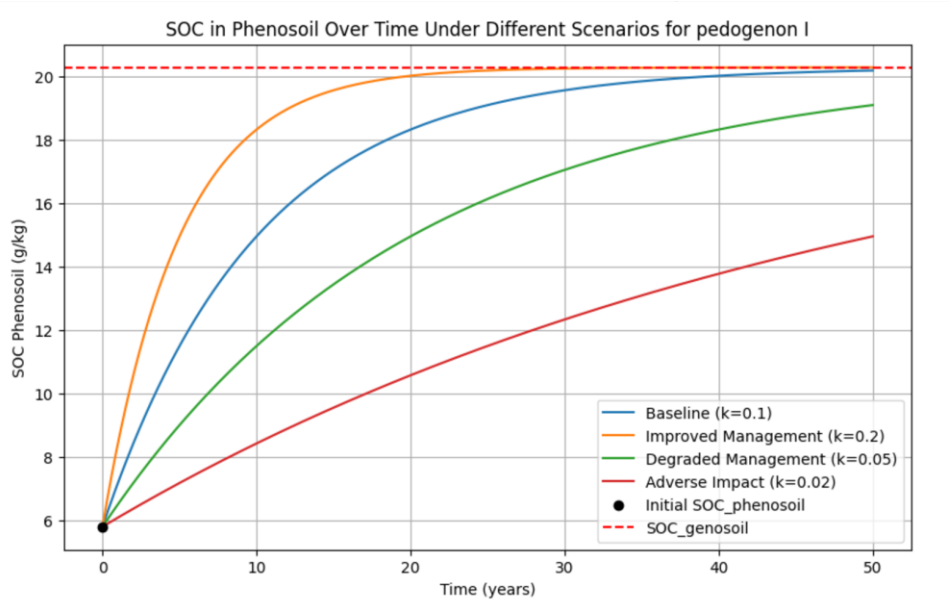

Fig.39. SOC restoration trajectories for Pedogenon I under varying management scenarios

4.5.3 Practical Implications for Soil Restoration

The exergy model is a promising approach with good potential for practical implications in land management, policy planning, and soil restoration. Although still at the pilot stage, it could have Implications in real-world environments as described below.

Guides targeted soil restoration: The model quantifies the exergy (energy requirement) needed to restore SOC in degraded soils. This allows land managers to identify which soils or regions require more investment for restoration. This helps in prioritization of areas with the highest restoration potential or lowest energy cost.

Decision-making for management practices: The model incorporates different management practices (e.g., composting, cover cropping) that influence the energy cost of SOC restoration. Knowing this, policymakers and farmers can choose cost-effective and energy-efficient strategies to increase carbon in the soil. Because it calculates parameters (SOC gap, recovery rate k, and cost α) for individual pedogenons, it can be adapted to local soil types and land uses, making it relevant for region-specific land management programs.

Enables Energy-Aware Soil Policies: With α representing the external energy investment, the model connects soil restoration to energy inputs. This connection is especially important for sustainability policies, carbon accounting, and strategies for reducing climate change. The model contributes to quantifying soil restoration as a measurable service, helping link soil security with broader goals like food security, biodiversity, and climate resilience.

Potential for scaling for larger land use planning tools: The exergy model can be turned into a mobile app for real-time SOC restoration monitoring and can be scaled to national or regional restoration planning.

4.5.4 Future Directions

The exergy model developed in this study serves as an accounting framework to quantify energy demands under different soil and management conditions. Future work could

empirically test this framework by applying it to long-term restoration monitoring projects.

Future studies could test how the framework performs in analyzing the influence of specific soil properties (e.g., texture, mineral composition) and historical management practices (e.g., tillage intensity, fertilization, crop rotation) on SOC recovery rates and exergy demands. This will allow for refinement of the model under different site conditions and support more targeted restoration strategies.

Refining the way α is estimated in this study by incorporating variability in SOC sequestration rates and differences across pedogenons would improve the model's precision. Including indirect costs, such as effects on crop production, would also enhance its relevance to real-world decision-making.

Future refinement of SOC restoration quantification can build on the exergy-based framework established in this study. Although the current model addresses the topsoil depth (0–30 cm) due to its high SOC levels, its extension to deeper profiles holds the potential for encompassing subsurface carbon dynamics and thus a more holistic perspective on soil health/condition, and carbon storage.

The addition of more parameters, like nutrient balance, salinity, and acidification, could expand the framework's scope and provide a general way to assess soil restoration. Likewise, testing the model with different management practices and in various soil types and agricultural systems would improve its flexibility and strength.

4.6. Conclusion

This study developed a thermodynamic framework with a simple equation to calculate total exergy, defined as the energy required to restore phenosoil to genosoil equilibrium. The model, expressed as the product of energy cost per unit (α), SOC gap (ΔSOC), and the inverse recovery rate (k), evaluates energy demands and recovery dynamics across diverse pedogenons.

Pedogenons with large SOC gaps and low k values, such as Pedogenon I, exhibited the highest exergy demands, benefiting from long-term management to leverage their

recovery potential. In contrast, pedogenons like M and D, with smaller SOC gaps and higher k values, require targeted soil incorporation improvements. These findings emphasize the importance of strategies that address specific pedogenon conditions, optimizing SOC recovery while minimizing energy demands.

Among management practices, compost application and crop cover practices had the lowest exergy demands, while irrigated cotton-to-wheat rotations incurred higher values. Wheat-to-sorghum rotations in dry areas demonstrated lower exergy requirements, reflecting the inherent energy efficiency of sorghum production.

Sensitivity analysis identified k as the primary driver of total exergy, with ΔSOC contributing moderately and α offering secondary benefits. This framework provides a tool for assessing energy demands in soil restoration, enabling stakeholders to design site-specific strategies. While not implemented in this study, the framework could be integrated into digital tools for real-time monitoring and decision-making, promoting sustainable soil management globally across diverse land uses.

Supplementary

S.1. Modeled Soc recovery and gap decay over 50 years, provided as supplementary material.

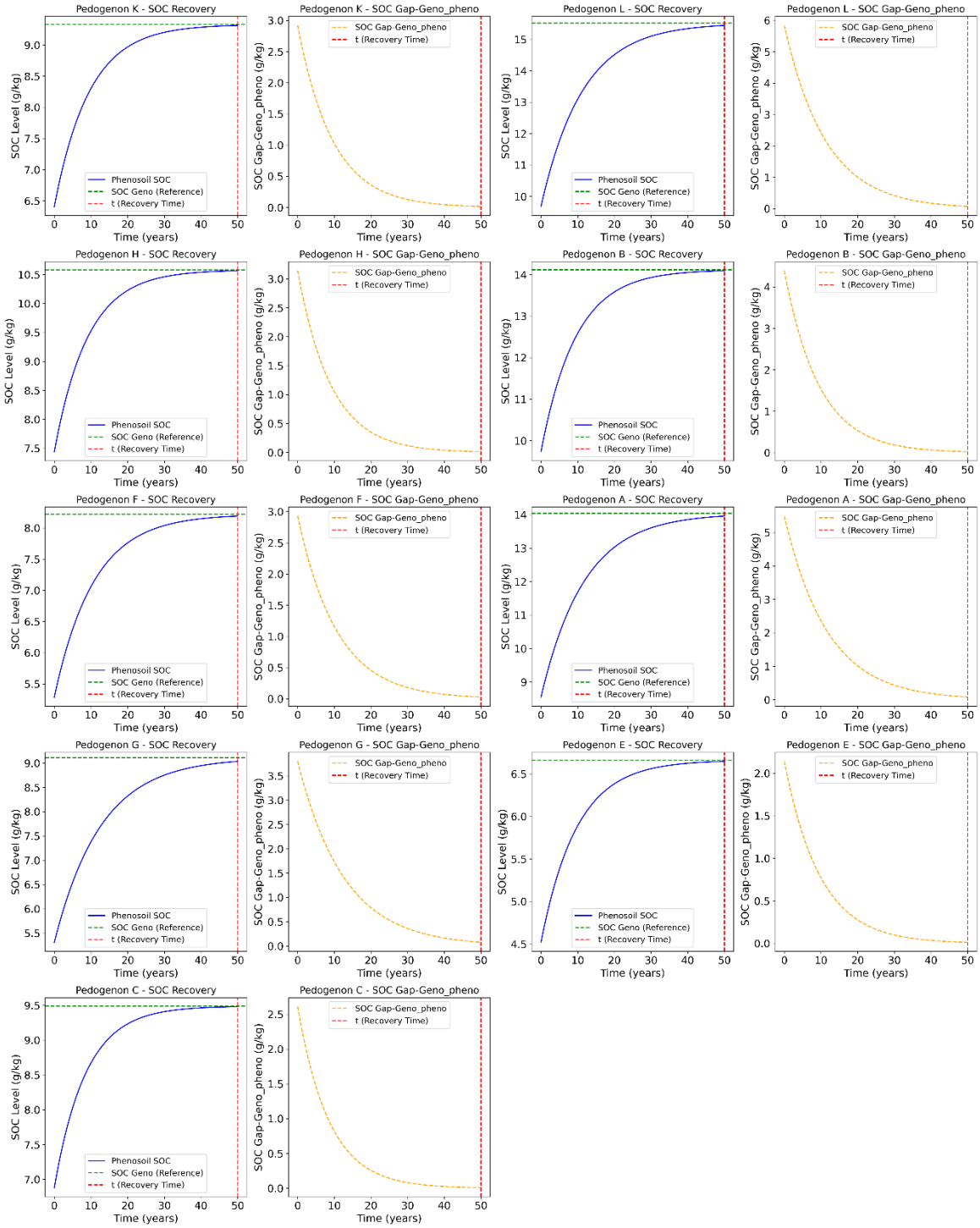

4.7. References

Angelopoulou, T., Tziolas, N., Balafoutis, A., Zalidis, G., Bochtis, D., 2019. Remote Sensing Techniques for Soil Organic Carbon Estimation: A Review. Remote Sensing, 116, 676. https://doi.org/10.3390/rs11060676

Alvarez, R., & Alvarez, C. R. 2000. Soil Organic Matter Pools and Their Associations with Carbon Mineralization Kinetics. Soil Science Society of America Journal, 64(1), 184–189. https://doi.org/10.2136/sssaj2000.641184x

Baumhardt, R., Stewart, B., Sainju, U., 2015. North American Soil Degradation: Processes, Practices, and Mitigating Strategies. Sustainability, 73, 2936–2960. https://doi.org/10.3390/su7032936

Bieluczyk, W., Asselta, F O., Navroski, D., Gontijo, J. B., Venturini, A. M., Mendes, L. W., Simon, C. P., Camargo, P. B. D., Tadini, A. M., Martin-Neto, L., Bendassolli, J. A., Rodrigues, R. R., Van Der Putten, W. H., Tsai, S. M. 2023. Linking above and belowground carbon sequestration, soil organic matter properties, and soil health in Brazilian Atlantic Forest restoration. Journal of Environmental Management, 344, 118573. https://doi.org/10.1016/j.jenvman.2023.118573

Borgonovo, E., & Plischke, E. 2016. Sensitivity analysis: A review of recent advances. European Journal of Operational Research, 248(3), 869–887. https://doi.org/10.1016/j.ejor.2015.06.032

Brandão, M., Milà I Canals, L., , Clift, R, 2011. Soil organic carbon changes in the cultivation of energy crops: Implications for GHG balances and soil quality for use in LCA. Biomass and Bioenergy, 356, 2323–2336. https://doi.org/10.1016/j.biombioe.2009.10.019

Cao, H., Liu, J., Ma, S., Wu, X., Fu, Y., , Gao, Y, 2024. Selection of Suitable Organic Amendments to Balance Agricultural Economic Benefits and Carbon Sequestration. Plants, 1317, 2428. https://doi.org/10.3390/plants13172428

Caruso, T., De Vries, F, T., Bardgett, R. D., Lehmann, J. 2018. Soil organic carbon dynamics matching ecological equilibrium theory. Ecology and Evolution, 822, 11169–11178. https://doi.org/10.1002/ece3.4586

Cerri, C, E. P., Easter, M., Paustian, K., Killian, K., Coleman, K., Bernoux, M., Falloon, P., Powlson, D. S., Batjes, N., Milne, E., Cerri, C. C. 2007. Simulating SOC changes in 11 land use change chronosequences from the Brazilian Amazon with RothC and Century models. Agriculture, Ecosystems, Environment, 1221, 46–57. https://doi.org/10.1016/j.agee.2007.01.007

Ghimire, R., Khanal, B., R. 2020. Soil organic matter dynamics in semiarid agroecosystems transitioning to dryland. PeerJ, 8, e10199. https://doi.org/10.7717/peerj.10199

Halvorson, A, D., , Schlegel, A. J. 2012. Crop Rotation Effect on Soil Carbon and Nitrogen Stocks under Limited Irrigation. Agronomy Journal, 1045, 1265–1273. https://doi.org/10.2134/agronj2012.0113

Herman, J., & Usher, W. 2017. SALib: An open-source Python library for Sensitivity Analysis. The Journal of Open Source Software, 2(9), 97. https://doi.org/10.21105/joss.00097

Hossain, Md S., Islam, Md. N., Rahman, Md. M., Mostofa, M. G., Khan, Md. A. R. 2022. Sorghum: A prospective crop for climatic vulnerability, food and nutritional security. Journal of Agriculture and Food Research, 8, 100300. https://doi.org/10.1016/j.jafr.2022.100300

Hulugalle, N, R., , Scott, F. 2008. A review of the changes in soil quality and profitability accomplished by sowing rotation crops after cotton in Australian Vertosols from 1970 to 2006. Soil Research, 462, 173. https://doi.org/10.1071/SR07077

Hulugalle, N R., Weaver, T. B., Finlay, L. A. 2006. Residual effects of cotton-based crop rotations on soil properties of irrigated Vertosols in central-western and north-western New South Wales. Soil Research, 445, 467. https://doi.org/10.1071/SR05141

Iwanaga, T., Sun, X., Wang, Q., Guillaume, J. H. A., Croke, B. F. W., Rahman, J., & Jakeman, A. J. 2021. Property-based Sensitivity Analysis: An approach to identify model implementation and integration errors. Environmental Modelling & Software, 139, 105013. https://doi.org/10.1016/j.envsoft.2021.105013

Jandl, R., Rodeghiero, M., Martinez, C., Cotrufo, M, F., Bampa, F., Van Wesemael, B., Harrison, R. B., Guerrini, I. A., Richter, D. deB, Rustad, L., Lorenz, K., Chabbi, A., , Miglietta, F. 2014. Current status, uncertainty, and future needs in soil organic carbon monitoring. Science of The Total Environment, 468–469, 376–383. https://doi.org/10.1016/j.scitotenv.2013.08.026

Jang, H J., Dobarco, M. R., Minasny, B., Campusano, J. P., McBratney, A. 2023. Assessing human impacts on soil organic carbon change in the Lower Namoi Valley, Australia.
Anthropocene, 43, 100393. https://doi.org/10.1016/j.ancene.2023.100393

Lascalajr, N., Lopes, A., Spokas, K., Bolonhezi, D., Archer, D., & Reicosky, D. (2008). Short-term temporal changes of soil carbon losses after tillage described by a first-order decay model. Soil and Tillage Research, 99(1), 108–118. https://doi.org/10.1016/j.still.2008.01.006

Jian, J., Du, X., Reiter, M, S., Stewart, R. D. 2020. A meta-analysis of global cropland soil carbon changes due to cover cropping. Soil Biology and Biochemistry, 143, 107735. https://doi.org/10.1016/j.soilbio.2020.107735

Jørgensen, S. E., Nielsen, S. N., & Mejer, H. 1995. Emergy, environ, exergy and ecological modelling. Ecological Modelling, 77(2–3), 99–109. https://doi.org/10.1016/0304-3800(93)E0080-M

Jorgensen, S., & Norsnielsen, S. 2007. Application of exergy as thermodynamic indicator in ecology. Energy, 32(5), 673–685. https://doi.org/10.1016/j.energy.2006.06.011

Khan, S., Khan, M A., Latif, N. 2010. Energy requirements and economic analysis of wheat, rice and barley production in Australia.

Kong, A., Y. Y., Six, J., Bryant, D. C., Denison, R. F., Van Kessel, C. 2005. The Relationship between Carbon Input, Aggregation, and Soil Organic Carbon Stabilization in Sustainable Cropping Systems. Soil Science Society of America Journal, 694, 1078–1085. https://doi.org/10.2136/sssaj2004.0215

Kuesters, J., Lammel, J, 1999. Investigations of the energy efficiency of the production of winter wheat and sugar beet in Europe. European Journal of Agronomy, 111, 35–43. https://doi.org/10.1016/S1161-03019900015-5

Lal, R., 2004. Soil Carbon Sequestration Impacts on Global Climate Change and Food Security. Science, 3045677, 1623–1627. https://doi.org/10.1126/science.1097396

Lal, R., 2015. Restoring Soil Quality to Mitigate Soil Degradation. Sustainability, 75, 5875–5895. https://doi.org/10.3390/su7055875

Larney, F J., Angers, D. A. 2012. The role of organic amendments in soil reclamation: A review. Canadian Journal of Soil Science, 921, 19–38. https://doi.org/10.4141/cjss2010-064

Lehmann, J., , Kleber, M, 2015. The contentious nature of soil organic matter. Nature, 5287580, 60–68. https://doi.org/10.1038/nature16069

Lützow, M, V., Kögel-Knabner, I., Ekschmitt, K., Matzner, E., Guggenberger, G., Marschner, B., , Flessa, H. 2006. Stabilization of organic matter in temperate soils: Mechanisms and their relevance under different soil conditions – a review. European Journal of Soil Science, 574, 426–445. https://doi.org/10.1111/j.1365-2389.2006.00809.x

Manzoni, S., Piñeiro, G., Jackson, R, B., Jobbágy, E. G., Kim, J. H., , Porporato, A. 2012. Analytical models of soil and litter decomposition: Solutions for mass loss and time-dependent decay rates. Soil Biology and Biochemistry, 50, 66–76. https://doi.org/10.1016/j.soilbio.2012.02.029

Maraseni, T., Chen, G., Banhazi, T., Bundschuh, J., Yusaf, T., 2015. An Assessment of Direct on-Farm Energy Use for High Value Grain Crops Grown under Different Farming Practices in Australia. Energies, 811, 13033–13046. https://doi.org/10.3390/en81112353

Montgomery, D. R. 2007. Soil erosion and agricultural sustainability. Proceedings of the National Academy of Sciences, 10433, 13268–13272. https://doi.org/10.1073/pnas.0611508104

Morais, T, G., Domingos, T., , Teixeira, R. F. M. 2016. A spatially explicit life cycle assessment midpoint indicator for soil quality in the European Union using soil organic carbon. The International Journal of Life Cycle Assessment, 218, 1076–1091. https://doi.org/10.1007/s11367-016-1077-x

Morais, T, G., Teixeira, R. F. M., , Domingos, T. 2019a. Detailed global modelling of soil organic carbon in cropland, grassland, and forest soils. PLOS ONE, 149, e0222604. https://doi.org/10.1371/journal.pone.0222604

Monti, A., & Venturi, G. 2003. Comparison of the energy performance of fibre sorghum, sweet sorghum, and wheat monocultures in northern Italy. European Journal of Agronomy, 19(1), 35–43. https://doi.org/10.1016/S1161-0301(02)00017-5

Morais, T, G., Teixeira, R. F. M., , Domingos, T. 2019b. Detailed global modelling of soil organic carbon in cropland, grassland, and forest soils. PLOS ONE, 149, e0222604. https://doi.org/10.1371/journal.pone.0222604

Murphy, B W. 2015. Impact of soil organic matter on soil properties—A review with emphasis on Australian soils. Soil Research, 536, 605. https://doi.org/10.1071/SR14246

Murindangabo, Y. T., Kopecký, M., Konvalina, P., Ghorbani, M., Perná, K., Nguyen, T. G., Bernas, J., Baloch, S. B., Hoang, T. N., Eze, F. O., & Ali, S. (2023). Quantitative Approaches in Assessing Soil Organic Matter Dynamics for Sustainable Management. Agronomy, 13(7), 1776. https://doi.org/10.3390/agronomy13071776

Padarian, J., Stockmann, U., Minasny, B., McBratney, A., B. 2022. Monitoring changes in global soil organic carbon stocks from space. Remote Sensing of Environment, 281, 113260. https://doi.org/10.1016/j.rse.2022.113260

Parton, W. J., Schimel, D. S., Cole, C. V., & Ojima, D. S. 1987. Analysis of Factors Controlling Soil Organic Matter Levels in Great Plains Grasslands. Soil Science Society of America Journal, 51(5), 1173–1179. https://doi.org/10.2136/sssaj1987.03615995005100050015x

Palacino, B., Ascaso, S., Valero, A., , Valero, A, 2024. Regeneration costs of topsoil fertility: An exergy indicator of agricultural impacts. Journal of Environmental Management, 369, 122297. https://doi.org/10.1016/j.jenvman.2024.122297

Pimentel, D., 2006. Soil Erosion: A Food and Environmental Threat. Environment, Development and Sustainability, 81, 119–137. https://doi.org/10.1007/s10668-005-1262-8

Pimentel, D., Burgess, M, 2013. Soil Erosion Threatens Food Production. Agriculture, 33, 443–463. https://doi.org/10.3390/agriculture3030443

Post, W, M., Izaurralde, R. C., Mann, L. K., , Bliss, N. 2001. Monitoring and Verifying Changes of Organic Carbon in Soil. Climatic Change, 511, 73–99. https://doi.org/10.1023/A:1017514802028

Powlson, D, S., Gregory, P. J., Whalley, W. R., Quinton, J. N., Hopkins, D. W., Whitmore, A. P., Hirsch, P. R., Goulding, K. W. T. 2011. Soil management in relation to sustainable agriculture and ecosystem services. Food Policy, 36, S72–S87. https://doi.org/10.1016/j.foodpol.2010.11.025

Pratibha, G., Srinivas, I., V., Rao, K., M.K. Raju, B., Shanker, A. K., Jha, A., Uday Kumar, M., Srinivasa Rao, K., Sammi Reddy, K. 2019. Identification of environment friendly tillage implement as a strategy for energy efficiency and mitigation of climate change in semiarid rainfed agro ecosystems. Journal of Cleaner Production, 214, 524–535. https://doi.org/10.1016/j.jclepro.2018.12.251

R Lal, D. J. Eckert, N. R. Fausey, W. M. Edwards. 1990. Conservation Tillage in Sustainable Agriculture 1st Edition. CRC Press.

Rochester, I.J. 2011. Sequestering carbon in minimum-tilled clay soils used for irrigated cotton and grain production. Soil and Tillage Research, 1121, 1–7. https://doi.org/10.1016/j.still.2010.10.012

Román Dobarco, M., Wadoux, A, M. J.-C., Malone, B., Minasny, B., McBratney, A. B., , Searle, R. 2023. Mapping soil organic carbon fractions for Australia, their stocks, and uncertainty. Biogeosciences, 208, 1559–1586. https://doi.org/10.5194/bg-20-1559-2023

Ros, M, 2003. Soil microbial activity after restoration of a semiarid soil by organic amendments. Soil Biology and Biochemistry, 353, 463–469. https://doi.org/10.1016/S0038-07170200298-5

Rosen, M A., Dincer, I. 2001. Exergy as the confluence of energy, environment and sustainable development. Exergy, An International Journal, 11, 3–13. https://doi.org/10.1016/S1164-02350100004-8

Saby, N, P. A., Bellamy, P. H., Morvan, X., Arrouays, D., Jones, R. J. A., Verheijen, F. G. A., Kibblewhite, M. G., Verdoodt, A., Üveges, J. B., FREUDENSCHUß, A., , Simota, C. 2008. Will European soil-monitoring networks be able to detect changes in topsoil organic carbon content? Global Change Biology, 1410, 2432–2442. https://doi.org/10.1111/j.1365-2486.2008.01658.x

Saltelli, A., 2002. Making best use of model evaluations to compute sensitivity indices. Computer Physics Communications, 1452, 280–297. https://doi.org/10.1016/S0010-46550200280-1

Sato, N, 2004. Thermodynamic state variables. In Chemical Energy and Exergy pp. 1–7. Elsevier. https://doi.org/10.1016/B978-044451645-9/50001-7

Sierra, C. A., & Müller, M. 2015. A general mathematical framework for representing soil organic matter dynamics. Ecological Monographs, 85(4), 505–524. https://doi.org/10.1890/15-0361.1

Smith, L G., Williams, A. G., Pearce, Bruce. D. 2015. The energy efficiency of organic agriculture: A review. Renewable Agriculture and Food Systems, 303, 280–301. https://doi.org/10.1017/S1742170513000471

Smith, P., Smith, J, U., Powlson, D. S., McGill, W. B., Arah, J. R. M., Chertov, O. G., Coleman, K., Franko, U., Frolking, S., Jenkinson, D. S., Jensen, L. S., Kelly, R. H., Klein-Gunnewiek, H., Komarov, A. S., Li, C., Molina, J. A. E., Mueller, T., Parton, W. J., Thornley, J. H. M., , Whitmore, A. P. 1997. A comparison of the performance of nine soil organic matter models using datasets from seven long-term experiments. Geoderma, 811–2, 153–225. https://doi.org/10.1016/S0016-70619700087-6

Sobol′, I, M. 2001. Global sensitivity indices for nonlinear mathematical models and their Monte Carlo estimates. Mathematics and Computers in Simulation, 551–3, 271–280. https://doi.org/10.1016/S0378-47540000270-6

Status of the World's Soil Resources: Main Report. n.d..

Stewart, C E., Paustian, K., Conant, R. T., Plante, A. F., Six, J. 2007. Soil carbon saturation: Concept, evidence and evaluation. Biogeochemistry, 861, 19–31. https://doi.org/10.1007/s10533-007-9140-0

Stepanchenko, O., Shostak, L., Moshynskyi, V., Kozhushko, O., & Martyniuk, P. 2023. Simulating Soil Organic Carbon Turnover with a Layered Model and Improved Moisture and Temperature Impacts. In S. Babichev & V. Lytvynenko (Eds.), Lecture Notes in Data Engineering, Computational Intelligence, and Decision Making (Vol. 149, pp. 74–91). Springer International Publishing. https://doi.org/10.1007/978-3-031-16203-9_5

Stoner, C D. 2000. Inquiries into the Nature of Free Energy and Entropy in Respect to Biochemical Thermodynamics. Entropy, 23, 106–141. https://doi.org/10.3390/e2030106

Van Der Werf, H, M. G., Knudsen, M. T., , Cederberg, C. 2020. Towards better representation of organic agriculture in life cycle assessment. Nature Sustainability, 36, 419–425. https://doi.org/10.1038/s41893-020-0489-6

Wendt, J W., Hauser, S. 2013. An equivalent soil mass procedure for monitoring soil organic carbon in multiple soil layers. European Journal of Soil Science, 641, 58–65. https://doi.org/10.1111/ejss.12002

Yang, L., Pan, J., , Yuan, S, 2006. Predicting dynamics of soil organic carbon mineralization with a double exponential model in different forest belts of China. Journal of Forestry Research, 171, 39–43. https://doi.org/10.1007/s11676-006-0009-1

Zhou, X., Chen, C., Lu, S., Rui, Y., Wu, H., , Xu, Z, 2012. The short-term cover crops increase soil labile organic carbon in southeastern Australia. Biology and Fertility of Soils, 482, 239–244. https://doi.org/10.1007/s00374-011-0594-9

Zhou, S., Xiang, D., Wang, G., Zhang, L., Lv, Z., Qi, S., & Li, W. 2025. Reevaluating multi-pool first-order kinetic models for fitting soil incubation data. Geoderma, 455, 117218. https://doi.org/10.1016/j.geoderma.2025.117218

Zhou, X., Wu, H., Li, G., Chen, C, 2016. Short-term contributions of cover crop surface residue return to soil carbon and nitrogen contents in temperate Australia. Environmental Science and Pollution Research, 2322, 23175–23183. https://doi.org/10.1007/s11356-016-7549-5

Chapter 5: Quantum Soil Science: A New Frontier for Soil Formation, Function, and Security

5.1 Abstract

Quantum effects such as proton tunnelling and electron coherence have been extensively studied in disciplines like chemistry, biology, and materials science, but remain largely underexplored in soil systems. This chapter introduces Quantum Soil Science as a conceptual research direction, proposing that quantum processes may contribute to fundamental soil formation processes, including mineral weathering and enzymatic decomposition. Classical thermodynamics and kinetics models may not full capture observed reaction behaviours, particularly under low-temperature or energy-limited conditions. We propose a conceptual framework linking potential quantum contributions to soil function and describe how quantum-informed perspectives could guide targeted management strategies that consider both bulk soil properties and microenvironmental conditions relevant to molecular scale reactions. Finally, we highlight the need for quantum-informed soil metrics and falsifiable experimental approaches to evaluate these mechanisms in soil systems.

Keywords: Quantum Soil Science; Soil formation; Proton tunneling; Soil function

5.2. Introduction

Soil forms the foundation of the terrestrial ecosystems, playing a crucial role in sustaining food production, climate change mitigation, biodiversity protection, water and energy securing, and human health mitigation. This dynamic system driven by ongoing organic/inorganic transformations (Li et al., 2023) demands study of both bulk properties (e.g., organic carbon, nutrients) and underlying pedogenic/mechanistic processes for resilience under environmental constraints. Soil is inherently dynamic across space and time, as soil properties continuously evolve under the influence of both natural forces and human activity (Lin, 2011). Yet, soil exhibits a remarkable capacity for self-organisation, maintaining structure and function through feedback mechanisms that operate across multiple scales (Young & Crawford, 2004; Targulian & Krasilnikov, 2007). This organisation emerges from underlying energy gradients and the constant tension between aggregation and disaggregation. Aggregates, cohesive groupings of solids and pores, form through energetically driven interactions, serving as fundamental units of soil structure and function (Yudina & Kuzyakov, 2023). These patterns of energy-based

structuring raise an important question: could subatomic, quantum-scale processes contribute to the efficiency and adaptability of soil systems? Exploring this possibility may offer new insight into the molecular foundations of soil formation.

Classical models explain many soil transformations through thermodynamic and kinetic principles but often fail to account for unexpectedly rapid or efficient behaviour under cold low-energy, or diffusion -limited microsites (Pot et al., 2021; Vereecken et al., 2016; Yan et al., 2023). Here, "low-energy" refers to constrained thermal energy, substrate availability, or molecular mobility-such as subzero alpine/tundra soils, deep subsoils with low microbial turnover, or mineral-organic/redox microzones. These highlight where classical limitations become most evident, though quantum effects are not exclusive to them. For example, classical Michaelis-Menten kinetics does not capture realistic soil enzyme behaviour, while the Equilibrium Chemistry Approximation better simulates decomposition across heterogeneous microsites (Wang & Allison, 2019). Such deviations may also stem from multi-enzyme interactions and microsite heterogeneity.

Consistent with this limitation of simplified formulations, results from the microbial-enzyme-mediated decomposition (MEND) model show that incorporating enzyme specificity and dynamic microbial traits yields decomposition patterns that deviate significantly from those predicted by classical pool-based SOC models, especially under warming scenarios (Wang et al., 2013a).

These limitations are not only relevant to modelling, they also reflect broader discrepancies in how classical theory explains real-world soil processes. For example, mineral weathering, a foundational component of soil genesis, often proceeds at rates far exceeding those predicted by Arrhenius-based models, under environmentally constrained conditions (Sverdrup & Warfvinge, 1988). Likewise, enzymatic decomposition of organic matter remains active even under suboptimal conditions where classical thermodynamics would predict minimal biochemical activity. Recent studies show that the decomposition of plant litter with a low C:P ratio progresses more rapidly than its optimal ratio, and that long-term breakdown is strongly linked to extracellular enzyme activity (Liu et al., 2025). The study further provided evidence of the limits of the classical stoichiometric framework.

Even under environmentally constrained settings, microbial communities in alpine and cold ecosystems can maintain enzyme activity, demonstrating a biochemical resilience that is not readily explained by classical models (Shan et al., 2024). In addition, several studies on microbial respiration have observed that electron transfers to mineral-bound acceptors are primarily carried out through the extracellular insulating outer layer of microbial cells. These redox processes seem to involve c-type cytochromes and conductive nanowires-mechanisms (Shi et al., 2016) that are difficult to reconcile with classical frameworks. Quantum mechanical phenomena such as proton tunnelling and electron coherence are well established in fundamental physics and chemistry (Devault, 1980), but their functional importance in complex biological and catalytic systems has gained increasing recognition over the past two decades (Lloyd, 2011; Kim et al., 2021). These mechanisms may offer a basis for explaining unexpectedly efficient transformation processes in soils. In classical physics, particles must possess sufficient energy to overcome an energy barrier. But in quantum mechanics, particles like protons can "tunnel through" the barrier, even if they lack sufficient energy. Electron coherence, meanwhile, refers to the preservation of the phase relationship between components of an electron’s wavefunction as it moves through a system, enabling quantum interference effects that can enhance reactivity and transport efficiency.

Recent research supports the relevance of these quantum processes in soil systems. For example, a study on soil-derived dissolved organic matter (DOM) shows that the photochemical reactivity of DOM, measured via quantum yields of reactive intermediates like triplet-state DOM and singlet oxygen, varies systematically with mineral weathering and oxidation states (Ren et al., 2025).

Advances in quantum enzymology have demonstrated that classical kinetic models relying solely on thermal energy to drive enzymatic processes fail to capture critical aspects of catalysis, such as proton abstraction and hydride transfer. These reactions often depend on quantum mechanical phenomena like multidimensional tunnelling and quantized vibrational energy states, which have been shown to significantly enhance reaction efficiency under constrained conditions (Truhlar et al., 2002).

These observations raise a critical question: What mechanisms allow such reactions to persist under constrained conditions? The answer may lie in quantum mechanisms that

allow particles to traverse energy barriers or synchronise reaction pathways in ways classical models cannot account for. If so, the implications for soil science would be significant.

Given the biochemical parallels observed in microbial respiration and organic matter turnover, incorporating quantum principles into soil models may help explain the persistence of biochemical activity under constrained environmental conditions. This paper explores the potential for quantum mechanical principles, particularly tunnelling and coherence, to contribute to key soil processes and support a refined mechanistic framework for interpreting soil processes. By focusing on two representative processes, mineral weathering and enzymatic decomposition, we examine how quantum effects might operate at the molecular level to enhance reaction efficiency in soils.

Drawing from recent advances in quantum biology, catalysis, and theoretical modelling, we propose a conceptual framework for integrating quantum thinking into soil science. This includes identifying relevant quantum phenomena, assessing their implications for soil system behaviour, and outlining how quantum-informed models and interventions could inform more mechanistically grounded soil management strategies. Our goal is to stimulate dialogue and research toward the development of quantum-informed approaches in soil science as a complementary direction capable of extending current soil modelling frameworks across diverse environments contexts.

5.3. Quantum contributions to Soil Formation and Function

Quantum-scale processes may contribute to specific reaction pathways involved in soil biogeochemical transformations. Mechanisms such as proton tunnelling, electron coherence, and quantum-assisted bond rearrangements influence how activation barriers are traversed at the molecular level (Devault, 1980; Strandh et al., 1997a). In classical transition-state theory, reactants must acquire sufficient thermal to overcome an energy barrier, whereas quantum mechanics allows particles such as protons or electrons to penetrate barriers through tunnelling, thereby modifying reaction probabilities (Schreiner, 2020).

Although direct empirical evidence of quantum processes operating in soil systems is still limited, analogous mechanisms are well-established in enzymology, molecular

biology, and geochemistry (McMahon, 2003; Sousa et al., 2017). In these fields, quantum effects have been shown to markedly improve reaction efficiency under constrained environmental conditions. Notably, even within enzymology, researchers have begun adopting quantum-enabled tools such as quantum dot nanoprobes from biomedical sciences to improve the spatial resolution and detection of enzyme activity in complex environments like soils (Nannipieri et al., 2011). Given the similar kinetic challenges and microenvironments present in soils, it is reasonable to examine whether comparable quantum contributions may operate in soil contexts.

Fig. 40 Conceptually contrasts classical and quantum-modified reaction pathways. Under a classical description, reaction rates depend strongly on the height and shape of the activation barrier; when tunnelling is operative, the effective transmission probability across that barrier increases, reducing the strict dependence of reaction rates on thermal activation energy and altering the effective rate constant under certain structural and energetic configurations.

For example, in iron-containing minerals, quantum tunnelling facilitates the transfer of electrons from Fe^{3+} to Fe^{2+}, enhancing mineral weathering even when classical conditions would suggest minimal reactivity. This kind of subatomic efficiency could help explain why certain soil systems maintain microbial activity and nutrient cycling under stress, a phenomenon that would be underestimated if only classical chemistry were considered (Shi et al., 2016).

These quantum effects may initiate a cascading sequence of outcomes Fig. 41:

- Quantum effects (e.g., tunnelling, coherence) enable low-energy, high-efficiency reactions such as enzymatic decomposition and electron transfer.
- Geochemical transformations, including mineral weathering, ion exchange, and organic matter stabilisation, are accelerated as a result.
- Soil formation advances through these pathways, laying the foundation for biophysical soil functions like nutrient cycling and carbon stabilisation.
- Ecosystem services, such as food production, water filtration, and climate moderation, emerge from this soil functionality.

- Soil security is achieved when this chain remains intact and resilient over time.

Although a wide range of soil-forming processes could be influenced by quantum phenomena, this conceptual examination focuses on two representative pathways where quantum contributions are both theoretically supported and functionally critical to soil development:

- Mineral Weathering and Electron Transfer: Governs the release of nutrients from primary minerals and mediates redox reactions vital to soil chemistry.
- Enzymatic Reactions in Soil Organic Matter Decomposition: Catalyses the breakdown of complex organic compounds, driving carbon cycling and microbial metabolism.

The following sections will examine each process in depth, beginning with a review of its classical mechanistic understanding, followed by an exploration of how quantum phenomena may modify or enhance these mechanisms.

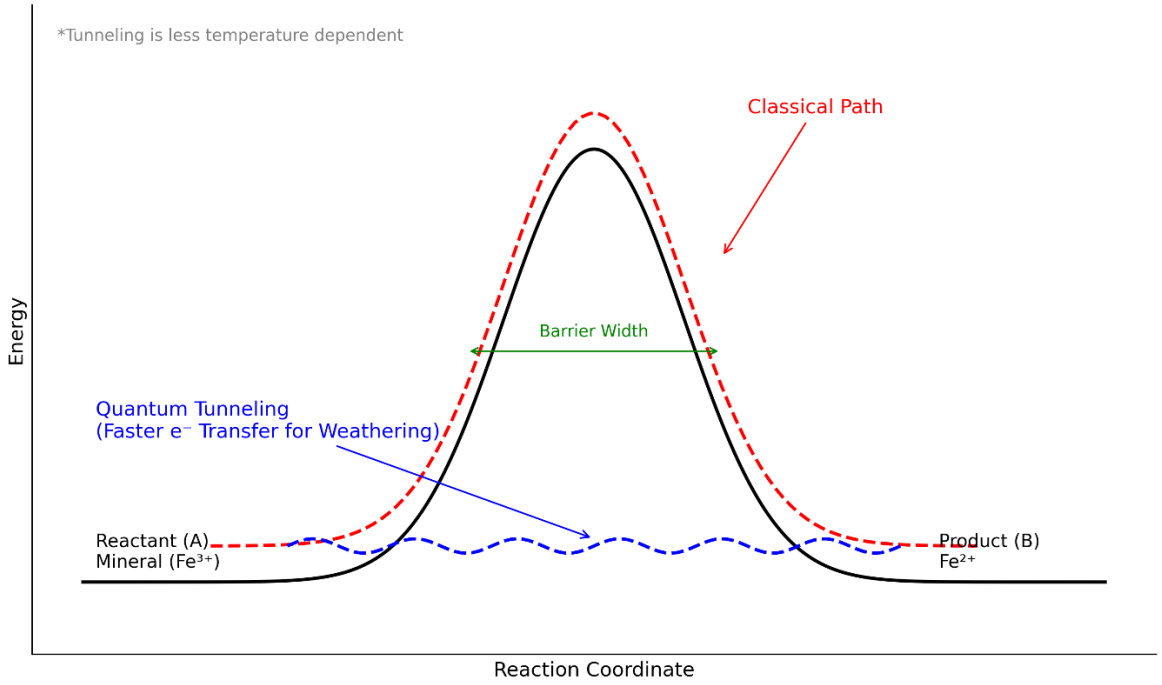

Fig 40. Comparison of classical and quantum tunneling pathways in mineral weathering. Quantum tunneling enables faster electron transfer (Fe^{3+} to Fe^{2+}) by

bypassing the activation barrier, explaining enhanced soil weathering under low-energy conditions.

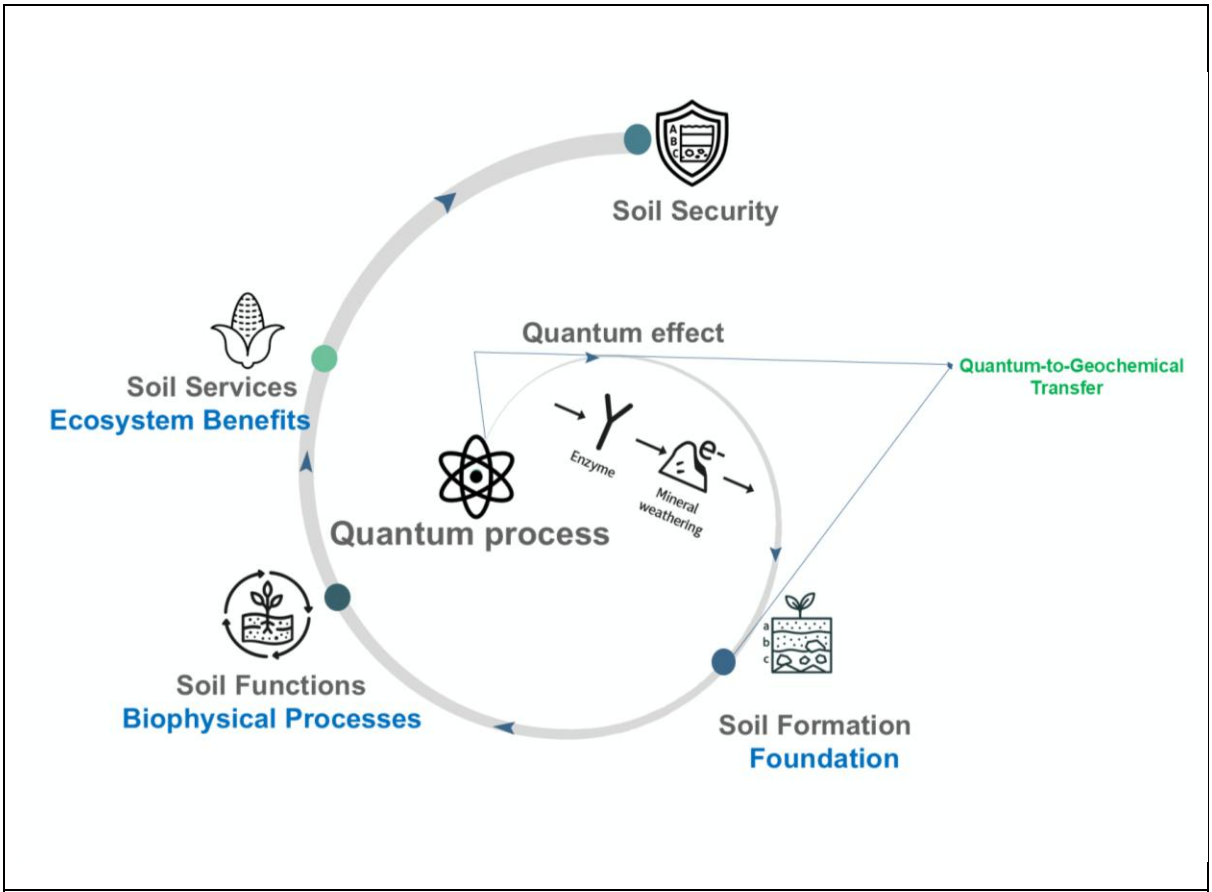

Fig 41. Conceptual framework linking quantum processes to soil formation, soil functions, and soil security. Quantum effects in mineral weathering and enzymatic reactions underpin soil development, ecosystem benefits, and long-term resilience.

5.4. Mineral Weathering and Electron Transfer

Soil formation fundamentally depends on mineral weathering, a process by which primary minerals such as feldspar, olivine, pyroxenes, amphiboles, micas, and chlorites break down to release essential nutrients (Wilson, 2004). The rate of weathering is classically described by the Arrhenius equation:

$$k = Ae^{-\frac{E_a}{RT}}$$

where *k* is the reaction rate constant, *A* the pre-exponential factor, E_a the activation energy, *R* the universal gas constant, and *T* the temperature in Kelvin. According to this model, reaction rates increase with temperature and are constrained by an energy barrier (E_a), beyond which molecular transformations proceed.

However, a growing body of empirical evidence challenges the sufficiency of this classical approach, especially under extreme environmental conditions such as low temperatures and limited energy availability. Several studies (Sverdrup & Warfvinge, 1988; Duan et al., 2002) have reported that silicate mineral weathering occurs several orders of magnitude faster than predicted by classical kinetics. These deviations suggest that additional mechanisms or microenvironmental effects may influence mineral dissolution beyond simplified classical formulations.

A particularly well-documented example is the dissolution of feldspar, a key silicate mineral involved in early-stage soil genesis (Cronan, 2018; Zhu, Zhao, et al., 2024). Reactions such as:

$$CaAl_2Si_2O_8 + 2H^+ + 2HCO_3^- + H_2O \rightarrow Al_2Si_2O_5(OH)_4 + Ca^{+2} + 2HCO_3^-$$

Experimental evidence indicates that feldspar dissolution rates are significantly higher than those anticipated by classical models (Velbel, 1990; Duan et al., 2002; Deng et al., 2022). For instance, comparative dissolution experiments involving anorthite ($CaAl_2Si_2O_8$) and albite ($NaAlSi_3O_8$) in carbonic acid demonstrate that Ca-rich feldspars weather significantly faster than their Na-rich counterparts (Huang et al., 1972).

To address these discrepancies, several studies have modified the Arrhenius equation to account for pH dependence, ionic strength effects, surface interactions, and deviations from equilibrium. One notable adjustment, proposed by (Cama et al., 1999), introduces a deviation-from-equilibrium factor into the reaction rate equation:

$$\text{Rate} = k_o e^{-\frac{E_a}{RT}} a_{H^+}^{n_{H^+}} g(I) \prod a_{ij}^{n_{ij}} f(\Delta G_r)$$

k_o=Pre-exponential factor (baseline reaction rate)

$e^{-\frac{E_a}{RT}}$ = Arrhenius temperature-dependent term, where:

E_a=Apparent activation energy

R =Universal gas constant

T = Temperature (Kelvin)

$a_{H^+}^{n_{H^+}}$ = Hydrogen ion activity raised to the reaction order n_{H^+}

$g(I)$ = Function accounting for the effect of ionic strength (I)

$\prod a_{ij}^{n_{ij}}$ = Product term that includes contributions from various species i and j, each raised to their respective reaction orders n_{ij}.

$f(\Delta G_r)$ = Function describing the impact of reaction affinity (ΔG_r), which accounts for deviations from equilibrium.

This multi-parameter approach provides a more realistic model of soil mineral reactivity by accounting for coupled chemical interactions in complex soil solutions. Additional evidence from far-from-equilibrium databases (Heřmanská, 2023) shows that over 65% of silicate minerals exhibit comparable dissolution rates at neutral pH, implying that the Si–O bond is a key rate-limiting step, rather than hydrogen ion concentration alone. Similarly, (Opolot & Finke, 2015) found that mineral dissolution kinetics vary not only with mineralogical properties but also with environmental conditions. Despite these refinements, discrepancies remain in some systems, indicating that further mechanistic refinement may be required.

Recent advances in quantum chemistry could provide new explanations for mineral dissolution behaviour that cannot be accounted for by classical or modified kinetic models alone. In particular, quantum tunnelling and electron coherence have been in related catalytic and mineral systems as mechanism that may contribute to barrier crossing under certain molecular configurations.

For example, (Strandh et al., 1997a) used density functional theory (DFT) simulations to show that proton adsorption weakens siloxane (Si–O–Si) bonds in feldspar, significantly lowering the energy barrier for bond cleavage. This behaviour indicates that protonation significantly reduces activation barriers. Whether such reductions involve tunnelling contributions requires further investigation.

Building on this, (Kubicki et al., 2012) incorporated quantum-derived parameters into modified Arrhenius equations. Their DFT-based molecular dynamics simulations revealed that protonation and hydrolysis of bridging oxygen atoms (Obr) are facilitated by internal surface hydrogen bonds, rather than depending exclusively on external water-mediated interactions. These atomistic simulations demonstrate how local hydrogen bonding networks can modify reaction pathways and activation barriers. Moreover, their findings showed that ionic strength modulates hydrogen bond formation, increasing the pre-exponential factor (A) in the Arrhenius equation and thereby accelerating dissolution rates.

Together, these studies demonstrate that atomistic-scale mechanisms significantly influence mineral dissolution kinetics. Whether quantum tunnelling or related nuclear quantum effects contribute measurably under soil conditions remains an open but testable question.

Tunnelling allows protons or electrons to bypass classical energy barriers, enabling bond dissociation to occur more rapidly, even at low temperatures or near-neutral pH levels. Such mechanisms may contribute to reconciling discrepancies between laboratory derived kinetics and field-observed weathering rates.

Further empirical and theoretical studies reinforce this perspective. For instance, Cama et al., 1999 and Kubicki et al. 2012 demonstrate that:

- Activation energy may decrease as a function of pH, a pattern consistent with quantum tunnelling-assisted bond cleavage.
- Electron transfer processes in minerals may involve delocalised or hopping mechanisms what warrant quantum-level investigation.

Although additional mechanisms, such as enhanced surface area from nanopores (Parry et al., 2015), mineral-organic interfaces (Mendez et al., 2020), and surface roughness-induced reactivity also contribute to mineral dissolution, While these factors account for may rate discrepancies, some inconsistencies remain in certain systems, motivating further mechanistic exploration.

5.5. Enzymatic Reactions in Soil Organic Matter Decomposition

The decomposition of soil organic matter (SOM) is a core process in soil formation, directly contributing to the development of stable organic-mineral associations, nutrient availability, and carbon stabilisation (Cotrufo & Lavallee, 2022).Soil microbes facilitate this process through the secretion of extracellular enzymes, which catalyse the breakdown of complex organic matter into simpler compounds usable by the microbes and involved in mineral interactions (Serrano-Grijalva et al., 2024).

Classical enzyme kinetics, particularly the Michaelis-Menten equation, initially formulated in biochemistry to describe enzyme-substrate interactions under steady-state conditions (Johnson & Goody, 2011), forms the basis of SOM decomposition models (Cecilia et al., 2019). In the context of SOM decomposition, this kinetic framework has been adapted to model the relationship between reaction velocity and substrate concentrations, providing a basis for understanding how enzymes facilitate the breakdown of organic matter in soils (Davidson et al., 2012; Y. Chen et al., 2016). This equation is written as:

$$V=\frac{V_{max}[s]}{K_m+[s]}$$

Where: V= reaction rate; Vmax= enzyme velocity; [S]= substrate concentration; Km= Michaelis constant.

The Michaelis-Menten equation usually rooted within first-order decay models to simulate SOM turnover across different pools (e.g., particulate, dissolved, or mineral-associated organic matter), governed by the equation:

$$\frac{\mathrm{dC}}{\mathrm{dt}} = -k\mathrm{C}$$

While these classical models have enhanced our ability to model microbial-driven organic matter transformations, they assume constant enzyme activity and linear microbial responses, often resulting in poor predictive power under variable or extreme environmental conditions (Schimel, 2003).

In response to these limitations, G. Wang et al., 2013b developed the Microbial-Enzyme-Mediated Decomposition (MEND) model, explicitly incorporating enzyme pools,

microbial biomass, and diverse organic carbon fractions (particulate, mineral-associated, dissolved). Despite the dynamic feedback and temperature sensitivities that have been incorporated to improve classical models, such models remain grounded in classical thermodynamics and Arrhenius-type kinetics and may not fully capture enzyme behaviour under certain environmental extremes. A growing number of empirical studies report inconsistencies between observed enzyme behaviour and classical model predictions. For example, Zhu, Zhang, et al., 2024 found that only certain enzymes (e.g., β-glucosidase, β-xylosidase) were significantly correlated with SOC increases under conservation tillage, contrary to assumptions of uniform enzymatic behaviour. Qi et al., 2016 and Xu et al., 2023 reported nonlinear enzyme responses to warming and significant shifts in enzyme ratios (hydroplase:oxidase), while Ali et al., 2018 demonstrated that microbial biomass and local soil physicochemical conditions had a stronger influence on enzyme temperature sensitivity than expected under classical models.

D. Li et al., 2017 observed that Vmax and Km co-varied systematically across elevational gradients, suggesting changes in underlying enzyme energetics that are not explicitly represented within classical Michaelis-Menten formulations. Similarly, Leifeld & Von Lützow, 2014 showed that although enzymatic catalysis reduces activation energy (from ~136 to ~87 kJ mol^{-1}), the temperature sensitivity of decomposition remained decoupled from classical predictions.

Together, these findings point to nonlinear behaviour, variable microbial control, and biochemical specificity, all of which challenge the assumptions of steady-state kinetics and first-order decay. As Schimel, 2003 notes, the complexity of microbial-enzyme interactions in soil environments demands models that go beyond classical frameworks.

Quantum mechanics descriptions of enzyme catalysis provide a mechanistic framework that may help interpret such observations. Two major quantum phenomena are relevant in this context: proton/electron tunnelling and quantum coherence.

5.6. Quantum Tunnelling in Proton and Electron Transfers

Soil enzymes involved in redox reactions, including phenol oxidases, laccases, and peroxidases, mediate key steps in organic matter decomposition (Sinsabaugh, 2010). These reactions are commonly described using transition state theory (TST), in which rate

constants depend on thermal activation over an energy barrier (Ptáček et al., 2018). In soil microenvironments, however, enzyme structure, mineral surfaces, electrostatic fields, and hydration networks influence donor–acceptor distances and energy landscapes. Under such conditions, tunnelling-corrected formulations allow for barrier penetration by light particles such as protons and electrons, modifying effective rate constants relative to purely over-barrier predictions. Proton transfer along narrow reaction coordinates is particularly sensitive to these quantum contributions (Benderskii et al., 1993).

To incorporate these effects, theoretical chemists have developed tunnelling-corrected transition state theories, in which TST rate expressions are modified by a tunnelling correction factor (κ). For example, Truhlar et al., 1996 proposed the following formulation:

$$k_{tunnel} = \kappa . \frac{k_B T}{h} . e^{-\Delta G ‡ / RT}$$

Where, k_{tunnel} is the tunnelling-corrected reaction rate, k_B is Boltzmann's constant, T the absolute temperature, h Planck's constant, ΔG ‡ the Gibbs free energy of activation, and R the universal gas constant and $\kappa \geq 1$ quantifies the contribution of tunnelling.

Applying quantum-corrected reaction rate concepts to soil enzyme systems provides a mechanistic hypothesis that may help explain the persistence of enzymatic activity under otherwise unfavourable conditions. Here, the theory refers to tunnelling-corrected transition state theory applied to enzyme-mediated proton and electron transfer within soil micro-environments.

For reactions with moderately high activation energies, classical kinetics predict strongly reduced rates at low temperatures (e.g.,5-10 C°). Under specific molecular configurations that reduce donor-acceptor distances, tunnelling corrections may partially mitigate this decline, such that:

$$k^{tunnel} \geq k^{Arrhenius}$$

Such quantum corrections are expected to become relevant only when donor–acceptor distances are sufficiently compressed and the reaction coordinate is narrow, conditions

that may arise within enzyme active sites but are not assumed to occur uniformly across soil systems.

Recent theoretical developments extend these ideas. Constrained Nuclear-Electronic Orbital Transition State Theory (CNEO-TST) incorporates nuclear quantum effects directly into the potential energy surface representation (Chen et al., 2025). While originally developed outside the soil contexts, CNEO-TST incorporates zero-point energy and shallow tunnelling directly onto the potential energy surface via a constrained minimized energy surface (CMES):

$$k_{SOC} = \kappa . \frac{k_B\, T}{h} . \, e^{-\Delta G \ddagger_{CMES}/_{RT}}$$

Here, $\Delta G \ddagger_{CMES}$ inherently includes quantum effects such as delocalisation and tunnelling. This framework has been demonstrated in model hydrogen-atom transfer systems and provides a theoretical basis that could, in principle, be extended to proton-coupled electron transfer in enzyme systems.

Parallel to this Jara et al., 2025 demonstrated that enzyme catalysis can proceed through a conformationally broad transition-state ensemble (TSE), not a single rigid saddle point. Their combined QM/MM and kinetic analyses showed that such a delocalized TSE reduces the activation entropy penalty, thereby enhancing catalytic efficiency. While some methodological limitations remain (e.g., free energy profile discrepancies), this supports the relevance of quantum-informed rate descriptions for enzymes operating in complex biological systems like soils. These formulations provide mechanistic hypotheses for quantum effects in soil microenvironments, not direct soil-scale kinetic models.

5.7. Quantum Coherence in Enzyme Dynamics

Enzymatic reactions occur within highly structured protein environments that create favourable conditions for catalysis. In this context, quantum coherence refers to the temporary preservation of phase relationships between quantum states, allowing coordinated electron or proton movement during a reaction. Any potential coherence effects would occur within enzyme-defined catalytic energy landscapes, not independently of classical catalytic structure. In some biological systems, such as

photosynthetic complexes, coherence has been show to enhance energy transfer efficiency by enabling more organised exploration of reaction pathways (Wang et al., 2019).

Although soil enzymes operate in heterogeneous environments, coherence effects could operate at active-site level (Jeon et al., 2012). Many key soil enzymes including laccases, peroxidases, and phenol oxidases mediate multi-step electron transfer (Jeon et al., 2012) and proton-coupled electron transfer (PCET) reactions (Jeon et al., 2012). If coherence influences these dynamics, it could potentially modify charge-transfer organisation and catalytic efficiency under low-energy/redox-variable conditions.

Such effects would not replace classical kinetics but could contribute to modifications of effective rate constants through changes in charge-transfer organisation within enzyme-substrate complexes. In soils characterised by fluctuating moisture, temperature, and substrate availability, even small changes in catalytic coordination could influence decomposition dynamics under specific environmental constraints.

At present, direct experimental evidence for quantum coherence in soil enzymes remains limited. However, the structural and kinetic parallels between soil oxidoreductases and well-studied biological systems (Jones & Solomon., 2015) suggest that coherence-related mechanisms merit investigation. If demonstrated, these effects could refine mechanistic understanding of soil organic matter turnover.

5.8. Conceptual Framework: Linking Quantum Effects to Accelerated Soil Formation

Building on the preceding sections, this framework recognises that molecular-scale processes may contribute to soil formation pathways and should therefore be considered in modelling, assessment, and intervention strategies. Rather than replacing classical drivers of soil development, quantum-informed perspectives provide an additional mechanistic layer that may refine interpretation under specific microenvironmental conditions. Given ongoing anthropogenic pressures on soils (Chapter 3), we propose a generalised decision-support structure in which microscale process understanding supports context-specific and mechanistically informed

management pathways. Although Sections 5.4-5.7 examined mineral weathering and enzymatic decomposition as representative examples, the framework is designed to be generalisable across multiple soil-forming processes. The following subsections outline its core components (Fig. 42).

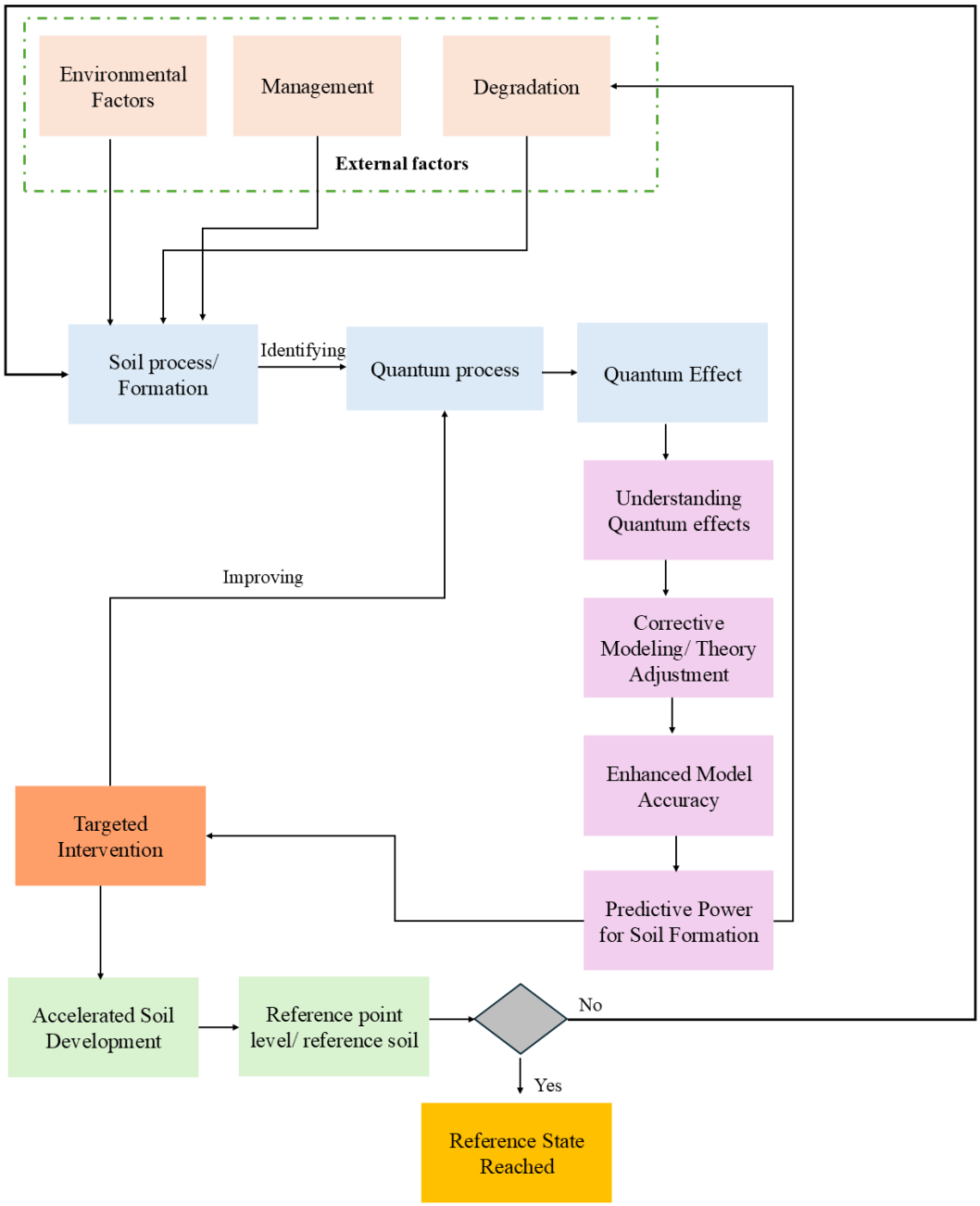

Fig 42. Conceptual framework integrating quantum processes into soil formation pathways. External drivers shape soil processes, where recognition of quantum-scale mechanisms supports mechanistic interpretation and targeted interventions. Quantum effects are represented as microscale modifiers of reaction kinetics within

environmental boundary conditions and do not override long-term climatic, geological, or environmental variability. Given the inherent uncertainty in long-term soil formation, quantum contributions are proposed to refine local mechanistic understanding under defined conditions, not to eliminate environmental noise or provide deterministic large-scale predictions.

5.8.1. External Drivers of Soil Processes

Soil formation is governed by environmental and management conditions including temperature, moisture regimes, land use practices, and degradation stressors such as erosion or salinity (He et al., 2009; Amundson, 2021). These factors influence both classical biogeochemical pathways and the microenvironmental boundary conditions under which molecular-scale reactions occur.

Cold or diffusion-limited settings may create circumstances where tunnelling contributions become kinetically relevant (Kästner, 2014), whereas disturbance, compaction, or structural degradation can disrupt the microzones that support organised redox cycling or enzymatic stability (Beylich et al., 2010). Management does not directly control quantum processes; rather, it modulates hydration states, redox gradients, enzyme distributions, and mineral interfaces that shape reaction energetics at the microscale.

5.8.2. Quantum Processes in Soil Systems: Identification and interpretive value

Persistent microbial and enzymatic function under constrained environmental settings motivates examination of mechanisms operating below the bulk scale (Gómez et al., 2020). At this scale, proton and electron tunnelling may influence charge transfer in enzymatic and mineral systems (Moser et al., 2010), while coherence effects have been observed in structured biological environments and proton-coupled electron transfer systems (Wang et al., 2019).

Direct measurement of such effects in intact soils remains challenging. Consequently, their possible relevance is inferred through diagnostic patterns such as deviations from classical Arrhenius behaviour, kinetic isotope effects, temperature-insensitive rates, and

consistency with quantum-informed simulations (e.g., QM/MM, DFT) (Truhlar et al., 1996; Acevedo & Jorgensen, 2010; Klinman, 2006; Kim et al., 2021), as outlined in Section 5.9.4.

Quantum-informed approaches are not intended to resolve the substantial uncertainties inherent in soil system modelling or to improve large-scale predictive accuracy. As demonstrated in erosion modelling (Govers, 2011), increasing mechanistic complexity does not automatically translate into improved predictions across space or time. Instead, the primary value of quantum-informed frameworks lies in mechanistic interpretation. However, by improving mechanistic understanding at the microscale, such frameworks may enhance context-dependent and scenario-based predictive insight under well-defined environmental and management conditions. Incorporating tunnelling-corrected kinetics and related quantum effects provides a more physically grounded framework for interpreting microscale processes such as enzymatic activity, redox cycling, mineral weathering, and SOC decomposition under low-energy conditions (Klinman & Kohen, 2013; Kim et al., 2021).

5.8.3. Targeted Interventions and Accelerated Soil Formation

Extending the interpretive framework above Section 5.8.3, this section outlines how quantum-relevant mechanisms can inform experimental design and management hypotheses. These interventions do not constitute new prescriptions; rather, they reinterpret established soil practices through a molecular-scale lens.

Microenvironmental factors including hydration films, redox gradients, enzyme density, and mineral-organic organisation strongly influences enzymatic and geochemical reaction pathways. Many conventional practices already modify these factors (Table 5). Recognising their potential molecular relevance allows these practices to be reframed as microenvironment-supportive strategies that may influence reaction efficiencies under particular conditions.

At present, such interventions should be viewed as hypothesis-generating guidance for experimental research and long-term management thinking. Direct empirical validation of quantum effects in soil systems remains limited and requires further investigation.

Table 5. Soil interventions that enhance quantum processes relevant to soil formation and restoration.

Intervention	How it Improves Soil	How it Enhances Quantum Processes
Organic amendments (e.g., compost, biochar)	Boosts microbial biomass and enzyme production (Guo, 2020).	High local enzyme concentrations can enhance the probability of proton tunnelling by optimizing substrate proximity and reducing activation barriers (Klinman & Kohen, 2013).
Moisture regulation (e.g., mulching, drip irrigation)	Improves microbial activity, nutrient diffusion, and aggregate formation (Zong et al., 2023).	Maintains hydration films supporting electron/proton coherence (Messori, 2019).
Mineral additives (e.g., basalt, wollastonite)	Promote nutrient release (Ribeiro et al., 2020).	Stimulates quantum-assisted bond breaking in weathering reactions (e.g., Si–O bonds in feldspars) (Xiao & Lasaga, 1994; Strandh et al., 1997b).
Microbial inoculation with redox-active species	Reestablishes functional microbial networks (Pidello & Monrozier, 2006).	Enhances tunnelling in redox enzyme cycles (e.g., laccase/peroxidase activity) (Xin et al., 2019).
Reducing disturbance (e.g., minimal tillage)	Preserves fungal communities, enzyme stability (Liu et al., 2023)	Protects structured microzones critical for quantum coherence.

5.8.4. Reference Soils

Reference soils (genosoils or benchmark soils) represent soil states typical of undisturbed, well-functioning ecosystems and provide comparative baselines for assessing soil condition and recovery (Alex. B. McBratney et al., 2019; Maharjan et al., 2020; Schram et al., 2024). Within the proposed framework (Fig. 42), reference soils define the endpoint against which managed or restored soils are evaluated.

From a mechanistic perspective, reference soils are characterised by stable structure and efficient functional performance, such as organic matter turnover and nutrient

cycling. Progress toward these reference conditions provides a practical criterion for evaluating whether soil formation pathways are moving toward long-term soil security.

5.9. Discussion

5.9.1 Limitations of Conventional Soil Indicators

Classic indicators of soil quality, health, and security, like SOC, aggregate stability, pH, and nutrient levels, continue to be utilised largely for assessing surface and bulk soil conditions (Carter, 2002; Lehmann et al., 2020). Although these parameters are indeed valuable, they report more on the consequences of soil processes while largely leaving unassessed the mechanisms driving the formation, transformation and resilience of soil.

Recent work by Ren et al., 2025 illustrates the quantum sensitivity of soil processes, showing that the quantum yields of soil-derived DOM associated with singlet oxygen, excited triplet states, and hydroxyl radicals vary systematically with mineral weathering and DOM composition across geographic gradients. Because of this variability, bulk soil pH, despite its widespread use may not adequately reflect underlying molecular-scale chemical reactivity, including processes with quantum sensitivity, particularly at soil-aquatic interfaces. Subatomic processes that may persist across a range of bulk pH conditions are therefore obscured by traditional indicators such as pH risk, which may not fully capture the complexity of underlying biochemical environments.

Beyond traditional soil measurements, new kinds of indicators and modelling techniques are needed to detect these quantum phenomena. Empirical evidence reinforces this gap. For example, (Koorneef et al., 2024) found that total SOC explained only 9% of the variation in functional soil indicators, with limited improvement even when SOC quality was included, particularly for microbial and nutrient cycling processes. Similarly, studies have shown that biological indicators, although promising, often fail to capture functional efficiency under stress or disturbance (Schoenholtz et al., 2000;Knoepp et al., 2000; Pulleman et al., 2012).

This discrepancy points to the need for complementary diagnostics that reflect molecular-scale mechanisms influencing soil processes. We emphasise that the following indicators are conceptual and research-oriented, intended to guide

mechanistic understanding and not to serve as routine field measurements, which may currently be accessible only through proxies or experimental approaches, including:

- Redox microheterogeneity (Dorau et al., 2024), which can be assessed using microelectrodes, redox-sensitive dyes, optodes, or spectroscopic techniques to resolve microscale electron-transfer environments.
- The stability of the hydration shell (Dragulet et al., 2022), currently explored primarily through molecular simulations and spectroscopic methods (e.g. neutron scattering, NMR, IR spectroscopy). While not directly measurable in intact field soils, hydration-shell stability may be indirectly inferred through water-mineral interaction proxies and modelling approaches.
- The efficiency of enzyme-substrate interactions (Yang et al., 2023), not as directly measured binding constants in soils, but inferred through microbial metabolic efficiency and enzymatic turnover proxies.

Although sophisticated methods like isotopic tracing, microelectrodes, or spectroscopic instruments can be used to evaluate some of these new molecular and quantum-sensitive metrics, these methods are still mostly limited to specialised research environments and are not yet incorporated into standard soil monitoring frameworks.

For broad-scale evaluation, classical indicators remain useful and practical. However, reliance on bulk measurements alone may limit insight into molecular-scale mechanisms operating within soils. Quantum-informed indicators are therefore proposed as complementary, research-oriented diagnostics to enhance mechanistic understanding alongside established monitoring tools.

5.9.2. Designing Interventions to Support Quantum Soil Processes

Quantum mechanical principles underlie all chemical reactions, including those occurring in soils. They become more apparent when classical pathways are constrained. The aim of quantum-informed soil management is not to create stress but to maintain microstructural and molecular conditions that sustain efficient reactions within natural energy and climate regimes.

Accelerating or sustaining soil formation, particularly under conditions where classical pathways are constrained, may benefit from targeted interventions that maintain microenvironments where molecular-scale reaction mechanisms, including quantum contributions, can operate efficiently. While mechanisms such as proton tunnelling and electron coherence are well-documented in biological systems (Kohen & Klinman, 1999; Marais et al., 2018), their expression in soils depends on specific physicochemical conditions.

These conditions include:

- Nanoscale water films and confinement, where hydrogen bonding networks may support tunnelling and coherence (Knight et al., 2019);
- Structured redox gradients, shaped by microbial metabolism and hydrologic variation (Zhang & Furman, 2021);
- Mineral and organic matter organisation, including clay surfaces that may facilitate electromagnetic oscillations relevant to coherence effects (Geesink et al., 2020).

Designing interventions that improve quantum-relevant conditions in soil systems becomes possible when these dependencies are understood. Some possible strategies are:

- Maintaining hydration films (e.g., through mulching or precision irrigation) to support coherent charge transfer.
- Enhancing enzyme-substrate coupling via microbial consortia or tailored organic amendments.
- Stabilizing redox gradients by leveraging plant–microbe interactions that support proton-coupled electron transfer (PCET).

While such interventions may overlap with conventional practices, the intentional targeting of microstructural and molecular environments differentiates them. Importantly, many widely adopted practices that improve surface-level metrics such as SOC or moisture do not always foster these deeper functional dynamics. In some cases,

they may alter microscale physicochemical conditions in way that could influence these processes Table 6.

This shift toward quantum-aware soil management becomes particularly relevant in degraded or slow-regenerating soils under environmental stress, where classical intervention strategies alone may be insufficient to explain or enhance observed soil formation dynamics. The next section outlines how this understanding can be operationalised into a decision-making framework for quantum-informed soil management.

Table 6. Conventional Soil Interventions and Potential Conflicts with Quantum-Process Optimisation

Intervention	Improved soil quality outcome	Reasons quantum processes may be disrupted
Heavy compost application	Increased SOC content (Baldi et al., 2018)	May induce anoxic conditions, disrupting redox enzyme pathways, (Wu et al., 2019; Zhu, Zhao, et al., 2024).
Irrigation in saline soils	Maintains soil moisture under stress when combined with drainage(Liu et al., 2024)	High ionic strength disrupts H-bond networks critical for tunnelling (DelloStritto et al., 2016).
Deep plowing	Alleviated soil compaction (Baumhardt et al., 2008)	Destroys fungal hyphal networks and structured microzones (Kabir, 2005), reducing coherence potential.

5.9.3. Integrating Quantum Thinking into Soil Management

Quantum-informed soil science combines theory with application to develop a complementary mechanistic approach for informing and refining strategies for land stewardship, as illustrated in the Fig.43, which demostrates compatibility with traditional methods under quantum-favourable micro-conditions.

The process begins with a common challenge in land systems: soil degradation or reduced formation rates. Traditional interventions, such as compost addition, mulching, or reduced tillage, are typically applied to improve bulk soil properties like structure, organic carbon content, and water retention. However, an essential question must follow: do these interventions also foster the microstructural environments relevant to quantum-scale contributions to mineral weathering, enzyme catalysis, or redox cycling?

If the response is negative, the intervention may still improve bulk soil properties, but its influence on specific molecular-scale processes may remain limited under certain conditions. In such cases, the management strategy must be adapted, for example, by adding redox-active microbial consortia, fine-tuning soil moisture to maintain hydration films, or using amendments that stimulate enzymatic efficiency. Once such modifications are effective, both classical and quantum mechanisms may contribute to sustaining soil formation.

Three conceptual shifts in soil management are central to this strategy:

- Greater consideration of molecular-sale quantities such as activation energies, electron transfers, enzyme mobility, hydration shells. Typically accessible through proxies, experimental studies, or modelling then the direct field measurement.
- Instead of concentrating solely on bulk soil properties, target interventions at quantum-enabling microenvironments (e.g. water films and organic-mineral interfaces).
- Integrate quantum- informed indicators into models and field trials to explore and test hypotheses about where quantum-scale contributions may influence soil processes.

Essentially, quantum-informed soil management expands mechanistic understanding and supports hypothesis-driven refinement of soil management strategies under changing environmental conditions. The development of quantum-informed field techniques and the careful scaling of these frameworks from experimental plots to landscape levels should be recognised as long-term research priorities, not immediate operational solutions.

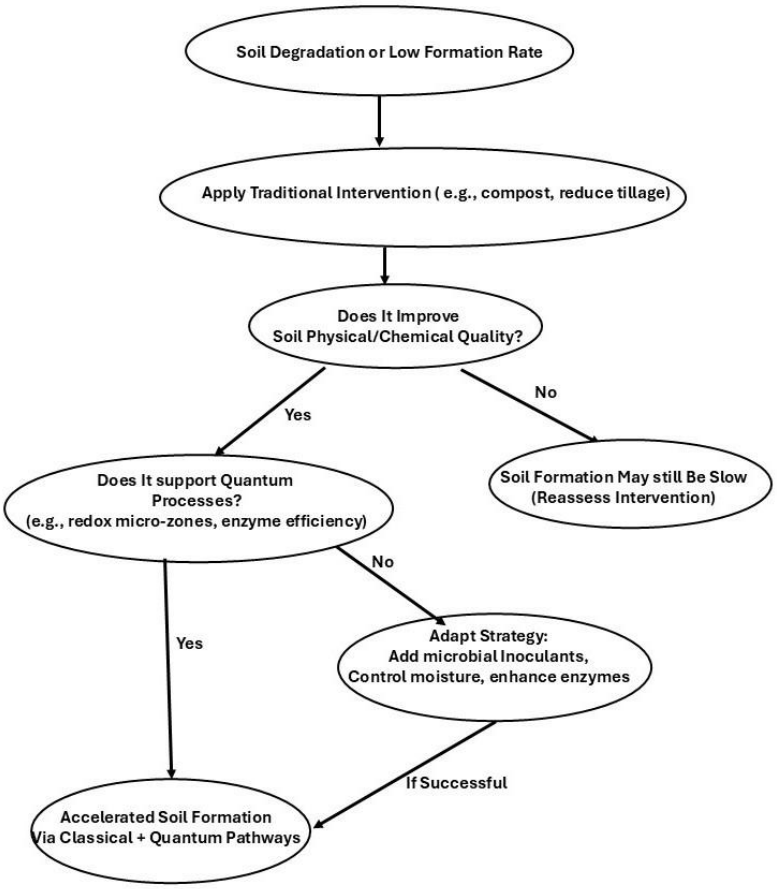

Fig 43. Decision pathway for integrating quantum process support into soil management interventions. Traditional improvements are evaluated for their ability to enhance quantum-relevant microenvironments, guiding adaptive strategies to accelerate soil formation via classical and quantum pathways.

5.9.4 Assessing Quantum Effects in Soil Systems

Quantum perspectives provide testable criteria for when tunnelling and nuclear effects become important in soil microbial and enzymatic reactions, particularly under low-temperature, low-energy, or diffusion-limited conditions. These concepts reframe observed biogeochemical deviations, such as non-Arrhenius temperature responses and unusually large kinetic isotope effects as potential signature of quantum modified energy landscape.

A falsifiable, method-driven framework is therefore required to diagnose quantum contributions in soils. This can couple targeted experimental diagnostics with quantum-corrected reaction modelling. Experimentally, candidate soil processes (e.g. extracellular oxidases, hydrolases, or redox enzymes bound to minerals) can be probed

using: (1) primary H/D and ^{13}C kinetic isotope effects, including temperature-dependent KIEs, as established probes of tunnelling in enzymes (Sutcliffe et al., 2006; Roston et al., 2014); (2) high-resolution temperature-response assays to detect curvature or plateaus in Arrhenius plots, beyond explanations such as denaturation (McLeod et al., 2025) (Kunze et al., 2014) ; and (3) microprofiling of redox and pH gradients using enzymatic microbiosensors to identify sub-millimeter zones where local conditions favour the tunnelling-ready configurations of soil enzymes (Mendes et al., 2024; De Smit et al., 2023). (4) ultrafast 2D IR spectroscopy of purified soil-derived enzymes or enzymes enzyme-mineral complexes at low temperatures, pending advances in mineral scattering mitigation. Under such controlled conditions, reduced decoherence rates may allow detection of vibrational coherence signals consistent with quantum effects beyond classical dephasing, as reported for hydrogenases (Hill et al., 2023; Wrathall et al., 2022). Quantum relevance is inferred when observables, such as temperature-independent KIEs or strong non-Arrhenius trends systematically deviate from classical predictions.

On the modelling side, variational transition state theory with tunnelling corrections (e.g., small-curvature tunnelling) applied to QM/MM- or DFT-derived reaction paths provides a practical route to estimate transmission coefficients and reproduce measured KIEs for soil-relevant enzymes (Soler et al., 2020; Pu et al., 2006). Path integral approaches, while more demanding, provide a robust framework to quantify nuclear quantum effects in complex catalysts (Wang et al., 2016; Vardi-Kilshtain et al., 2015). When extended to mineral-water-enzyme interfaces and constrained by soil-like hydration, crowding, and mineral surface structures, these models allow direct comparison between classical and quantum-corrected rate predictions under environmentally realistic conditions.

This integrated experimental-theoretical pathway offers a concrete route forward: (1) use enzyme assays and microprofiling to flag candidate systems exhibiting anomalous temperature or isotope behaviour; (2) construct simplified enzyme-substrate-mineral models; and (3) apply tunnelling-corrected QM/MM methods to test whether quantum-enabled mechanisms better reproduce the data than classical kinetics. Progress is feasible in controlled experimental systems using established tools from enzymology and quantum chemistry.

At the applied level, a more quantitative Quantum Soil Science could, if supported by empirical validation, inform soil restoration strategies that exploit quantum-favourable microenvironments defined by specific moisture, redox, or mineralogical conditions to stabilise organic matter, enhance nutrient cycling, and improve forecasts of soil responses to environmental stress.

5.10. Conclusion

This thesis introduces Quantum Soil Science as an emerging conceptual direction that invites reconsideration of how fundamental soil processes are interpreted. We suggest that subatomic phenomena such as proton tunnelling, electron coherence, and quantum-assisted bond transformations may contribute to key soil processes in ways that complement, and potentially extend, classical descriptions.

Traditional thermodynamic and kinetic models remain foundational to soil science. However, through careful understanding of mineral weathering and enzymatic decomposition this research proposes that incorporating quantum-scale considerations may refine mechanistic understanding under certain microenvironmental conditions. Quantum-informed perspectives thus sit alongside classical approaches, extending the framework available for interpreting soil dynamics across diverse environmental contexts.

Building upon these observations, we propose a conceptual framework that articulates the relationship between quantum-level phenomena, soil formation processes, and soil function. This framework envisions a shift in emphasis from purely bulk-scale management toward consideration of molecular and energetic foundations. It discusses how targeted interventions such as maintaining hydration shells, stabilising redox microenvironments, and optimising enzyme-substrate interactions can foster microconditions favourable to quantum activity, thereby offering a potential pathway for enhancing soil regeneration and resilience.

The paper also discusses the important limitations in conventional soil indicators. Practical, standard metrics such as pH, SOC, and aggregate stability may not capture the biochemical and energetic complexity governed by quantum processes. To fill this gap, we support the development of quantum-informed indicators of redox

microheterogeneity, hydration shell integrity, and enzyme binding efficiency, supported by advanced analytical techniques such as isotopic tracing and high-resolution spectroscopy.

Looking ahead, this study calls for greater integration of quantum chemistry, molecular biophysics, and soil biogeochemistry within soil science. A falsifiable experimental–modelling pathway, combining isotope effects, temperature diagnostics, and quantum-corrected rate modelling, provides a structured approach for evaluating potential quantum contributions.

5.11. References

Acevedo, O., & Jorgensen, W. L. (2010). Advances in Quantum and Molecular Mechanical (QM/MM) Simulations for Organic and Enzymatic Reactions. Accounts of Chemical Research, 43(1), 142–151. https://doi.org/10.1021/ar900171c

Adhikari, K., & Hartemink, A. E. (2016). Linking soils to ecosystem services—A global review. Geoderma, 262, 101–111. https://doi.org/10.1016/j.geoderma.2015.08.009

Ali, R. S., Kandeler, E., Marhan, S., Demyan, M. S., Ingwersen, J., Mirzaeitalarposhti, R., Rasche, F., Cadisch, G., & Poll, C. (2018). Controls on microbially regulated soil organic carbon decomposition at the regional scale. Soil Biology and Biochemistry, 118, 59–68. https://doi.org/10.1016/j.soilbio.2017.12.007

Amundson, R. (2021). Factors of soil formation in the 21st century. Geoderma, 391, 114960. https://doi.org/10.1016/j.geoderma.2021.114960

Baldi, E., Cavani, L., Margon, A., Quartieri, M., Sorrenti, G., Marzadori, C., & Toselli, M. (2018). Effect of compost application on the dynamics of carbon in a nectarine orchard ecosystem. Science of The Total Environment, 637–638, 918–925. https://doi.org/10.1016/j.scitotenv.2018.05.093

Banning, N. C., Grant, C. D., Jones, D. L., & Murphy, D. V. (2008). Recovery of soil organic matter, organic matter turnover and nitrogen cycling in a post-mining forest rehabilitation chronosequence. Soil Biology and Biochemistry, 40(8), 2021–2031. https://doi.org/10.1016/j.soilbio.2008.04.010

Baumhardt, R. L., Jones, O. R., & Schwartz, R. C. (2008). Long-Term Effects of Profile-Modifying Deep Plowing on Soil Properties and Crop Yield. Soil Science Society of America Journal, 72(3), 677–682. https://doi.org/10.2136/sssaj2007.0122

Baldrian, P. (2006). Fungal laccases – occurrence and properties. FEMS Microbiology Reviews, 30(2), 215–242. https://doi.org/10.1111/j.1574-4976.2005.00010.x

Benderskii, V. A., Goldanskii, V. I., & Makarov, D. E. (1993). Quantum dynamics in low-temperature chemistry. Physics Reports, 233(4–5), 195–339. https://doi.org/10.1016/0370-1573(93)90136-2

Beylich, A., Oberholzer, H.-R., Schrader, S., Höper, H., & Wilke, B.-M. (2010). Evaluation of soil compaction effects on soil biota and soil biological processes in soils. Soil and Tillage Research, 109(2), 133–143. https://doi.org/10.1016/j.still.2010.05.010

Cama, J., Ayora, C., & Lasaga, A. C. (1999). The deviation-from-equilibrium effect on dissolution rate and on apparent variations in activation energy. Geochimica et Cosmochimica Acta, 63(17), 2481–2486. https://doi.org/10.1016/S0016-7037(99)00144-1

Carter, M. R. (2002). Soil Quality for Sustainable Land Management: Organic Matter and Aggregation Interactions that Maintain Soil Functions. Agronomy Journal, 94(1), 38–47. https://doi.org/10.2134/agronj2002.3800

Chen, Y., Chen, G., Robinson, D., Yang, Z., Guo, J., Xie, J., Fu, S., Zhou, L., & Yang, Y. (2016). Large amounts of easily decomposable carbon stored in subtropical forest subsoil are associated with r-strategy-dominated soil microbes. Soil Biology and Biochemistry, 95, 233–242. https://doi.org/10.1016/j.soilbio.2016.01.004

Chen, Z., Zheng, J., Truhlar, D. G., & Yang, Y. (2025). Constrained Nuclear-Electronic Orbital Transition State Theory Using Energy Surfaces with Nuclear Quantum Effects. Journal of Chemical Theory and Computation, 21(2), 590–604. https://doi.org/10.1021/acs.jctc.4c01521

Cronan, C. S. (2018). Ecosystem Biogeochemistry. Springer International Publishing. https://doi.org/10.1007/978-3-319-66444-6

Cotrufo, M. F., & Lavallee, J. M. (2022). Soil organic matter formation, persistence, and functioning: A synthesis of current understanding to inform its conservation and regeneration. In Advances in Agronomy (Vol. 172, pp. 1–66). Elsevier. https://doi.org/10.1016/bs.agron.2021.11.002

Davidson, E. A., Samanta, S., Caramori, S. S., & Savage, K. (2012). The D ual A rrhenius and M ichaelis– M enten kinetics model for decomposition of soil organic matter at hourly to seasonal time scales. Global Change Biology, 18(1), 371–384. https://doi.org/10.1111/j.1365-2486.2011.02546.x

DelloStritto, M. J., Kubicki, J. D., & Sofo, J. O. (2016). Effect of Ions on H-Bond Structure and Dynamics at the Quartz(101)–Water Interface. Langmuir, 32(44), 11353–11365. https://doi.org/10.1021/acs.langmuir.6b01719

Deng, K., Yang, S., & Guo, Y. (2022). A global temperature control of silicate weathering intensity. Nature Communications, 13(1), 1781. https://doi.org/10.1038/s41467-022-29415-0

De Smit, S. M., Langedijk, J. J. H., Van Haalen, L. C. A., Lin, S. H., Bitter, J. H., & Strik, D. P. B. T. B. (2023). Methodology for In Situ Microsensor Profiling of Hydrogen, pH, Oxidation–Reduction Potential, and Electric Potential throughout Three-Dimensional Porous Cathodes of (Bio) Electrochemical Systems. Analytical Chemistry, 95(5), 2680–2689. https://doi.org/10.1021/acs.analchem.2c03121

Devault, D. (1980). Quantum mechanical tunnelling in biological systems. Quarterly Reviews of Biophysics, 13(04), 387. https://doi.org/10.1017/S003358350000175X

Dominati, E., Patterson, M., & Mackay, A. (2010). A framework for classifying and quantifying the natural capital and ecosystem services of soils. Ecological Economics, 69(9), 1858–1868. https://doi.org/10.1016/j.ecolecon.2010.05.002

Dorau, K., Zanger, T., Bolten, A., & Mansfeldt, T. (2024). Soil redox maps: Assessment of small field-scale redox zonation by Mn and Fe oxide-coated IRIS films. Journal of Soils and Sediments, 24(3), 1206–1219. https://doi.org/10.1007/s11368-023-03705-6

Dragulet, F., Goyal, A., Ioannidou, K., Pellenq, R. J.-M., & Del Gado, E. (2022). Ion Specificity of Confined Ion–Water Structuring and Nanoscale Surface Forces in Clays. The Journal of Physical Chemistry B, 126(26), 4977–4989. https://doi.org/10.1021/acs.jpcb.2c01738

Duan, L., Hao, J., Xie, S., Zhou, Z., & Ye, X. (2002). Determining weathering rates of soils in China. Geoderma, 110(3–4), 205–225. https://doi.org/10.1016/S0016-7061(02)00231-8

Fleming, G. R., Scholes, G. D., & Cheng, Y.-C. (2011). Quantum effects in biology. Procedia Chemistry, 3(1), 38–57. https://doi.org/10.1016/j.proche.2011.08.011

Geesink, H., Meijer, D., & Jerman, I. (2020). Clay minerals: Information network linking quantum coherence and first life.

Guo, X. (2020). The role of biochar in organic waste composting and soil improvement: A review. Waste Management.

Govers, G. (2011). Misapplications and Misconceptions of Erosion Models.

He, X., Bao, Y., Nan, H., Xiong, D., Wang, L., Liu, Y., & Zhao, J. (2009). Tillage pedogenesis of purple soils in southwestern China. Journal of Mountain Science, 6(2), 205–210. https://doi.org/10.1007/s11629-009-1038-y

Hill, T. D., Basnet, S., Lepird, H. H., Rightnowar, B. W., & Moran, S. D. (2023). Anisotropic dynamics of an interfacial enzyme active site observed using tethered substrate analogs and ultrafast 2D IR spectroscopy. The Journal of Chemical Physics, 159(16), 165101. https://doi.org/10.1063/5.0167991

Heřmanská, M. (2023). A comprehensive and consistent mineral dissolution rate database: Part II: Secondary silicate minerals. Chemical Geology.

Hunakunti, A., McBratney, A., & Minasny, B. (2025). Towards soil security: Understanding soil erosion footprints and their implications in NSW. Soil Security, 19, 100184. https://doi.org/10.1016/j.soisec.2025.100184

Jara, G. E., Pontiggia, F., Otten, R., Agafonov, R. V., Martí, M. A., & Kern, D. (2025). Wide transition-state ensemble as key component for enzyme catalysis. eLife, 12, RP93099. https://doi.org/10.7554/eLife.93099

Jeon, J., Baldrian, P., Murugesan, K., & Chang, Y. (2012). Laccase-catalysed oxidations of naturally occurring phenols: From in vivo biosynthetic pathways to green synthetic applications. Microbial Biotechnology, 5(3), 318–332. https://doi.org/10.1111/j.1751-7915.2011.00273.x

Johnson, K. A., & Goody, R. S. (2011). The Original Michaelis Constant: Translation of the 1913 Michaelis–Menten Paper. Biochemistry, 50(39), 8264–8269. https://doi.org/10.1021/bi201284u

Joseph, S., Husson, O., Graber, E., Van Zwieten, L., Taherymoosavi, S., Thomas, T., Nielsen, S., Ye, J., Pan, G., Chia, C., Munroe, P., Allen, J., Lin, Y., Fan, X., & Donne, S. (2015). The Electrochemical Properties of Biochars and How They Affect Soil Redox Properties and Processes. Agronomy, 5(3), 322–340. https://doi.org/10.3390/agronomy5030322

Jones, S. M., & Solomon, E. I. (2015). Electron transfer and reaction mechanism of laccases.

Kabir, Z. (2005). Tillage or no-tillage: Impact on mycorrhizae. Canadian Journal of Plant Science, 85(1), 23–29. https://doi.org/10.4141/P03-160

Kästner, J. (2014). Theory and simulation of atom tunneling in chemical reactions. WIREs Computational Molecular Science, 4(2), 158–168. https://doi.org/10.1002/wcms.1165

Kim, Y., Bertagna, F., D'Souza, E. M., Heyes, D. J., Johannissen, L. O., Nery, E. T., Pantelias, A., Sanchez-Pedreño Jimenez, A., Slocombe, L., Spencer, M. G., Al-Khalili, J., Engel, G. S., Hay, S., Hingley-Wilson, S. M., Jeevaratnam, K., Jones, A. R., Kattnig, D. R., Lewis, R., Sacchi, M., … McFadden, J. (2021). Quantum Biology: An Update and Perspective. Quantum Reports, 3(1), 80–126. https://doi.org/10.3390/quantum3010006

Klinman, J. P. (2006). Linking protein structure and dynamics to catalysis: The role of hydrogen tunnelling. Philosophical Transactions of the Royal Society B: Biological Sciences, 361(1472), 1323–1331. https://doi.org/10.1098/rstb.2006.1870

Klinman, J. P., & Kohen, A. (2013). Hydrogen Tunneling Links Protein Dynamics to Enzyme Catalysis. Annual Review of Biochemistry, 82(1), 471–496. https://doi.org/10.1146/annurev-biochem-051710-133623

Knight, A. W., Kalugin, N. G., Coker, E., & Ilgen, A. G. (2019). Water properties under nano-scale confinement. Scientific Reports, 9(1), 8246. https://doi.org/10.1038/s41598-019-44651-z

Knoepp, J. D., Coleman, D. C., Crossley, D. A., & Clark, J. S. (2000). Biological indices of soil quality: An ecosystem case study of their use. Forest Ecology and Management, 138(1–3), 357–368. https://doi.org/10.1016/S0378-1127(00)00424-2

Kohen, A., & Klinman, J. P. (1999). Hydrogen tunneling in biology. Chemistry & Biology, 6(7), R191–R198. https://doi.org/10.1016/S1074-5521(99)80058-1

Koorneef, G. J., Pulleman, M. M., Comans, R. Nj., Van Rijssel, S. Q., Barré, P., Baudin, F., & De Goede, R. Gm. (2024). Assessing soil functioning: What is the added value of soil organic carbon quality measurements alongside total organic carbon content? Soil Biology and Biochemistry, 196, 109507. https://doi.org/10.1016/j.soilbio.2024.109507

Kubicki, J. D., Sofo, J. O., Skelton, A. A., & Bandura, A. V. (2012). A New Hypothesis for the Dissolution Mechanism of Silicates. The Journal of Physical Chemistry C, 116(33), 17479–17491. https://doi.org/10.1021/jp300623v

Kunze, M., Lattermann, C., Diederichs, S., Kroutil, W., & Büchs, J. (2014). Minireactor-based high-throughput temperature profiling for the optimization of microbial and enzymatic processes. Journal of Biological Engineering, 8(1), 22. https://doi.org/10.1186/1754-1611-8-22

Kumar, D., Gupta, S., Hasan, W., Hussain, B., Ansari, M. J., & Singh, S. (2024). Rhizosphere Revolution: Unveiling the Secrets of Insect Pheromones in Soil Health and Vermicompost Production (1st ed.). CRC Press. https://doi.org/10.1201/9781003570295

la Cecilia, D., Riley, W.J. and Maggi, F. (2019). Biochemical modeling of microbial memory effects and catabolite repression on soil organic carbon compounds. Soil Biology and Biochemistry, 128, pp.1-12.

Lehmann, J., Bossio, D. A., Kögel-Knabner, I., & Rillig, M. C. (2020). The concept and future prospects of soil health. Nature Reviews Earth & Environment, 1(10), 544–553. https://doi.org/10.1038/s43017-020-0080-8

Leifeld, J., & Von Lützow, M. (2014). Chemical and microbial activation energies of soil organic matter decomposition. Biology and Fertility of Soils, 50(1), 147–153. https://doi.org/10.1007/s00374-013-0822-6

Li, D., Fan, J., Zhang, X., Xu, X., He, N., Wen, X., Sun, X., Blagodatskaya, E., & Kuzyakov, Y. (2017). Hydrolase kinetics to detect temperature-related changes in the rates of soil organic matter decomposition. European Journal of Soil Biology, 81, 108–115. https://doi.org/10.1016/j.ejsobi.2016.10.004

Li, Q., Wang, L., Fu, Y., Lin, D., Hou, M., Li, X., Hu, D., & Wang, Z. (2023). Transformation of soil organic matter subjected to environmental disturbance and preservation of organic matter bound to soil minerals: A review. Journal of Soils and Sediments, 23(3), 1485–1500. https://doi.org/10.1007/s11368-022-03381-y

Lin, H. (2011). Three Principles of Soil Change and Pedogenesis in Time and Space. Soil Science Society of America Journal, 75(6), 2049–2070. https://doi.org/10.2136/sssaj2011.0130

Liu, W.-S., Wei, Y.-X., Deng, P.-P., Oladele, O. P., N'Dri Bohoussou, Y., Dang, Y. P., Zhao, X., & Zhang, H.-L. (2023). Conservation tillage increases surface soil organic carbon stock by altering fungal communities and enzyme activity. Environmental Science and Pollution Research, 30(33), 80901–80915. https://doi.org/10.1007/s11356-023-28062-2

Liu, X., Tou, C., Zhou, J., Chen, J., Wanek, W., Chadwick, D. R., Jones, D. L., Wu, L., & Ma, Q. (2025). Plant litter decomposition is regulated by its phosphorus content in the short term and soil enzymes in the long term. Geoderma, 457, 117283. https://doi.org/10.1016/j.geoderma.2025.117283

Liu, Y., Hu, Y., Wei, C., Zeng, W., Huang, J., & Ao, C. (2024). Synergistic regulation of irrigation and drainage based on crop salt tolerance and leaching threshold. Agricultural Water Management, 292, 108679. https://doi.org/10.1016/j.agwat.2024.108679

Lloyd, S. (2011). Quantum coherence in biological systems. Journal of Physics: Conference Series, 302, 012037. https://doi.org/10.1088/1742-6596/302/1/012037

Maharjan, B., Das, S., & Acharya, B. S. (2020). Soil Health Gap: A concept to establish a benchmark for soil health management. Global Ecology and Conservation, 23, e01116. https://doi.org/10.1016/j.gecco.2020.e01116

Marais, A., Adams, B., Ringsmuth, A. K., Ferretti, M., Gruber, J. M., Hendrikx, R., Schuld, M., Smith, S. L., Sinayskiy, I., Krüger, T. P. J., Petruccione, F., & Van Grondelle, R. (2018). The future of quantum biology. Journal of The Royal Society Interface, 15(148), 20180640. https://doi.org/10.1098/rsif.2018.0640

McBratney, A., Field, D. J., & Koch, A. (2014). The dimensions of soil security. Geoderma, 213, 203–213. https://doi.org/10.1016/j.geoderma.2013.08.013

McBratney, Alex. B., Field, D., Morgan, C. L. S., & Huang, J. (2019). On Soil Capability, Capacity, and Condition. Sustainability, 11(12), 3350. https://doi.org/10.3390/su11123350

McMahon, R. J. (2003). Chemical Reactions Involving Quantum Tunneling. Science, 299(5608), 833–834. https://doi.org/10.1126/science.1080715

McLeod, M. J. (n.d.). A structural perspective on the temperature dependent activity of enzymes.

Meisner, J., & Kästner, J. (2016). Atom Tunneling in Chemistry. Angewandte Chemie International Edition, 55(18), 5400–5413. https://doi.org/10.1002/anie.201511028

Mendez, J. C., Hiemstra, T., & Koopmans, G. F. (2020). Assessing the Reactive Surface Area of Soils and the Association of Soil Organic Carbon with Natural Oxide Nanoparticles Using Ferrihydrite as Proxy. Environmental Science & Technology, 54(19), 11990–12000. https://doi.org/10.1021/acs.est.0c02163

Mendes, B., Brissos, V., Martins, L. O., & Conzuelo, F. (2024). Enzyme-Modified Microelectrode for Simultaneous Local Measurements of O2 and pH. Analytical Chemistry, 96(41), 16244–16251. https://doi.org/10.1021/acs.analchem.4c03150

Messori, C. (2019). Deep into the Water: Exploring the Hydro-Electromagnetic and Quantum-Electrodynamic Properties of Interfacial Water in Living Systems. OALib, 06(05), 1–50. https://doi.org/10.4236/oalib.1105435

Moser, C. C., Anderson, J. L. R., & Dutton, P. L. (2010). Guidelines for tunneling in enzymes. Biochimica et Biophysica Acta (BBA) - Bioenergetics, 1797(9), 1573–1586. https://doi.org/10.1016/j.bbabio.2010.04.441

Nannipieri, P., Landi, L., Giagnoni, L., & Renella, G. (2011). Past, Present and Future in Soil Enzymology. In C. Trasar-Cepeda, T. Hernández, C. García, C. Rad, & S. González-Carcedo (Eds.), Soil Enzymology in the Recycling of Organic Wastes and Environmental Restoration (pp. 1–17). Springer Berlin Heidelberg. https://doi.org/10.1007/978-3-642-21162-1_1

Opolot, E., & Finke, P. A. (2015). Evaluating sensitivity of silicate mineral dissolution rates to physical weathering using a soil evolution model (SoilGen2.25). Biogeosciences, 12(22), 6791–6808. https://doi.org/10.5194/bg-12-6791-2015

Palansooriya, K. N., Wong, J. T. F., Hashimoto, Y., Huang, L., Rinklebe, J., Chang, S. X., Bolan, N., Wang, H., & Ok, Y. S. (2019). Response of microbial communities to biochar-amended soils: A critical review. Biochar, 1(1), 3–22. https://doi.org/10.1007/s42773-019-00009-2

Parry, S. A., Hodson, M. E., Kemp, S. J., & Oelkers, E. H. (2015). The surface area and reactivity of granitic soils: I. Dissolution rates of primary minerals as a function of depth and age deduced from field observations. Geoderma, 237–238, 21–35. https://doi.org/10.1016/j.geoderma.2014.08.004

Pidello, A., & Monrozier, L. J. (2006). Inoculation of the redox effector Pseudomonas fluorescens C7R12 strain affects soil redox status at the aggregate scale. Soil Biology and Biochemistry, 38(6), 1396–1402. https://doi.org/10.1016/j.soilbio.2005.10.010

Pot, V., Gerke, K. M., Ebrahimi, A., Garnier, P., & Baveye, P. C. (2021). Editorial: Microscale Modelling of Soil Processes: Recent Advances, Challenges, and the Path Ahead. Frontiers in Environmental Science, 9, 818038. https://doi.org/10.3389/fenvs.2021.818038

Ptáček, P., Šoukal, F., & Opravil, T. (2018). Introduction to the Transition State Theory. In P. Ptáček, T. Opravil, & F. Šoukal (Eds.), Introducing the Effective Mass of Activated Complex and the Discussion on the Wave Function of this Instanton. InTech. https://doi.org/10.5772/intechopen.78705

Pulleman, M., Creamer, R., Hamer, U., Helder, J., Pelosi, C., Pérès, G., & Rutgers, M. (2012). Soil biodiversity, biological indicators and soil ecosystem services—An overview of European approaches. Current Opinion in Environmental Sustainability, 4(5), 529–538. https://doi.org/10.1016/j.cosust.2012.10.009

Pu, J., Gao, J., & Truhlar, D. G. (2006). Multidimensional Tunneling, Recrossing, and the Transmission Coefficient for Enzymatic Reactions. Chemical Reviews, 106(8), 3140–3169. https://doi.org/10.1021/cr050308e

Qi, R., Li, J., Lin, Z., Li, Z., Li, Y., Yang, X., Zhang, J., & Zhao, B. (2016). Temperature effects on soil organic carbon, soil labile organic carbon fractions, and soil enzyme activities under long-term fertilization regimes. Applied Soil Ecology, 102, 36–45. https://doi.org/10.1016/j.apsoil.2016.02.004

Ren, D., Yang, B., Wang, Y., & Wang, J. (2025). Molecular-level insight into the role of soil-derived dissolved organic matter composition in regulating photochemical reactivity. Water Research, 268, 122765. https://doi.org/10.1016/j.watres.2024.122765

Ribeiro, I. D. A., Volpiano, C. G., Vargas, L. K., Granada, C. E., Lisboa, B. B., & Passaglia, L. M. P. (2020). Use of Mineral Weathering Bacteria to Enhance Nutrient Availability in Crops: A Review. Frontiers in Plant Science, 11, 590774. https://doi.org/10.3389/fpls.2020.590774

Roston, D., Islam, Z., & Kohen, A. (2014). Kinetic isotope effects as a probe of hydrogen transfers to and from common enzymatic cofactors. Archives of Biochemistry and Biophysics, 544, 96–104. https://doi.org/10.1016/j.abb.2013.10.010

Schimel, J. (2003). The implications of exoenzyme activity on microbial carbon and nitrogen limitation in soil: A theoretical model. Soil Biology and Biochemistry, 35(4), 549–563. https://doi.org/10.1016/S0038-0717(03)00015-4

Schoenholtz, S. H., Miegroet, H. V., & Burger, J. A. (2000). A review of chemical and physical properties as indicators of forest soil quality: Challenges and opportunities. Forest Ecology and Management, 138(1–3), 335–356. https://doi.org/10.1016/S0378-1127(00)00423-0

Schram, M., Wubs, E. R. J., & Van Der Putten, W. H. (2024). Benchmarking for soil health improvement. One Earth, 7(12), 2099–2102. https://doi.org/10.1016/j.oneear.2024.11.015

Schreiner, P. R. (2020). Quantum Mechanical Tunneling Is Essential to Understanding Chemical Reactivity. Trends in Chemistry, 2(11), 980–989. https://doi.org/10.1016/j.trechm.2020.08.006

Serrano-Grijalva, L., Van Der Putten, W. H., Ochoa-Hueso, R., Margenot, A. J., Van Rijssel, S. Q., Koorneef, G. J., & Veen, G. F. (Ciska). (2024). Soil extracellular enzyme activity increases during the transition from conventional to organic farming. Agriculture, Ecosystems & Environment, 375, 109202. https://doi.org/10.1016/j.agee.2024.109202

Shan, C., Wang, M., Yang, Y., Shen, F., Ji, L., & Yang, L. (2024). Microbial carbon and nitrogen limitation in Larix gmelinii forests along an altitudinal gradient: Evidence from ecoenzymatic stoichiometry and vector analysis. Applied Soil Ecology, 195, 105257. https://doi.org/10.1016/j.apsoil.2023.105257

Shi, L., Dong, H., Reguera, G., Beyenal, H., Lu, A., Liu, J., Yu, H.-Q., & Fredrickson, J. K. (2016). Extracellular electron transfer mechanisms between microorganisms and minerals. Nature Reviews Microbiology, 14(10), 651–662. https://doi.org/10.1038/nrmicro.2016.93

Sinsabaugh, R. L. (2010). Phenol oxidase, peroxidase and organic matter dynamics of soil. Soil Biology and Biochemistry, 42(3), 391–404. https://doi.org/10.1016/j.soilbio.2009.10.014

Sousa, S. F., Ribeiro, A. J. M., Neves, R. P. P., Brás, N. F., Cerqueira, N. M. F. S. A., Fernandes, P. A., & Ramos, M. J. (2017). Application of quantum mechanics/molecular mechanics methods in the study of enzymatic reaction mechanisms. WIREs Computational Molecular Science, 7(2), e1281. https://doi.org/10.1002/wcms.1281

Soler, J., González-Lafont, À., & Lluch, J. M. (2020). A protocol to obtain multidimensional quantum tunneling corrections derived from QM(DFT)/MM calculations for an enzyme reaction. Physical Chemistry Chemical Physics, 22(46), 27385–27393. https://doi.org/10.1039/D0CP05265E

Strandh, H., Pettersson, L. G. M., Sjöberg, L., & Wahlgren, U. (1997a). Quantum chemical studies of the effects on silicate mineral dissolution rates by adsorption of alkali metals. Geochimica et Cosmochimica Acta, 61(13), 2577–2587. https://doi.org/10.1016/S0016-7037(97)00118-X

Strandh, H., Pettersson, L. G. M., Sjöberg, L., & Wahlgren, U. (1997b). Quantum chemical studies of the effects on silicate mineral dissolution rates by adsorption of alkali metals. Geochimica et Cosmochimica Acta, 61(13), 2577–2587. https://doi.org/10.1016/S0016-7037(97)00118-X

Sverdrup, H., & Warfvinge, P. (1988). Weathering of primary silicate minerals in the natural soil environment in relation to a chemical weathering model. Water, Air, and Soil Pollution, 38(3–4), 387–408. https://doi.org/10.1007/BF00280768

Sutcliffe, M. J., Masgrau, L., Roujeinikova, A., Johannissen, L. O., Hothi, P., Basran, J., Ranaghan, K. E., Mulholland, A. J., Leys, D., & Scrutton, N. S. (2006). Hydrogen tunnelling in enzyme-catalysed H-transfer reactions: Flavoprotein and quinoprotein systems. Philosophical Transactions of the Royal Society B: Biological Sciences, 361(1472), 1375–1386. https://doi.org/10.1098/rstb.2006.1878

Targulian, V. O., & Krasilnikov, P. V. (2007). Soil system and pedogenic processes: Self-organization, time scales, and environmental significance. CATENA, 71(3), 373–381. https://doi.org/10.1016/j.catena.2007.03.007

Truhlar, D. G., Gao, J., Alhambra, C., Garcia-Viloca, M., Corchado, J., Sánchez, M. L., & Villà, J. (2002). The Incorporation of Quantum Effects in Enzyme Kinetics Modeling. Accounts of Chemical Research, 35(6), 341–349. https://doi.org/10.1021/ar0100226

Truhlar, D. G., Garrett, B. C., & Klippenstein, S. J. (1996). Current Status of Transition-State Theory. The Journal of Physical Chemistry, 100(31), 12771–12800. https://doi.org/10.1021/jp953748q

Vardi-Kilshtain, A., Nitoker, N., & Major, D. T. (2015). Nuclear quantum effects and kinetic isotope effects in enzyme reactions. Archives of Biochemistry and Biophysics, 582, 18–27. https://doi.org/10.1016/j.abb.2015.03.001

Velbel, M. A. (1990). Influence of Temperature and Mineral Surface Characteristics on Feldspar Weathering Rates in Natural and Artificial Systems: A First Approximation. Water Resources Research, 26(12), 3049–3053. https://doi.org/10.1029/WR026i012p03049

Vereecken, H., Schnepf, A., Hopmans, J. W., Javaux, M., Or, D., Roose, T., Vanderborght, J., Young, M. H., Amelung, W., Aitkenhead, M., Allison, S. D., Assouline, S., Baveye, P., Berli, M., Brüggemann, N., Finke, P., Flury, M., Gaiser, T., Govers, G., … Young, I. M. (2016). Modeling Soil Processes: Review, Key Challenges, and New Perspectives. Vadose Zone Journal, 15(5), 1–57. https://doi.org/10.2136/vzj2015.09.0131

Wang, B., & Allison, S. D. (2019). Emergent properties of organic matter decomposition by soil enzymes. Soil Biology and Biochemistry, 136, 107522. https://doi.org/10.1016/j.soilbio.2019.107522

Wang, G., Post, W. M., & Mayes, M. A. (2013a). Development of microbial-enzyme-mediated decomposition model parameters through steady-state and dynamic analyses. Ecological Applications, 23(1), 255–272. https://doi.org/10.1890/12-0681.1

Wang, G., Post, W. M., & Mayes, M. A. (2013b). Development of microbial-enzyme-mediated decomposition model parameters through steady-state and dynamic analyses. Ecological Applications, 23(1), 255–272. https://doi.org/10.1890/12-0681.1

Wang, L., Isborn, C. M., & Markland, T. E. (2016). Simulating Nuclear and Electronic Quantum Effects in Enzymes. In Methods in Enzymology (Vol. 577, pp. 389–418). Elsevier. https://doi.org/10.1016/bs.mie.2016.05.047

Wang, L., Allodi, M. A., & Engel, G. S. (2019). Quantum coherences reveal excited-state dynamics in biophysical systems. Nature Reviews Chemistry, 3(8), 477–490. https://doi.org/10.1038/s41570-019-0109-z

Wu, J.-H., Chen, W.-Y., Kuo, H.-C., & Li, Y.-M. (2019). Redox fluctuations shape the soil microbiome in the hypoxic bioremediation of octachlorinated dibenzodioxin- and dibenzofuran-contaminated soil. Environmental Pollution, 248, 506–515. https://doi.org/10.1016/j.envpol.2019.02.053

Wilson, M. J. (2004). Weathering of the primary rock-forming minerals: Processes, products and rates. Clay Minerals, 39(3), 233–266. https://doi.org/10.1180/0009855043930133

Wrathall, S. L. D., Procacci, B., Horch, M., Saxton, E., Furlan, C., Walton, J., Rippers, Y., Blaza, J. N., Greetham, G. M., Towrie, M., Parker, A. W., Lynam, J., Parkin, A., & Hunt, N. T. (2022). Ultrafast 2D-IR spectroscopy of [NiFe] hydrogenase from E. coli reveals the role of the protein scaffold in controlling the active site environment. Physical Chemistry Chemical Physics, 24(40), 24767–24783. https://doi.org/10.1039/D2CP04188J

Xiao, Y., & Lasaga, A. C. (1994). Ab initio quantum mechanical studies of the kinetics and mechanisms of silicate dissolution: H+(H3O+) catalysis. Geochimica et Cosmochimica Acta, 58(24), 5379–5400. https://doi.org/10.1016/0016-7037(94)90237-2

Xin, H., Sim, W. J., Namgung, B., Choi, Y., Li, B., & Lee, L. P. (2019). Quantum biological tunnel junction for electron transfer imaging in live cells. Nature Communications, 10(1), 3245. https://doi.org/10.1038/s41467-019-11212-x

Xu, M., Zhi, R., Jian, J., Feng, Y., Han, X., & Zhang, W. (2023). Changes in Soil Organic C Fractions and C Pool Stability Are Mediated by C-Degrading Enzymes in Litter Decomposition of Robinia pseudoacacia Plantations. Microbial Ecology, 86(2), 1189–1199. https://doi.org/10.1007/s00248-022-02113-6

Yan, Z., Wang, Z., Fu, Z., Zhang, Y., Peng, X., & Zheng, J. (2023). Microscale heterogeneity controls macroscopic soil heterotrophic respiration by regulating resource availability and environmental stress. Biogeochemistry, 164(2), 431–449. https://doi.org/10.1007/s10533-023-01044-9

Yang, Y., Chen, Y., Li, Z., Zhang, Y., & Lu, L. (2023). Microbial community and soil enzyme activities driving microbial metabolic efficiency patterns in riparian soils of the Three Gorges Reservoir. Frontiers in Microbiology, 14, 1108025. https://doi.org/10.3389/fmicb.2023.1108025

Young, I. M., & Crawford, J. W. (2004). Interactions and Self-Organization in the Soil-Microbe Complex. Science, 304(5677), 1634–1637. https://doi.org/10.1126/science.1097394

Yudina, A., & Kuzyakov, Y. (2023). Dual nature of soil structure: The unity of aggregates and pores. Geoderma, 434, 116478. https://doi.org/10.1016/j.geoderma.2023.116478

Zhang, Z., & Furman, A. (2021). Soil redox dynamics under dynamic hydrologic regimes—A review. Science of The Total Environment, 763, 143026. https://doi.org/10.1016/j.scitotenv.2020.143026

Zhu, Y., Zhang, H., Wang, Q., Zhu, W., & Kang, Y. (2024). Soil extracellular enzyme activity linkage with soil organic carbon under conservation tillage: A global meta-analysis. European Journal of Agronomy, 155, 127135. https://doi.org/10.1016/j.eja.2024.127135

Zhu, Y., Zhao, Z., Li, X., Liu, C., Yu, S., Lu, Y., & Du, X. (2024). Influence of Feldspar Dissolution on the Pore Structure and Characteristics of a Tight Sandstone Reservoir: A Case Study From the Northeast Margin of Ordos Basin, China. Geofluids, 2024(1), 9069384. https://doi.org/10.1155/2024/9069384

Zong, R., Wang, Z., Li, W., Li, H., & Ayantobo, O. O. (2023). Effects of practicing long-term mulched drip irrigation on soil quality in Northwest China. Science of The Total Environment, 878, 163247. https://doi.org/10.1016/j.scitotenv.2023.163247

Chapter 6. Overall Discussion and Conclusions

6.1. Erosion Risk Capability as a Metric for Assessing Threats to Soil

Accelerated soil erosion, influenced by anthropogenic pressures, is one of the most widespread threats to soil security (Shojaeezadeh et al., 2024; Koch et al., 2015). A major challenge in most current approaches is the lack of assessment methods that consider both soil capacity and condition to understand how well soils can withstand future erosion risks (Nosrati & Collins, 2019; Fang et al., 2024). This thesis addresses this gap by introducing the Erosion Risk Capability (ERC) metric, which evaluates erosion vulnerability across space and time by explicitly integrating inherent soil capacity (e.g clay ratio and topsoil thickness) with current soil condition (chapter 2). ERC quantifies the gap between these two states, providing a spatially explicit measure of a soil's ability to resist ongoing and future erosion pressures.

The ERC metric is grounded in the Genosoil-Phenosoil concept, which represents soils at different stages of pedogenesis and human influence (Huang et al., 2018). Genosoil represents the past state, and Phenosoil represents the current state where active human modifications are noticed (Francos et al., 2024). The space for time substitution approach is embedded in the metric, ERC enables assessment of how erosion vulnerability emerges as soil condition diverges from its natural capacity over time (Jang et al., 2022).

Many studies have highlighted the need for simple indicators to communicate threats to soil and raise awareness among the broader community (García-Gamero et al., 2024; Mason et al., 2025). The metric introduced in this thesis addresses that need. It is easy to interpret that a larger gap indicates a higher risk of soil erosion, providing a straightforward indicator to support efforts in achieving soil security.

The proposed Capacity-Condition Framework (CCF) advances a new approach to assessing soil erosion that is more directly targeted than general composite indices that combine multiple soil properties, and more integrative than traditional erosion rate models (Chapter 2). As shown in Chapter 2, the ERC was able to spatially delineate erosion vulnerability across New South Wales. It identified critical zones where mismatches between soil capacity and current condition reveal areas of high erosion risk, even where the actual erosion rate is low. This helps pinpoint regions where soil

management practices are most needed to mitigate erosion and maintain soil security. These findings demonstrated that ERC functions not only as a vulnerability indicator but also as a practical metric for threat assessment within the broader Soil Security Assessment Framework (Evangelista et al., 2023).

6.2. Soil Footprint as a Metric of Soil Security

Soil footprint is a simple indicator or metric used to communicate soil security (García-Gamero et al., 2024) . However, the current soil footprint concept is underdeveloped due to the lack of a general definition and a framework to serve as a comprehensive metric for soil security (Chapter 3). This thesis introduces a generalised soil footprint concept within a broader and more flexible framework that accommodates both simplified and detailed assessments. It proposes a unified metric that links different degradation processes, service loss, and intrinsic mitigation capability. The metric naturally captures the imbalance between threats to soil and its ability to sustain services-an imbalance that underlies the challenge of sustainable soil formation (Chapter 3) (Chapter 1).

In principle, the soil footprint has the potential to serve as a tool for assessing whether soils are operating within their regenerative limits. However, this aspect requires further investigation in future studies. The metric is designed to be interpretable even by non-scientific audiences: a higher soil footprint indicates a greater imbalance between degradation and the soil's service or mitigation capacity, while a lower footprint implies a smaller imbalance. Importantly, while existing soil degradation assessments often evaluate services and threats separately and rarely include mitigation capability, the proposed framework integrates all three dimensions (Schwilch et al., 2016). This indicates its potential as a practical tool for informing policy decisions and soil management priorities.

As demonstrated in the results (Chapter 3), the soil footprint framework was applied in New South Wales (NSW), using different soil services to calculate separate soil erosion footprints. This dual application showed how the metric can flexibly capture both agronomic and hydrological service losses under erosion as the main degradation process (soil erosion) (Chapter 3). The findings suggest that soil footprints not only quantify the imbalance between threats and services but also help prioritise areas for

intervention based on both vulnerability and economic importance, supporting the broader goals of soil sustainability and soil security (A. McBratney et al., 2014) (Chapter 3).

6.2.1. Soil security dimensions and Soil footprint framework

The soil footprint model proposed in this thesis naturally integrates the dimensions of soil security, making it a more comprehensive indicator for representing soil security. For instance,

- The condition of soil can be captured in the soil footprint equation, expressed through the soil service ratio, where reflects the condition of the soil by quantifying the deviation between its natural state (genosoil) and current state (phenosoil) (Chapter 3) (Alex. B. McBratney et al., 2019).
- The capacity of soil, representing its inherent ability to mitigate degradation within the soil system, is integrated into the equation through the term called mitigation capability (Chapter 3) (Alex. B. McBratney et al., 2019).
- Capital value of soil is reflected in service loss or retention. A lower footprint indicates capital retention; a higher footprint indicates depletion, affecting productivity and ecological resilience (Chapter 3). The soil footprint framework's flexibility allows a different capital dimension to be reflected depending on the indicator used. For example, AWC reflects natural capital, while Yield emphasises economic or produced capital, highlighting soil security's capital dimension (Francos et al., 2024).
- Connectivity (Pachón Maldonado et al., 2024)- Footprint maps or results serve as tools for communicating spatial patterns of degradation, enhancing stakeholder awareness and engagement. They bridge the gap between complex scientific assessments and practical intervention, where intervention is most needed for soil restoration. Successful restoration required farmer involvement, which connects people to soil (Maniraho et al., 2023; Hailemichael et al., 2025).
- As a standardised, quantifiable indicator, the soil footprint offers a pathway for institutional integration (García-Gamero et al., 2024). It can be codified into

national monitoring systems, regulatory frameworks, or international soil health targets similar to how water and carbon footprints have informed policy action (Pierrat et al., 2023).

6.3. Exergy as a Regenerative Pathway for Restoring Soils

Soil degradation often occurs at a higher rate than natural soil regeneration, particularly in intensively managed agricultural systems (Hossain et al., 2020). Soil security depends not only on assessing soil conditions but also on the efficient restoration of degraded soils (chapter 1). There is already an established solution, including practices such as composting, cover cropping, and agroecological design (Khangura et al., 2023). However, a critical question remains largely unaddressed in both literature and policy: How much energy is required to restore or regenerate degraded soil to its natural state? This thesis addresses this gap by developing exergy model to quantify the energy demand of soil restoration, especially on the restoration of SOC (Chapter 1, Chapter 4).

This thesis demonstrated the use of the exergy concept, with results from chapter 4 showing, for example, that organic amendments required less exergy input than intensive crop rotations in some pedogenons. This indicates that soil restoration is not only soil-dependent but also management-dependent, and that energy-efficient strategies can be identified and periodized through this model. Thus, the model has potential as a regenerative pathway tool, as it makes regenerative feasibility measurable – showing where and how much energy is needed for soil restoration (Chapter 4). It enables more efficient, goal-directed efforts to rebuild soil organic carbon and restore degraded soils to their reference state.

This process-based insight highlights that not all restoration efforts are equally energy-efficient; therefore, energy-efficient pathways must be prioritised to secure soil through strategies that contribute to soil security. The thesis argues that the exergy-based model has the potential to serve as a quantifiable, regenerative pathway for soil security. Its inclusion enhances the soil security assessment framework by addressing one of its current limitations - the lack of operational tools to guide and evaluate restoration, ensuring that the soils we aim to secure can also be feasibly restored.

6.4 Quantum Soil Science as a Future Pathway for Accelerated Regeneration

The thesis has introduced novel metrics (Erosion Risk Capability and soil footprint) and a thermodynamic restoration framework for soil assessment and restoration. However, securing soil requires more than these tools. We need a deeper understanding of soil formation processes to explore whether there is an opportunity to enhance the soil formation process itself- to boost soil's inherent ability to regenerate rather than merely applying remediation (Chapter 5).

Chapter 5 suggests that this may be possible by recognising quantum processes in the soil. The thesis argues that classical soil models, which are based on thermodynamics and kinetics, often struggle to explain why soil processes such as enzymatic decomposition and mineral weathering continue efficiently even under cold, low-energy, or stressed conditions. This leads the thesis to explore alternative theories of quantum mechanics, where subatomic phenomena like proton tunnelling and electron coherence could provide the hidden mechanisms that make soils resilient and regenerative, thus proposing a new pathway for soil security (Chapter 5).

The current soil restoration approach is effective but often a slow process to rebuild soil or soil fertility (Khangura et al., 2023). This thesis introduced the concept of quantum thinking in soil management, which could accelerate soil formation by targeting interventions at quantum-enabling microenvironments, where suitable conditions are created for quantum processes to foster soil processes (Chapter 5). This thinking is especially necessary in the current context of global soil degradation, where incremental improvements are no longer sufficient. By focusing on both quantum soil management and current soil management, we could boost the soil's capacity to regenerate, providing a pathway to restore soils more effectively than was previously possible.

Chapter 5 presents a conceptual perspective by proposing Quantum Soil Science as a potential extension of soil science, focused on the systematic investigation of quantum-scale processes. It also encourages interdisciplinary research, bringing scientists from different fields to engage in soil research and foster innovation, which has not been seen before. However, more empirical evidence and further research are still needed for a stronger understanding and identification of quantum processes in soil. Nonetheless, if

developed in the future, the quantum field may revolutionise soil science, optimise land-use planning and interventions, and enhance forecasting of soil response under various environmental stress.

6.5. A Holistic Vision for an Adaptive soil systems Framework

This thesis proposes an integrated decision-support framework that connects threat evaluation, soil condition assessment, restoration feasibility, and process-level enhancement within a closed-loop system: diagnose → prioritise → restore → accelerate → reassess. Erosion Risk Capability (ERC) quantifies vulnerability gaps between inherent capacity and current condition, while Soil Footprint evaluates operations beyond regenerative limits by integrating threats, service loss, and mitigation. Where footprints exceed limits, exergy-based restoration tests energetic feasibility and optimal low-input pathways, and Quantum Soil Science targets microenvironments to accelerate enzymatic and mineral processes. This vision transforms soil security from a static assessment into a dynamic management system. The framework can be implemented as a modular digital tool, where different data resolutions (field measurements, remote sensing, modelling outputs) populate each component. As new data or improved process understanding becomes available, particularly from quantum-informed experiments or restoration trials, the system can be iteratively updated without redefining the core structure.

6.6. Future direction

This thesis introduced a set of novel metrics and regenerative pathways that support securing soils in the face of accelerating degradation. The novel metrics, such as the Erosion Risk capability (ERC) and the Soil Footprint, represent an important shift in how soil degradation is assessed (chapter 2). These are communicable indicators that are spatially explicit and policy-relevant, and can be used by land managers, scientists, and policymakers.

Furthermore, these metrics need to be understood in terms of how they interact with climate, and different management practices, because soil degradation, especially soil erosion is influenced by climate change (Eekhout & De Vente, 2022). The interaction between climate variables and the proposed metrics was not fully explored in this work.

Future research could integrate climate projections and long-term climate scenarios (e.g., from CMIP6 models) into the ERC and Footprint frameworks to improve their adaptive capacity and forecasting utility. For instance, climate-adjusted ERC maps could inform land-use planning and resilience strategies, while dynamic Soil Footprint models could help track shifting pressures on soil services under different climate futures. These additions would enhance the policy relevance of the proposed metrics and support alignment with climate-smart agriculture and Land Degradation Neutrality (LDN) targets.

These metrics also have the potential to be transferred to other regions, similar to the capacity and condition framework (CCF) and the soil footprint framework; however, utility functions need to be calibrated to local conditions (chapter 2, 3).

Furthermore, future research could integrate frameworks developed in this thesis to develop machine learning models, as explored by Padarian et al. (2019), for continuous monitoring and for developing intelligent decision-support systems. This can be achieved by integrating artificial intelligence (AI) and machine learning frameworks with satellite remote sensing approaches to predict both indicators at different spatial and temporal scales, under various management and climate scenarios.

Future research can explore the socio-economic and human dimensions, since the adoption of these metrics depends on stakeholder engagement and supportive policy environments. Studies could examine in more detail the socioeconomic factors, cultural contexts, and behavioural drivers that influence farmers' decisions to adopt management practices informed by the ERC and Soil Footprint metrics (Khuraijam et al., 2025; Winowiecki et al., 2025). This direction could strengthen the connectivity dimension of soil security.

The exergy model demonstrated feasibility for quantifying the requirements of SOC restoration across various pedogenons and management systems in New South Wales. The model can be transferred to other regions by calculating k, α and the change in SOC between degraded soils and their reference soils. In practical applications, this framework could be tested by applying it to long-term restoration monitoring projects for further evaluation of the model.

One of the potential future extensions of this model lies in its ability to assess net climate benefits. Since many countries are moving towards net-zero emissions (eg.,Australia's Net Zero Plan and the EU Soil Strategy 2030 and soil systems are increasingly recognized for their potential role in carbon sequestration and emission offsetting (De Rosa et al., 2024; White, 2022), the model could be extended to calculate the balance between CO_2 equivalent emissions from restoration activities (e.g., transport, application of amendments, fertilizer production) and the sequestration potential via restored SOC stocks. This potential can be used both for soil restoration as a regenerative approach to soil security and as a quantifiable input to national carbon budgets and climate mitigation goals.

The thesis introduces the concept of quantum thinking in soil science, a novel conceptual advancement that provides new perspectives for a regenerative pathway to secure soil. If targeted management focuses on both quantum-scale processes and improvements in bulk soil properties, it could accelerate soil regeneration, something that has not been previously discussed in soil science. This chapter is conceptual, with some support from literature from enzymology and microbial behaviour under low-energy conditions, which attempts to understand quantum effects in soil processes. However, experimental validation in real soil systems remains a critical next step. Section 5.9.4 explicitly outlines a methodological pathway for such validation, including the use of kinetic isotope effects, temperature response analyses, redox microprofilling and quantum-corrected modelling approaches and related quantum contribution under soil-relevant condition. If validated, these approaches could advance our mechanistic understanding of soil process and inform future soil restoration strategies.

6.6 . References

De Rosa, D., Ballabio, C., Lugato, E., Fasiolo, M., Jones, A., & Panagos, P. (2024). Soil organic carbon stocks in European croplands and grasslands: How much have we lost in the past decade? Global Change Biology, 30(1), e16992. https://doi.org/10.1111/gcb.16992

Eekhout, J. P. C., & De Vente, J. (2022). Global impact of climate change on soil erosion and potential for adaptation through soil conservation. Earth-Science Reviews, 226, 103921. https://doi.org/10.1016/j.earscirev.2022.103921

Evangelista, S. J., Field, D. J., McBratney, A. B., Minasny, B., Ng, W., Padarian, J., Román Dobarco, M., & Wadoux, A. M. J.-C. (2023). A proposal for the assessment of soil security: Soil functions, soil services and threats to soil. Soil Security, 10, 100086. https://doi.org/10.1016/j.soisec.2023.100086

Fang, H., Zhai, Y., & Li, C. (2024). Evaluating the impact of soil erosion on soil quality in an agricultural land, northeastern China. Scientific Reports, 14(1), 15629. https://doi.org/10.1038/s41598-024-65646-5

Francos, N., McBratney, A. B., Field, D. J., Minasny, B., Pachon, J. C., Padarian, J., Hunakunti, A., Ng, W., Evangelista, S. J., & O'Donoghue, T. (2024). Valuing and integrating soil roles in assessing the capital dimension of soil security: An Australian case study. Soil Security, 16, 100141. https://doi.org/10.1016/j.soisec.2024.100141

García-Gamero, V., Vanwalleghem, T., & Peñuela, A. (2024). Soil footprint: A simple indicator to communicate and quantify soil security. Soil Security, 16, 100156. https://doi.org/10.1016/j.soisec.2024.100156

Hailemichael, B., Bekele, M., & Tamirat, T. (2025). Impact of Socio-economic and Environmental Factors on Land Restoration Initiatives by Farmers: Evidence from Soddo Zuria Woreda, Southern Ethiopia. World Journal of Agricultural Science and Technology, 3(1), 1–11. https://doi.org/10.11648/j.wjast.20250301.11

Hossain, A., Krupnik, T. J., Timsina, J., Mahboob, M. G., Chaki, A. K., Farooq, M., Bhatt, R., Fahad, S., & Hasanuzzaman, M. (2020). Agricultural Land Degradation: Processes and Problems Undermining Future Food Security. In S. Fahad, M. Hasanuzzaman, M. Alam, H. Ullah, M. Saeed, I. Ali Khan, & M. Adnan (Eds.), Environment, Climate, Plant and Vegetation Growth (pp. 17–61). Springer International Publishing. https://doi.org/10.1007/978-3-030-49732-3_2

Huang, J., McBratney, A. B., Malone, B. P., & Field, D. J. (2018). Mapping the transition from pre-European settlement to contemporary soil conditions in the Lower Hunter Valley, Australia. Geoderma, 329, 27–42. https://doi.org/10.1016/j.geoderma.2018.05.016

Jang, H. J., Román Dobarco, M., Minasny, B., McBratney, A., & Jones, E. (2022). Developing and testing of pedogenons in the lower Namoi valley, NSW, Australia. Geoderma, 428, 116182. https://doi.org/10.1016/j.geoderma.2022.116182

Khangura, R., Ferris, D., Wagg, C., & Bowyer, J. (2023). Regenerative Agriculture—A Literature Review on the Practices and Mechanisms Used to Improve Soil Health. Sustainability, 15(3), 2338. https://doi.org/10.3390/su15032338

Khuraijam, S., Wechtler, H., Higgins, V., & Seshadri, B. (2025). Understanding the impact of identity and socio-economic factors on the adoption of soil conservation practices: Empirical evidence from Australia. Journal of Rural Studies, 116, 103636. https://doi.org/10.1016/j.jrurstud.2025.103636

Koch, A., Chappell, A., Eyres, M., & Scott, E. (2015). Monitor Soil Degradation or Triage for Soil Security? An Australian Challenge. Sustainability, 7(5), 4870–4892. https://doi.org/10.3390/su7054870

Maniraho, L., Frietsch, M., Sieber, S., & Löhr, K. (2023). A framework for drivers fostering social-ecological restoration within forest landscape based on people's participation. A systematic literature review. Discover Sustainability, 4(1), 26. https://doi.org/10.1007/s43621-023-00141-x

Mason, E., Cornu, S., Froger, C., Saby, N. P. A., & Chenu, C. (2025). Scientific Indicators and Stakeholders' Perceptions on Soil Threats in France: How Do They Compare? European Journal of Soil Science, 76(5), e70190. https://doi.org/10.1111/ejss.70190

McBratney, A., Field, D. J., & Koch, A. (2014). The dimensions of soil security. Geoderma, 213, 203–213. https://doi.org/10.1016/j.geoderma.2013.08.013

McBratney, Alex. B., Field, D., Morgan, C. L. S., & Huang, J. (2019). On Soil Capability, Capacity, and Condition. Sustainability, 11(12), 3350. https://doi.org/10.3390/su11123350

Nosrati, K., & Collins, A. L. (2019). A soil quality index for evaluation of degradation under land use and soil erosion categories in a small mountainous catchment, Iran. Journal of Mountain Science, 16(11), 2577–2590. https://doi.org/10.1007/s11629-019-5567-8

Padarian, J., Minasny, B., & McBratney, A. B. (2019). Using deep learning for digital soil mapping. SOIL, 5(1), 79–89. https://doi.org/10.5194/soil-5-79-2019

Pachón Maldonado, J. C., Leonard, E. C., Field, D. J., McRobert, K., Heath, R., & McBratney, A. B. (2024). Quantifying the connectivity dimension of the soil security assessment framework. Soil Security, 17, 100175. https://doi.org/10.1016/j.soisec.2024.100175

Pierrat, É., Laurent, A., Dorber, M., Rygaard, M., Verones, F., & Hauschild, M. (2023). Advancing water footprint assessments: Combining the impacts of water pollution and scarcity. Science of The Total Environment, 870, 161910. https://doi.org/10.1016/j.scitotenv.2023.161910

Schwilch, G., Bernet, L., Fleskens, L., Giannakis, E., Leventon, J., Marañón, T., Mills, J., Short, C., Stolte, J., Van Delden, H., & Verzandvoort, S. (2016). Operationalizing ecosystem services for the mitigation of soil threats: A proposed framework. Ecological Indicators, 67, 586–597. https://doi.org/10.1016/j.ecolind.2016.03.016

Shojaeezadeh, S. A., Al-Wardy, M., Nikoo, M. R., Mooselu, M. G., Alizadeh, M. R., Adamowski, J. F., Moradkhani, H., Alamdari, N., & Gandomi, A. H. (2024). Soil erosion in the United States: Present and future (2020–2050). CATENA, 242, 108074. https://doi.org/10.1016/j.catena.2024.108074

White, R. E. (2022). The Role of Soil Carbon Sequestration as a Climate Change Mitigation Strategy: An Australian Case Study. Soil Systems, 6(2), 46. https://doi.org/10.3390/soilsystems6020046

Winowiecki, L. A., Linden, H., Alexander, S., Bargués Tobella, A., Campari, J., Christensen, C., Choudhury, D., Van Duijn, H., Fleckenstein, M., Harz-Pitre, Y., Hussain, Z., Kakade, B., Kamau, D., Luu, P., Magaju, C., Makiyi, V., Mbabazi, P., Morgan, C., Snapp, S., … Lal, R. (2025). Multistakeholder Engagement to Scale Soil Health Globally: The Coalition of Action 4 Soil Health. European Journal of Soil Science, 76(3), e70128. https://doi.org/10.1111/ejss.70128